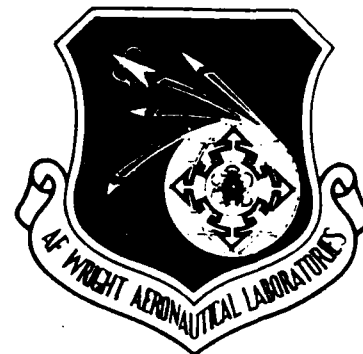


DTIC FILE COPY

2

AFWAL-TR-87-3115

Volume I



STABILITY AND CONTROL METHODOLOGY FOR
CONCEPTUAL AIRCRAFT DESIGN

VOLUME I: METHODOLOGY MANUAL

Terry S. Smith
Design Branch
Technology Assessment Office
Flight Dynamics Laboratory

December 1987

Final Report for Period June 85 - June 87

AD-A191 314

APPROVED FOR PUBLIC RELEASE; DISTRIBUTION UNLIMITED

DTIC
SELECTED
FEB 29 1988
S H D

- FLIGHT DYNAMICS LABORATORY
AIR FORCE WRIGHT AERONAUTICAL LABORATORIES
AIR FORCE SYSTEMS COMMAND
WRIGHT-PATTERSON AIR FORCE BASE, OHIO 45433-6553

88 2 26 178

NOTICE

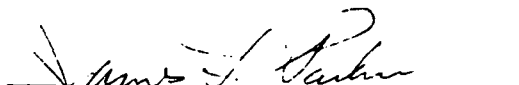
When Government drawings, specifications, or other data are used for any purpose other than in connection with a definitely Government-related procurement, the United States Government incurs no responsibility or any obligation whatsoever. The fact that the Government may have formulated or in any way supplied the said drawings, specifications, or other data, is not to be regarded by implication, or otherwise in any manner construed, as licensing the holder, or any other person or corporation; or as conveying any rights or permission to manufacture, use, or sell any patented invention that may in any way be related thereto.

This report has been reviewed by the Office of Public Affairs (ASD/PA) and is releasable to the National Technical Information Service (NTIS). At NTIS, it will be available to the general public, including foreign nations.

This technical report has been reviewed and is approved for publication.



TERRY S. SMITH
Aerospace Engineer
Technology Assessment Office
Flight Dynamics Laboratory



JAMES L. PARKER, Chief
Design Branch
Technology Assessment Office
Flight Dynamics Laboratory

FOR THE COMMANDER



SQUIRE L. BROWN, Chief
Technology Assessment Office
Flight Dynamics Laboratory

If your address has changed, if you wish to be removed from our mailing list, or if the addressee is no longer employed by your organization please notify AFWAL/FIAD, Wright-Patterson AFB, OH 45433-6553 to help us maintain a current mailing list.

Copies of this report should not be returned unless return is required by security considerations, contractual obligations, or notice on a specific document.

UNCLASSIFIED

SECURITY CLASSIFICATION OF THIS PAGE

REPORT DOCUMENTATION PAGE

Form Approved OMB No. 0704-0188

1a. REPORT SECURITY CLASSIFICATION UNCLASSIFIED		1b. RESTRICTIVE MARKINGS	
2a. SECURITY CLASSIFICATION AUTHORITY		3. DISTRIBUTION/AVAILABILITY OF REPORT Approved for public release; distribution unlimited	
2b. DECLASSIFICATION/DOWNGRADING SCHEDULE		4. PERFORMING ORGANIZATION REPORT NUMBER(S) AFWAL-TR-87-3115, Vol I	
4. PERFORMING ORGANIZATION REPORT NUMBER(S)		5. MONITORING ORGANIZATION REPORT NUMBER(S)	
6a. NAME OF PERFORMING ORGANIZATION Design Branch Technology Assessment Office	6b. OFFICE SYMBOL (If applicable) AFWAL/FIAD	7a. NAME OF MONITORING ORGANIZATION	
6c. ADDRESS (City, State, and ZIP Code) AFWAL/FIA Wright-Patterson AFB OH 45433-6553		7b. ADDRESS (City, State, and ZIP Code)	
8a. NAME OF FUNDING / SPONSORING ORGANIZATION	8b. OFFICE SYMBOL (If applicable)	9. PROCUREMENT INSTRUMENT IDENTIFICATION NUMBER	
8c. ADDRESS (City, State, and ZIP Code)		10. SOURCE OF FUNDING NUMBERS	
		PROGRAM ELEMENT NO 62201F	PROJECT NO 2404
		TASK NO 01	WORK UNIT ACCESSION NO 97
11. TITLE (Include Security Classification) Stability and Control Methodology for Conceptual Aircraft Design Vol I - Methodology Manual			
12. PERSONAL AUTHOR(S) Smith, Terry S.			
13a. TYPE OF REPORT Final	13b. TIME COVERED FROM Jun 85 TO Jun 87	14. DATE OF REPORT (Year, Month, Day) December 87	15. PAGE COUNT 179
16. SUPPLEMENTARY NOTATION			
17. COSATI CODES		18. SUBJECT TERMS (Continue on reverse if necessary and identify by block number)	
FIELD	GROUP	Aircraft > Trim Drag	
01	01	Stability and Control	
01	03	Aerodynamics	
19. ABSTRACT (Continue on reverse if necessary and identify by block number) This report contains methodology for predicting stability and control characteristics of conceptual flight vehicles. The methodology presented is a combination of existing methodology, modified existing methodology, and newly developed methodology. The methodology is divided into three main sections: 1) Aerodynamics or Longitudinal stability coefficients, 2) Lateral Stability coefficients, and 3) Static and Dynamic Stability Analysis.			
20. DISTRIBUTION/AVAILABILITY OF ABSTRACT <input type="checkbox"/> UNCLASSIFIED/UNLIMITED <input type="checkbox"/> SAME AS RPT <input checked="" type="checkbox"/> DTIC USERS		21. ABSTRACT SECURITY CLASSIFICATION UNCLASSIFIED	
22a. NAME OF RESPONSIBLE INDIVIDUAL Terry Smith		22b. TELEPHONE (Include Area Code) (513) 255-5288	22c. OFFICE SYMBOL AFWAL/FIAD

FOREWORD

This report describes the methodology that is used by the Flight Dynamics Laboratory, Technology Assessment Office, Design Branch for stability and control analyses of in-house conceptual aircraft designs. The method was developed and coded into the Stability and Control Program by Terry Smith to be compatible with the unique constraints of the conceptual design environment. The computer program and the user's manual are available upon request. The assistance of Tracy Smith in documenting the methods and the user's manual is gratefully acknowledged. The validation of the method and the many corrections to the code provided by Dr Richard Walker and the students of Miami University was invaluable. The Technical Report Committee chaired by Mr William Blake, with the participation of Greg Staley and Stan Levy, provided many valuable suggestions and comments. The final preparation of the report by Cecilia Brewer, Donna Swabey and Maureen Conway is also much appreciated.



Accession For	
NTIS GRA&I	<input checked="" type="checkbox"/>
DTIC TAB	<input type="checkbox"/>
Unannounced	<input type="checkbox"/>
Justification	
By	
Distribution/	
Availability Codes	
Dist	Avail and/or Special
A-1	

TABLE OF CONTENTS

TITLE	PAGE
1.0 INTRODUCTION	1
2.0 AERODYNAMIC METHODS	2
2.1 CRITICAL MACH NUMBER (MCR)	2
2.1.1 Pressure Coefficient Calculations	3
2.1.2 Critical Mach Number Calculation from Crestline Pressure	4
2.2 AERODYNAMIC CENTER	10
2.2.1 Aerodynamic Center of Forebody	10
2.2.2 Aerodynamic Center of Surface (Single Panel).	10
2.2.3 Aerodynamic Center of Multi Panel Surfaces	18
2.2.4 Aerodynamic Center of Wing-Lift Carryover on the Body .	19
2.2.5 Total Aerodynamic Center	22
2.3 ZERO-LIFT PITCHING MOMENT (CMO)	24
2.4 ZERO ALPHA LIFT COEFFICIENT (CLO)	27
2.4.1 Lifting Surface CLO	27
2.4.2 Body and Nacelle CLO	29
2.4.3 Total Aircraft CLO	30
2.5 ZERO LIFT DRAG (CDO)	31
2.5.1 Friction Drag (CF)	31
2.5.2 Form Factors	32
2.5.3 Interference Factors	39
2.5.4 Wave Drag	42
2.5.4.1 Surface Wave Drag	42
2.5.4.2 Body Wave Drag	45
2.5.4.3 Nacelle Wave Drag	46
2.5.5 Camber Drag	47
2.5.6 Base Drag	47
2.5.7 Drag Rise	47
2.6 SURFACE INTERACTIONS	50
2.6.1 Downwash Effects on Angle of Attack	50
2.6.2 Wing Lift	52

2.7	LIFT, LIFT CURVE SLOPE, AND DRAG DUE TO LIFT	55
2.7.1	Incompressible Flow Zone 1 ($M < 0.1$)	55
2.7.2	Compressible, Shock-Free Flow Zone 2	57
2.7.3	Leading-edge Mach-limited Flow Zone 3	58
2.7.4	Surface Mach-limited Zone 4	60
2.7.5	Supersonic Attached-Shock Zone 5	62
2.7.6	Supersonic Detached-Shock Zone 6	63
2.7.7	Lift and Drag for Bodies and Nacelles	64
2.8	DYNAMIC PRESSURE RATIO	67
2.8.1	Dynamic Pressure at Down Stream Surfaces	67
2.8.2	Side-Wash-Factor * Dynamic Pressure Ratio of the Vertical Tail	68
2.9	TRIM AERODYNAMICS	70
2.9.1	Body Engines or Nacelle Engines	70
2.9.2	All Moveable Surfaces	70
2.9.3	Flaps	71
2.10	PITCHING MOMENT CURVE SLOPE (CM_{α})	73
2.11	THE VARIATION OF PITCHING MOMENT COEFFICIENT WITH ANGLE OF ATTACK RATE ($CM_{\dot{\alpha}}$)	74
2.12	THE VARIATION OF PITCHING MOMENT COEFFICIENT WITH PITCH RATE ($CM_{\dot{q}}$)	75
2.13	HIGH-LIFT SYSTEM AERODYNAMICS	77
2.13.1	Aerodynamic Characteristics of Two-Dimensional High-Lift Devices	77
2.13.2	Lift of High-Lift Devices	92
2.13.3	Drag of High-Lift Devices	96
2.13.4	Moment of High-Lift Devices	99
3.0	STABILITY COEFFICIENTS METHODS	103
3.1	CLP	103
3.1.1	CLP For Lifting Surfaces	103
3.1.2	CLP For the Vertical Tail	110
3.1.3	CLP for Wing-Body Interaction	110
3.2	CLDA	110
3.3	CLB	123
3.3.1	CLB for Vertical Tails	123
3.3.2	CLB for Lifting Surfaces	123

3.4	CNB	131
3.4.1	CNB for Bodies and Nacelles	131
3.4.2	CNB for Lifting Surfaces	131
3.4.3	CNB for Vertical Tails	140
3.4.4	CNB for Fins	140
3.4.5	CNB for the Vertical Component of the Horizontal Tail	140
3.5	CNDELTR	142
3.6	CNR	144
3.6.1	CNRWB	144
3.6.2	CNRV	144
4.0	DYNAMIC ANALYSIS ROUTINES	148
4.1	SHORT PERIOD MODE EQUATION	148
4.2	PHUGOID MODE EQUATION	150
4.3	DUTCH-ROLL MODE EQUATION	151
4.4	ROLLING MODE EQUATION	152
5.0	STATIC ANALYSIS METHODS	153
5.1	ENGINE OUT CONDITIONS	153
5.2	TAKEOFF ROTATION	156
5.3	CROSS-WIND LANDING	160
Appendix A	Sign Conventions	A1
Appendix B	Geometry	B1
References	R1

LIST OF FIGURES

	<u>Figure</u>	<u>Page</u>
2.1.1	Mach Critical Prediction Chart	6
2.1.2	Prediction of Fuselage Critical Mach Number	8
2.1.3	Correlation of Critical Mach Number for Conventional Wings	9
2.2.1	Wing-Body Geometry	11
2.2.2	Supersonic Center of Pressure of Ogive with Cylindrical Afterbody	12
2.2.3	Wing Aerodynamic-Center Position	13
2.2.4	Transonic Wing Aerodynamic-Center Location	16
2.2.5	Geometry for the Multi Panel Surfaces	20
2.2.6	Parameter Used in Accounting for Wing-Lift Carryover on the Body	21
2.2.7	Effective Ratio of Body Diameter to Root Chord	23
2.3.1	Effect of Linear Twist on the Wing Zero-Lift Pitching Moment	25
2.5.1	Turbulent Skin Friction Coefficient on an Adiabatic Flat Plate	33
2.5.2	Skin Friction on an Adiabatic Flat Plate, $X_{TR} = 0.1$	34
2.5.3	Skin Friction on an Adiabatic Flat Plate, $X_{TR} = 0.2$	35
2.5.4	Skin Friction on an Adiabatic Flat Plate, $X_{TR} = 0.3$	36
2.5.5	Skin Friction on an Adiabatic Flat Plate, $X_{TR} = 0.4$	37
2.5.6	Skin Friction on an Adiabatic Flat Plate, $X_{TR} = 0.5$	38
2.5.7	Supercritical Wing Compressibility Factor	40
2.5.8	Wing-Body Correlation Factor for Subsonic Minimum Drag	41
2.5.9	Lifting Surface Correlation Factor For Subsonic Minimum Drag	43
2.5.10	Transonic Drag Buildup	49
2.7.1	Flow Zones	56
2.7.2	Surface Mach number Limited Transonic Flow	61
2.7.3	Contour of Cross-Flow Drag Coefficient with Cross- Flow Mach and Reynolds Numbers	66
2.13.1	Incremental Effect of Flaps	79
2.13.2	Flap Chord Factor	80
2.13.3	Flap Span Lift Factor	80
2.13.4	Slat Span Lift Factor	81
2.13.5	Flap Span Drag Factor	81
2.13.6	Flap-Induced Drag Factors	83
2.13.7	Span Effect on Moments	84
2.13.8	Span Effect on Moments of Sweptback Wings	84
2.13.9	Theoretical Lifting Effectiveness of Trailing- Edge Flaps	86
2.13.10	Turning Efficiency of Plain Trailing-Edge Flaps	86
2.13.11	Turning Efficiency of Single-Slotted Flaps	86
2.13.12	Turning Efficiency of Double-Slotted Flaps	88
2.13.13	Turning Efficiency of Triple-Slotted Flaps	88
2.13.14	Principle of Superposition Theory and Extended Slotted-Flap Geometry	89
2.13.15	Maximum Lift Correlation Factor for Trailing Edge Flaps	90
2.13.16	Flap Angle Correlation Factor Versus Flap Deflection	91

2.13.17	Leading Edge Flap Maximum Lift Effectiveness	93
2.13.18	Maximum Lift Efficiency for Leading-Edge Devices	94
2.13.19	Leading Edge Device Deflection Angle Correction Factor	95
2.13.20	Flap Center of Pressure Location as given by Thin Airfoil Theory	97
2.13.21	Moment Correlation Factor Versus Flap Chord	98
2.13.22	Two-Dimensional Drag Increment Due to Plain Flaps	100
2.13.23	Two-Dimensional Drag Increment Due to Single- Slotted Flaps	101
2.13.24	Drag Increment for Double-Slotted Flaps Versus Lift Increment at $\alpha = 0^\circ$	102
3.1.1	Roll-Damping Parameter at Zero Lift	104
3.1.2	Drag-Due-To-Lift Roll-Damping Parameter	109
3.1.3	Roll-Damping Parameter	111
3.1.4	Damping-in-Roll Correction Factor for Sonic-Leading- Edge Region	113
3.1.5	Effect of the Fuselage on Roll Damping	115
3.2.1	Subsonic Aileron Rolling-Moment Parameter	117
3.2.2	Instructions for Using Figure 3.2.1	120
3.2.3	Theoretical Lift Effectiveness of Plain Trailing- Edge Flaps	122
3.2.4	Empirical Correction for Lift Effectiveness of Plain Trailing-Edge Flaps	122
3.3.1	Wing Sweep Contribution to CLBETA	125
3.3.2	Compressibility Correction Factor to Sweep Contribution to Wing CLBETA	126
3.3.4	Aspect Ratio Contribution to Wing CLBETA	126
3.3.3	Fuselage Correction Factor	127
3.3.5	Effect of Uniform Geometric Dihedral on Wing CLBETA	128
3.3.6	Compressibility Correction to Dihedral Effect on Wing CLBETA	129
3.3.7	Effect of Wing Twist on Wing CLBETA	129
3.4.1	Empirical Factor KN Related to Sideslip Derivative CNBETA for Body + Wing-Body Interference	132
3.4.2	Effect of Fuselage Reynolds Number on Wing-Body CNBETA	133
3.4.3	Elliptic Integral Factors of the Stability Derivative	136
3.4.4	$F_0(N)$ Factor of the Stability Derivative	137
3.4.5	$F(N)$ Factors of the Stability Derivative	138
3.4.6	Elliptic Integral Factor of the Stability Derivative	139
3.5.1	Angle-of-Attack Effectiveness of Trailing Edge Control Surfaces	143
3.6.1	Low-Speed Drag-Due-To-Lift Yaw-Damping Parameter	145
3.6.2	Low-Speed Profile-Drag Yaw-Damping Parameter	146
5.1.1	Angle-of-Attack Effectiveness of Trailing Edge Control Surfaces	155
A1	Arm Definition	A2
A2	Force Definition	A2
A3	Moment Definition	A2
A4	Surface Moment Arm Definition	A3
B1	Wing Surface Geometry	B2

1.0 INTRODUCTION

The Stability and Control Program (SACP) is a computerized set of methods for predicting stability and control characteristics of conceptual level flight vehicles. The program was developed as an in-house effort, by the design branch (AFWAL/FIAD), to fill a deficiency in the stability and control analysis area.

The methodology used in SACP is a combination of existing methodology, modified existing methodology, and newly created methods. The program is divided into three major modules: 1) aerodynamics and longitudinal coefficients, 2) stability coefficients and lateral coefficients, and 3) stability analysis. The program is set up to run on the design branches PRIME 750 computer and uses TEKTRONIX's PLOT10 IGL graphics software for graphical output.

Volume I of this report documents the methods used by the program. Volume II is a user's manual and computer program description for SACP.

2.0 AERODYNAMIC METHODS

The methods described here compute the critical Mach number, aerodynamic center, and the longitudinal stability derivatives for the specified aircraft. The coefficients computed include lift, drag, pitching moment, the variations in these with angle of attack, and the dynamic pressure ratios. Methods are used to compute coefficients for untrimmed, trimmed, and high lift conditions ensuring a good coverage of aircraft configurations. Each method, and its use, is discussed below.

2.1 CRITICAL MACH NUMBER (MCR)

The drag-divergence Mach number or Mach critical, is defined as the Mach number at which a rapid drag rise interrupts the subsonic trend in drag. The British method of predicting the critical Mach number for two-dimensional airfoils as described by the Royal Aerodynamic Society (3) appears to be the most accurate empirical method available. This method uses the Sinnott "crest criteria", where the low speed pressure at the airfoil crest is related to the drag-divergence.

The SACP program uses a method, taken from the Large Aircraft Program (1), (2), that is analogous to the British two-dimensional critical Mach number prediction procedure in order to predict the critical Mach number for a finite-aspect-ratio swept wing. The critical Mach number is defined as the value of free stream Mach number which produces a local supersonic flow measured normal to the sweep of the isobar at the crest. The local Mach number normal to the crest isobar is taken to be 1.02 for conventional airfoils and 1.05 for supercritical airfoils in order to define free stream critical Mach number. The sonic condition at the crest can be predicted by means of a simple equation in which the incompressible pressure at the crest of the airfoil and compressibility factors are used.

The value of 1.02 local Mach number for the weak shock at crest condition for drag rise used in Sinnotts transonic airfoil theory (4) was established empirically. The Royal Aerodynamic Society (3) shows that this method should predict critical Mach to within ± 0.015 for the majority of conventional two-dimension airfoils. However, as shown in reference (3), with "peaky" airfoils (as in the supercritical airfoil) the onset of rapid drag rise may be delayed until the shock is substantially downstream of the crest. The predicted value of critical Mach based on a local Mach of 1.02 at the crest may thus be conservative by more than 0.02, and a local Mach of 1.05 is needed to achieve good correlation.

The following sections discuss the methods used to predict the pressure distribution around an airfoil and to determine critical Mach from the pressure at the crest along with the method used to estimate the drag rise above critical Mach.

2.1.1 Pressure Coefficient Calculations

The incompressible, inviscid pressure distribution around the airfoil is first defined. From this, the pressure at the crest can be determined. The method of Weber (5) was used for the pressure distribution calculations. This method requires the airfoil surface coordinates to be determined at the chordwise locations defined by

$$XU(IV) = .5 * (1 + \text{COS}(IV * \text{PI}/N)); \quad (2.1.1)$$

Where IV takes on the integer values between zero and N, and N may be any integer, in this program N is set equal to 32.

The Weber formula is essentially a second-order linear theory whereby the pressures are determined from multiplication of the matrix of thickness and camber ordinates of the airfoil by a matrix of constants given by the Royal Aerodynamic Society (5).

The formula for the incompressible pressure distribution on an infinite sheared wing was obtained from the incompressible form of equation 93 in reference (5) resulting in

$$\begin{aligned} 1 - CP = & (1/(1 + ((SA(IV) \pm SE(IV))/\text{COS } L)^2)) \\ & * ((\text{COS } A * \text{COS } L * (1 + SA(IV) \pm SD(IV)) \\ & \pm \text{SIN } A * \text{COS } L * (1 + SC(IV)/\text{COS } L) * \text{SQRT}((1 - IV)/IV))^2 \\ & \pm (\text{COS } A * \text{SIN } L * (SA(IV) \pm SD(IV)) \\ & \pm \text{SIN } A * \text{SIN } L * (1 + SC(IV)/\text{COS } L) * \text{SQRT}((1 - IV)/IV))^2 \\ & + \text{SIN}^2 L * \text{COS}^2 A * (1 - (1/(1 + ((SB(IV) \pm SE(IV))/\text{COS } L)^2)))) \end{aligned} \quad (2.1.2)$$

For CP on the upper surface the + is used, and for the lower surface CP the - is used. Also,

$$SA(IV) = \sum_{IU=1}^N S1(IU,IV) * ZT(IU)$$

$$SB(IV) = \sum_{IU=1}^N S2(IU,IV) * ZT(IU)$$

$$SC(IV) = \sum_{IU=1}^N S3(IV,IV) * ZT(IU) + S3(NX,IV) * SQRT(ROC/2)$$

$$SD(IV) = \sum_{IU=1}^N S4(IU,IV) * ZS(IU)$$

$$SE(IV) = \sum_{IU=1}^N S5(IU,IV) * ZS(IU)$$

Where the S1, S2, S3, S4, and S5 matrices are constants given by the Royal Aerodynamic Society (5). ZT(IU) and ZS(IU) are the thickness and camber distribution at the control point IU given by

$$ZT(IU) = .5(YU + YL)^1$$

and

$$ZS(IU) = .5(YU - YL)^1$$

Where YU and YL are the upper- and lower-surface ordinates at the control point IU given by

$$X(IU) = .5(1 + \cos(IU * \pi/N))$$

2.1.2 Critical Mach Number Calculation from Crestline Pressure.

The procedure followed to determine critical Mach for swept wings is similar to the procedure outline in reference (3) to predict the critical Mach for two-dimensional sections. In the procedure, Equation 2.1.1 is used to compute the pressure distribution around the airfoil at a sweep angle determined from

¹ the actual computations for ZT and ZS are dependent on the type of airfoil represented

$$L = \text{ARCOS} (\text{COS}(\text{C2SWEEP}))^n; \quad \text{WHEN C2SWEEP} \leq 40$$

$$L = \text{ARCOS} (\text{COS}(\text{C2SWEEP}))^n + .76604^n / 2; \quad \text{WHEN C2SWEEP} > 40$$

(2.1.3)

where C2SWEEP is the mid chord sweep at the semi-span of the wing and the factor n is determined from

$$n = \text{ARW} / (1.4 + \text{ARW})$$

and ARW is the aspect ratio of the wing.

The angle L represents an effective isobar sweep angle at the mid span region of the wing. The procedure used to determine critical Mach based on the crest pressures is as follows:

1. Determine a chordwise incompressible, inviscid pressure distribution for an angle of incidence (A). Integrate the pressure distribution to obtain the lift coefficient (CLI)
2. Determine the chordwise position of the crest for each A, the crest being defined as the point at which the airfoil surface is tangential to the undisturbed freestream direction.
3. Determine the incompressible pressure coefficient at the crest (CPCRST).
4. Use CPCRST to determine critical Mach from the relation

$$\text{CPCRST} = \frac{(P/PT) * (1 + .02 * \text{MCR}^2 * \text{COS}^2 L)^{3.5} - 1}{0.7 * \text{MCR}^2 / \text{SQRT}(1 - \text{MCR}^2 * \text{COS}^2 L)} \quad (2.1.4)$$

where (P/PT) is the ratio of local static pressure to freestream stagnation pressure as determined by

$$P/PT = (1 + 0.2 * \text{ML}^2)^{3.5}$$

where ML is the local Mach normal to the isobar sweep L at the crest of the airfoil. ML is set equal to 1.02 for conventional airfoils and 1.05 for "peaky" or supercritical airfoils. Equation 2.1.4 uses a Prandtl-Glauert compressibility factor to correct the incompressible pressure coefficient for Mach number rather than the Karman-Tsien factor used in reference 3. Miller (6) and the Royal Aerodynamic Society (7) recommend using the Prandtl-Glauert factor instead of the Karman-Tsien factor in the critical Mach prediction method for highly cambered airfoils or general airfoils at high-lift coefficients. The relationship determined by Equation 2.1.4 is plotted in Figure 2.1.1.

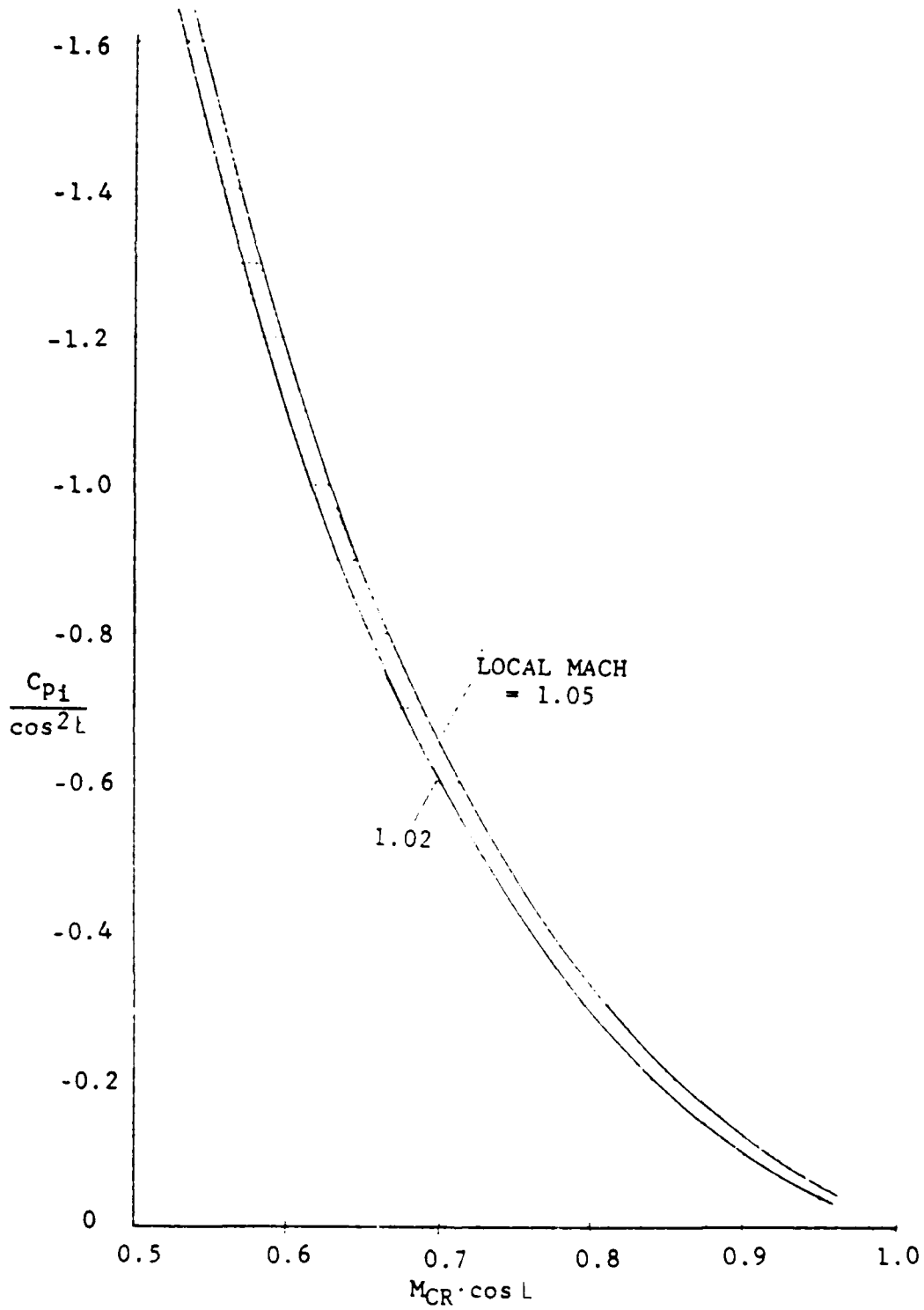


Figure 2.1.1 Mach Critical Prediction Chart

5. Use the Prandtl-Glauert compressibility factor (BMDD2) evaluated at critical Mach to obtain the lift coefficient CLMDD from

$$CLMDD = CLI/BMDD2$$

6. Repeat Steps 1 through 5 for a set of incidence in order to obtain a drag-rise boundary from the set of points (CLMDD, MCR).

The critical Mach number predicted by the above six steps is prevented from exceeding the critical Mach number of the fuselage alone (shown plotted in figure 2.1.2). For aircraft that are not area-ruled, where the isobars are allowed to upsweep at the wing-fuselage juncture, the method would tend to over predict MCR when the value approaches the fuselage MCR. The prediction - versus - test MCR correlation shown in figure 2.1.3 is thus applied for conventional-wing predictions.

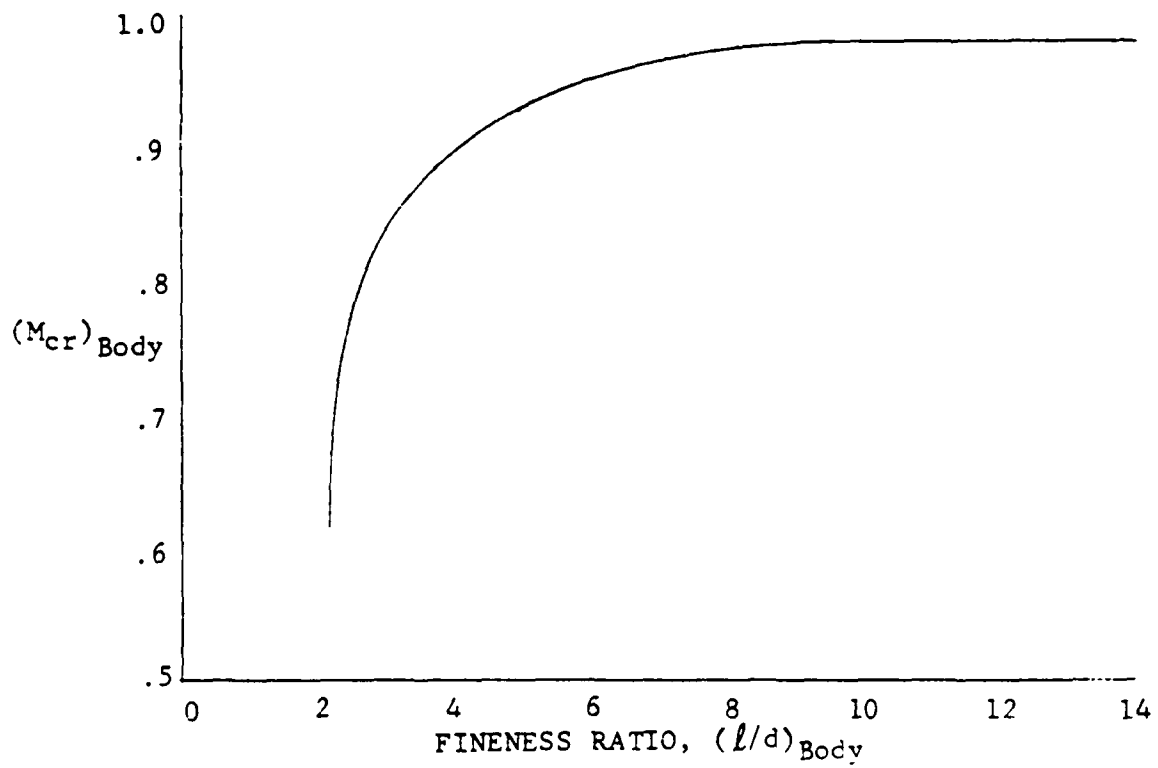


Figure 2.1.2 Prediction of Fuselage Critical Mach Number

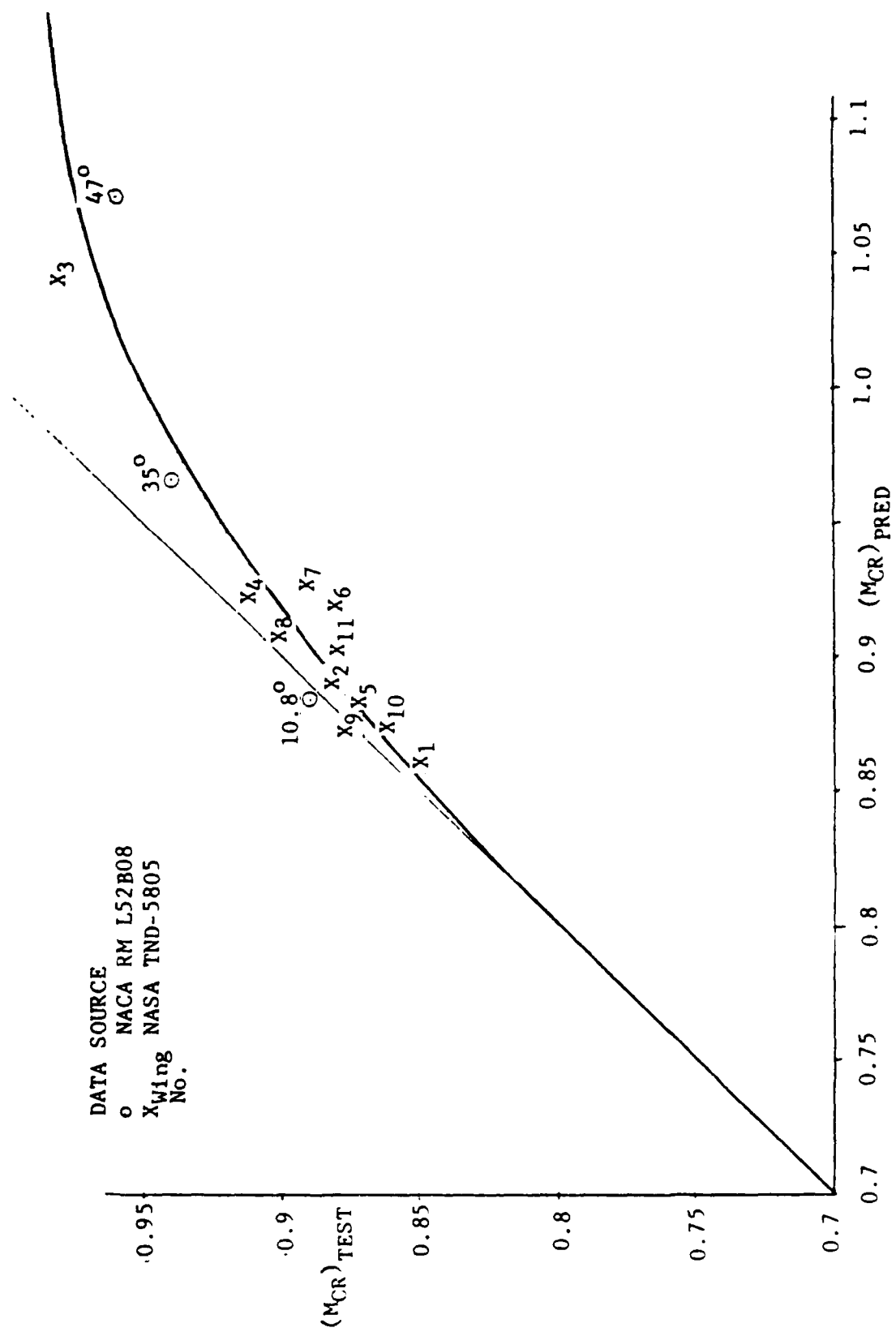


Figure 2.1.3 Correlation of Critical Mach Number for Conventional Wings

2.2 AERODYNAMIC CENTER

The methods for calculation of aerodynamic center locations are those of the DATCOM (8). They have largely been taken from the Large Aircraft Program (1) with modifications made to incorporate more complex airframes.

2.2.1 Aerodynamic Center of Forebody

The subsonic location of the aerodynamic center for forebodies with ogive nosecones is approximated in the DATCOM (8) as

$$XACNO = -0.54 * (BLN + 1.6 * (XCREW - BLN))/CREW \quad (2.2.1)$$

where

CREW is the wing exposed root chord length

BLN is the body nose length

XCREW is the x location of wing exposed root chord leading edge

Figure 2.2.1 defines the geometric parameters BLN, XCREW, and CREW. The supersonic forebody aerodynamic center is obtained from

$$XACNO = XCREW/CREW * (XCPOL - 1) \quad (2.2.2)$$

where the term XCPOL is obtained from figure 2.2.2

2.2.2 Aerodynamic Center of Surface (Single Panel).

The aerodynamic center of exposed surfaces is determined from the DATCOM charts presented in figures 2.2.3a through 2.2.3f. These charts are valid for subsonic Mach numbers less than Mach critical and supersonic Mach numbers greater than 1.2. For transonic conditions, the data presented in the DATCOM in terms of transonic similarity parameters (Figures 2.2.4a through 2.2.4d) are used to determine the aerodynamic center position.

The procedure for obtaining aerodynamic center can be summarized as:

For Mach \leq MCR or Mach \geq 1.2

$$XACR = XAC1$$

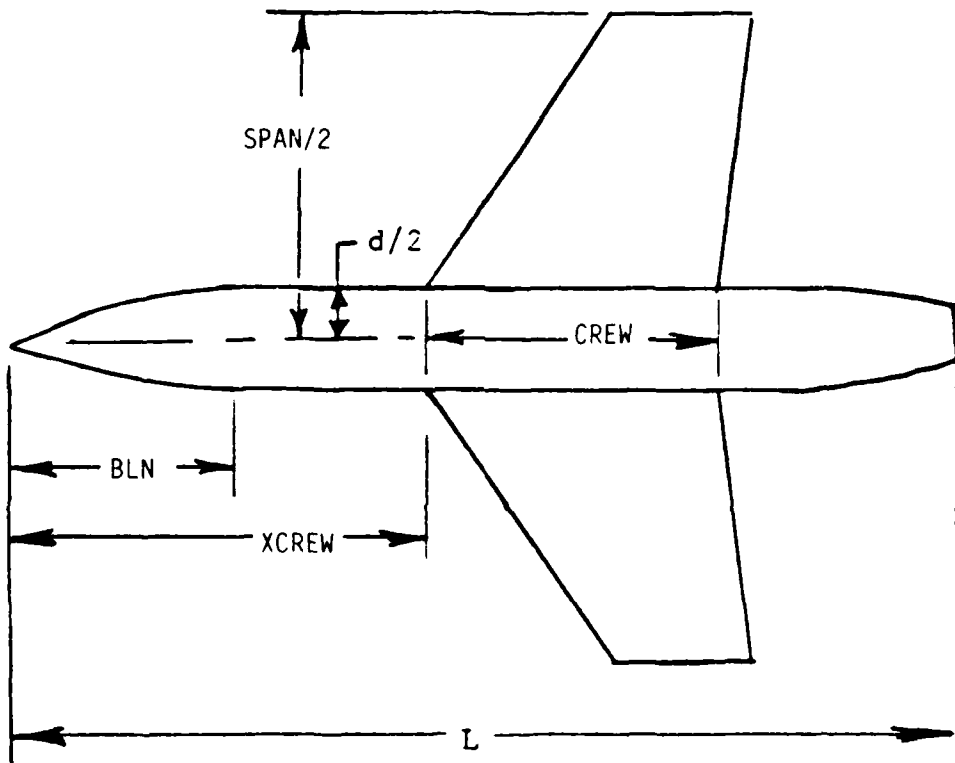


Figure 2.2.1 Wing-Body Geometry

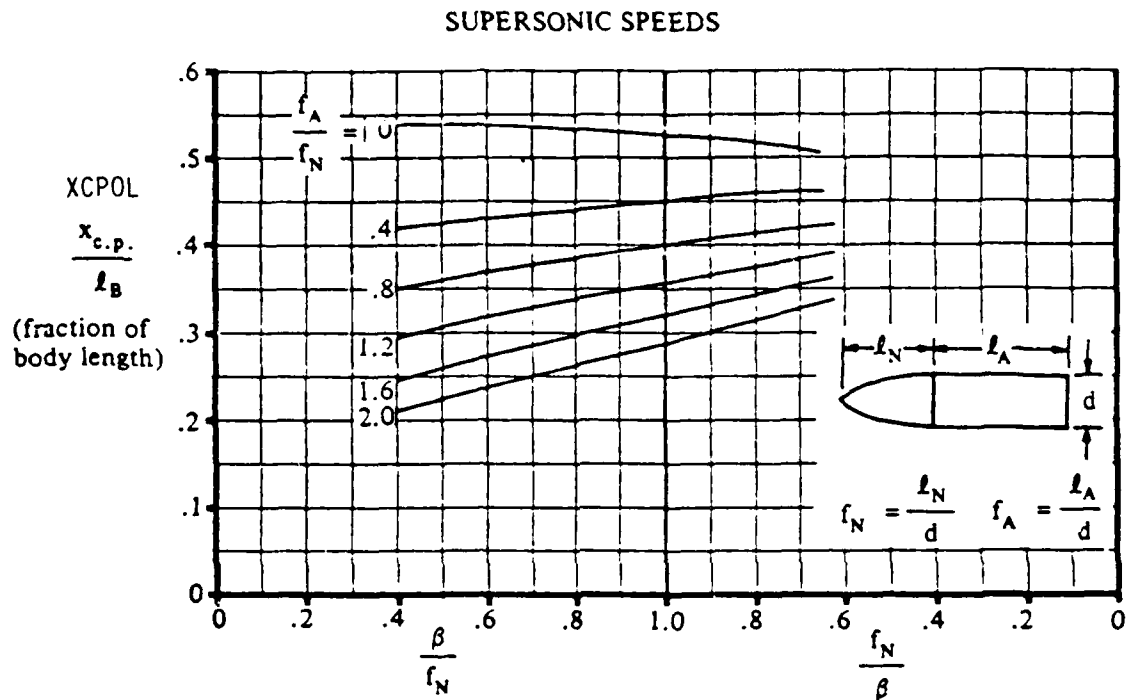


Figure 2.2.2 Supersonic Center of Pressure of Ogive with Cylindrical Afterbody

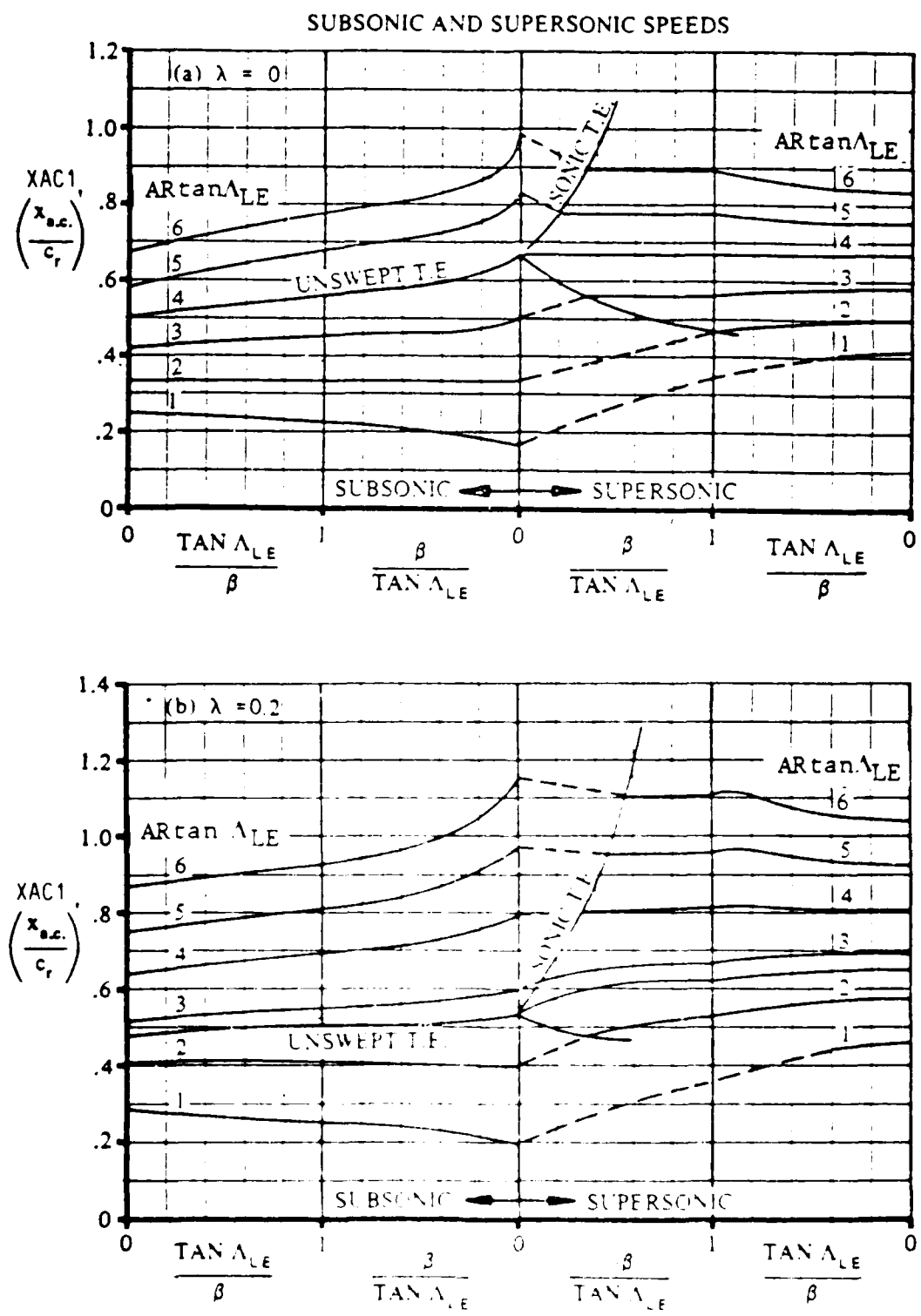


Figure 2.2.3 Wing Aerodynamic-Center Position

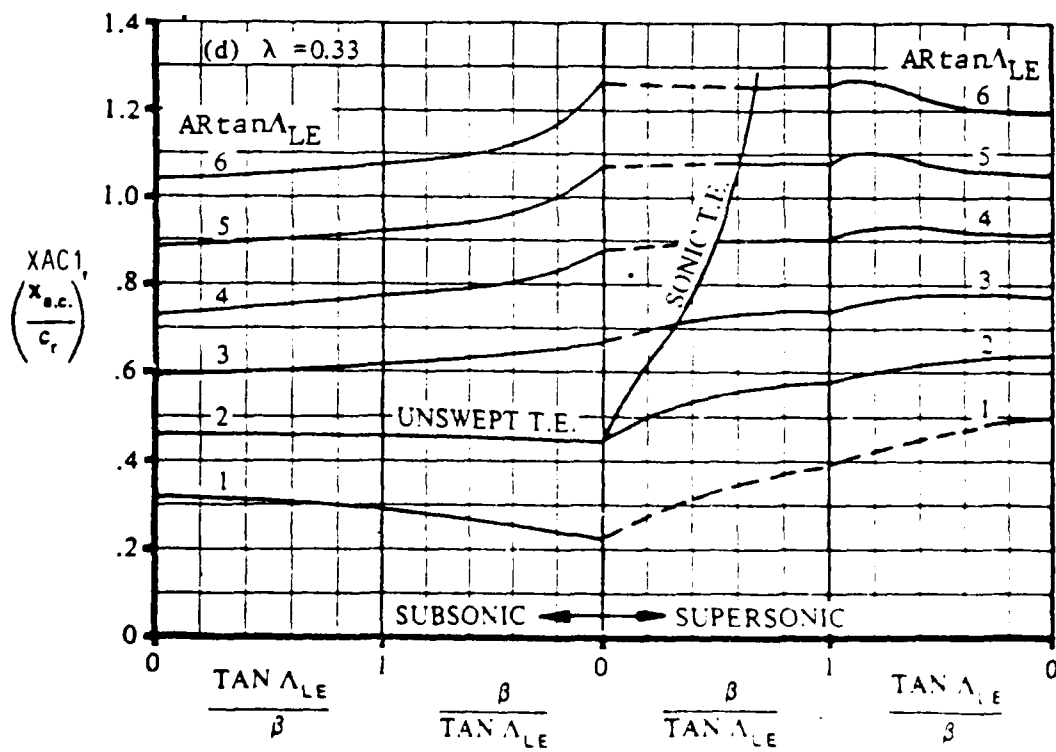
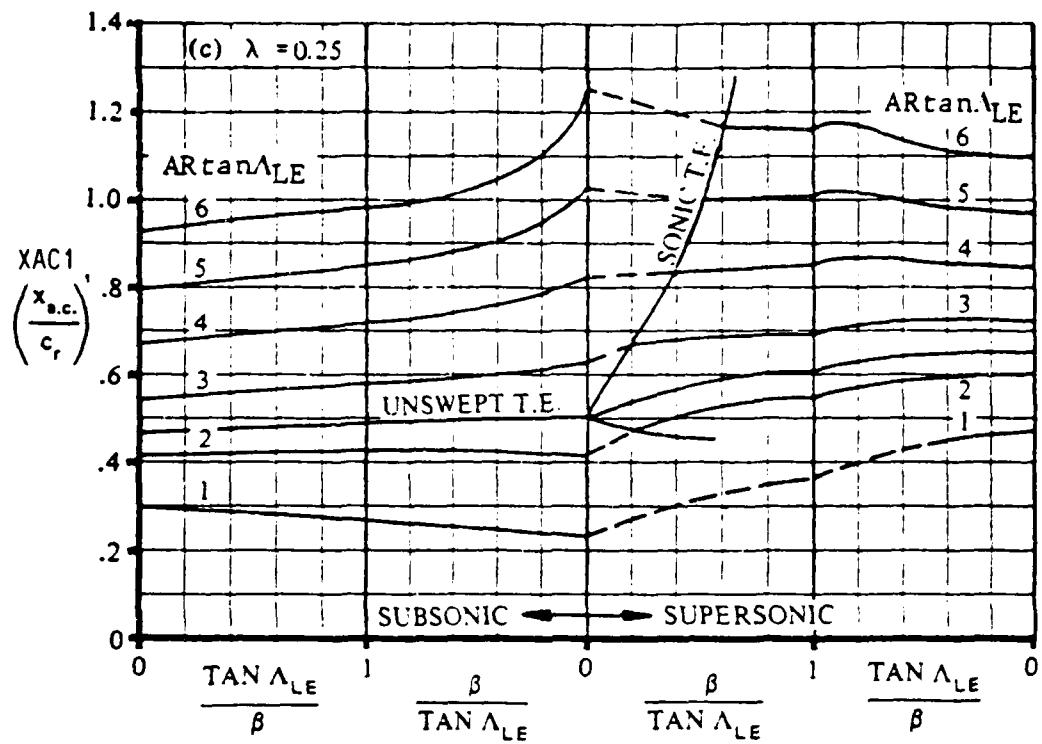


Figure 2.2.3 (Cont'd)

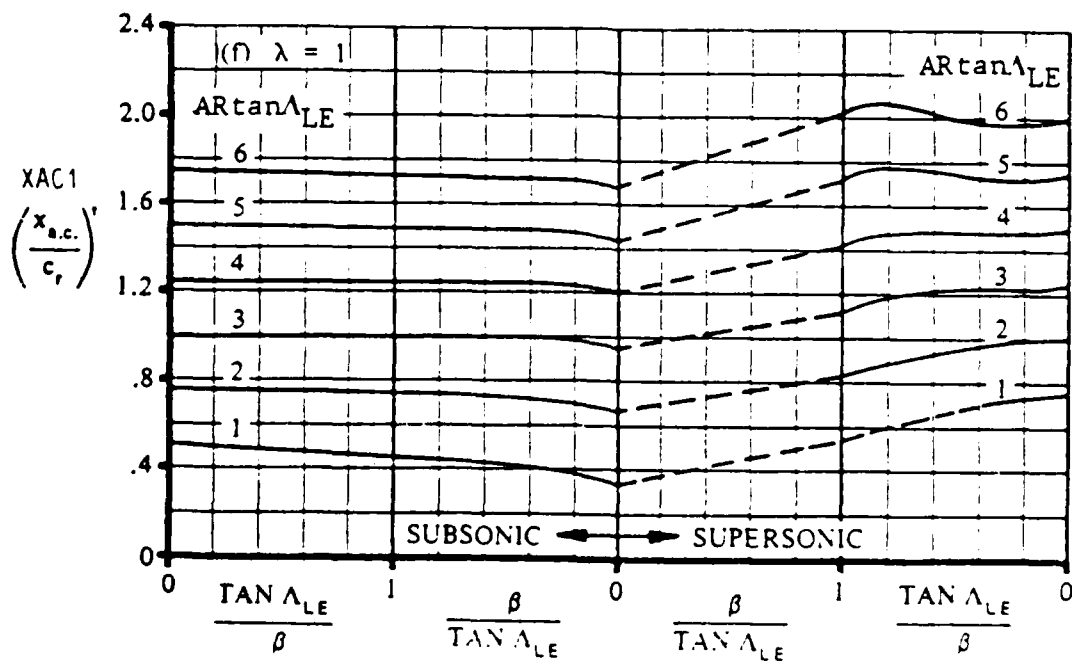
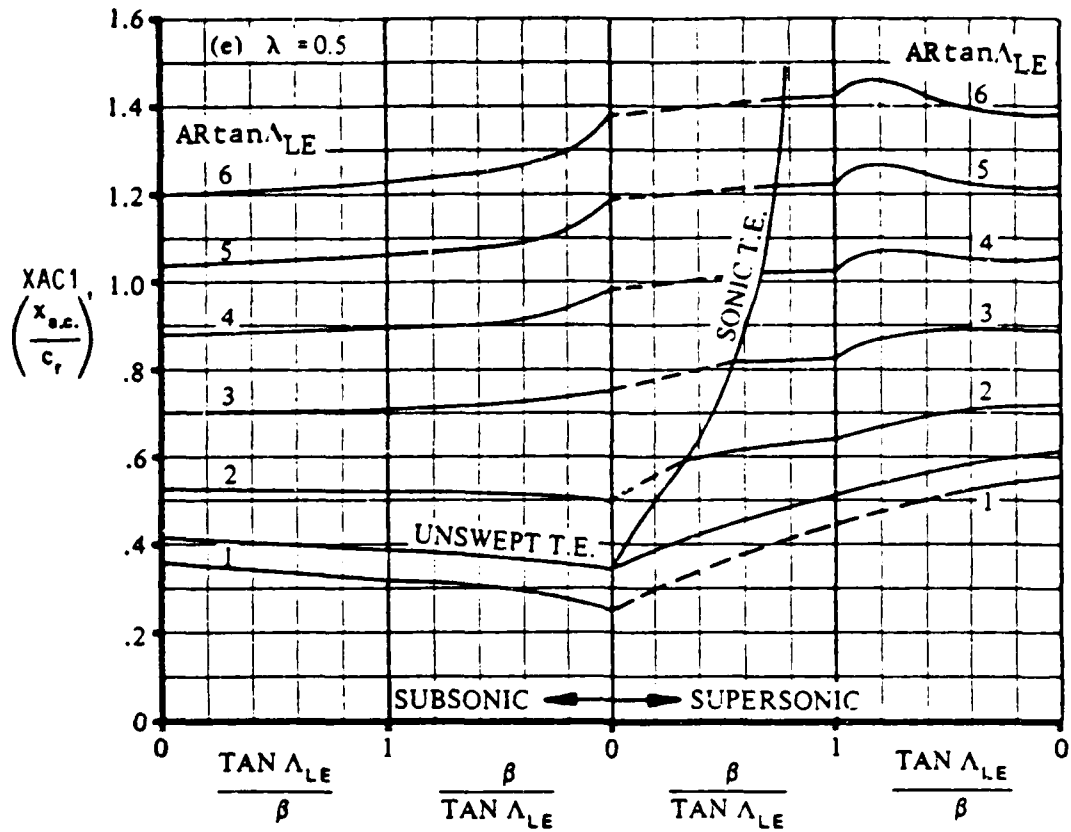


Figure 2.2.3 (Cont'd)

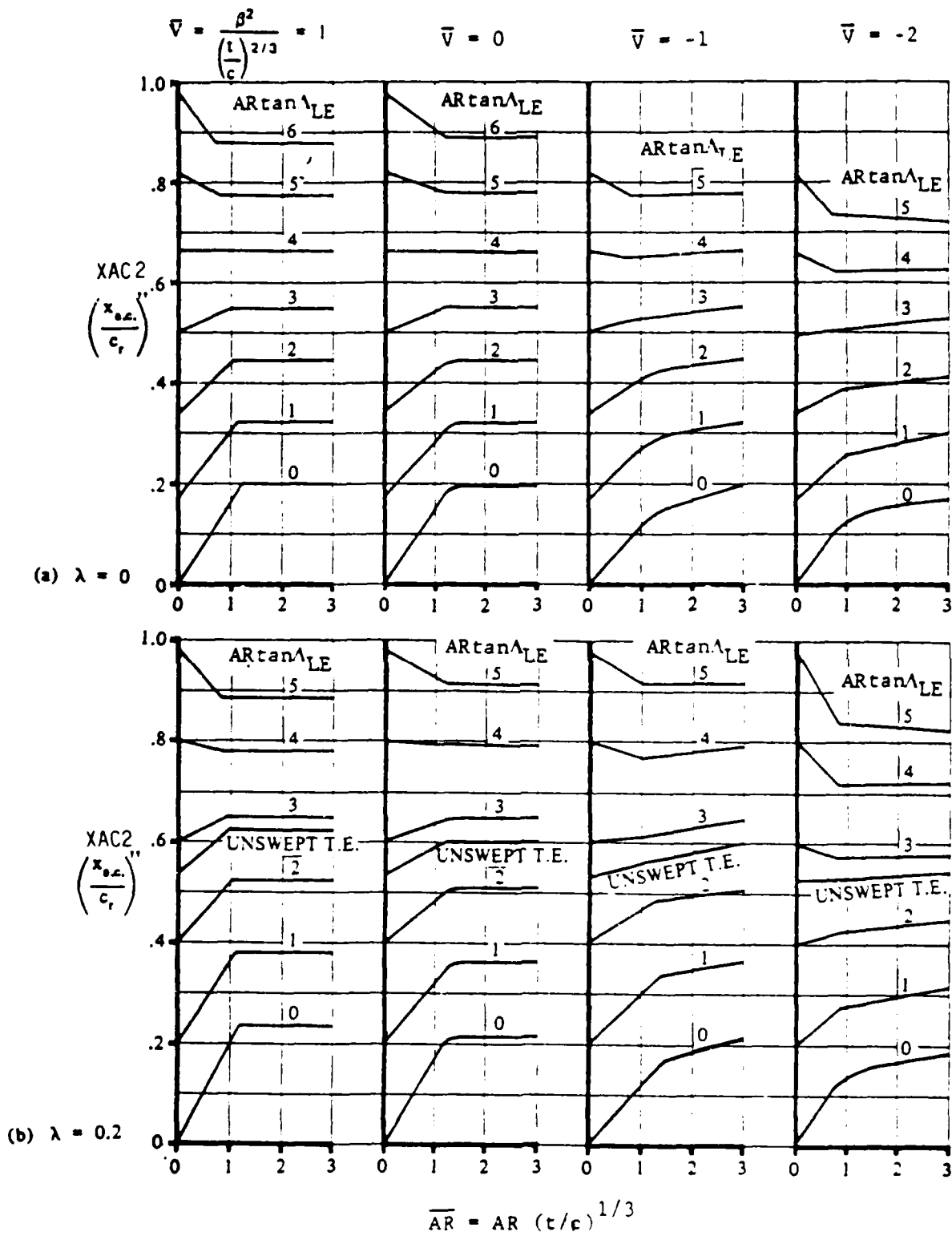


Figure 2.2.4 Transonic Wing Aerodynamic-Center Location

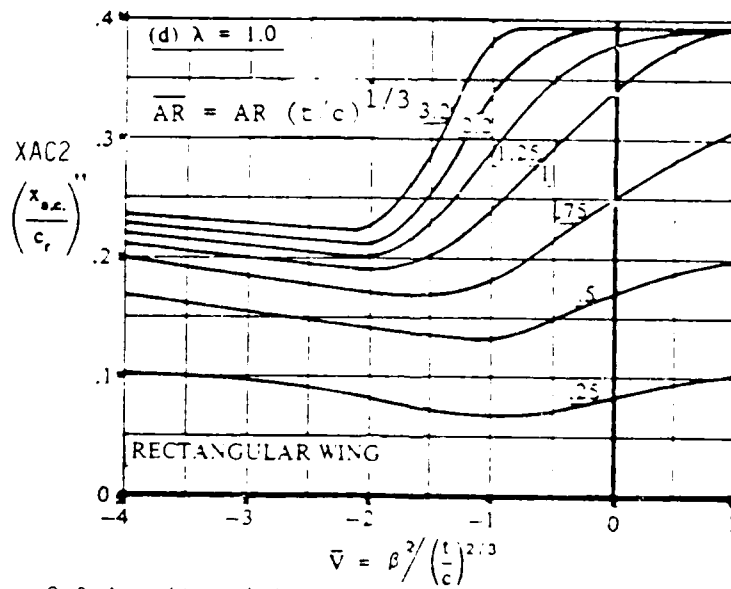
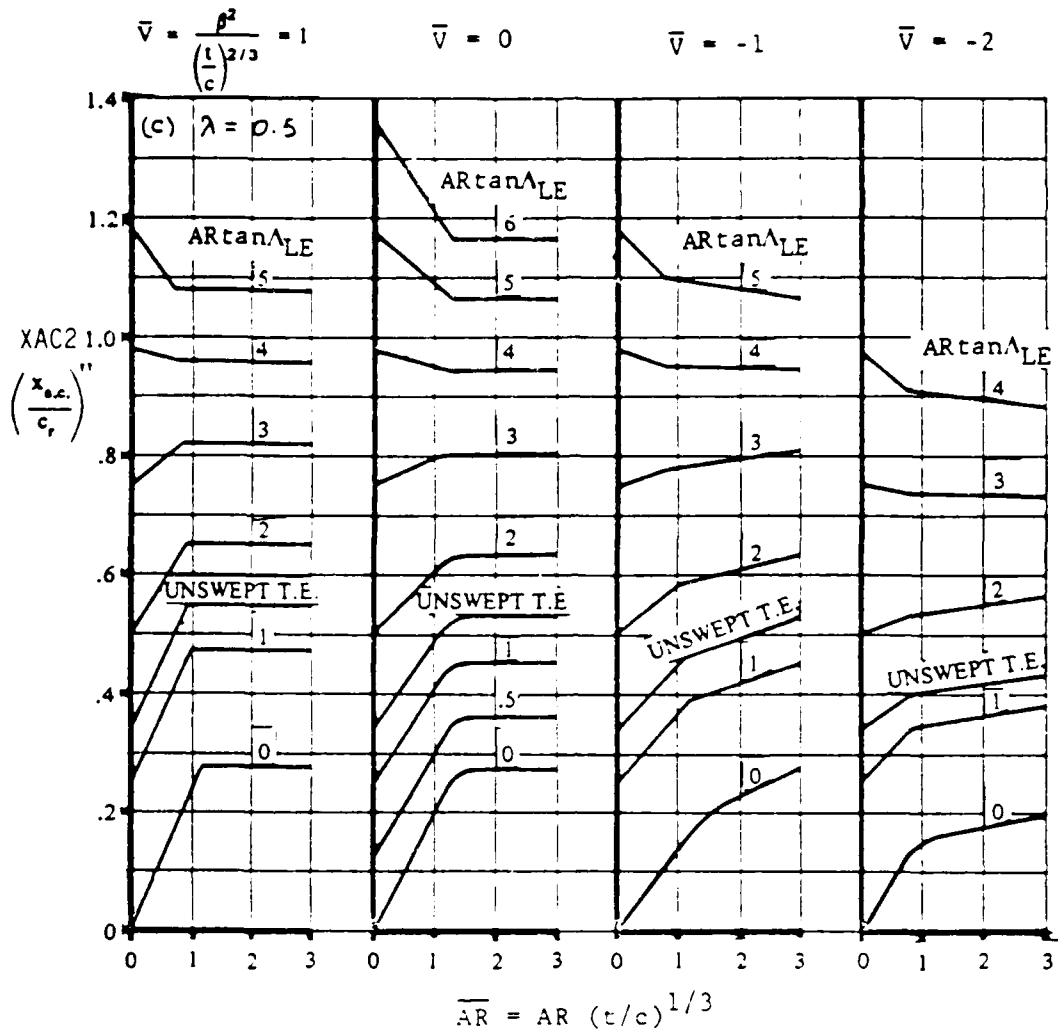


Figure 2.2.4 (Cont'd)

For $MCR + .05 \geq Mach > MCR$

$$XACR = XAC1 + (XAC2 - XAC1) * (Mach - MCR)/.05$$

For $FM2 > Mach > MCR + .05$

$$XACR = XAC2$$

For $1.2 > Mach \geq FM2$

$$XACR = XAC1 + (XAC2 - XAC1) * (Mach - FM2)/(1.2 - FM2) \quad (2.2.3)$$

where

FM2 $\text{SQRT}(1 + \text{TOCS} \cdot 6667)$
MCR is the critical Mach
TOCS is the thickness to chord ratio of the surface
XAC1 is given by figure 2.2.3
XAC2 is given by figure 2.2.4

2.2.3 Aerodynamic Center of Multi Panel Surfaces.

The prediction of the aerodynamic center location of multi panel surfaces is taken from the method developed at Convair Aerospace as reported by Henderson (9). The non-straight-tapered wing is divided into panels, with each panel having conventional, straight-tapered geometry. The individual lift-curve slope and aerodynamic center are estimated for each panel, using the technique described above for the single panel wing and treating each constructed panel as an isolated wing. The individual lift and aerodynamic center locations for each constructed panel are then combined, using an inboard-outboard weighted-area relationship

XASCR =

$$\frac{XACR(1) * CLALPSO(1) * SXXO(1) + XACR(2) * CLALPSO(2) * SXXO(2) + \dots}{CLALPSO(1) * SXXO(1) + CLALPSO(2) * SXXO(2) + \dots} \quad (2.2.4)$$

where the outboard wing aerodynamic center is referenced to the total surface root chord length given by

$$XACR = ((XACR * CRO) + (XCRO - XCRES))/CRES$$

and

CLALPSO(i) is the zero AoA lift curve slope of the panel
SXXO(i) is the area of the panel
CRO is the panel exposed root chord
XCRO is the X location of the panel root chord leading edge

XGRES is the X location of the surface root chord leading edge
GRES is the surface exposed root chord

The geometry for the multi panel arrangement is illustrated in figure 2.2.5.

2.2.4 Aerodynamic Center of Wing-Lift Carryover on the Body.

The location of the aerodynamic center due to the wing-lift carryover on the body is determined by use of the DATCOM method. For $BARE \geq 4$ the subsonic aerodynamic center location is obtained from

$$XACBW = .25 + DXQC * FDOB * TAN(C4SWEEP)$$

$$DXQC = (SPANW - BDW)/(2 * CREW) \quad (2.2.5)$$

where

SPANW is the span of the wing
BDW is the body diameter along the wing root chord
CREW is the wing exposed root chord length
C4SWEEP is the wing quarter chord sweep
BARE is the Prandtl-Glauert compressibility factor times the effective aspect ratio

and FDOB is determined from the plot in figure 2.2.6. For $BARE < 4$ the aerodynamic center location is determined from

$$XACBW = (XACBWO - XACBW) * (BARE - 4)^2/16 + XACBW \quad (2.2.6)$$

where XACBW is from the equation (2.2.5) and XACBWO is determined by

$$XACBWO = .5 * .25 * ARWE * TAN(LESWEEP) * (1 + TRWE) \quad (2.2.7)$$

and

ARWE is the exposed aspect ratio of the wing
TRWE is the exposed taper ratio of the wing
LESWEEP is the leading edge sweep of the wing

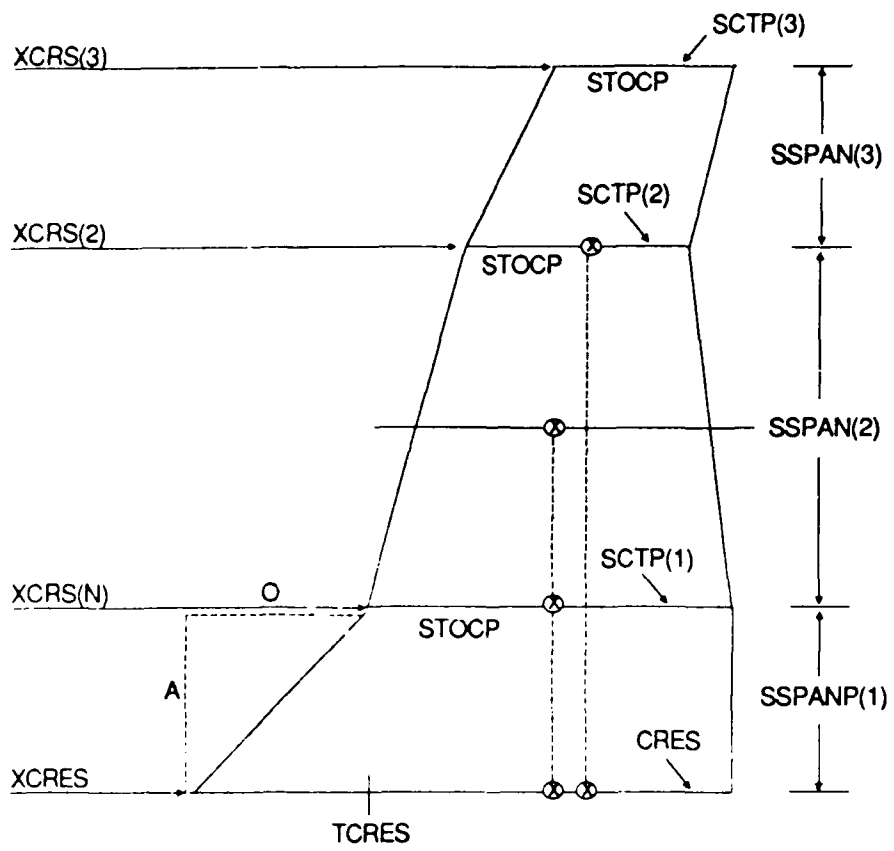


Figure 2.2.5 Geometry for the Multi-Panel Surfaces

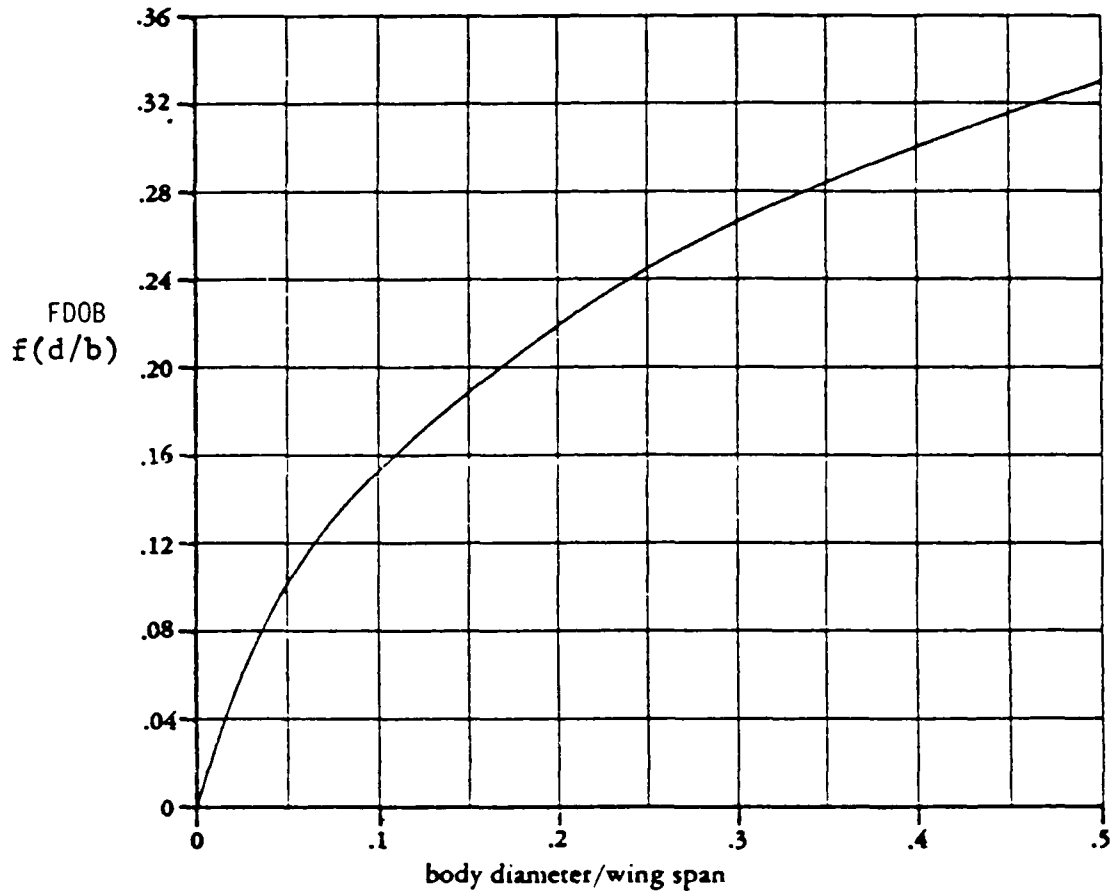


Figure 2.2.6 Parameter Used in Accounting for Wing-Lift Carryover on the Body

Equation 2.2.7 is limited to values less than or equal to 0.5. For supersonic conditions, the aerodynamic center location is estimated from figure 2.2.7. For transonic conditions, the aerodynamic center location is determined by linear interpolation of the aerodynamic center values determined at the critical Mach number and Mach 1.1.

2.2.5 Total Aerodynamic Center.

With the above computed values, the location of aerodynamic center for a wing body configuration is given by the DATCOM as

$$XAC = \frac{XACWB + KS * XACS(i)}{1 + KS} \quad (2.2.8)$$

where the XACS(i) are the aerodynamic centers of the aircraft components

$$KS = \frac{CLAS}{CLAWB} * \frac{NS}{NW} * \frac{AS}{AW} * \cos(DIHS) * (1 - DEWS) \quad (2.2.9)$$

and

CLAS	is the zero alpha lift curve slope for the surface
CLAWB	is the zero alpha lift curve slope for the wing-body
NS	is the dynamic pressure ratio at the surface (from section 2.8)
NW	is the dynamic pressure ratio at the wing (from section 2.8)
AS	is the exposed area of the surface
AW	is the exposed area of the wing
DIHS	is the dihedral angle of the surface
DEWS	is the downwash factor for the surface from the wing (from section 2.6)

Equation 2.2.9 is summed over all of the surfaces on the airframe.

Ref. 8, FIGURE 4.3.2.1-37

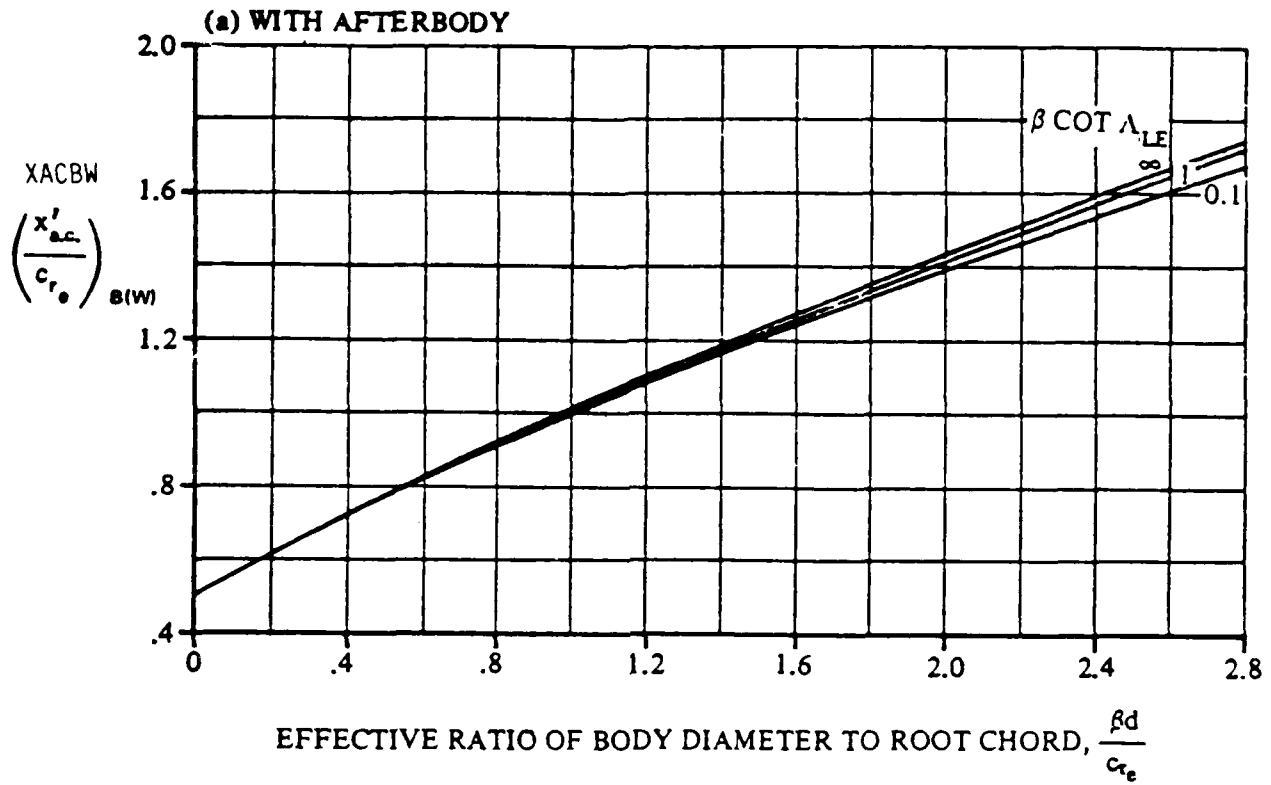


Figure 2.2.7 Aerodynamic-Center Locations for Lift Carry-over onto Body at Supersonic Speeds

2.3 ZERO-LIFT PITCHING MOMENT (CMO)

The method for predicting the zero-lift pitching moment for an aircraft configuration considers only the effects of surface components on CMO. It does not include the effect of an asymmetrical fuselage or the effect of stores and nacelles located near the surfaces.

The subsonic zero-lift pitching moment for lifting surfaces with linear twist, up to the critical Mach number, is given in the DATCOM as

$$CMOS = (CMON + CMOOT * TWIST) * CMACH \quad (2.3.1)$$

where CMON is the CMO of an untwisted surface given by

$$CMON = (ARS * \cos^2(C4SWEEP)) / (ARS + 2 * \cos(C4SWEEP)) * CMOSECT \quad (2.3.2)$$

CMOSECT is the average section pitching moment coefficient determined by averaging the section CMO for each surface panel using

$$CMOSECT = (\text{SCAMP}(i) * \text{SXXS}(i) * \text{CMC4}(i)) / \text{ASEXS} \quad (2.3.3)$$

CMOOT is determined by a table lookup from lifting line theory graphs as shown in figure 2.3.1

$$CMACH = (1 + 5.9 * \text{TOCS} * \text{MACH}^5) / (\text{SQRT}(1 - \text{MACH}^2 * \cos^2(C4SWEEP))) \quad (2.3.4)$$

and

TWIST is the twist on the surface
ARS is the aspect ratio of the surface
C4SWEEP is the quarter chord sweep of the surface
SCAMP is the camber on the panel
SXXS is the exposed area of the panel
CMC4 is a constant based on the airfoil type
ASEXS is the exposed area of the surface
TOCS is the thickness to chord ratio
MACH is the current Mach number (not greater than Mach critical)

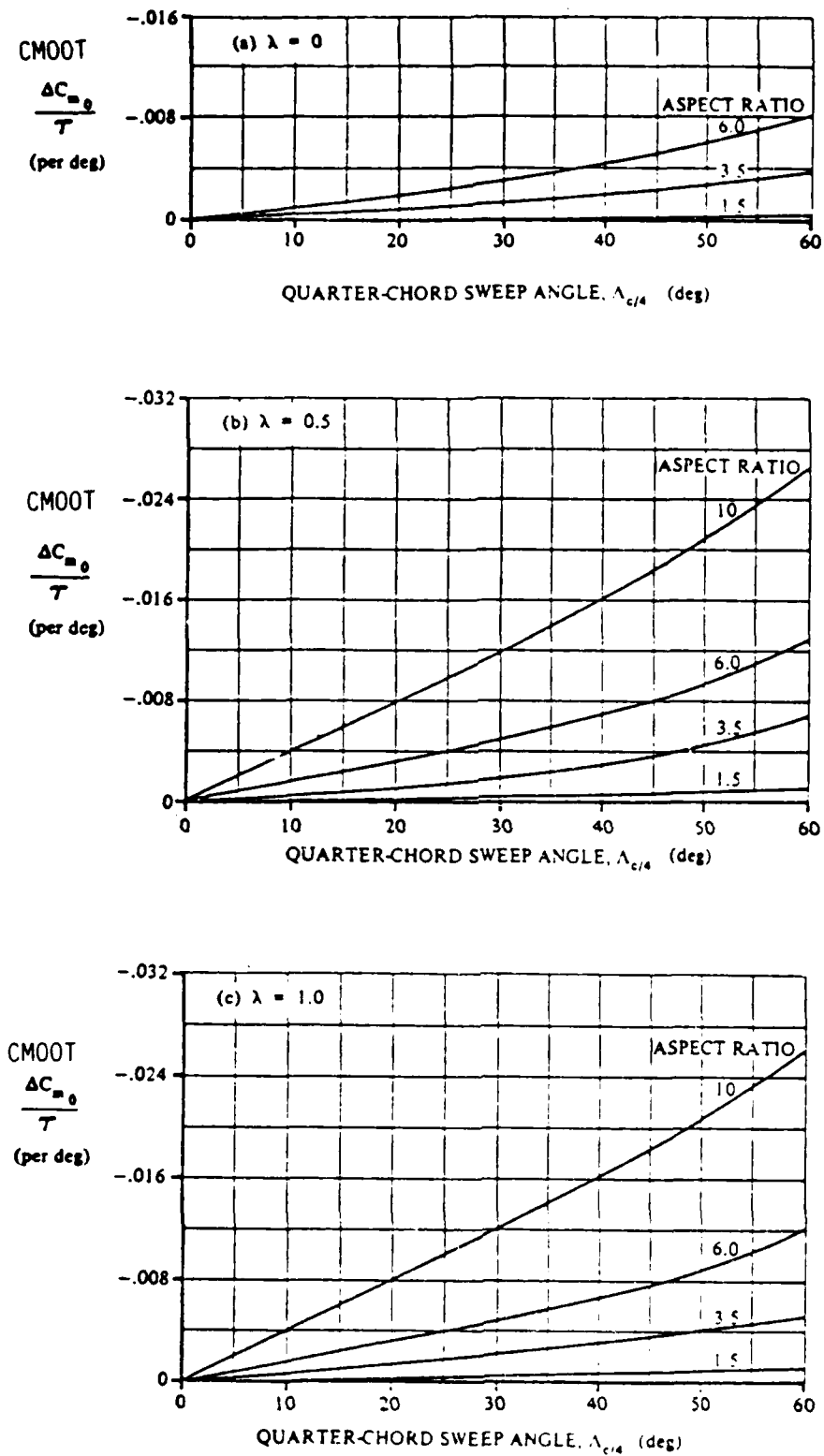


Figure 2.3.1 Effect of Linear Twist on the Wing Zero-Lift Pitching Moment

The CMO for the total configuration can then be computed by summing the individual CMOs for surfaces after they have been converted to the reference area. The equation is

$$\text{CMO} = \sum \text{CMOS}(i) * S(i) / \text{SREF} \quad (2.3.5)$$

where

$S(i)$ is the area of the surface

SREF is the reference area

2.4 ZERO ALPHA LIFT COEFFICIENT (CLO)

The method for predicting the zero alpha lift coefficient has been taken from the Large Aircraft Program (LACP) (1). The method first computes the lift curve slope and the ALPHA where zero lift occurs. CLO is then computed as the product of these two values;

$$CLO = CLA * -ALO$$

This equation holds for all surfaces, bodies, and nacelles.

2.4.1 Lifting Surface CLO

For each surface of interest the lift curve slope, CLA, is defined by

$$CLA = CLAB * KT \quad (2.4.1)$$

where

CLAB is the surface alone CLA with no thickness effects. The factor KT accounts for the effect of airfoil thickness plus camber. The equation for CLAB was originally taken from Polhamus (10) and adopted for the LACP. The final form is;

$$CLAB = 1.0 / (57.3 * ((M^*/MACH)^Z / CLAO + BETAP / 4.0)); \text{ WHEN } MACH > M^* \quad (2.4.2)$$

and

$$CLAB = (.0548311 * ARS) / [1.0 + \text{SQRT}(1.0 + (1.0 - \text{COS}(C2\text{SWEEP}))^{1.334} * (MACH/M^*)^{2.667}) * (ARS / (2.0 * \text{COS}(C2\text{SWEEP})))^2]; \\ \text{ WHEN } MACH \leq M^* \quad (2.4.3)$$

Where M^* , a function of ARS and C2SWEEP, is the limiting Mach, and is defined by;

$$M^* = \text{CSUBO} + (1.0 - \text{CSUBO}) * (1.0 - \text{COS}(C2\text{SWEEP}))^2$$

and

$$\text{CSUBO} = (10.0 + 0.91 * ARS^3) / (10.0 + ARS^3)$$

$$\text{BETAP} = (MACH - M^*) * (1.0 + (M^*/MACH)^Y)^2$$

$$Y = (1 + \text{PI} * ARS) / (3 + \text{PI} * ARS) * (2 + .667 * \text{SQRT}(\text{TRS}) - \text{TRS}^2)$$

$$Z = M^* * CLAO + ARS^2 / (3 * \text{PI} * ARS / CLAO * (\text{PI} * ARS / CLAO - 1.0) * \text{COS}(C2\text{SWEEP})^{.667})$$

where

CLAO is defined as CLAB at MACH = M*
C2SWEEP is the half chord sweep of the theoretical surface
ARS is the aspect ratio of the theoretical surface
TRS is the taper ratio of the theoretical surface

Wings having thick airfoils undergo a degradation in CLA beginning at MACH > M*. The level of CLA versus Mach dips, usually reaching a minimum at MACH < 1.0, and then recovers to a second peak at M > 1.0. To account for this phenomenon, the basic CLA equations have been modified by a factor KT, as defined by;

$$KT = 1.0 - (4.0 * SIG1 * (1.0 - SIG1))^3 * GAMMA; M1 < MACH < M2$$

$$KT = 1.0 - (4.0 * SIG2 * (1.0 - SIG2))^3 * GAMMA; M2 < MACH < M3$$

$$KT = 1.0; M1 \geq MACH \geq M3$$

(2.4.4)

where the factors GAMMA, SIG1, SIG2, M1, M2 and M3 are defined by the equations that follow:

$$GAMMA = 9.0 * DTOCL / (1.0 + .5 * ARDT)$$

$$DTOCL = (TOCS - TOCL) / \cos(C2SWEEP)$$

$$TOCL = 1.0 / (4.4 * ARS * \cos(C2SWEEP)^{1.5})$$

$$ARDT = ARS * DTOCL \quad (2.4.5)$$

$$SIG1 = .5 * (MACH - M1) / (M2 - M1)$$

$$SIG2 = .5 * (1.0 + (MACH - M2)) / (M3 - M2)$$

$$M1 = 1.0 - 2.0 * TOCS * (ARS^3 / (4.0 + ARS^3)) * \cos(C2SWEEP)^{1.5} * (1.0 + 1.5 * CLD^{1.5})$$

$$M2 = M1 + TOCS$$

$$M3 = 1.0 + TOCS \quad (2.4.6)$$

and

TOCS is the thickness to chord ratio of the surface
CLD is the camber of the surface

NOTE:

If DTOCL > .07 then DTOCL = .07
If ARDT > .1 then ARDT = .1

$0 \leq M1 \leq M^*$
If $M1 > M^*$ then $M1 = M^*$

The derivation of equation 2.4.4 is based on the data trends and analysis of Polhumas (11) and on other limited data (e.g., Nelson and McDevitt (12), and Tinling and Kolk (13)). It should be noted that a CLA "bucket" is predicted only if the wing streamwise airfoil TOCS exceeds the limit thickness defined by equation 2.4.5. The limit thickness boundary was established from the statistical boundaries presented by Donlan and Weil (14).

The angle of attack at zero lift, ALO is determined by

$$ALO = AALOT * TWIST \quad (2.4.7)$$

where

TWIST is the twist on the surface (- for washout)
AALOT is obtained from a curve fit of parametric data reported by Gilman and Burdges (15) for wings with linear element twist. The derived equation for AALOT is;

$$AALOT = .093 - (.000571 * SPBETA) + (.5761 * TRW) - (.2645 * TRS^2) \quad (2.4.8)$$

where

SPBETA = ATAN(TAN(ABS(C4SWEEP/BETA)))
BETA = SQRT(ABS(1 - MACH²))

and

C4SWEEP is the quarter chord sweep of the surface

2.4.2 Body and Nacelle CLO

The equations for calculation of CLA for aircraft bodies and nacelles in LACP have been simplified for SACP. CLA is now defined as;

$$CLA = 2.0 * CSA/SREF \quad (2.4.9)$$

where

CSA is the maximum cross sectional area of the component
SREF is the aircraft reference area.

ALO in this case is also simplified. For nacelle components ALO is just the incidence of the nacelle. For bodies ALO is defined as

$$ALO = ATAN((BTL * TAN(BTUSA))/(BL/2.0)) \quad (2.4.10)$$

where

BTL is the boattail length
BTUSA is the boattail upsweep angle
BL is the length of the body

2.4.3 Total Aircraft CLO

Once all of the component CLO terms have been computed and referenced to the aircraft reference area, then the total CLO is expressed as the sum of all of the components as;

$$CLOT = CLOB + CLON + CLOW * (SW/SREF) + CLOC * (SC/SREF) \\ + CLOH * (SH/SREF) + CLOV * (SV/SREF) + CLOF * (SF/SREF) \quad (2.4.11)$$

CLOB is the CLO for the body
CLON is the CLO for the nacelles
CLOW is the CLO for the wing
CLOC is the CLO for the canard
CLOH is the CLO for the horizontal tail
CLOV is the CLO for the vertical tail
CLOF is the CLO for the fins

The effect of wing incidence is not included in the CLO calculation. The wing incidence is added into the total effective angle of attack (See section 2.6.1)

2.5 ZERO LIFT DRAG (CDO)

The drag of an aircraft can be represented as the sum of minimum drag, plus drag due to lift, plus drag due to trim. The SACP program maintains separately, the minimum drag (or zero lift drag) and the trim drag. CDO is comprised of the drag items that are assumed to be independent of lift, such as friction, form, interference, wave, base, and camber. These components and drag rise are discussed below.

A large part of the subsonic CDO is comprised of the sum of the above mentioned items. The drag of each component, then, is computed as

$$CD = CF * (AWET/SREF) * FF * IF * CDW * CDC$$

for surfaces and

$$CD = CF * (AWET/SREF) * FF * IF * CDW * CDB \quad (2.5.1)$$

for bodies and nacelles, where

CF	is the compressible flat plate skin-friction coefficient
AWET	is the component wetted area
SREF	is the reference area
FF	is the form factor
IF	is the interference factor
CDW	is the wave drag
CDC	is the drag due to camber and twist of surfaces
CDB	is the base drag for bodies and nacelles

2.5.1 Friction Drag (CF)

The flat-plate, compressible, turbulent, skin-friction coefficient is determined from methods given in the Large Aircraft Program (1). These methods are based on work by White and Christoph (16) and give the following expression for CF:

$$CF = T * F^2 * .430 / (\text{LOG}_{10}(\text{RNL} * L * T^{1.67} * F))^{2.56} \quad (2.5.2)$$

where

$$T = 1.0 / (1.0 + 0.178 * \text{MACH}^2)$$

$$F = 1.0 + 0.03916 * \text{MACH}^2 * T$$

L is the characteristic length of the component (mean aerodynamic chord for surfaces or length for bodies and nacelles).

RNL is based on either component length or an admissible surface roughness, whichever produces a smaller value of Reynolds number, as follows:

$$RNL = \text{MIN}((RNF * L), (K1 * (L/K)^{1.0489})) \quad (2.5.3)$$

where

RNF is the Reynolds number per foot determined from standard atmospheric tables
K is admissible surface roughness and is an input quantity

and

$$K1 = 37.587 + 4.617 * \text{MACH} + 2.949 * \text{MACH}^2 + 4.132 * \text{MACH}^3$$

For mixed laminar-turbulent flow, transition location is specified for the upper and lower surfaces of the wing. For the laminar portion of the flow, the Blasius skin-friction relation is

$$CF(XR) = CFCFIL * 1.328/\text{SQRT}(RNL * XR) \quad (2.5.4)$$

where

CFCFIL = $(1.0 + 0.1256 * \text{MACH}^2)^{-.12}$, is used up to the transition point, XR, the laminar momentum thickness, which begins some fictitious distance, DX, ahead of transition. The skin-friction coefficient for the turbulent part of the flow is calculated from equation (2.5.2), where the Reynolds number is calculated from

$$RNL = (DX + L - XR) * RNF \quad (2.5.5)$$

The value of CF with transition is finally given by

$$CF = (DX + L - XR)/L * CFTURB \quad (2.5.6)$$

Calculated values of CF versus RNL are presented in figures 2.5.1 through 2.5.6 for mixed laminar-turbulent flow.

2.5.2 Form Factors

The component form factors, FF, account for the increased skin-friction caused by the super velocities of the flow over the body or surface and the boundary-layer separation at the trailing edge. The form factor for the "body" component is computed as

$$FF = 1.0 + 60.0/FR^3 + 0.0025 * FR \quad (2.5.7)$$

where

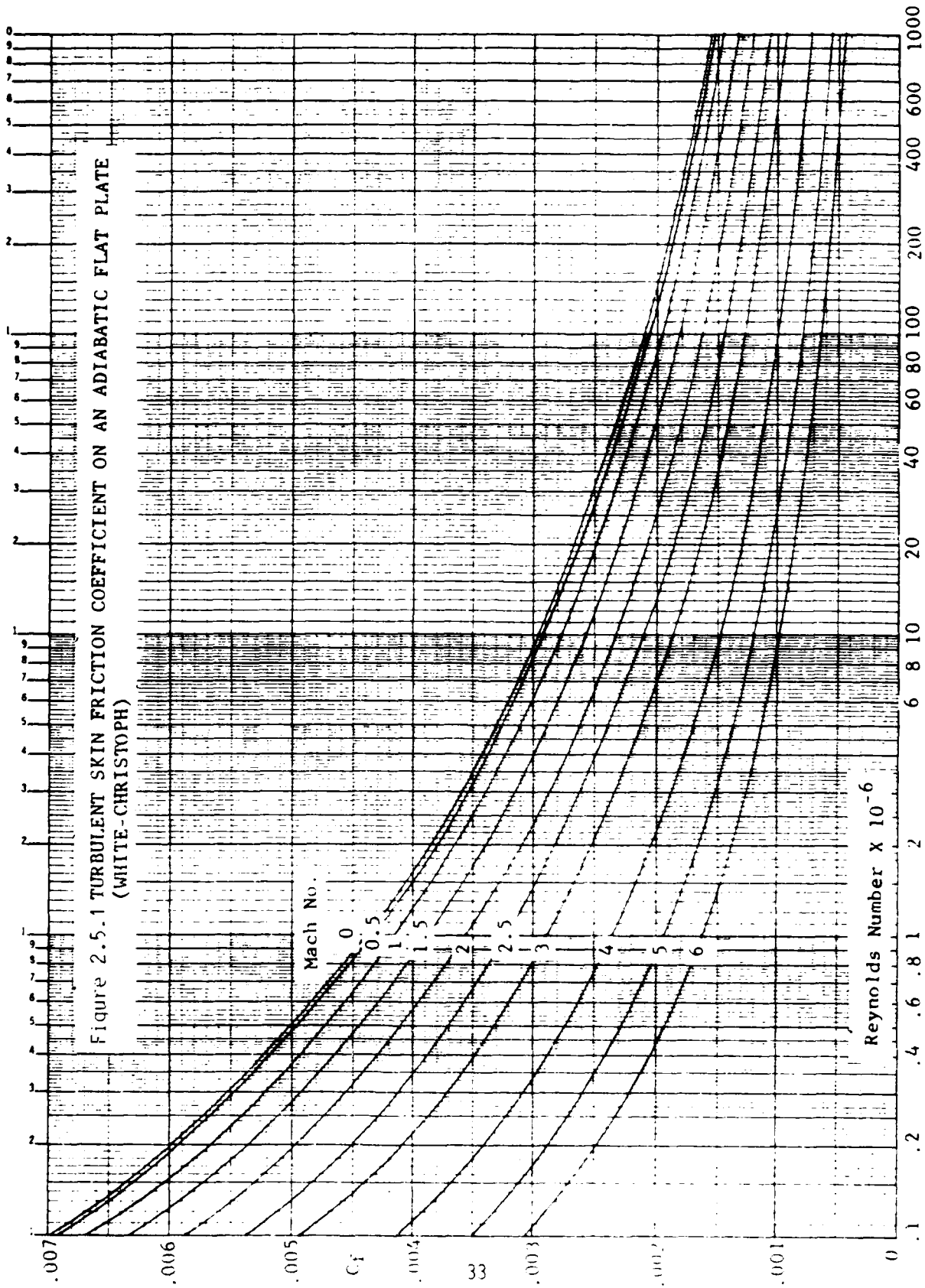


Figure 2.5.1 TURBULENT SKIN FRICTION COEFFICIENT ON AN ADIABATIC FLAT PLATE (WHITE-CHRISTOPH)

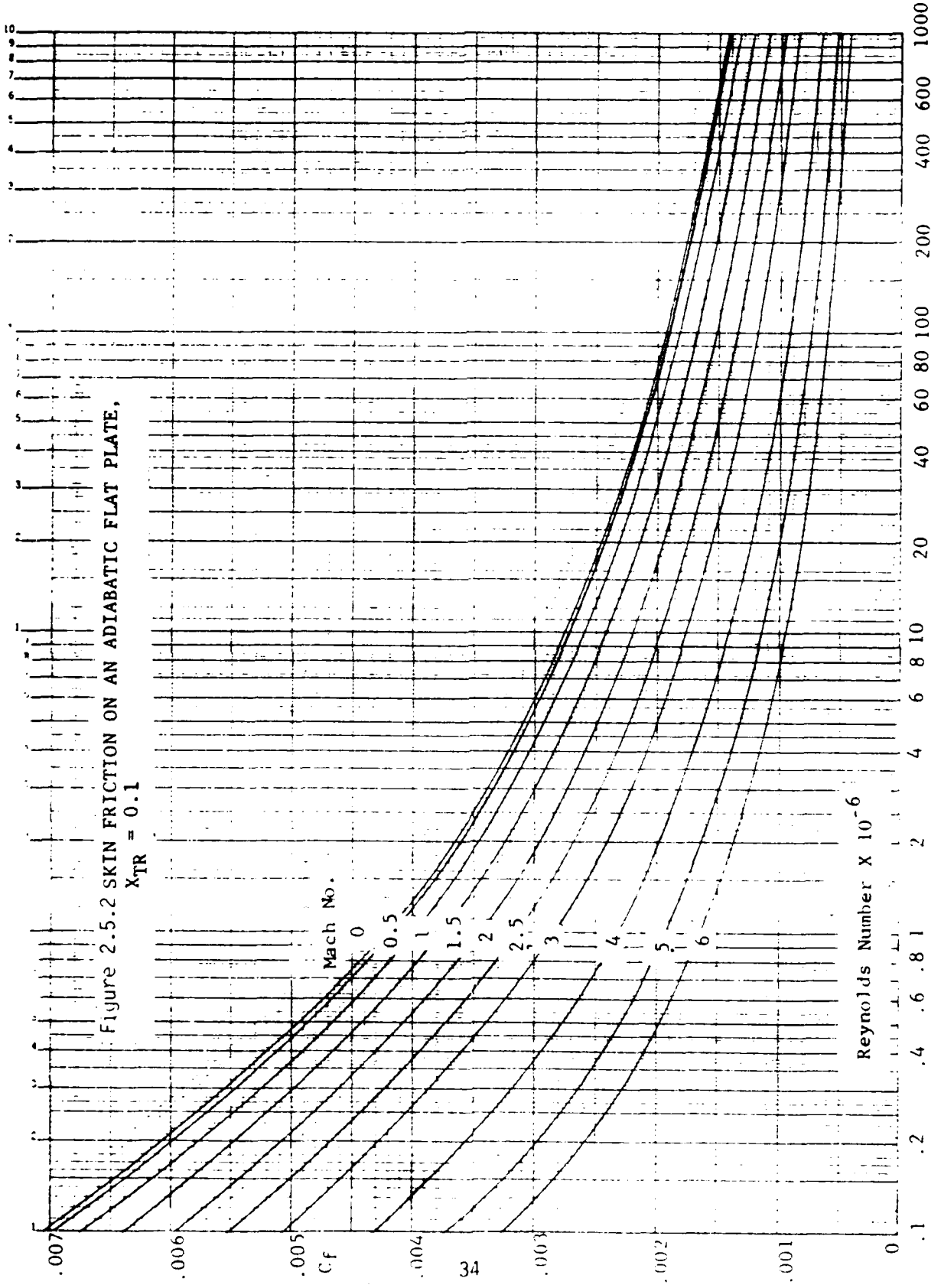
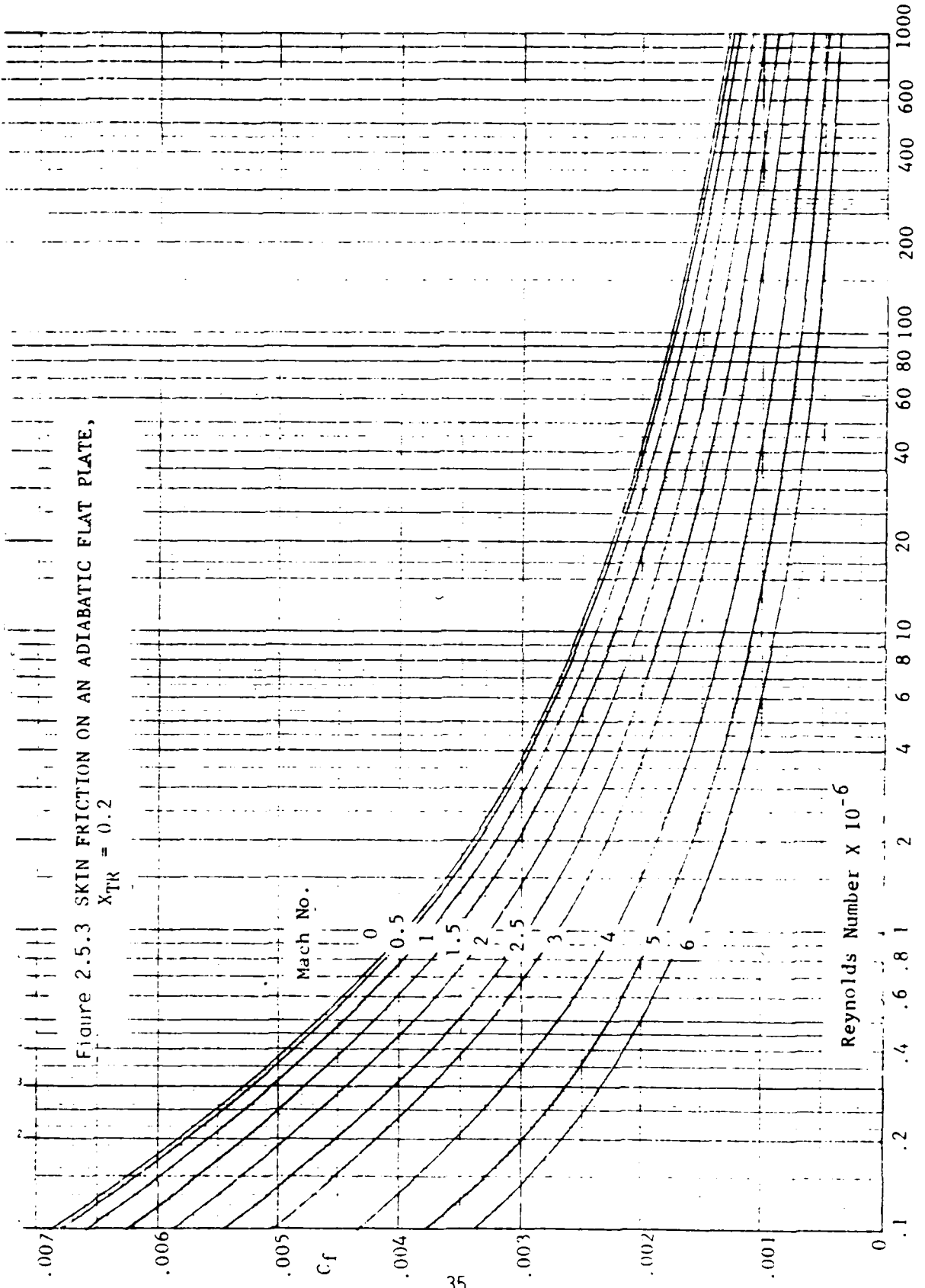


Figure 2.5.2 SKIN FRICTION ON AN ADIABATIC FLAT PLATE,
 $X_{TR} = 0.1$



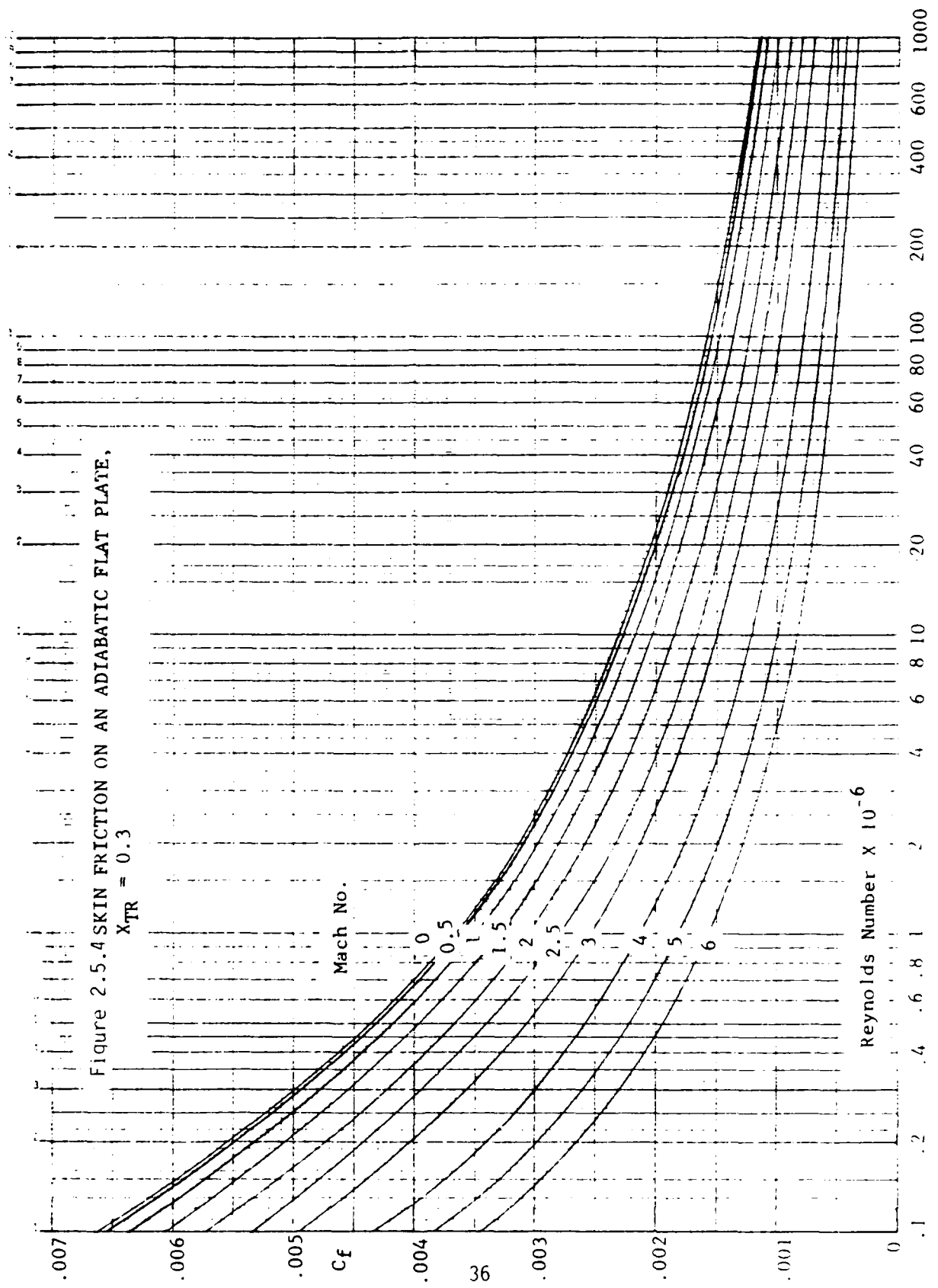


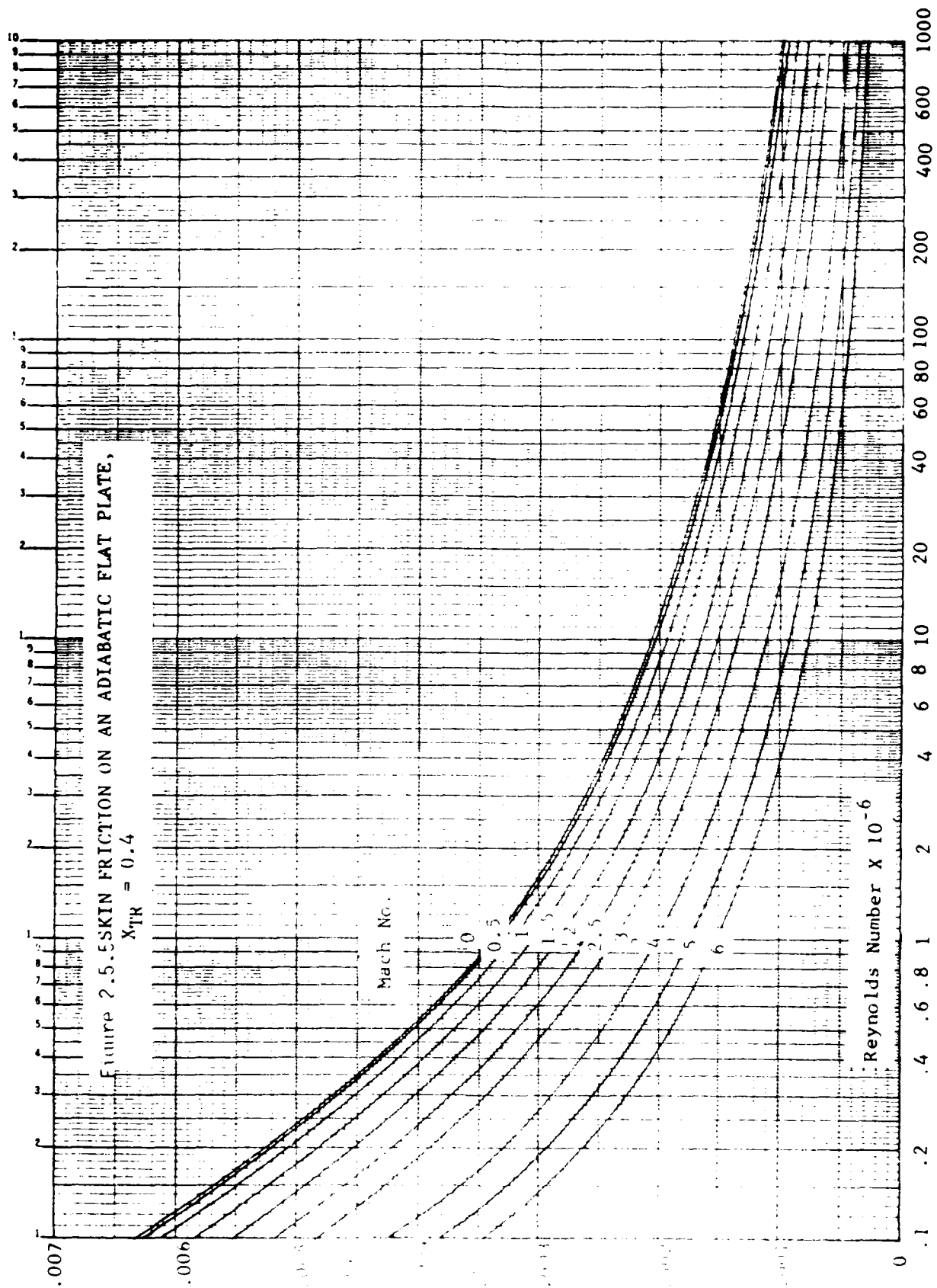
Figure 2.5.4 SKIN FRICTION ON AN ADIABATIC FLAT PLATE,
 $X_{TR} = 0.3$

Mach No.

C_f

Reynolds Number $\times 10^{-6}$

36



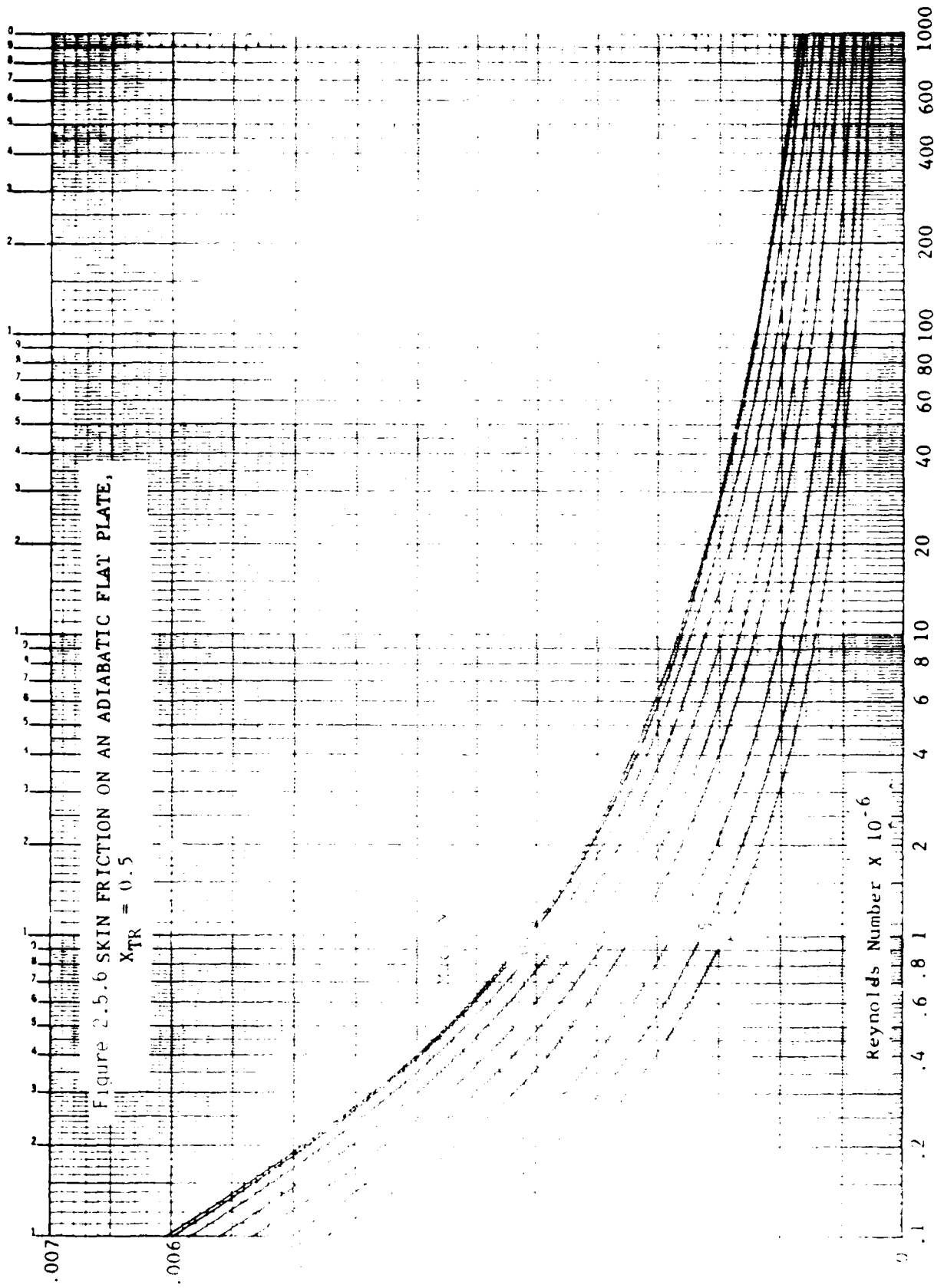


Figure 2.5.6 SKIN FRICTION ON AN ADIABATIC FLAT PLATE,
 $X_{TR} = 0.5$

Reynolds Number $\times 10^{-6}$

FR is the fineness ratio of the component.

For "nacelle" components, the form factor is given by

$$FF = 1.0 + 0.35/FR \quad (2.5.8)$$

Equations 2.5.7 and 2.5.8 were obtained from the Convair Aerospace Handbook (17) and also appears in the DATCOM (8).

The airfoil form factors depend upon airfoil type and streamwise thickness ratio. For 6-series airfoils, the form factor is given by

$$FF = 1.0 + 1.44 * TOCS + 2.0 * TOCS^2 \quad (2.5.9)$$

where

TOCS is the surface thickness to chord ratio.

For 4-digit airfoils, the form factor is given by

$$FF = 1.0 + 1.68 * TOCS + 3.0 * TOCS^2 \quad (2.5.10)$$

For biconvex airfoils, the form factor is given by

$$FF = 1.0 + 1.2 * TOCS + 100.0 * TOCS^4 \quad (2.5.11)$$

And for supercritical airfoils, the form factor is given by

$$FF = 1.0 + ZK * (CLD/.4) + 1.44 * TOCS + 2.0 * TOCS^2 \quad (2.5.12)$$

The factor $ZK * CLD/.4$ in equation 2.5.12 is an empirical relationship which shifts the 6-series form factor equation to account for the increased super velocities caused by the supercritical section design camber CLD. The factor $ZK/.4$ (derived from experimental data) is shown plotted in figure 2.5.7, as a function of the Mach number relative to the wing Mach critical. The equations above were extracted from the Large Aircraft Program (1).

2.5.3 Interference Factors

The component interference factors, IF, account for the mutual interference between components. For the fuselage, the interference factor is given by

$$\begin{aligned} IF &= RWB && ; && \text{WHEN MACH} < 1.0 \\ IF &= RLS * RWB && ; && \text{WHEN MACH} \geq 1.0 \end{aligned} \quad (2.5.13)$$

where

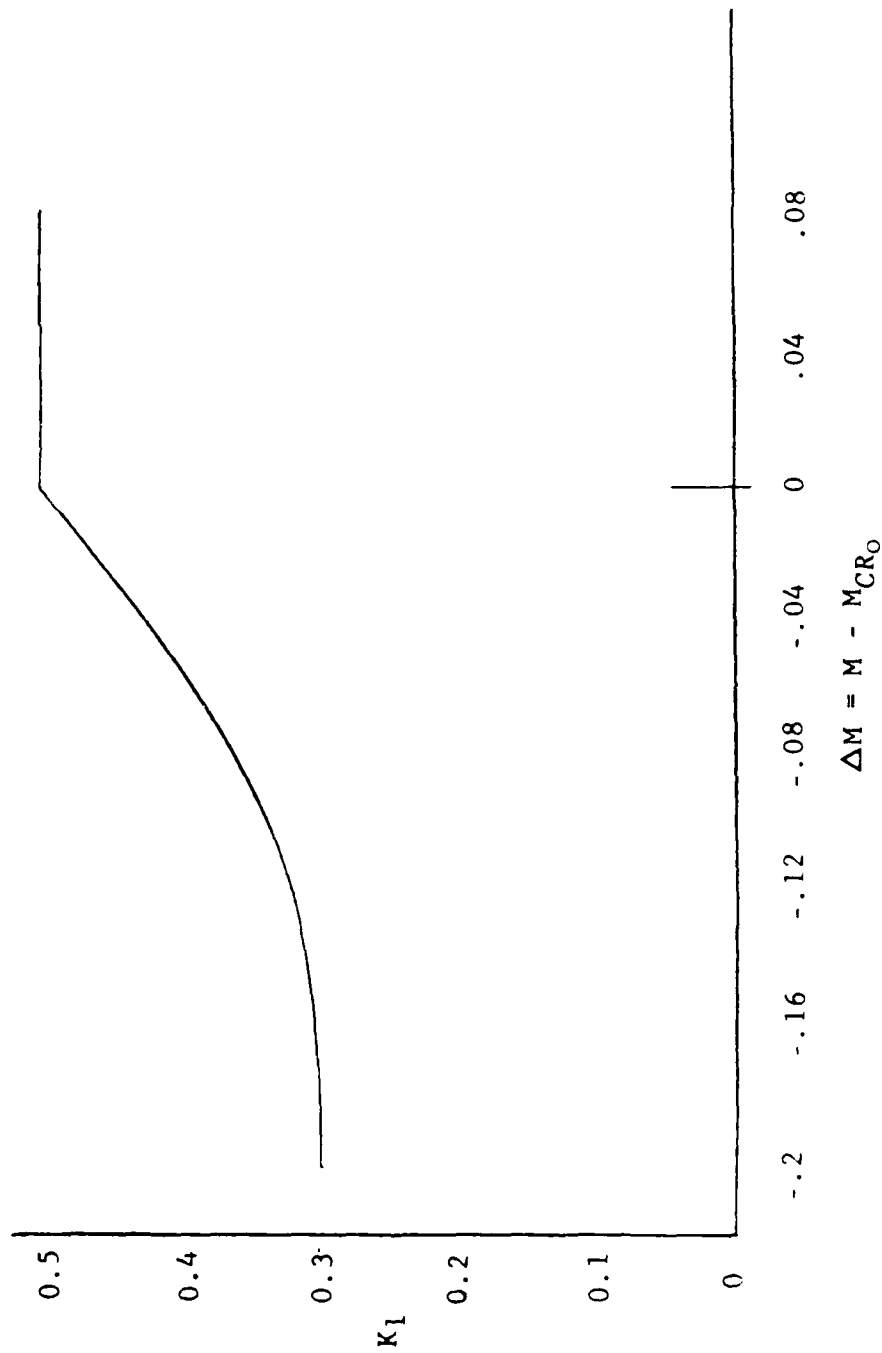


Figure 2.5.7 Supercritical Wing Compressibility Factor

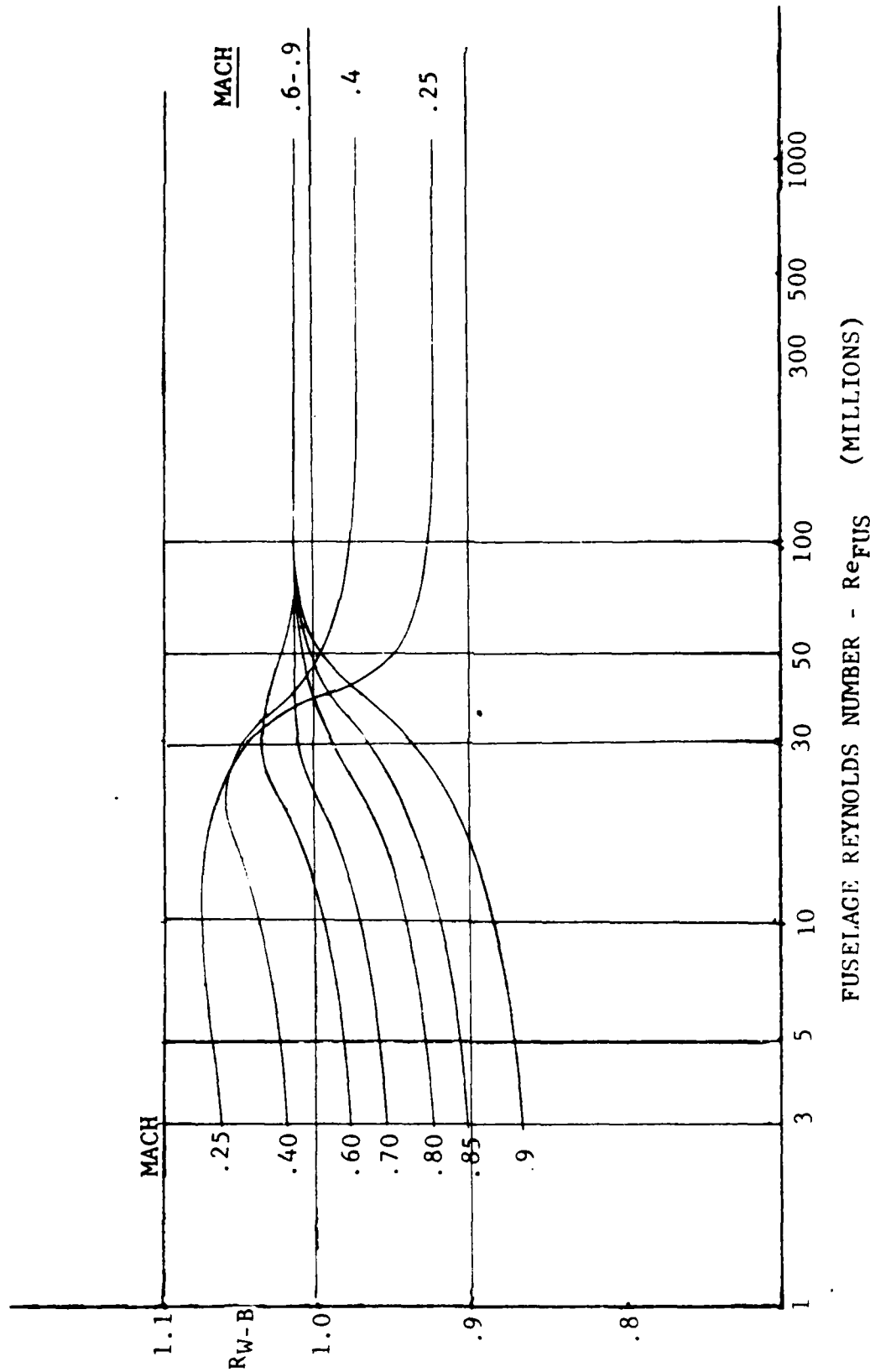


Figure 2.5.8 Wing-Body Correlation Factor for Subsonic Minimum Drag

RWB is shown plotted in figure 2.5.8 as a function of fuselage Reynolds number and Mach.

For other bodies, such as engine nacelles, the interference factor is given based on experimental experience with similar configurations. The Convair Aerospace Handbook (17) recommends using

IF = 1.0 for nacelles mounted out of the local velocity field of the wing

IF = 1.3 for nacelles mounted in moderate proximity to the wing

IF = 1.5 for nacelles and stores mounted flush to the wing or fuselage

SACP currently requires the user to input the interference factor for nacelles.

The interference factor for the surfaces is computed as

IF = RLS

where RLS is the lifting surface interference factor presented in figure 2.5.9.

If the Mach number is greater than 1.0 then the interference factors for both bodies, and surfaces are set to 1.0.

2.5.4 Wave Drag

Supersonic wave drag is determined on the basis of a component buildup for which simplified shapes are assumed. Three basic simplified shapes are used to represent the airplane: bodies, nacelles, and surfaces. The component buildup assumes that the total drag is the sum of the isolated wave drag of each component and does not allow for the mutual interference between components. However, the component buildup method does give wave-drag results comparable to favorable and unfavorable interference.

2.5.4.1 Surface Wave Drag

The technique used to estimate surface wave drag evolved from a method that applies transonic similarity theory to straight surfaces. Data correlations at Mach 1 were performed on a large number of unswept surface configurations with blunt and sharp leading-edge airfoils. For SACP, these results were represented by an analytical function common to both types. The equations, which are taken from the Large Aircraft Program (1), were modified for $M > 1$ to produce a peak value at low

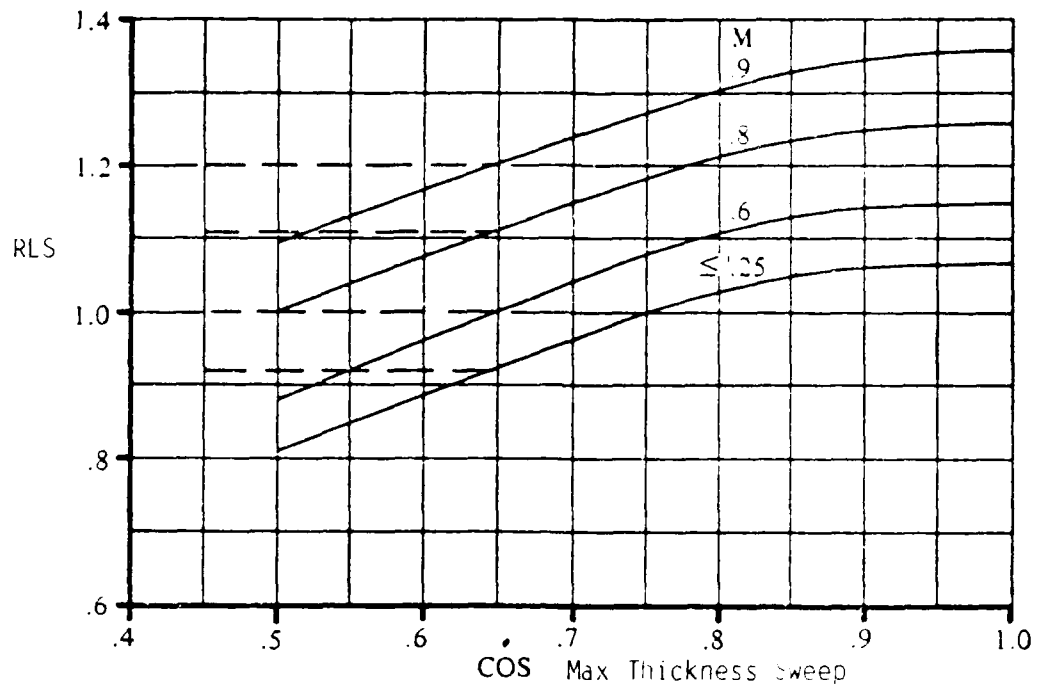


Figure 2.5.9 Lifting Surface Correlation Factor For Subsonic Minimum Drag

supersonic speeds and then to decrease at high Mach numbers to values predicted by straight-wing linear theory for equivalent two-dimensional configurations. Finally, sweep effects were included. The resulting semi-empirical equations are presented below

$$CDW = \frac{2 * Kt * Kw * Kc * Kb * TOC^{1.667}}{BETAW * Kb * Kw * FBXM + T1 + T2} + \frac{3.33 * Kt * Kw * Kc * Kb * TOC^{1.667}}{BETAW * Kb * KW1 * FBXM + T3 + T4} \quad (2.5.14)$$

where

Kt is airfoil thickness distribution factor

$$Kt = 1.0 + 4.0 * (.5 - XTOC * (1.0 + .5 * SQRT(ROT)))^2 - .25 * SQRT(ROT) * (1.0 - XTOC)^2 \quad (2.5.15)$$

Kb and Kw are airfoil factors

$Kb = 1.0$, $Kw = 1.2$ for double-wedge sections
 $Kb = 1.069$, $Kw = 1.0$ for curved-type sections
 $XTOC =$ is the location of airfoil section mean Y ordinate
 $ROT =$ is the leading edge radius to thickness ratio
 $Kc =$ is the airfoil camber factor given by

$$Kc = 1.0 + 2.5 * HOT^2$$

$$HOT = CAMBER * .055/TOC \quad (2.5.16)$$

$$Kp = \frac{(\cos(LESWEEP) + TR1 * (\tan(LESWEEP)^2 - \tan(LESWEEP)^2))}{(1 + TR2 * (\tan(LESWEEP) + \tan(LESWEEP))^2)} \quad (2.5.17)$$

$$TR1 = 0.5 / (1.0 + ZLAM)^2$$

$$TR2 = 1.0 / (1.0 + ZLAM)^2$$

$LESWEEP$ is the leading edge sweep
 $TESWEEP$ is the trailing edge sweep
 $ZLAM$ is the exposed taper ratio

$$T1 = (1.0/ARE) / (1.0 + (1.0 + ZLAM) * FB * BETAW^{1+Kw})$$

$$T2 = ARE^3 / (1.0 + .33 * ARE^3 * BETAW^4)$$

$$T3 = (2/ARE^3) / (1.0 + (.667 + ZLAM) * FB * BETAW^{1+Kw1})$$

$$T4 = 1.0 / (1.0 + 3.0 * ARE * BETAW^4)$$

$$Kw1 = Kw^{3.8}$$

$$BETAW = SQRT(M^2 - 1) / TOC * 333$$

$$FBXM = FB^{XM}$$

$$FB = .3 + .7 * Kp$$

$$FEX = 1.0 + 2.0 * ZLAM * 333$$

$$XM = .5 * (1.0 + ZLAM^2 * (2.0 - ZLAM)^3)$$

If $\text{Beta} (\text{SQRT}(M^2 - 1.0)) > \text{TAN}(\text{LESWEEP})$

$$\begin{aligned} XM &= (\text{TAN}(\text{LESWEEP})/\text{BETA})^2 \\ Z &= \text{COS}(\text{LESWEEP}) + \text{COS}(\text{TESWEEP}) \end{aligned}$$

where

ARE is the straight-surface ARW having the same value of CDW at $M = 1.0$ as ARW, where;

$$\text{ARW} = \text{AR} * (\text{TOCS})^{.333}$$

and

AR is the aspect area of the exposed surface

M is the Mach number

TOCS is the thickness ratio of the surface

The value of ARE is determined by solving the following equation using an iterative method

$$\begin{aligned} &\frac{2.0 * \text{ARE}}{\text{ARE}^4 + 1.0} + \frac{3.33 * \text{ARE}^3}{\text{ARE}^3 + 2.0} - (3.667 * \text{ARW}^3 + 2 * \text{ARW} + 1.667) * Kp \\ &= \frac{2.0 - 6.0 * \text{ARE}^4}{(\text{ARE}^4 + 1.0)^2} + \frac{20.0 * \text{ARE}^2}{(\text{ARE}^3 + 2)^2} \end{aligned} \quad (2.5.18)$$

$\text{TAN}(\text{LESWEEP})$ represents the approximate value of BETA at which CDW will maximize, provided the body is essentially cylindrical where the wing is attached. If the body is area-ruled, the peak value of CDW may or may not be closely approximated.

2.5.4.2 Body Wave Drag

The fuselage body wave drag is computed by dividing the body into two parts, consisting of a simplified pointed nose and a simplified boattail. That is,

$$\text{CDW} = (\text{CDPN} + \text{CDBT}) * \text{AMAX}/\text{SREF} \quad (2.5.19)$$

Nose wave drag, CDPN, is determined from Linnell's empirical equation for the supersonic wave drag of parabolic noses (Ref. 18).

$$\text{CDPN} = (1.2 + 1.5 * X) / ((1.0 + 1.9 * X) * (1.0 + \text{ELOD}^2)) \quad (2.5.20)$$

The nose fineness ratio ELOD is calculated from the nose length, LNOS and the maximum cross-sectional area, AMAX, as

$$\text{ELOD} = \text{LNOS}/\text{SQRT}(\text{AMAX} * 4.0/\text{PI}) \quad (2.5.21)$$

Boattail wave drag, CDBT is determined as a function of the boattail fineness ratio, ELOD, base diameter to maximum diameter, DBOD, and Mach number. This is done by computing CDBT at five values of DBOD and interpolating to the desired value. The general form of these equations is given below:

For $X \leq 1$

$$CDBT(i) = (A_0(i) + A_1(i) * X + A_2(i) * X^2 + A_3(i) * X^3) / ELOD^2 \quad (2.5.22)$$

and for $X > 1$

$$CDBT(i) = A_4(i) / (X * ELOD^2) \quad (2.5.23)$$

where

$$X = BETA / ELOD$$

The polynomial coefficients of equations 2.5.22 and 2.5.23 are determined from a least-square fit of Fig. III.B.10-9 of Aerospace Handbook (17) for ogive boattails and are tabulated below:

I	DBOD	A ₀	A ₁	A ₂	A ₃	A ₄
1	0.0	1.165	-0.5112	-0.5376	0.3964	0.513
2	0.4	1.067	-1.709	1.6632	-0.686	0.3352
3	0.6	0.7346	-1.4618	1.5795	-0.6542	0.198
4	0.8	0.2555	-0.5008	0.5024	-0.2077	0.0494
5	1.0	0.0	0.0	0.0	0.0	0.0

2.5.4.3 Nacelle Wave Drag

The nacelle wave drag is calculated by a method similar to that used for the fuselage:

$$CDW = (CDON + CDBT) * A_{MAX} / SREF \quad (2.5.24)$$

where CDBT, A_{MAX}, and SREF are as before and the equation used to calculate CDON for open-nose bodies is

$$CDON = ((1.0 - 2.0 * RIN / D_{MAX}) / ELOD)^{1.5} / SQRT(BETA) \quad (2.5.25)$$

where

RIN is the nose inlet area and D_{MAX}, ELOD, and BETA are as before.

This equation is a curve fit of Figure III.B.10-6 of Aerospace Handbook (17).

2.5.5 Camber Drag

The minimum drag contribution of the surface twist and camber is related to the lift coefficient of the polar displacement, POLARD, by the equation

$$CDC = 1.0 / (\text{PI} * \text{ARS} * (1.0 - E)) * \text{POLARD} \quad (2.5.26)$$

This increment is called camber drag and represents a drag increment between minimum profile drag and drag minimum. The span efficiency value, E, is related to the induced drag factor and is computed by

$$\begin{aligned} E &= \text{SQRT}(\text{EAR} * \text{ELE}) \\ \text{EAR} &= 1.0 - .45 * \text{ARS}^{.68} \\ \text{ELE} &= 1.0 - .000392 * \text{ABS}(\text{LESWEEP})^{1.615} \end{aligned} \quad (2.5.27)$$

If for some reason $E > 1$, and alternate equation, obtained from The Aerospace Handbook (17), is used

$$CDC = .7 * \text{POLARD}^2 * \text{AEXP} / \text{SERF} \quad (2.5.28)$$

where

AEXP is the exposed area of the surface
ARS is the surface aspect ratio
LEWSWEEP is the surface leading edge sweep angle

2.5.6 Base Drag

Data represented in Hoerner (19) were used to establish equations from which the base drag of bodies could be determined. The trends of these data show three different phases: (1) a gradual rise in CDB at transonic speeds up to Mach = 1.0, (2) a relatively constant drag level supersonically up to about Mach = 1.8 and (3) a steadily decreasing value of drag above Mach = 1.8. The resulting empirical equations are given as

$$\begin{aligned} \text{CDB} &= (.1 + .122 * \text{MACH}^8) * \text{SBASE} / \text{SREF}; & \text{WHEN } \text{MACH} < 1 \\ \text{CDB} &= .222 * \text{SBASE} / \text{SREF}; & \text{WHEN } 1 < \text{MACH} < 1.8 \\ \text{CDB} &= (1.42 * \text{SBASE} / \text{SREF}) / (3.15 + \text{MACH}^2); & \text{WHEN } \text{MACH} > 1.8 \end{aligned} \quad (2.5.29)$$

where

SBASE is the base area.

2.5.7 Drag Rise

For Mach numbers less than Mach critical the drag increases slowly with increasing Mach number. This drag component is known as compressible drag, or drag creep. Methodology for estimating this component of drag for conventional or supercritical wings was included in the subsonic drag buildup described above. For

Mach numbers greater than Mach critical, drag rise begins and increases rapidly with Mach. Figure 2.5.10 illustrates the drag bookkeeping system followed in SACP. This is the same as the system used in the Large Aircraft program whereby beyond Mach 1.0 the drag rise and the interference plus form drag are replaced by wave drag. The drag rise is separated into two components, drag rise due to lifting components and drag rise due to all other components on the aircraft. However, at this point only the total drag rise, at zero lift due to lifting and non-lifting components is addressed. This value is determined by

$$CDDR = A_2 * (MACH - MCR)^2 + A_3 * (MACH - MCR)^3 \quad (2.5.30)$$

where A_2 and A_3 are defined to produce a continuous zero-lift drag curve between MCR and MACH 1.0. The drag rise is curve fitted to begin at MCR with zero slope and end at Mach = 1.0, matching the value and slope of the wave drag curve. The coefficients A_2 and A_3 are calculated from

$$A_2 = (3.0 * (CDW1 - CDFE) - (1.0 - MCR) * CDWP) / (1.0 - MCR)^2$$

$$A_3 = ((1.0 - MCR) * CDWP - 2.0 * (CDW1 - CDFE)) / (1.0 - MCR)^3$$

where CDW1, CDFE, and CDWP represent the Mach 1.0 value of the wave drag, form plus interference drag, and the slope of the wave drag respectively.

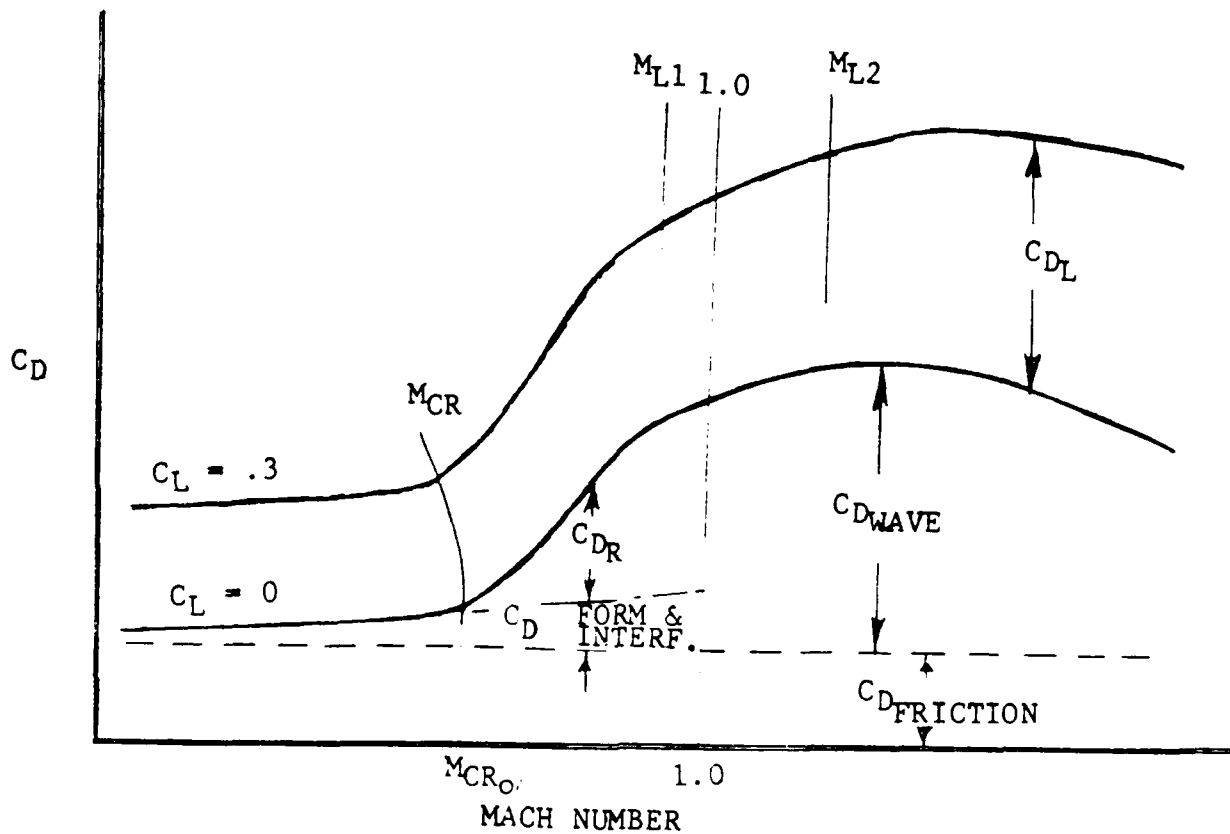


Figure 2.5.10 Transonic Drag Buildup

2.6 SURFACE INTERACTIONS

Interaction between various aircraft surfaces has an impact on several computed properties. The interactions between canards and wings or between wings and horizontal tails impact the calculations of angle of attack for these components, and also can affect the lift curve slope of the wing. The methods described below make the necessary adjustments to these values to account for the interactions.

2.6.1 Downwash Effects on Angle of Attack

Air passing over a surface causes a disturbance in the airflow, much like the wake produced by a boat. This disturbance effects other surfaces that fall within the wake area. This phenomenon is known as Downwash. Downwash alters the angle of attack on all of the aircraft surfaces. A set of equations for the calculation of the downwash has been adapted from the AEROX Computer Program for Transonic Aircraft (20 and 21) for use in SACP. These equations are:

$$\begin{aligned}T1 &= 2.0/ARS \\T2 &= \text{SQRT}(2.0 * \text{SPANS}/(3.0 * \text{MACS})) \\T3 &= \text{SQRT}(\text{SPANL}) \\T4 &= (1.3 - \text{CONAR})/(\text{SQRT}(1.0 + \text{TRS}))\end{aligned}$$

$$\begin{aligned}\text{SPANL} &= .5 * \text{SPANS}/\text{LTS} \\ \text{CONAR} &= 1.0/(3.0 * \text{ARS}^{\text{ARS}-3}) \\ \text{OSP NL} &= 1.0/\text{SPANL}\end{aligned}$$

The wake angle, EPSD, is

$$\text{EPSD} = \text{ALCAM} * T4 * (T1 + .1 * (T2 + T3)) \quad (2.6.1)$$

$$\text{ALCAM} = \text{ALPHA} + \text{CLO}/(2.0 * \text{PI} * \text{C4SWEEP} * \text{ARS}/(\text{ARS} + 2.0))$$

the nondimensional offset distance from the affected surface to the wake, AYOSS, is

$$\text{AYOSS} = \text{ABS}(((2.0 * \text{ZS})/\text{SPANS}) + \text{YDOSS}) \quad (2.6.2)$$

$$\text{YDOSS} = ((\text{OSP NL} - 1.5/\text{ARS}) * \text{SIN}(\text{EPSD})) - (\text{OSP NL} * \text{SIN}(\text{ALPHA}))$$

$$\begin{aligned}W1 &= .2/(\text{SQRT}(\text{OSP NL})) \\W2 &= (2.0 + \text{COS}(2.25 * \text{ALR}))/3.0 \\W3 &= 1.0 - (1.5 * \text{AYOSS}) \\W4 &= W2 - .75 * \text{ALPHA} * \text{SIN}(2.25 * \text{ALPHA})\end{aligned}$$

the downwash angle at the effected surface, DWASH, is

$$\text{DWASH} = \text{ALCAM} * T4 * (W1 + T1) * W2 * W3 * \text{ATENF} \quad (2.6.3)$$

and the downwash derivative with respect to angle of attack, DEPDA, is

$$\text{DEPDA} = T4 * (W1 + T1) * W4 * W3 * \text{ATENF} \quad (2.6.4)$$

where

ATENF is the supersonic downwash attenuation factor that is only used if Mach 1, is defined as

$$\text{ATENF} = 1.0 - .1 * \text{SQRT}(\text{MACH}^2 - 1.0) * (1.0 + \text{TAN}(\text{LESWEEP}))/ \\ (T1 + \text{OSPNL}) \quad (2.6.5)$$

and

ARS is the aspect ratio of the effecting surface
SPANS is the span of the effecting surface
MACS is the mean aerodynamic chord of the effecting surface
LTS is the X distance between the aerodynamic centers of the effecting and affected surface
TRS is the taper ratio of the affecting surface
ALPHA is the total aircraft angle of attack
ZS is the Z distance between the two surfaces
C4SWEEP is the quarter chord sweep of the effecting surface
LESWEEP is the leading edge sweep of the effecting surface

This algorithm was developed for the downwash angle (DWASH) downstream of the wing at aft tail locations. For other interactions, the downwash angles must be adjusted. For use downstream of canards, the angle must be multiplied by the ratio of the canard span to the wing span

$$\text{ECW} = \text{DWASH} * \text{SPANC}/\text{SPANW} \quad (2.6.6)$$

For canards mounted outboard of widely spaced, wing mounted nacelles (NCAN = 2) where the wing inboard panels are out of the canard downwash,

$$\text{ECW} = 0$$

The wing will also produce an upwash disturbance at the canard. In this case, the ratio of the upwash velocity (upstream of the lateral or bound leg of the equivalent "horseshoe" vortex representing the wing) to the downwash velocity at an equal distance downstream of the lateral vortex leg was evaluated by the Biot-Savart law for vortex-induced velocities. This ratio is denoted by FWAC.

$$\text{FWAC} = 1.0 - (1.2 * (\text{LTC})/\text{SPANW}) \quad (2.6.7)$$

The upwash angle ahead of the wing is

$$EWC = DWASH * FWAC$$

Three additional conditions are now placed on the values of wing upwash angle. First, for sharp wings having aspect ratios greater than 2.5, the leading-edge Mach limited flow zone is assumed to cancel the upwash

$$EWC = 0; \text{ WHEN NATW} = 9 \text{ (B1 convex airfoil type) and ARW} > 2.5$$

Second, for canards mounted outboard of widely spaced, twin nacelles (NCAN = 2), the wing upwash angle is reduced by a factor involving the spans of the wing and canard and the nacelle spacing (SPANAC).

$$EWC = DWASH * FWAC * (1.0 - (\text{SPANAC} + \text{SPANC}/2.0)/\text{SPANW}) \quad (2.6.8)$$

Third, for supersonic Mach numbers, the wing upwash is attenuated by dividing by the Mach number.

$$EWC = DWASH * FWAC/\text{MACH}; \text{ WHEN MACH} > 1.0 \quad (2.6.9)$$

The relationship of the wing to the horizontal tail is similar with:

$$EWH = DWASH$$

$$\text{FHAW} = 1.0 - (1.2 * (\text{LTW})/\text{SPANH})$$

$$\text{EHW} = DWASH * \text{FHAW}$$

$$\text{EHW} = DWASH * \text{FHAW}/\text{MACH}; \text{ WHEN MACH} > 1.0$$

$$\text{EHW} = 0; \text{ FOR SHAPE LEADING EDGE AIRFOILS AND ARH.GT.2.5}$$

The downwash and upwash angles produced by the canard, wing, and horizontal tail can now be used to obtain the angles of attack for these three surfaces including the induced angle of attack:

$$\text{ALPHAC} = \text{ALPHA} + \text{IC} + \text{EWC} \quad (2.6.10)$$

$$\text{ALPHAW} = \text{ALPHA} + \text{IW} - \text{ECW} + \text{EHW} + \text{EWC} * \text{SPANC}/2.0 * \text{SPANW} \quad (2.6.11)$$

$$\text{ALPHAH} = \text{ALPHA} + \text{IH} - \text{EWH} + \text{EHW} * (\text{SPANW}/2.0 * \text{SPANH}) \quad (2.6.12)$$

where IC, IW, and IH are the incidence angles of the canard, wing, and horizontal tail.

2.6.2 Wing Lift

The possibility of favorable interference from close-coupled canards on wing lift was cited initially by Behrhohm (22). An aerodynamic lift interference factor (VORTEX) has been added to

SACP and may increase the upper surface lift of wings having aspect ratios near 2.0 and having close-coupled canards mounted above the wing plant. This factor, in effect, accounts for the "fluid end-plate action" of the canard trailing vortices which promote local two-dimensional flow over the inboard wing upper surface, when the wing operates with a subsonic leading edge. No evidence of similar vortex action has been observed with wings having supersonic leading edges. The interference factor is proportional to the square root of the absolute value of the canard lift coefficient (ABCLC), and decreases with further upstream positioning of the canard (GLC) and with vertical repositioning of the canard above or below the favorable, close coupled height zone (GCZ).

$$\begin{aligned} \text{GCL} &= 1.4 * \text{MACW}/\text{LTC}; && \text{WHEN } \text{LTC}/\text{MACW} \geq 1.4 \\ \text{GCL} &= 1.0; && \text{WHEN } \text{LTC}/\text{MACW} < 1.4 \end{aligned}$$

$$\begin{aligned} \text{GCZ} &= 1.0; && \text{WHEN } 0.0 < \text{ZCAN}/\text{MACW} \\ \text{GCZ} &= 1.0 + \text{ZCAN}/\text{MACW}; && \text{WHEN } 0.0 > \text{ZCAN}/\text{MACW} \\ \text{GCZ} &= 1.0 - \text{ZCAN}/(4.0 * \text{MACW}); && \text{WHEN } .2 < \text{ZCAN}/\text{MACW} \end{aligned}$$

For $1.75 < \text{ARW} < 2.5$, the interference factor is

$$\begin{aligned} \text{VORTEX} &= \text{GCL} * \text{GCZ} * \text{CLC}/(\text{ARWC} * \text{ABCLC}) \\ &* \text{SQRT}(\text{ABCLC} * \text{SPANC} * \text{MACW}/(\text{SPANW} * \text{MACC})) \\ &* (1.0 - \text{ABS}(\text{ARW} - 2.125)/.375) \end{aligned} \quad (2.6.13)$$

where

ARWC = $\text{ARW}/(\text{ARW} + 2.0)$
 CLC is the canard lift coefficient referenced to the wing area
 MACW is the mean aerodynamic chord of the wing
 MACC is the mean aerodynamic chord of the canard
 LTC is the X distance between canard and wing aerodynamic center
 ZCAN is the Z distance between canard and wing aerodynamic center
 ARW is the aspect ratio of the wing
 SPANC is the span of the canard
 SPANW is the span of the wing

The interference factor is reduced for wings having highly swept leading edges, because some leading edge vortex lifts already act on the wing with or without canard. For wings having leading edge sweep angle greater than 45° and aspect ratio between 1.75 and 2.5,

$$\text{VORTEX} = \text{VORTEX}/\text{TAN}(\text{LESWEEP})$$

For supersonic Mach numbers and subsonic wing leading edges,

$$\text{VORTEX} = \text{VORTEX}/\text{MACH}$$

The lift coefficient of the wing upper surface and the wing lift curve slope can now be computed by multiplying the interference factor as follows:

$$\text{CLWU} = \text{CLWU} * (1.0 + \text{VORTEX}) \quad (2.6.14)$$

$$\text{CLWALPHA} = \text{CLWALPHA} * (1.0 + \text{VORTEX}/2.0) \quad (2.6.15)$$

Again, the interference factor is used only for wings having aspect ratios between 1.75 and 2.50.

2.7 LIFT, LIFT CURVE SLOPE, AND DRAG DUE TO LIFT

Methods for the computation of lift, lift curve slope and drag due to lift were taken from the AEROX-Computer Program (20 and 21) for use in SACP. The equations are organized according to the division of the flight envelope into the flow zones depicted in figure 2.7.1. The cross-hatched viscous stall region is not included in the present method. The flow is considered incompressible for Mach numbers below 0.1. The compressible, shockless zone 2 covers airfoils with blunt leading edges and with surrounding flows having local Mach numbers everywhere below the Laitone limit value ($\text{SQRT}(1.4 + 3.0)/2.0$). The boundary between zones 2 and 3 is estimated by the equation for ALER, the angle of attack for onset of the limit Mach number at the leading edge. The onset of the surface limit-Mach number, zone 4, occurs when the super-surface lift for zone 2 or 3 reaches the limit lift corresponding to the designated chordwise shock location, XCD. Sharp airfoils are considered to have reached the leading-edge Mach limit for all subsonic flow, and are treated with the nonpotential lift equations of zones 3 and 4. Zone 5 applies only to sharp airfoils having supersonic leading edges with attached shocks. Finally, Flow zone 6 covers all airfoils with detached, leading edge shocks. The supersonic leading edges for zones 5 and 6 occur when the normal component of Mach number exceeds unity ($\text{Mach} * \text{COS}(\text{LESWEEP}) \geq 1.0$).

The following equations apply to an equivalent wing having straight leading and trailing edges. Account is made for strakes and wing forward-chord extensions in SACP by multiplying all of the following equations for lift coefficient and wing lift curve slope by the term $(1.0 + \text{FLEX})$. FLEX, the empirical lift factor for chord extension, is defined within the program and depends on Mach number, angle of attack, and whether the extension is sharp (IFLEX = 0) or blunt (IFLEX = 1).

2.7.1 Incompressible Flow Zone 1 ($M < 0.1$)

The incompressible lift equation for conventional airfoils is taken from the potential-flow theory of Kutta-Jowkowski. The lift equation for nonpotential flow, such as around sharp airfoils, is based upon the integration of downwash momentum. Both equations are extended to three-dimensional flows through the inclusions of the Prandtl aspect-ratio transformation and the cosine term involving the effective sweep of the quarter-chord line. The potential-flow equations for conventional airfoils are:

$$CL = 2.0 * PI * SIN(ALPHA) * COS(SQ) * AR / (AR + 2.0) \quad (2.7.1)$$

$$DLL = 2.0 * PI * COS(ALPHA) * COS(SQ) * AR / (AR + 2.0) \quad (2.7.2)$$

$$CD = CL^2 / (PI * AR) \quad (2.7.3)$$

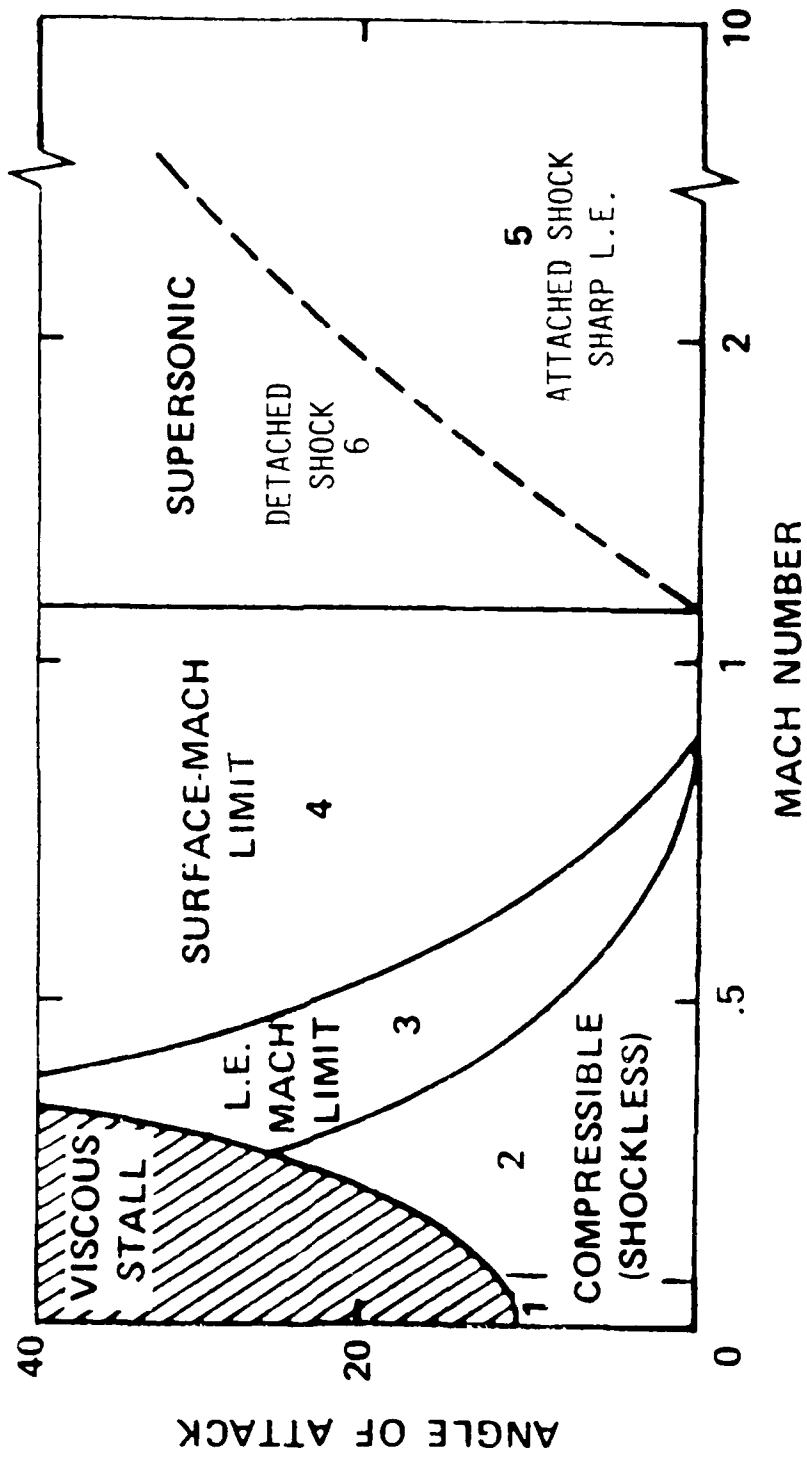


Figure 2.7.1 Flow zones.

where

ALPHA is the surface angle of attack
AR is the surface exposed aspect ratio
SQ is the effective quarter chord sweep of the surface

$$SQ = AR \sin(\sin(\text{SWEEP}) \cdot \cos(\text{ALPHA}))$$

The nonpotential equations derived for AEROX (20) are:

$$CL = 2 \cdot \pi \cdot \sin(\text{ALPHA}) \cdot \cos(\text{ALPHA})^2 \cdot (1 - \sin(\text{ALPHA})^2)^{1/2} \cdot \cos(SQ) \cdot AR / (AR + 2) \quad (2.7.4)$$

$$DCL = \pi \cdot \cos(\text{ALPHA}) \cdot (2 \cdot \sin(\text{ALPHA})^4 + 2 \cdot \cos(\text{ALPHA})^2 - 4 \cdot \sin(\text{ALPHA})^2 - 3 \cdot \sin(\text{ALPHA})^2 \cdot \cos(\text{ALPHA})^2) \cdot \cos(SQ) \cdot AR / (AR + 2) \quad (2.7.5)$$

$$= \pi \cdot \cos(\text{ALPHA}) \cdot (CISQ) \cdot \cos(SQ) \cdot AR / (AR + 2)$$

$$CD = CL \cdot \tan(\text{ALPHA})^{\text{DEXP}} \quad (2.7.6)$$

where

$$\text{DEXP} = 1.5 - \text{MACH} \cdot \cos(\text{LESWEEP})/4; \text{ WHEN } M < 1 \\ = 1.5 - \text{MACH}^2 \cdot \cos(\text{LESWEEP})/4; \text{ WHEN } M > 1$$

The incompressible lift is comprised of equal contributions from the upper and lower wing surfaces. The nonpotential equations asymptotically approach the potential equations at small angles of attack.

2.7.2 Compressible, Shock-free Flow Zone 2

In estimating the aerodynamics for airfoils having subsonic leading edges, separate compressibility factors are used for the lifts of the upper and lower surfaces. For compressible, shock-free flow (zone 2) on the upper surface of blunt airfoils, a Prandtl-Glauert factor is used involving the component of flight Mach number normal to the quarter-chord line and an angle-of-attack attenuation to value unity at 40° .

$$FU = 1.0 - (1.0 - \sqrt{1.0 - \text{MACH}^2 \cdot \cos(SQ)^2}) \cdot (\text{ALPHA}/40)^2 / \sqrt{1.0 - \text{MACH}^2 \cdot \cos(SQ)^2} \quad (2.7.7)$$

No compressibility factor is used for the upper-surface lift in nonpotential flow, because the onset of the local Mach-limit is considered to "freeze" the local flow.

Lower surface lifts in potential and nonpotential flows around airfoils having subsonic leading edges are evaluated using

a pitot-compressibility factor expressing the ratio of the leading-edge stagnation-line pressure in compressible flow to that in incompressible flow. Account is included for variations in the angles of attack and sweep, and for wing-body interference patterned after the FLAX parameter from references 24 and 25.

$$FL = CPMXS = 1.4285717/MACH^2 * ((1.0 + .2 * FINT * MACH^2 * \cos(ESWPLE)^2)^{3.5} - 1.0) / \cos(ESWPLE)^2 \quad (2.7.8)$$

where

ESWPLE is the effective leading edge sweep of the surface
 $= \text{ARCSIN}(\text{SIN}(\text{LESWEEP}) * \text{COS}(\text{ALPHA}))$

FINT = $((1.0 + \text{BDMAX})/\text{SPANS})^2$; WHEN $1.4 < \text{MACH}$

FINT = $(1.0 + (1.0 - (\text{ALPHA}/40) * (1.4 - \text{MACH})/.04)^2 * \text{BDMAX}/\text{SPANS})^2$; WHEN $(1 < \text{MACH} \leq 1.4)$

FINT = $(1.0 + (1.0 - \text{ALPHA}/40.)^2 * \text{BDMAX}/\text{SPANS})^2$; WHEN $(\text{MACH} \leq 1)$

BDMAX is the body width
 SPANS is the span of the surface

The compressible, potential-flow equations for conventional airfoils are obtained by incorporating the compressibility factors, equations 2.7.7 and 2.7.8 into equations 2.7.1 and 2.7.2.

$$CL = (\text{FU} * \text{FINT} + \text{FL}) * \text{PI} * \text{SIN}(\text{ALPHA}) * \text{COS}(\text{SQ}) * \text{AR}/(\text{AR} + 2.0) \quad (2.7.9)$$

$$\text{DCL} = ((\text{FU} * \text{COS}(\text{ALPHA}) + (\text{dFU}/\text{dALPHA}) * \text{SIN}(\text{ALPHA})) * \text{FINT} + \text{FL} * \text{COS}(\text{ALPHA})) * \text{PI} * \text{COS}(\text{SQ}) * \text{AR}/(\text{AR} + 2.0) \quad (2.7.10)$$

$$CD = CL^2/(\text{PI} * \text{AR})$$

Sharp airfoils in subsonic, compressible flow are treated as nonpotential, Mach-limited flows, and assigned to flow zones 3 or 4.

2.7.3 Leading-edge Mach-limited Flow Zone 3

The onset of the Laitone limit Mach number in the curvilinear flow around a blunt-airfoil leading edge is estimated by the value of the onset angle of attack, ALPHA_E. A brief discussion of the conceptual flow model undergoing the transition from compressible, potential flow to Mach-limited, nonpotential flow follows. For more information see the appendix in AEROX (20).

After attaining the local limit Mach number around the leading edge, further increases in angle of attack or in flight Mach number tend to enlarge the local Mach-limited region on the airfoil nose.

The enlargement of the constant velocity profile in the curvilinear flow around the nose disrupts the radial equilibrium between the local, radial static-pressure gradient and the local, centrifugal focus. (Irrotational, curvilinear flow exists only when radial equilibrium prevails, which requires an essentially inverse relationship between local velocity and local streamline radius of curvature.) The constant velocity profile may be accomplished by the dominance of the local centrifugal forces and the possible formation of a separation bubble. When the locally supersonic flow decelerates (and reattaches) just downstream of the nose (with or without the separation bubble), a "peaky" pressure distribution results, (shown in ref. 26). This flow is designated in AEROX as leading-edge Mach-limited or zone 3. When the separation bubble is present, the mixing action of the rotational-flow layers emanating from the disrupted nose flow may promote the flow reattachment.

When the supersonic limit-Mach number extends well back on the airfoil upper surface, resulting in the flat pressure distribution (also in ref 26), the flow is surface Mach-limited, and assigned to zone 4. Surface Mach-limited flow is modeled to have separation downstream of the surface limit shock, resulting in an additive drag component, CDSEP. Experimental confirmation of the separation appears in pressure distributions, samples of which were included in reference 26.

Sharp airfoils in compressible, subsonic flow are treated as leading-edge Mach-limited flow with the nonpotential zone 3 equations.

$$CL = (1.0 + FL) * PI * SIN(ALPHA) * COS(ALPHA)^2 * (1 - SIN(ALPHA)^2/2.0) * COS(SQ) * AR/(AR + 2.0) \quad (2.7.11)$$

$$DCL = (1 + FL) * PI * COS(ALPHA) * (CISQ) * COS(SQ) * AR/(AR + 2) \quad (2.7.12)$$

$$CD = CL * TAN(ALPHA)^{DEXP} \quad (2.7.13)$$

The lift curves for blunt airfoils traversing from compressible, potential flow (zone 2) into zone 3 are assigned a continuous mathematical transition, rather than a discontinuous jump, so that the program may be coupled to an optimizer program. The lift equation is the sum of the zone 2 lift (eg. 2.7.9) evaluated at ALPHA_E and an incremental lift for the interval (ALPHA - ALPHA_E) in zone 3, until equation 2.7.11 is reached.

CL = The greater of

Equation 2.7.11

or

$$CL = (FU * FINT + FL) * PI * SIN(ALPHAE) * COS(SQ) * AR / (AR + 2.0) + (dCLU/dALPHA + dCLl/dALPHA)(ALPHA - ALPHAE) \quad (2.7.14)$$

2.7.4 Surface Mach-Limited Zone 4

The conceptual flow model depicting surface Mach-number limited flow past an airfoil is shown in figure 2.7.2. The Laitone limit Mach number (ref. 27 and 28) corresponds to the maximization of the static pressure behind the surface limit shock.

$$MACH_{LIM} = 1.48 \quad (2.7.15)$$

This criterion is extended to swept wings in the AEROX program with the following limit pressure coefficient.

$$CPLIM = \frac{1.4285717}{3.58 - 1.0} MACH^2 * (1.0 + .2 * MACH^2 * COS(SXC)^2)^{3.5/2} \quad (2.7.16)$$

where

SXC is the effective sweep angle of the limit shock

The airfoil lift coefficient for zone 4 is the sum of the lower-surface nonpotential lift (equation 2.7.11) and the upper-surface limit lift, which is dependent upon the designated chordwise location, XCD of the surface limit shock. The program uses $XC = f(XCD)$ which moves the limit shock to the trailing edge as the sonic leading-edge condition is reached.

$$CL = -(CPLIM * XC + .5 * CPDS * (1.0 - XC)) * COS(ALPHA) + FL * PI * SIN(ALPHA) * COS(ALPHA)^2 * (1 - SIN(ALPHA))^2 / 2 * COS(SQ) * AR / (AR + 2) \quad (2.7.17)$$

$$DCL = (CPLIM * XC + .5(CPDS) * (1.0 - XC)) * SIN(ALPHA) + FL * PI * COS(ALPHA) * (CISQ) * CCS(SQ) * AR / (AR + 2.0) \quad (2.7.18)$$

$$CD = CL^2 / (PI * AR) + CL * TAN(ALPHA)^{DEXP} + CDSEP \quad (2.7.19)$$

where

CPDS is the pressure coefficient downstream of the limit shock, corresponding to P_2 in figure 2.7.2

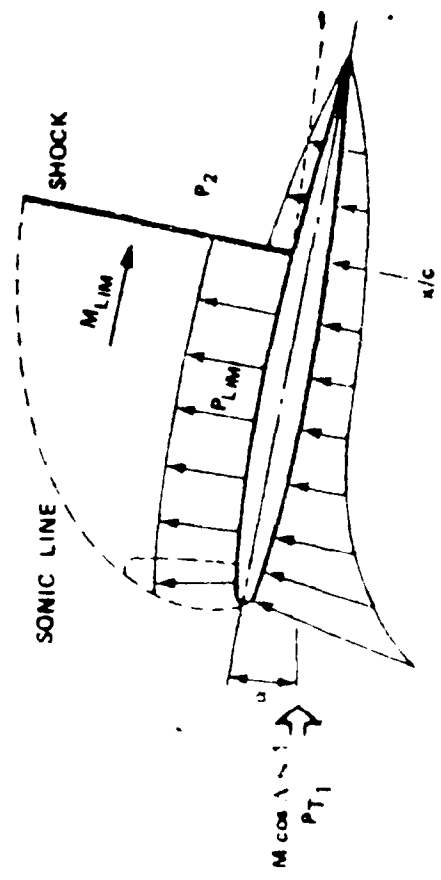


Figure 2.7.2 Surface Mach-number limited transonic flow.

CDSEP is the separation drag. It accounts for the momentum deficit in the modeled separation wake passing the trailing edge. The wake is assumed to originate at the base of the limit shock, to have its upper edge follow a line inclined at one-half the angle of attack, and to have a linear velocity profile between the zero value on the surface to the freestream value at the upper edge.

$$CPDS = 1.4285714/MACH^2 * (((2.8 * (2.2 + MACH^2 * SIN(SXC)^2) * COS(SXC)^2 - .4)/2.4) * ((2. + .4 * MACH^2)/ (.4 * (2.2 + MACH^2 * SIN(SXC)^2 + 2.)))^{3.5} - 1.)$$

$$CDSEP = (SPANS - BDMAX) * (1. - XC) * MACS/SREF * SIN(ALPHA)/2$$

where

SPANS is the span of the surface
 BDMAX is the body diameter
 MACS is the mean aerodynamic chord of the exposed surface
 SREF is the reference area
 SXC is the effective sweep angle of the limit shock

2.7.5 Supersonic Attached-Shock Zone 5

Airfoils having sharp leading edges with attached shocks are treated in zone 5. The upper boundary is the angle of attack for shock detachment, ARDET, which is evaluated by equations based on curve fitting figure 4 in reference 29 for supersonic speeds. The supersonic lift coefficients are estimated by the nonpotential equation (2.7.11) using the exposed wing area, an empirical, Mach-attenuated aspect-ratio transformation, and the wing-body interference factor of FLAX (ref. 24 and 25) applied to the lower surface lift.

$$CL = 2. * PI * SIN(ALPHA) * COS(ALPHA)^2 * (1. - SIN(ALPHA)^2/2. * ARX/(ARX + 2./MACH) * SX/SREF * FLAX * (1. - .65/MACH) + .65/MACH); \quad \text{when } (MACH \leq SQRT(2.)) \quad (2.7.20)$$

$$DCL = 2. * PI * COS(ALPHA) * (CISQ) * ARX/(ARX + 2./MACH) * SX/SREF * FLAX(1. - .65/MACH) + .65/MACH); \quad \text{when } (MACH \leq SQRT(2.)) \quad (2.7.21)$$

For $SQRT(2.) \leq Mach \leq 3.$ multiply the above equations by $1./SQRT(MACH^2 - 1.)$

At MACH numbers above 3., lift coefficients are evaluated by the explicit, oblique-shock theory of reference 30.

$$CL = .833 * SX/SREF * ARX/(ARX + 2./MACH) * (1. + 1.4 * \sin(\alpha)^2 - \cos(\alpha) * \sqrt{1. - 4./MACH^2 * \alpha/16. - 1.96 * \sin(\alpha)^2}) * \cos(\alpha);$$

when ($\alpha \leq 16.$ degrees; and $3. < MACH$) (2.7.22.A)

$$CL = .833 * SX/SREF * ARX/(ARX + 2./MACH) * (1. + 1.4 * \sin(\alpha)^2 - \cos(\alpha) * \sqrt{1. - 4./MACH^2 - 1.96 * \sin(\alpha)^2}) * \cos(\alpha);$$

when ($16.$ degrees $\leq \alpha$; and $3. < MACH$) (2.7.22.B)

$$DCL = SX/SREF * (.833 * 2.8 * \sin(\alpha) * \cos(\alpha)^2 + \sin(\alpha) * \cos(\alpha) * \sqrt{1. - 4./MACH^2 - 1.96 * \sin(\alpha)^2} + (1.96 * \sin(\alpha) * \cos(\alpha)^3) / \sqrt{1. - 4./MACH^2 - 1.96 * \sin(\alpha)^2}) * ARX/(ARX + 2./MACH) - CL * \tan(\alpha);$$

when ($3. < MACH$) (2.7.23)

$$CD = CL * \tan(\alpha) \quad (2.7.24)$$

where

ARX is the aspect ratio of the exposed surface
 SX is the area of the exposed surface
 SREF is the reference area

2.7.6 Supersonic Detached-Shock Zone 6

Blunt airfoils with supersonic leading edges and sharp airfoils with detached leading edge shocks are treated with the following equations combining the nonpotential equation (2.7.11) derived from diverted momentum and modified Newtonian impact theory, which assumes increased importance on the windward surface loading at hypersonic speed. The limit pressure coefficient for the upper surface undergoes a transition from a value of $-.68$ at $MACH = 1.$ and approaches the value $-1./MACH^2$ the well-known empirical value suggested by Mayer in reference 31.

$$CPLIM = -1./MACH^2 * (1. - .32/MACH^{2.5}) \quad (2.7.25)$$

The upper surface lift coefficient becomes a small fraction of the total lift coefficient as the Mach number increases.

CLU = the lesser of

$$-CPLIM * SX/SREF * \cos(\alpha)$$

or

$$PI * \sin(\alpha) * \cos(\alpha)^2 * (1. - \sin(\alpha)^2/2.) * SX/SREF * ARX/(ARX + 2./MACH) * FMOMU/DNBL \quad (2.7.26)$$

$$CLL = \pi * \sin(\alpha) * \cos(\alpha)^2 * (1. - \sin(\alpha)^2/2.) * SX / SREF * ARX / (ARX + 2./MACH) * FMOML/DNBL * FLAX * CPSTAG + CPSTAG * \sin(\alpha)^2 * \cos(\alpha) \quad (2.7.27)$$

$$CL = CLU + CLL$$

DCLU = the lesser of

$$CPLIM * SX/SREF * \sin(\alpha)$$

or

$$\pi * \cos(\alpha) * CISQ * ARX / (ARX + 2./MACH) * SX / SREF * FMOMU/DNBL \quad (2.7.28)$$

$$DCLL = \pi * \cos(\alpha) * (CISQ) * ARX / (ARX + 2./MACH) * SX/SREF * FMOMU/DNBL * FLAX * CPSTAG + CPSTAG * \sin(\alpha) * (2. * \cos(\alpha)^2 - \sin(\alpha)^2) \quad (2.7.29)$$

$$DCL = DCLU + DCLL$$

$$CD = CL * \tan(\alpha) \quad (2.7.30)$$

The empirical constants entering the diverted-momentum (nonpotential) lift contribution include DNBL, establishing the variation with Mach number, and FMOMU and FMOML, expressing the division of the diverted momentum lift to the upper and lower wing surfaces.

$$DNBL = MACH^{2/3}; \quad \text{when } MACH \leq 1.77$$

or

$$SQRT(MACH^2 - 1.); \quad \text{when } MACH > 1.77$$

$$FMOMU = 1.; \quad \text{when } MACH \leq 1.2$$

or

$$1./(\text{MACH} - 2.); \quad \text{when } MACH > 1.2$$

$$FMOML = 1.6 - .6 * MACH; \quad \text{when } MACH \leq 1.5$$

.7; \quad \text{when } 1.5 < MACH \leq 2.2

or

$$0.1 + 1./(\text{MACH} - .55); \text{when } MACH > 2.2$$

2.7.7 Lift and Drag for Bodies and Nacelles

The lift and drag forces on the body or on the nacelles are estimated by the equation summing the slender body contribution and the viscous cross flow drag. An updated discussion of the approach appears in reference 32, which was the principle source of the values used for constructing the contour plot of cross-

flow drag coefficient against cross-flow Reynolds number and cross-flow Mach number shown in figure 2.7.3. The BAERO subroutine contains explicit equations for each of the nine regions indicated.

$$CL = (\sin(2. * \alpha) * \cos(\alpha/2.) * ASECT + CDC * ETAN * \sin(\alpha)^2 * APLAN) / SREF * \cos(\alpha) + CLO \quad (2.7.30)$$

$$CD = (\sin(2. * \alpha) * \cos(\alpha/2.) * ASECT + CDC * ETAN * \sin(\alpha)^2 * APLAN) / SREF * \sin(\alpha) + CDO \quad (2.7.31)$$

where

$$ETAN = .55 + .0125 * LENGTH/DIAMETER$$

ASECT is the nose maximum cross sectional area
APLAN is the nose planform area
CLO is the zero AoA lift coefficient
CDO is the zero AoA drag coefficient

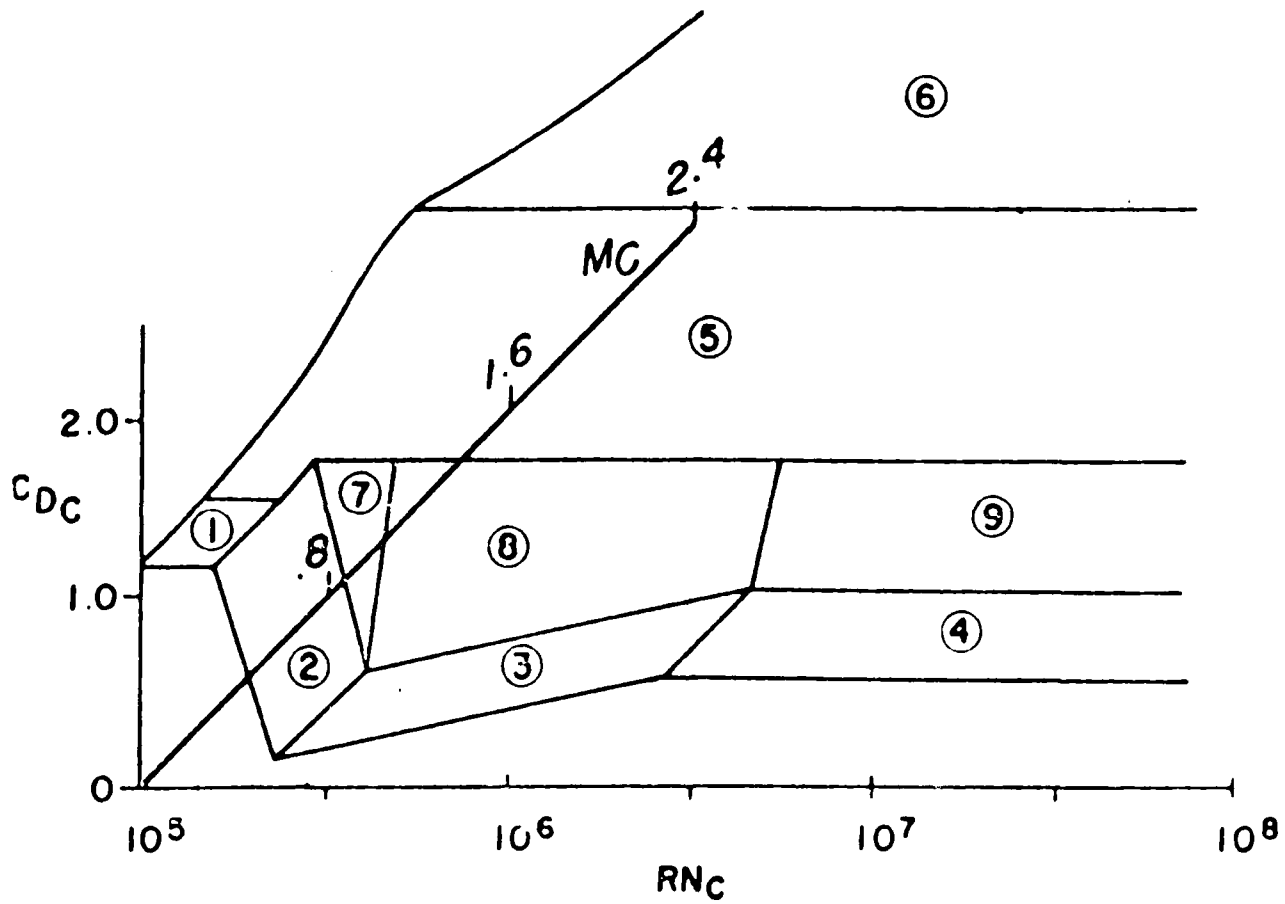


Figure 2.7.3 - CONTOUR OF CROSS-FLOW DRAG COEFFICIENT WITH CROSS-FLOW MACH AND REYNOLDS NUMBERS.

2.8 DYNAMIC PRESSURE RATIO

The dynamic pressure ratios are computed for horizontal downstream surfaces. In addition the sidewash times the dynamic pressure of the vertical tail can also be computed.

2.8.1 Dynamic Pressure at Down Stream Surfaces

The method for estimating the dynamic-pressure Q/Q at the downstream surfaces is based on the DATCOM method which relates the dynamic-pressure ratio to the drag coefficient of the upstream surface. The steps involved in determining the dynamic pressure at some distance aft of the wing root chord, outlined in section 4.4.1 of the DATCOM report are as follows:

1. Calculate the half-width of the wing wake by

$$ZWOC = 0.68 * \text{SQRT}(CDOUS * (XOC + .15)) \quad (2.8.1)$$

where

CDOUS is the wing zero-lift drag coefficient of the upstream surface
XOC is the distance measured from the upstream surface trailing edge to the down stream surface leading edge

2. Calculate the downwash in the plane of symmetry at the vortex sheet by

$$EW = 0.51566 * (2. * CLALPHA) / AR \quad (2.8.2)$$

where

CLALPHA is the lift curve slope of the upstream surface
AR is the aspect ratio of the upstream surface

3. Determine the vertical distance Z from the vortex sheet to the quarter-chord point of the mean aerodynamic chord of the downstream surface by

$$ZOC = XOC * \text{TAN}(GAMMA + EW - 2.) \quad (2.8.3)$$

where

GAMMA = $\text{ATAN}(ZMAC/XDIST)$
ZMAC is the Z location of the downstream mean aerodynamic chord
XDIST is the distance in feet between the upstream surface trailing edge and the downstream surface leading edge

4. Determine the dynamic-pressure-loss ratio at the wake center by

$$DQOQO = 2.42 * \text{SQRT}(CDOUS)/(XOC + .3) \quad (2.8.4)$$

5. Determine the dynamic-pressure-loss ratio for points not on the wake centerline by

$$DQOQ = DQOQO * (\text{COS}(\text{PI}/2 * ZOZW))^2 \quad (2.8.5)$$

where

$$ZOZW = ZOC/ZWOC$$

6. Determine the dynamic pressure ratio at an arbitrary distance X aft of the upstream-surface-root-chord trailing edge by

$$QOQ = 1 - DQOQ$$

2.8.2 Side-Wash-Factor * Dynamic Pressure Ratio of the Vertical Tail

For a wing-body combination there are two contributions to the sidewash present at a vertical tail - that due to the body and that due to the wing.

The sidewash due to a body arises from the side force developed by a body in yaw. As a result of this side force a vortex system is produced, which in turn induces lateral-velocity components at the vertical tail. This sidewash from the body causes a destabilizing flow in the airstream beside the body. Above and below the fuselage, however, the flow is stabilizing.

The sidewash arising from a wing in yaw is small compared to that of the body. The flow above the wake center line moves inboard and the flow below the wake center line moves outboard.

For conventional aircraft the combination of the wing-body flow fields is such as to cause almost no sidewash effect below the wake center line.

A single algebraic equation, taken from the DATCOM, is presented that predicts the combined sidewash and dynamic pressure parameter. This empirically derived expression is

$$\text{SWFNV} = .724 + (3.06 * ((\text{SV}/\text{SW})/1. + \text{COS}(C4\text{SWEEP}))) + (.4 * ZCGC4W/\text{BMW}) + (.009 * \text{ARW}) \quad (2.8.6)$$

where

SV	is the vertical tail total area
SW	is the wing total area
C4SWEEP	is the quarter chord sweep of the wing
ZCFC4W	is the distance parallel to the Z axis, from wing root quarter chord point to fuselage centerline.
BMW	is the maximum body width

2.9 TRIM AERODYNAMICS

Aircraft can be trimmed using any one or a combination of several devices. These trimming devices fall into one of three classes, engines, moveable surfaces such as canards and horizontal tails, or flaps. The aerodynamic methods for each of these are as follows.

2.9.1 Body Engines or Nacelle Engines

If engines are equipped with thrust vectoring devices, then these devices can be used to trim the aircraft. In this case the trim aero coefficients are simply computed from the thrust vector as

$$CLT = CT * SIN(ALPHAT) \quad (2.9.1)$$

$$CDT = CT * COS(ALPHAT) \quad (2.9.2)$$

$$CMT = CLT * XARM/MACW + CDT * ZARM/MACW \quad (2.9.3)$$

where

CLT is the lift coefficient due to trim on the engine
CDT is the drag coefficient due to trim on the engine
CMT is the pitching moment coefficient due to the trim on the engine
ALPHAT is the thrust vector angle for the trim in the plane of symmetry
XAMR is the X moment arm for the engine
ZAMR is the Z moment arm for the engine
MACW is the mean aerodynamic chord of the wing

2.9.2 All Moveable Surfaces

For all moveable surfaces, such as canards and horizontal tails, trim can be effected simply by changing the angle of attack on the device. In this case lift and drag can be computed from the methods described in section 2.7 and the pitching moment can be found from

$$CMT = (CLT * XARM/MACS + CDT * ZARM/MACS) * SS * MACS / (SREF * MACW) \quad (2.9.4)$$

where

CLT is the lift coefficient due to trim on the surface
CDT is the drag coefficient due to trim on the surface
XARM is the X moment arm of the surface
ZARM is the Z moment arm of the surface
MACS is the mean aerodynamic chord of the surface
MACW is the mean aerodynamic chord of the wing
SS is the surface area
SREF is the reference area

2.9.3 Flaps

Methods for computing the trim coefficients for flap are taken from AEROX (20). The methods are as follows:

Flap effectiveness. The nonlinear flap-effectiveness ratio is the average of the flap effectiveness ratios at zero angle of attack and at the prescribed higher angle of attack.

$$FER = (1. + \cos(\alpha + \delta)/\cos(\alpha)) * \sqrt{FLAPC/MACS * FLAPS / (.3 * (SPANS - BDMAXS))} \quad \text{when } MACH < 2.$$

or

$$FER = FLAPS * (1. + 1.4 * \sin(\alpha + \delta)^2) / (SS * (1. + 1.4 * \sin(\alpha)^2)) \quad \text{when } MACH \geq 2. \quad (2.9.5)$$

where

DELTA is the flap deflection angle
FLAPC is the flap average chord
MACS is the mean aerodynamic chord of the surface
FLAPS is the flap span
SPANS is the surface span
BDMAXS is the average body diameter along the surface

Flap-induced lift coefficient. The incremental lift coefficient accompanying trailing-edge flap deflection is

$$CL_{FLAP} = FER * CL_{\alpha} * \delta * FM \quad (2.9.6)$$

where

CL_α is the surface lift curve slope (unflapped)
FM accounts for variations over the Mach number range

$$\begin{aligned} FM &= .25; && \text{when } MACH < .4 \\ FM &= .322 - MACH/6.; && \text{when } .4 < MACH \leq 1.4 \\ FM &= .0835/\sqrt{MACH^2 - 1.}; && \text{when } 1.4 < MACH \leq 2.0 \\ FM &= 1.; && \text{when } MACH > 2.0 \end{aligned}$$

Flap-induced drag coefficient. The incremental drag coefficient accompanying deflection of the surface trailing-edge flaps is assumed to be:

$$CD_{FLAP} = CL_{FLAP} * \tan(\alpha + \delta/2.) \quad (2.9.7)$$

Flap-induced pitching moment coefficient. The incremental pitching moment coefficient produced by the flap is:

$$CM_{FLAP} = -CL_{FAP} * E_{FLAP}/MACS \quad (2.9.8)$$

where

E_{FLAP} accounts for the eccentricities of the centroids of the loading produced by the flaps

$$\begin{aligned} E_{FLAP} &= LACS - LCG + MACS/4; && \text{when } MACH \leq .4 \\ E_{FLAP} &= LACS - LCG + MACS * (.25 + (MACH - .4) * .5 - \\ &FLAPC/MACS)); && \text{when } .4 < MACH < 1.4 \\ E_{FLAP} &= LACS - LCG + MACS * (.75 - FLAPC/MACS); && \text{when } MACH > 1.4 \end{aligned}$$

where

LACS is the X location of the surface aerodynamic center
LCG is the X location of the aircraft center of gravity

The value of the pitching moment must now be referenced to the aircraft. This is accomplished by the factor.

$$CM_{FLAP} = CM_{FLAP} * SS * MACS/(SREF * MACW) \quad (2.9.9)$$

2.10 PITCHING MOMENT CURVE SLOPE (CMALPHA)

According to Roskam (23), CMALPHA can be estimated for all subsonic Mach numbers by the equation

$$CMALPHA = (XCG - XAC) * CLALPHA \quad (2.10.1)$$

where

XCG is the X location of the aircraft center of gravity
XAC is the X location of the aircraft aerodynamic center
CLALPHA is the lift curve slope of the aircraft determined by

$$CLALPHA = CLALPWB + CLALPC + CLALPH * (1 - DWF)$$

where the lift curve slopes for wing-body, canard, and nacelles are given by

$$CLALPWB = KWB * CLAW * TNW * SW/SREF$$

$$CLALPC = CLAC * TNC * SC/SREF$$

$$CLALPH = CLAH * TNH * SH/SREF$$

$$KWB = 1 - .25 * (BDW/SPANW)^2 + .025 * BDW/SPANW$$

and

BDW is the body width
SPANW is the wing span
CLAW is the wing lift curve slope from section 2.7
CLAC is the canard lift curve slope from section 2.7
CLAH is the horizontal tail lift curve slope from section 2.7
SW is the wing area
SC is the canard area
SH is the horizontal tail area
TNW is the wing dynamic pressure ratio from section 2.8
TNC is the canard dynamic pressure ratio from section 2.8
TNH is the horizontal tail dynamic pressure ratio from section 2.8
SREF is the reference area
DWF is the downwash factor from the wing to the horizontal tail

2.11 THE VARIATION OF PITCHING MOMENT COEFFICIENT WITH ANGLE OF ATTACK RATE (CMALPD)

Roskam (23) states that CMALPD can be expressed as the sum of components for canards and horizontal tails because wing and body contributions are small. With this CMALPD can be expressed as

$$\text{CMALPD} = \text{CMACD} + \text{CMAHD} \quad (2.11.1)$$

with

$$\text{CMACD} = -2. * \text{CLALPC} * (\text{XCG} - \text{XACC})^2 \quad (2.11.2)$$

and

$$\text{CMAHD} = -2. * \text{CLALPH} * (\text{XACH} - \text{XCG})^2 * \text{DWF} \quad (2.11.3)$$

where

CLALPC is the canard component lift curve slope from section 2.10
CLALPH is the horizontal tail component lift curve slope from section 2.10
XCG is the X location of aircraft center of gravity
XACC is the X location of the canard aerodynamic center
XACH is the X location of the horizontal tail aerodynamic center
DWF is the down wash factor from the wing the the horizontal tail

2.12 THE VARIATION OF PITCHING MOMENT COEFFICIENT WITH PITCH RATE (CMQ)

The methods for calculation of CMQ are taken from Roskam (23). The derivative CMQ may be considered to be the sum of a wing, canard, and a tail contribution, the effect of the fuselage being usually small:

$$CMQ = CMQW + CMQC + CMQH \quad (2.12.1)$$

For the canard contribution:

$$CMQC = -2. * CLALPC * (XCG - XACC)^2 \quad (2.12.2)$$

where

CLALPH is the canard component of lift curve slope from section 2.10

XCG is the X location of the aircraft center of gravity

XACC is the X location of the canard aerodynamic center

For the horizontal tail contribution:

$$CMQH = -2 * CLALPH * (XACH - XCG)^2 \quad (2.12.3)$$

where

CLALPC is the horizontal tail component of the lift curve slope from section 2.10

XACH is the X location of the horizontal tail aerodynamic center

For the wing contribution

$$CMQW = CMQWMO * (R1/R2 + 3./B)/(R3/R4 + 3.) \quad (2.12.4)$$

with

$$CMQWMO = CLAW * \cos(C4SWEEP) * (T1/T2 + .041667 * T3/T4 + .125)$$

and

$$B = \sqrt{1. - MACH^2 * C4SWEEP}$$

$$R1 = ARW^3 * \tan(C4SWEEP)^2$$

$$R2 = ARW * B + 6. * \cos(C4SWEEP)$$

$$R3 = R1$$

$$R4 = ARW + 6. * \cos(C4SWEEP)$$

$$T1 = ARW * (2. * XW^2 + .5 * XW)$$

$$T2 = ARW^3 + 2. * \cos(C4SWEEP)$$

$$T3 = ARW^3 * \tan(C4SWEEP)^2$$

$$T4 = ARW + 6. * \cos(C4SWEEP)$$

$$XW = XACW - XCG$$

where

CLAW is the lift curve slope of the wing
C4SWEEP is the quarter chord sweep of the wing
ARW is the aspect ratio of the wing
XACW is the X location of the aerodynamic center of the wing
XCG is the X location of the aircraft center of gravity

2.13 HIGH-LIFT SYSTEM AERODYNAMICS

The empirical method for predicting lift, drag, and moment of an airplane with flaps and slats deployed consist of adding the incremental effects of the high lift system to the clean airplane aerodynamics. Figure 2.13.1 illustrates the manner in which the incremental effects of a flap can be applied to the clean-wing aerodynamics. The following techniques for estimating these increments were taken from the Large Aircraft Program (1).

2.13.1 Aerodynamic Characteristics of Two-Dimensional High-Lift Devices

The lift effectiveness of plain trailing-edge flaps can be estimated from thin-airfoil theory. The rate of change of lift with flap deflection at a constant angle of attack is given by

$$C_{10} = 2 * (OF + \sin(OF)) \quad (2.13.1)$$

with

$$\cos(OF) = 1 - 2 * CFP$$

where

CPF is the flap to wing chord ratio

This equation is plotted in figure 2.13.1 as a function of flap-chord ratio. The theory considers only a bent flat plate and does not include effects of thickness or large deflection angles. The effects are accounted for in Reference 34 and 35 by empirical flap efficiency factors, as shown in figures 2.13.2 through 2.13.5. The lift of a plain flap may now be expressed as

$$DCL = \eta * C_{10} * DFR \quad (2.13.2)$$

where

ETA is the plain-flap efficiency factor from figure 2.13.2 depending on the flap deflection angle DFR, plus the included angle of the flap trailing edge PHI.

C10 is the rate of change of lift with flap deflection at constant angle of attack from equation 2.13.1

DFR is the flap deflection angle in radians

This procedure is extended to slotted flaps with Fowler motion by evaluating C10 at a flap-chord ratio based on the extended chord. For double - or triple - slotted Fowler flat segments the lift increment is obtained by summing the incremental lift increments for each flap segment. The result is

$$DCF1 = \sum_{i=1}^I \eta(i) * C_{10}(i) * DFR(i) \quad (2.13.3)$$

where

i is a subscript that indicates the 1st, 2nd, and 3rd flap segment of the slotted flap
 I is the number of slots or segments in the flap segment
 $\text{ETA}(i)$ is the slotted-flap efficiency factor from Figures 2.13.3, 2.13.4, or 2.13.5 for the i th flap segment
 $C_{10}(i)$ is the lift for the i th flap segment
 DFR is the flap deflection of the i th flap segment

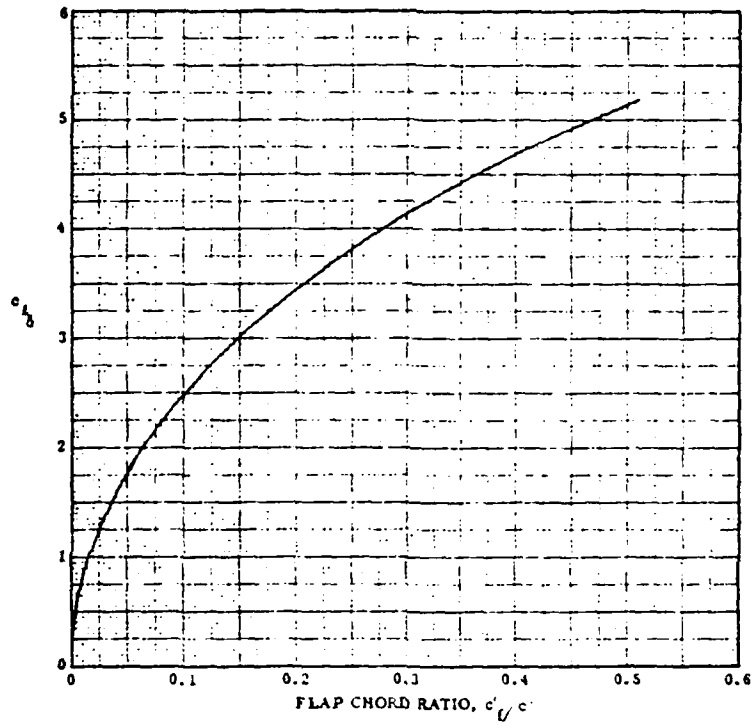


Figure 2.13.1 Theoretical Lifting Effectiveness of Trailing-Edge Flaps

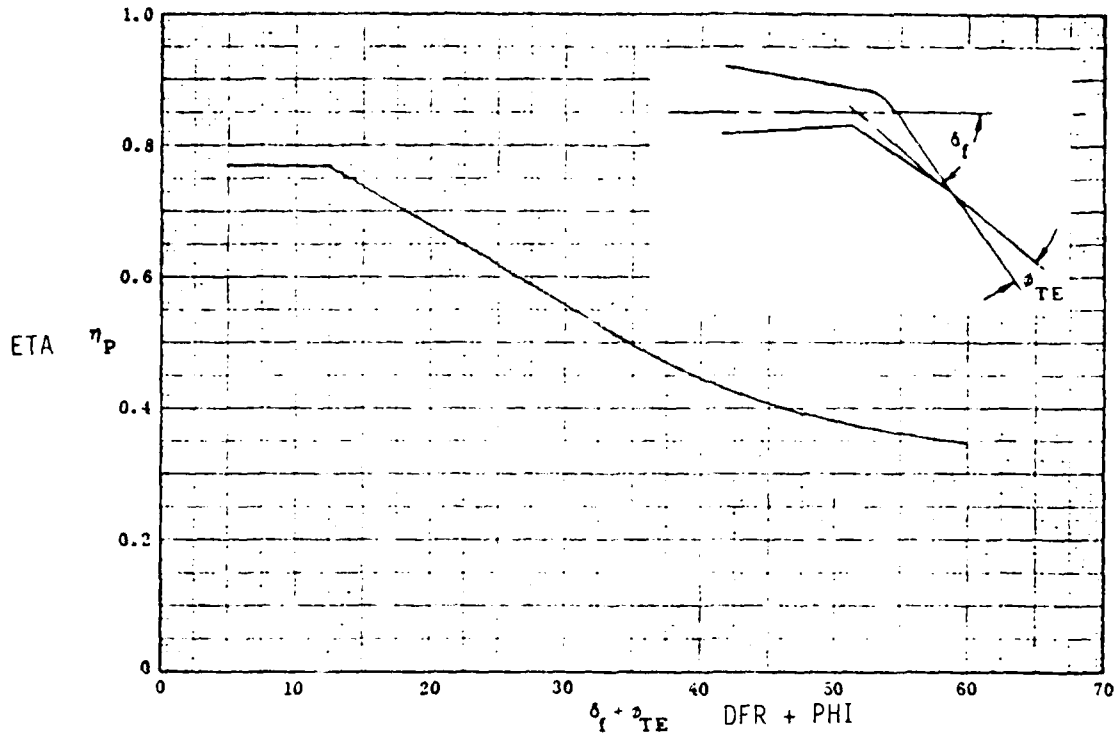


Figure 2.13.2 Turning Efficiency of Plain Trailing-Edge Flaps

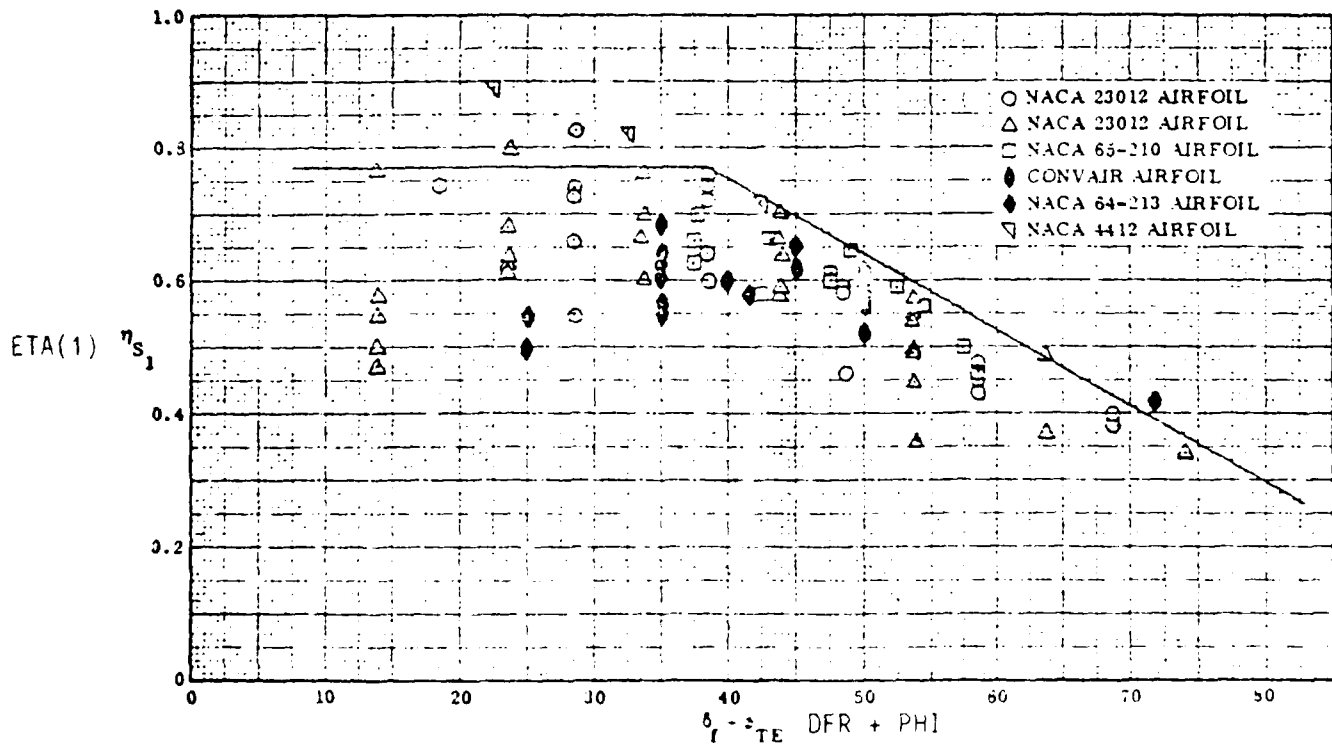


Figure 2.13.3 Turning Efficiency of Single-Slotted Flaps

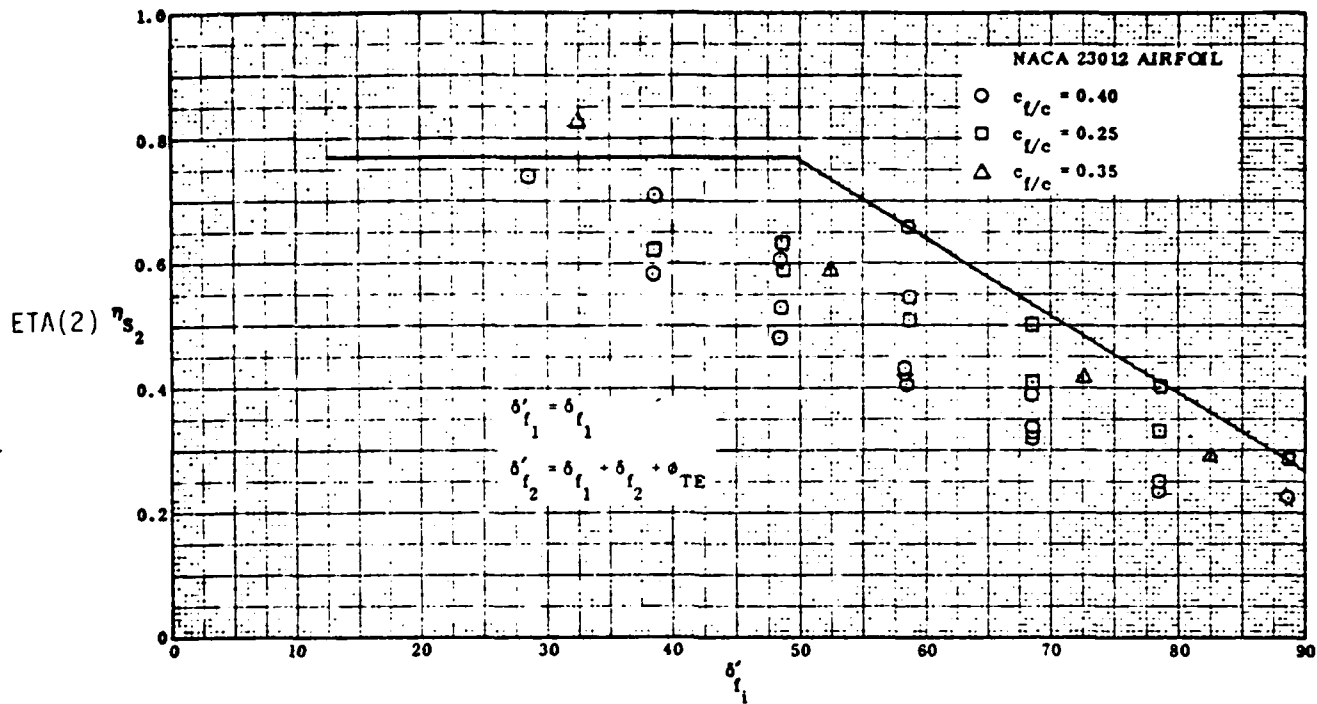


Figure 2.13.4 Turning Efficiency of Double-Slotted Flaps

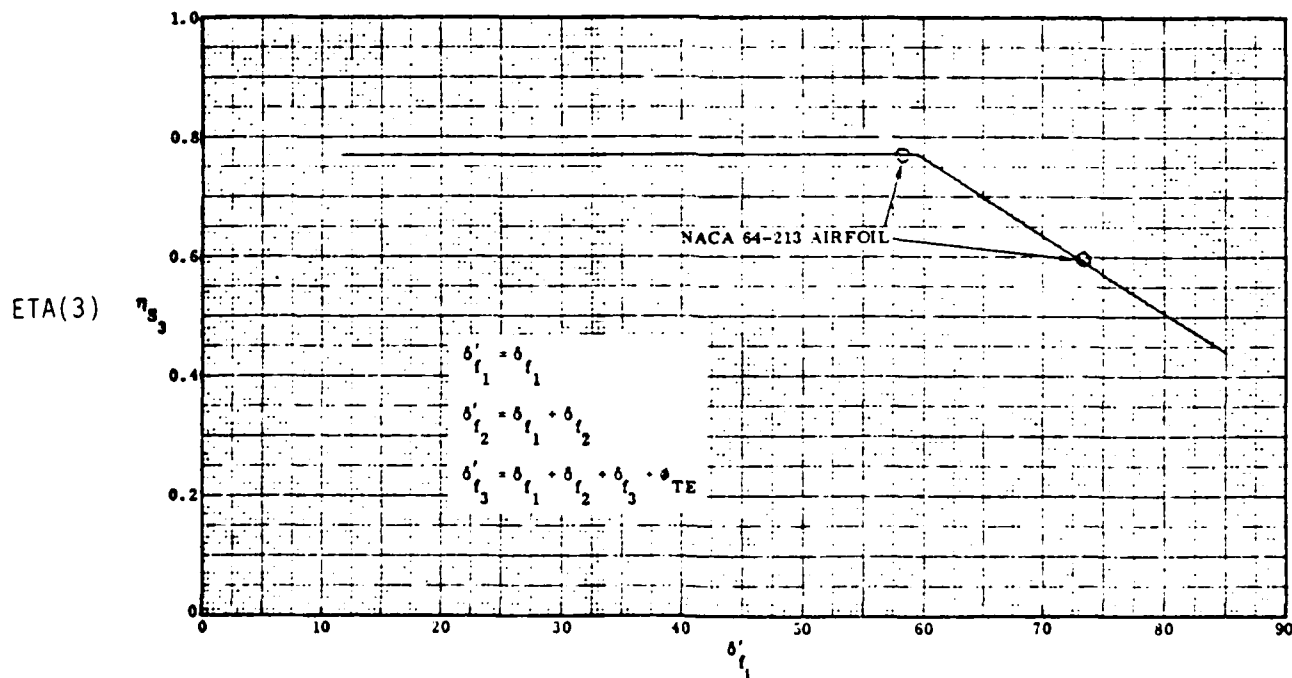


Figure 2.13.5 Turning Efficiency of Triple-Slotted Flaps

The method of summation and the geometry definition required to evaluate equation 2.13.3 is shown in figure 2.13.6.

The effects of leading-edge high-lift devices on the wing lift at zero angle of attack is estimated from thin-airfoil theory as

$$C_{1LE} = 2 * (\sin(OS) - OS) \quad (2.13.4)$$

where

$$\cos(OS) = 1 - 2 * CSOS$$

and

CSOS is the slat to wing chord ratio

Unlike trailing-edge flaps, the deflection of a nose flap causes a loss in lift at zero angle of attack. The increment in lift, DC1S is

$$DC1S = C_{1LE} * DSR \quad (2.13.5)$$

where DSR is the leading edge flap deflection angle in radians, positive nose down.

The two-dimensional maximum lift increment, DCLM, due to a trailing edge plain flap deflection is given in reference 34 as

$$DCLM = K_t * K_d * DCL * RMAX \quad (2.13.6)$$

and similarly, for single, double - or triple - slotted flaps the equation is

$$DC1MF = K_t * K_d * \sum_{i=1}^I DCL(i) * RMAX(i) \quad (2.13.7)$$

where

DCL(i) is the predicted lift increment determined for the ith flap segment from equation 2.13.7

K_t is taken from the plot in figure 2.13.7

K_d is taken from the plot in figure 2.13.8

RMAX is the theoretical relationships between DCLM and DCLO given in reference 35 as

$$RMAX = 1. - (OF / (OF + \sin(OF))) * (1. + \text{ALOG}(.5 * (X + OF)) / \sin(.5 * X - OF)) / (OF * \tan(.5 * X)) \quad (2.13.8)$$

where

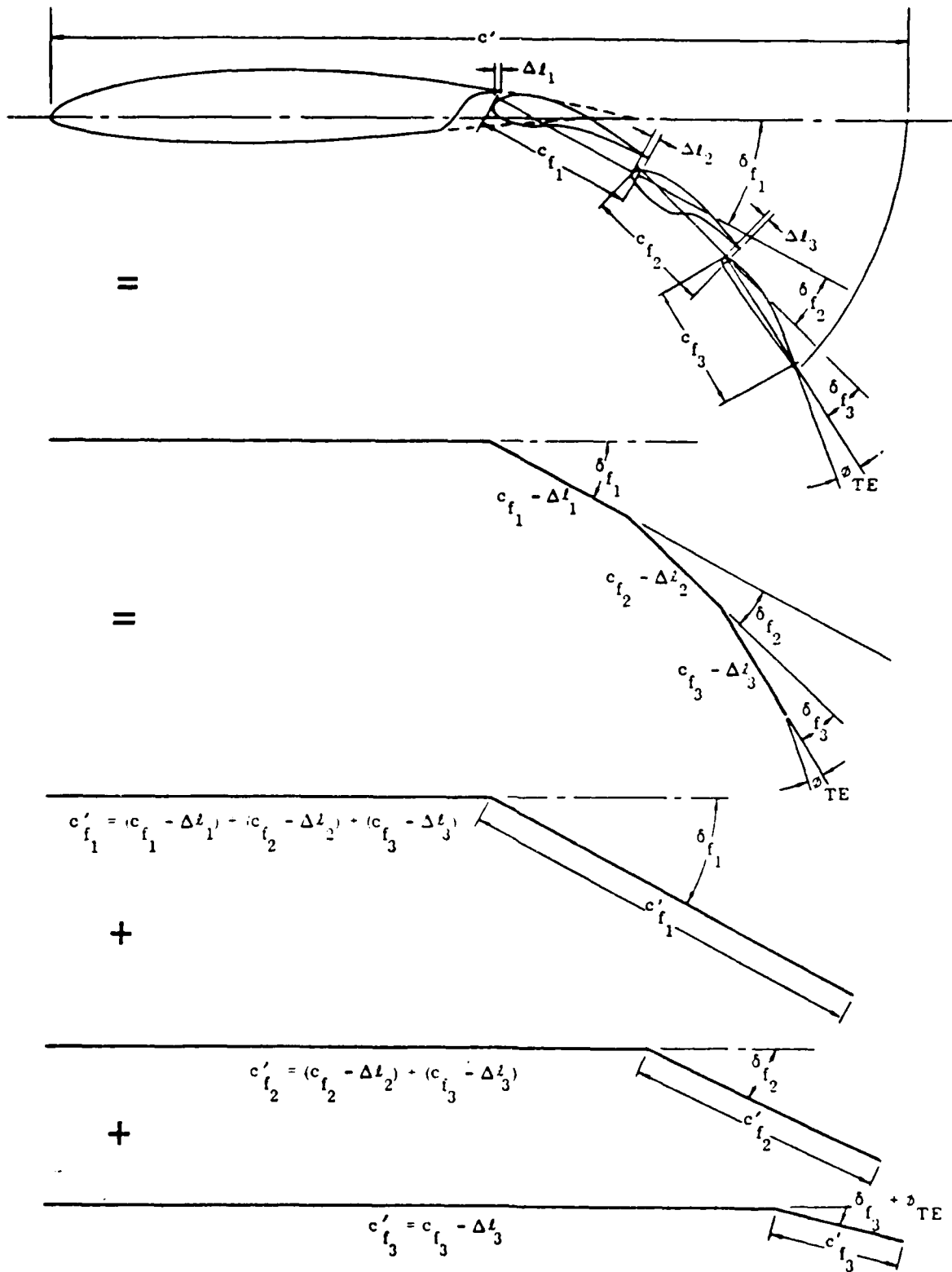


Figure 2.13.6 Principle of Superposition Theory and Extended Slotted-Flap Geometry

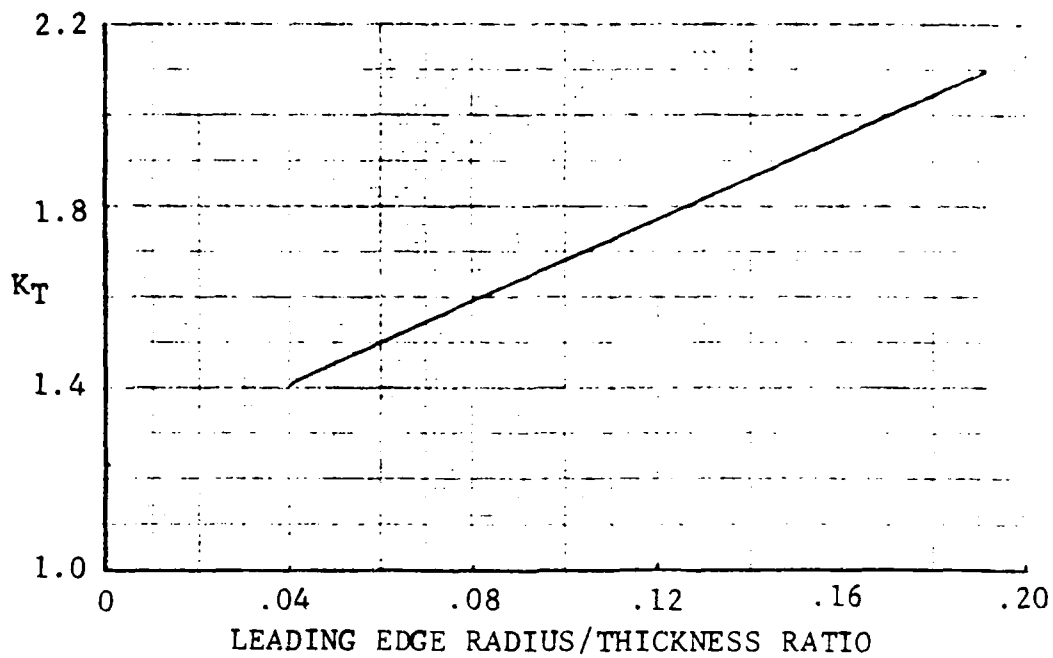


Figure 2.13.7 Maximum Lift Correlation Factor for Trailing-Edge Flaps

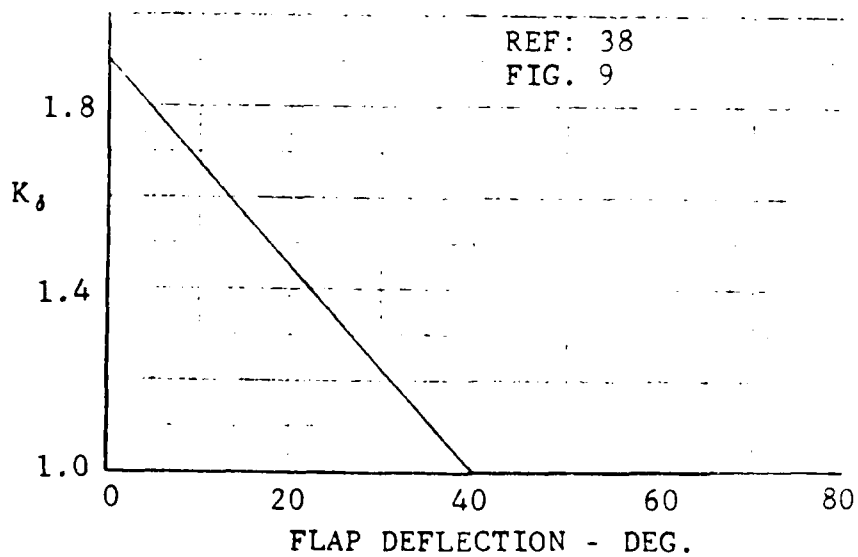


Figure 2.13.8 Flap Angle Correlation Factor Versus Flap Deflection

$$\text{COS}(X) = 2.0 * \text{CSOS} - 1.0$$

and

$$\text{COS}(\text{OF}) = 1.0 - 2.0 * \text{CFP}$$

with

XSOC is the position of separation
CFP is the sum of the flap to wing chord ratios

The equation relates the theoretical maximum-lift increment to the chord of the flap and the position of separation, XSOC, on the airfoil. The choice of the separation point, XSOC, to determine the maximum-lift ratio from equation 2.13.8 depends on the leading-edge configuration. For clean leading-edge airfoils, the point of flow separation is assumed at the leading edge, XSOC = 0. For airfoils with leading-edge high-lift devices, the point of flow separation is assumed to be at the knee of the leading edge device, XSOC = CSOS.

The two-dimensional increment in maximum-lift coefficient of leading-edge devices is predicted in reference 34 as follows:

$$\text{DC1MS} = \text{CMXLE} * \text{EMAX} * \text{ED} * \text{DSR} \quad (2.13.9)$$

where according to thin-airfoil theory,

$$\text{CMXLE} = 2.0 * \text{SIN}(\text{OS})$$

$$\text{COS}(\text{OS}) = (1. - 2. * \text{CSOC})$$

CMXLE is presented in figure 2.13.9
EMAX is taken from the plot in figure 2.13.10
ED is taken from the plot in figure 2.13.11
DSR is the slat deflection

The maximum-lift efficiency factor, EMAX, depends on the type of leading-edge device and on the ratio of leading-edge radius to maximum airfoil thickness; ED is an efficiency factor that accounts for large leading-edge-flap deflections.

In the case of two-dimensional moment increment, the methodology for predicting the pitching moment is developed parallel to the methods used for estimating the lift increment, which extends thin-airfoil theory to cover multiple-slotted flaps with extendable chords. The trailing-edge-flap pitching-moment increment at zero angle of attack is given in reference 34 as:

$$\text{DCM} = \text{DCL} * \text{RCM} * \text{Km} \quad (2.13.10)$$

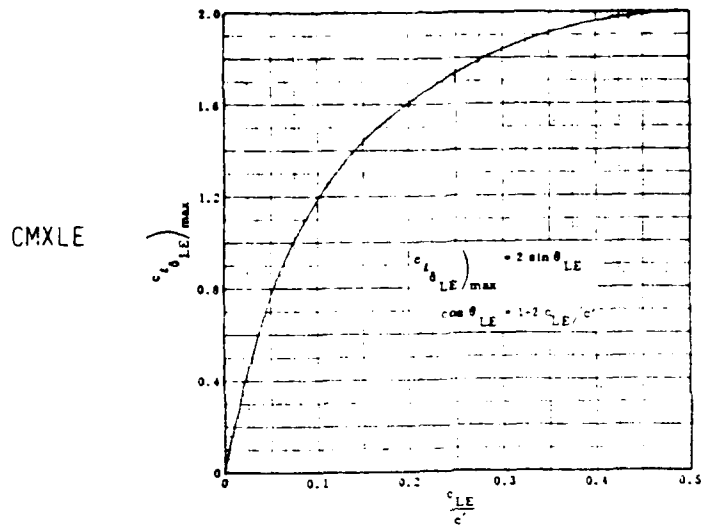


Figure 2.13.9 Leading Edge Flap Maximum Lift Effectiveness

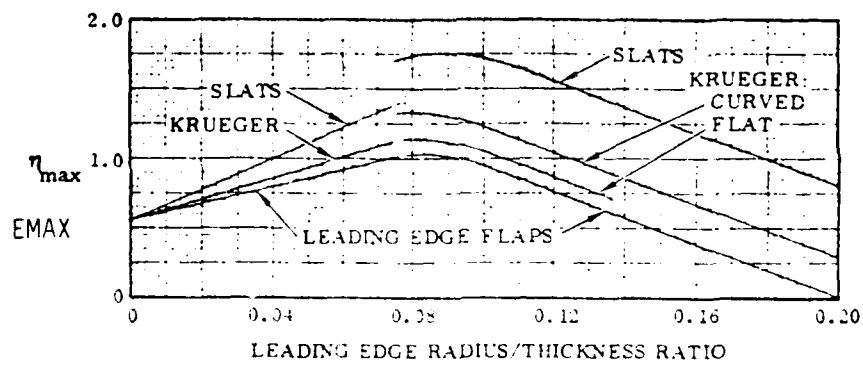


Figure 2.13.10 Maximum Lift Efficiency for Leading-Edge Devices

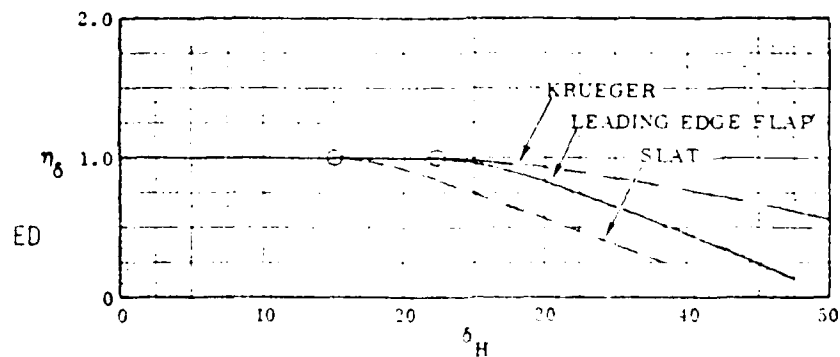


Figure 2.13. Leading Edge Device Deflection Angle Correction Factor

DCL is the predicted lift increment for either trailing-edge or leading-edge devices
RCM is the theoretical center-of-pressure location from thin-airfoil theory (figure 2.13.12)
Km is an empirical factor developed from experimental data (figure 2.13.13)

In the case of the profile drag increment, flap drag increments at ALPHA = 0 for plain and single-slotted flaps are obtained from Figure 2.13.14 and 2.13.15. These figures were obtained from Section 6.1.7 in the DATCOM. For double- and triple-slotted flaps, figure 2.13.16 is used to obtain the alpha = 0 drag increment.

AD-A191 314

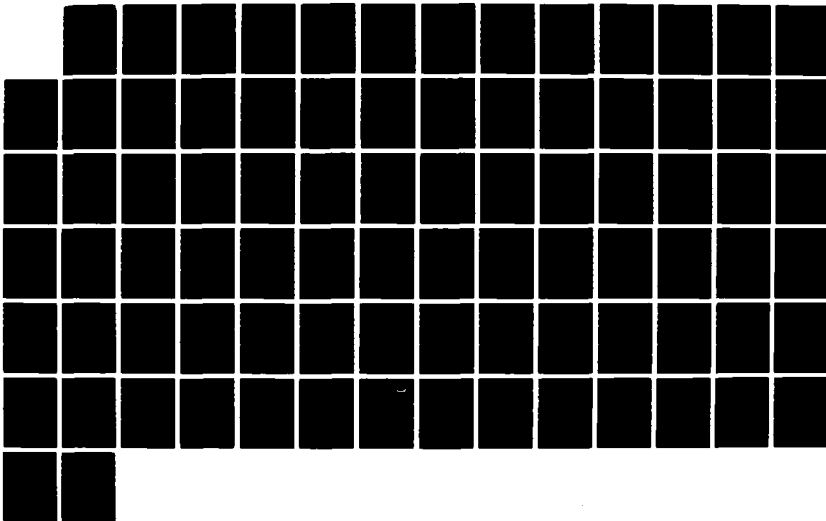
STABILITY AND CONTROL METHODOLOGY FOR CONCEPTUAL
AIRCRAFT DESIGN VOLUME 1. (U) AIR FORCE WRIGHT
AERONAUTICAL LABS WRIGHT-PATTERSON AFB OH. T S SMITH
DEC 87 AFMAL-TR-87-3115-VOL-1

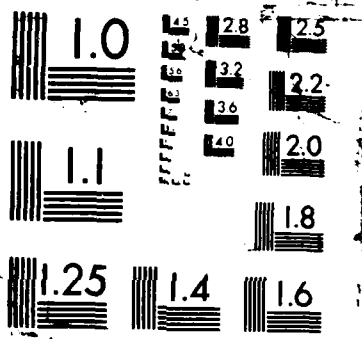
2/2

UNCLASSIFIED

F/G 1/1

ML





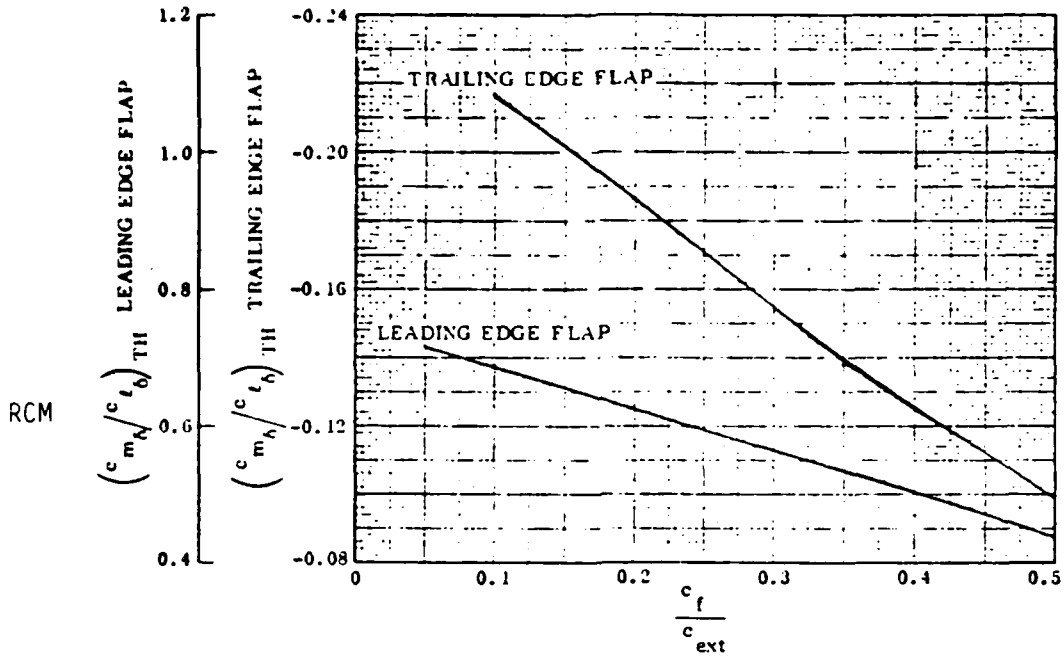


Figure 2.13.10 Flap Center of Pressure Location as given by Thin Airfoil Theory

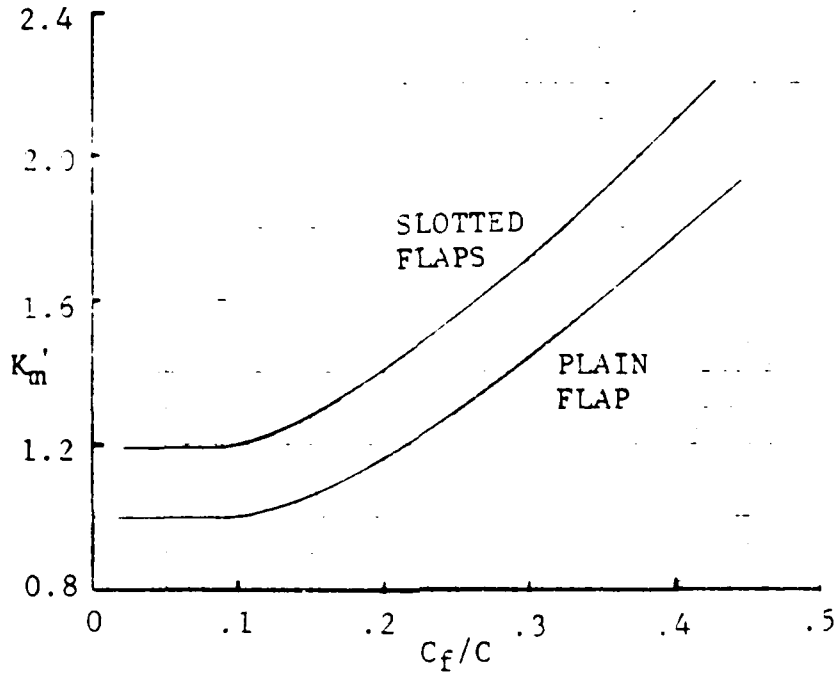


Figure 2.13.13 Moment Correlation Factor Versus Flap Chord

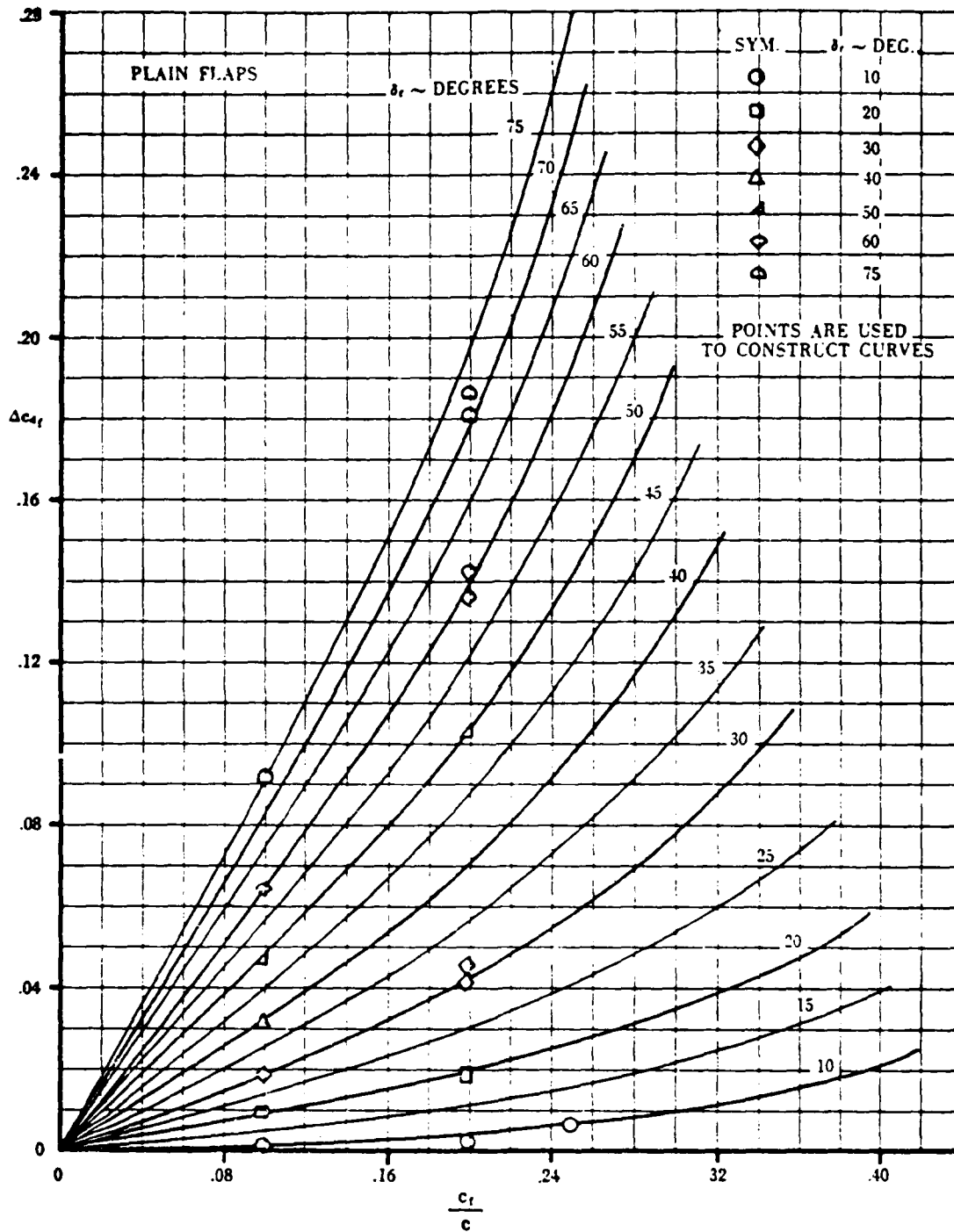


Figure 2.13.14 Two-Dimensional Drag Increment Due to Plain Flaps

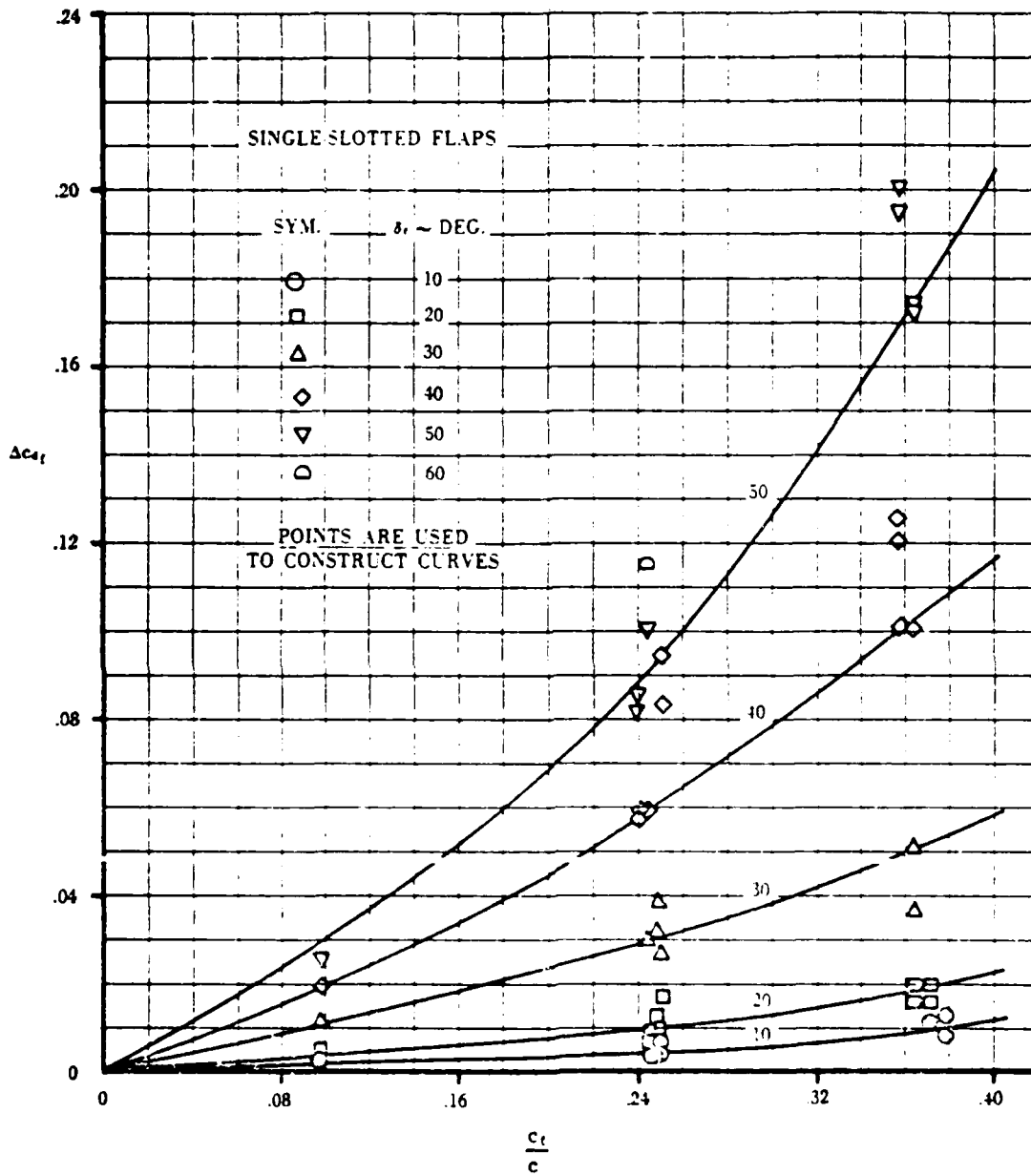


Figure 2.13.15 Two-Dimensional Drag Increment Due to Single-Slotted Flaps

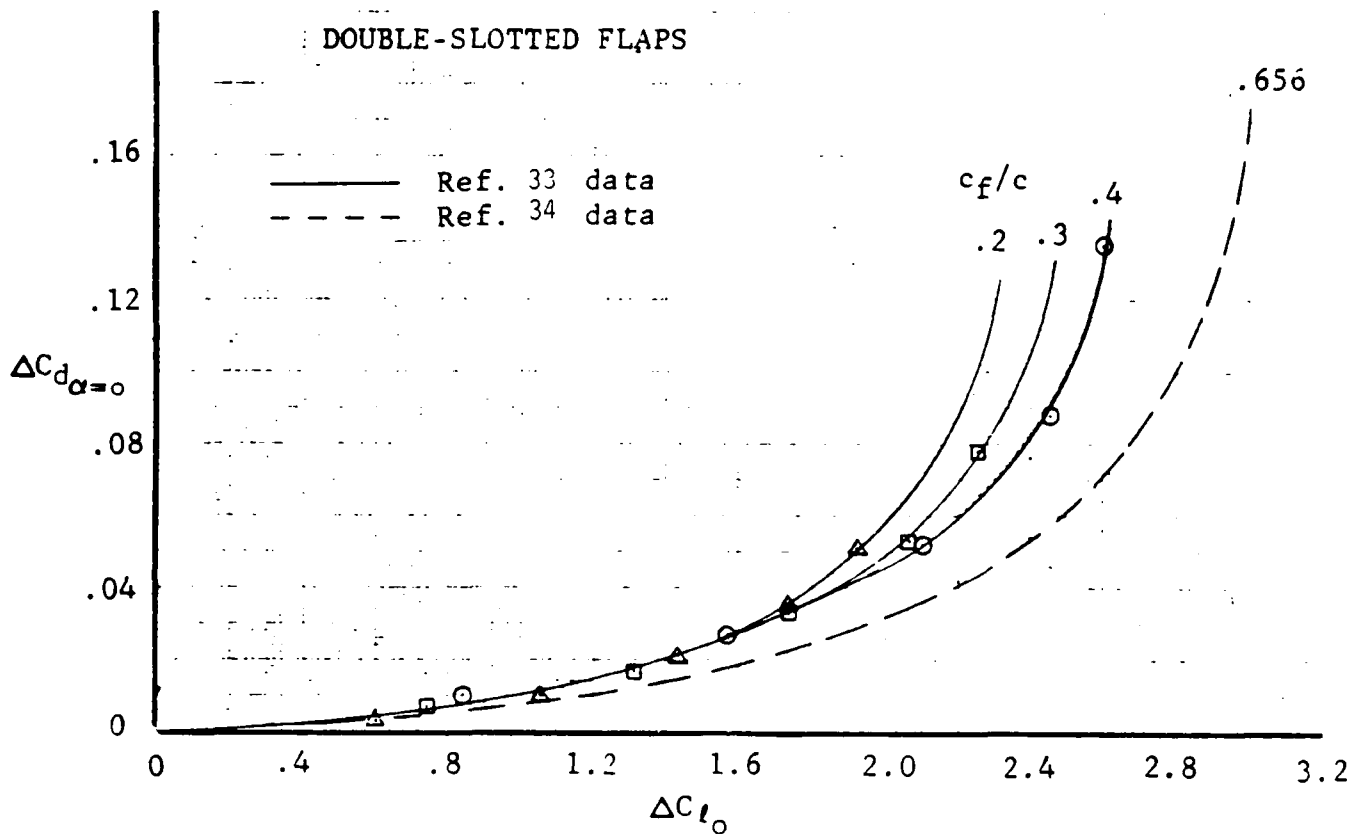


Figure 2.13.16 Drag Increment for Double-Slotted Flaps Versus Lift Increment at $\alpha = 0^\circ$

2.13.2 Lift of High-Lift Devices

The untrimmed equation for lift can be expressed as

$$CL = CLO + CLALPHA * ALPHA \quad (2.13.11)$$

The increment in CLO and CLMAX caused by a trailing-edge-flap deflection can be estimated from

$$DCLOF = DC1F * CLOC1 * Kc * Kb \quad (2.13.12)$$

$$DCLMF = DC1MF * CLOO1 * Kc * Kb * COS(SWEEPMT) \quad (2.13.13)$$

where

DC1F is defined in section 2.13.1
DC1MF is defined in section 2.13.1
Kc is taken from the plot in figure 2.13.18
Kb is taken from the plot in figure 2.13.19

The factor CLOC1, determined from the Polhamus lift equation

$$CLOC1 = ARW / (2.0 + SQRT(4.0 + (SW * ARW / SPLANX / COS(SWEEPMT))^2)) \quad (2.13.14)$$

where

ARW is the aspect ratio of the wing
SW is the area of the wing
SPLANX is the planform area of the wing with flaps extended
SWEEPMT is the maximum thickness sweep of the wing

and converts the sectional values DC1F and DC1MF to the three dimensional case. The sectional values are either obtained from input to the program or generated internally for certain types of high-lift system. The method of generating the section values is discussed in section 2.13.1.

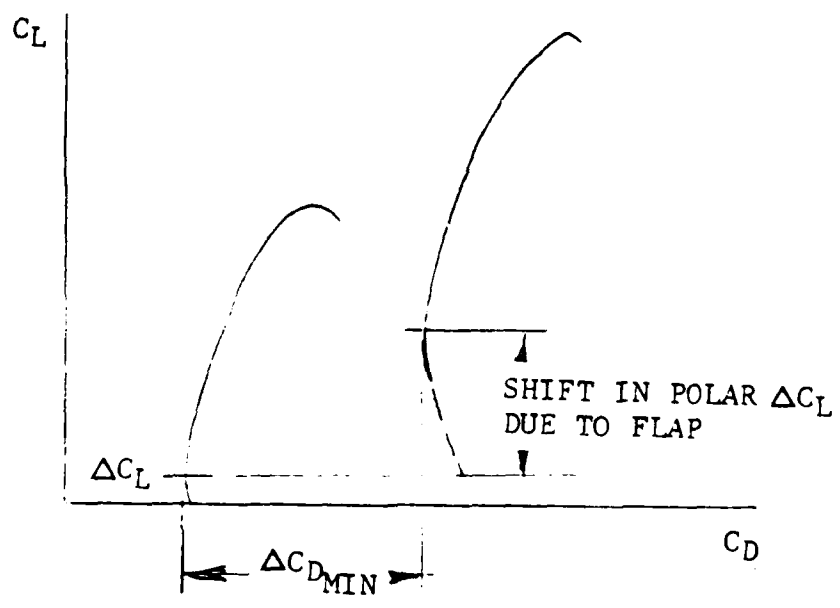
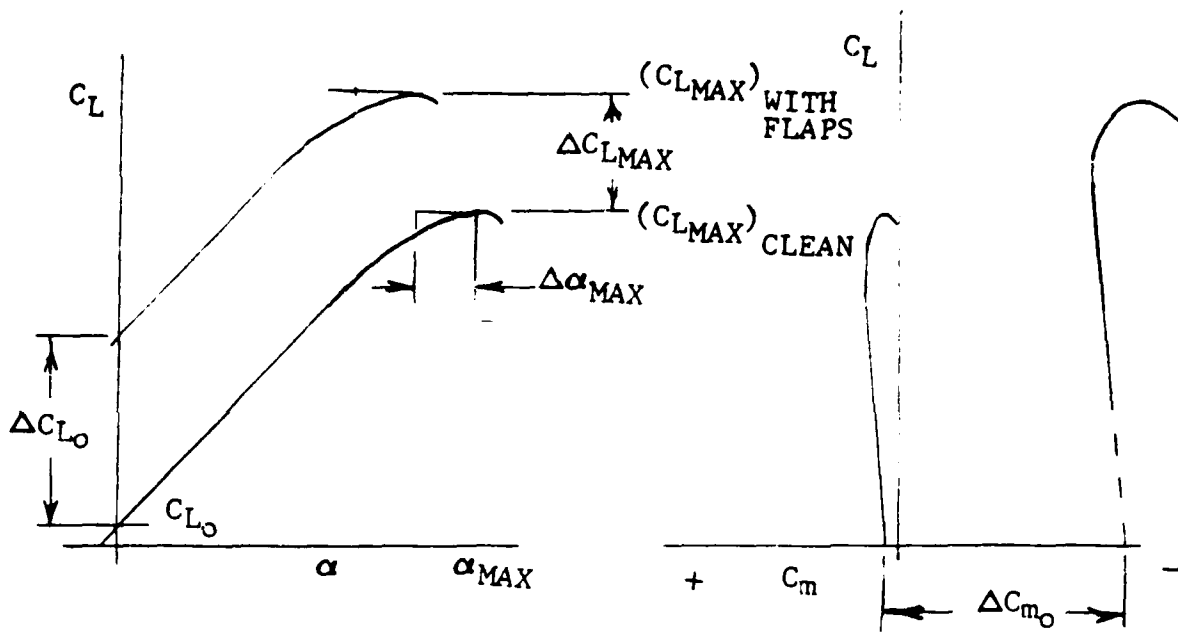


Figure 2.13.17 Incremental Effect of Flaps

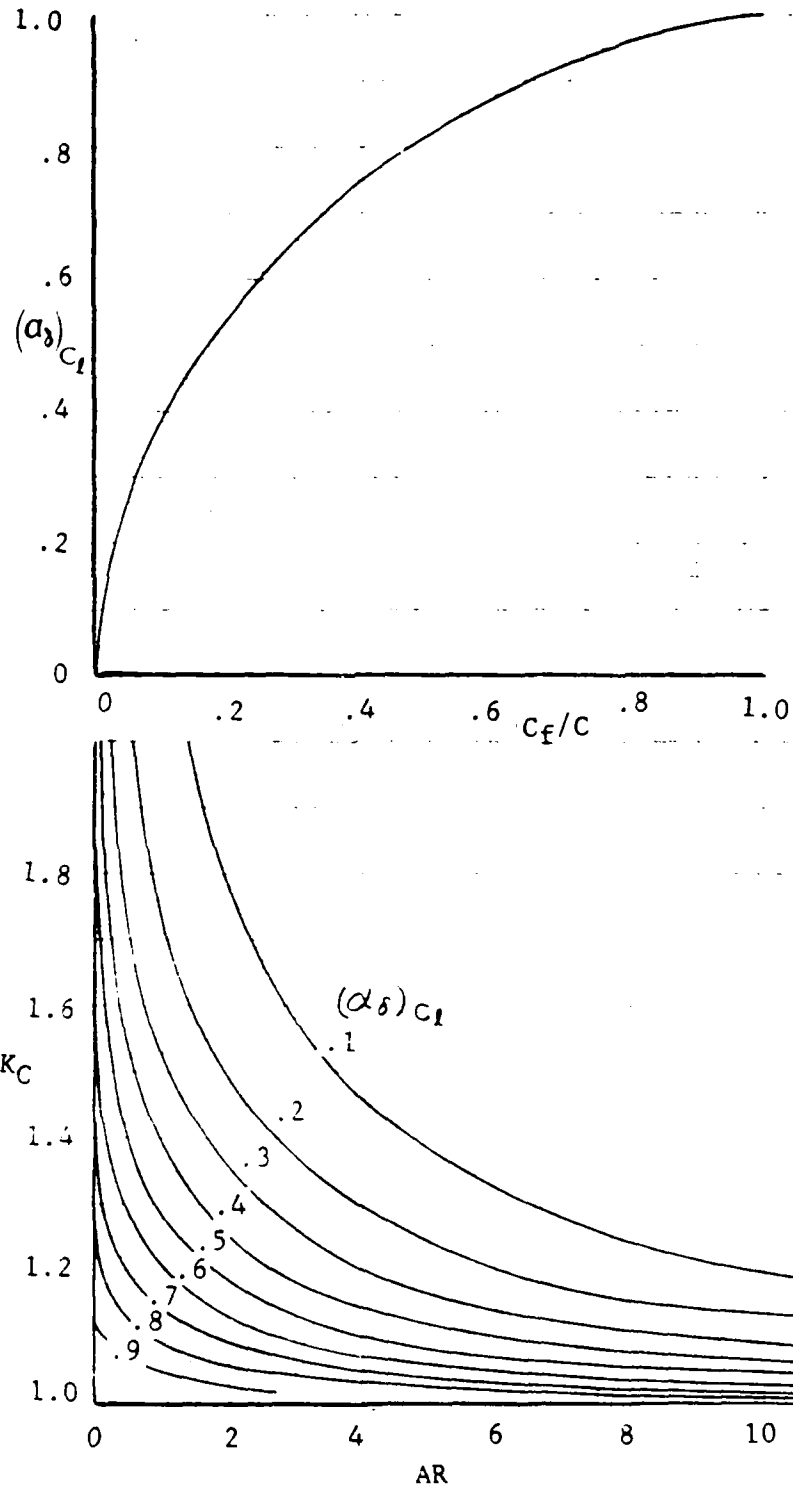


Figure 2.13. Flap Chord Factor

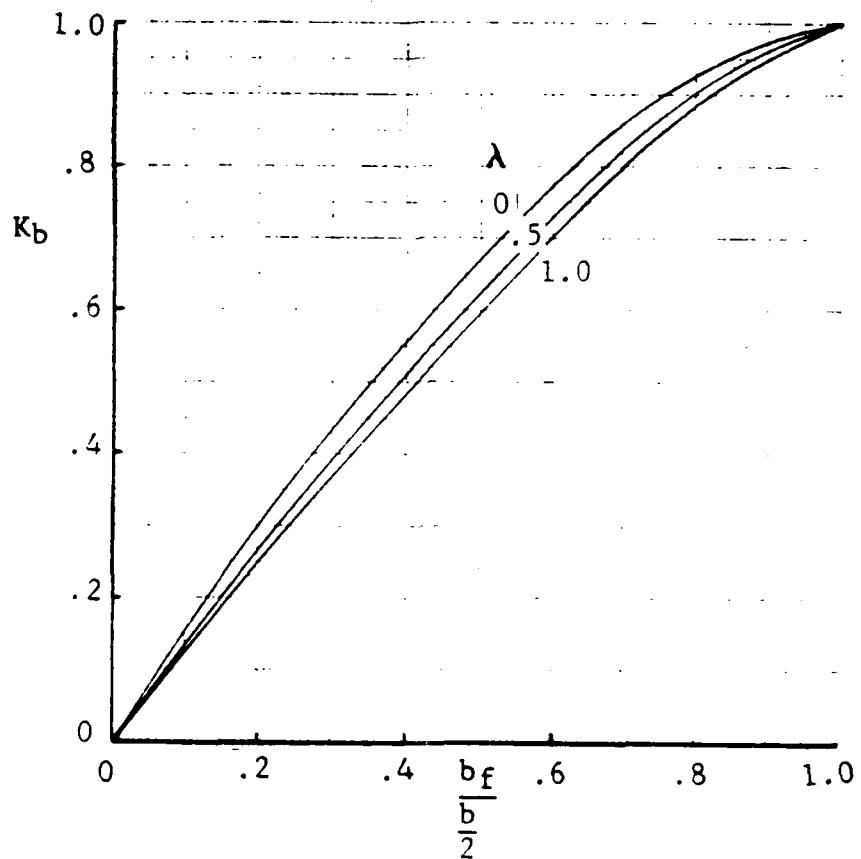
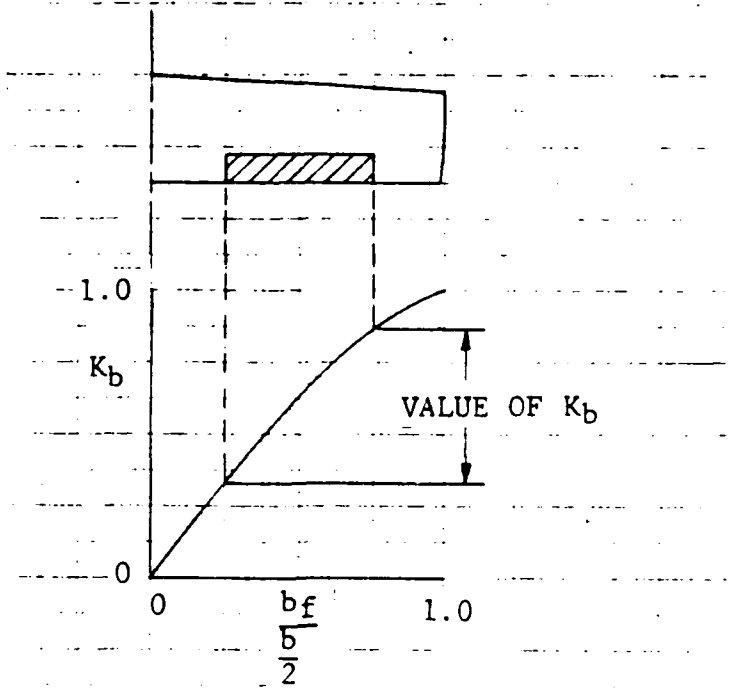


Figure 2.13.19 Flap Span Lift Factor

The increment in lift at zero angle of attack is approximately zero when a slat is deflected. The slat acts to delay separation from the wing leading edge and thus allows higher angles of attack and, consequently, higher values of maximum lift before the wing stalls. An estimate of the increase in maximum lift of a slat is represented by

$$DCLMS = DC1MS * CLOC1 * Ks * COS(SWEEPLE) \quad (2.13.15)$$

where

SWEEPLE is the leading edge sweep of the wing
 Ks is taken from the plot in figure 2.13.20
 DC1MS is the sectional increase in maximum lift of a slat

2.13.3 Drag of High-Lift Devices

The untrimmed equation for drag can be expressed by

$$CD = CDO + K * (CL - DCL)^2 \quad (2.13.16)$$

where the drag-due-to lift factor, K, with high lift devices can be estimated by

$$K = (CD - CDO / CL^2) * (SREF / SPLANX) \quad (2.13.17)$$

The change in minimum drag for the high-lift configuration is expressed as

$$DCDMIN = DCDF + DCDS + CDI + CDCLEAN \quad (2.13.18)$$

where increments are summed for the profile drag caused by the flaps (DCDF) and the slats (DCDS). The increment in profile drag of the flaps and slats can be estimated from sectional drag data, using

$$DCDF = DCDFS * COS(SWEEPHL) * Kd \quad (2.13.19)$$

$$DCDS = DCDSS * COS(SWEEPLE) * Kd \quad (2.13.20)$$

where

SWEEPHL is the sweep of the high-lift system
 Kd is taken from the plot in figure 2.13.21
 DCDFS is the section DCDF given in section 2.13.1
 DCDSS is the section DCDS given in section 2.13.1

Deflection of a flap produces an increase in lift at zero angle of attack which in turn produces an induced drag given by

$$CDI = Ka * Kf * DCLOF^2 / (PI * ARW) \quad (2.13.21)$$

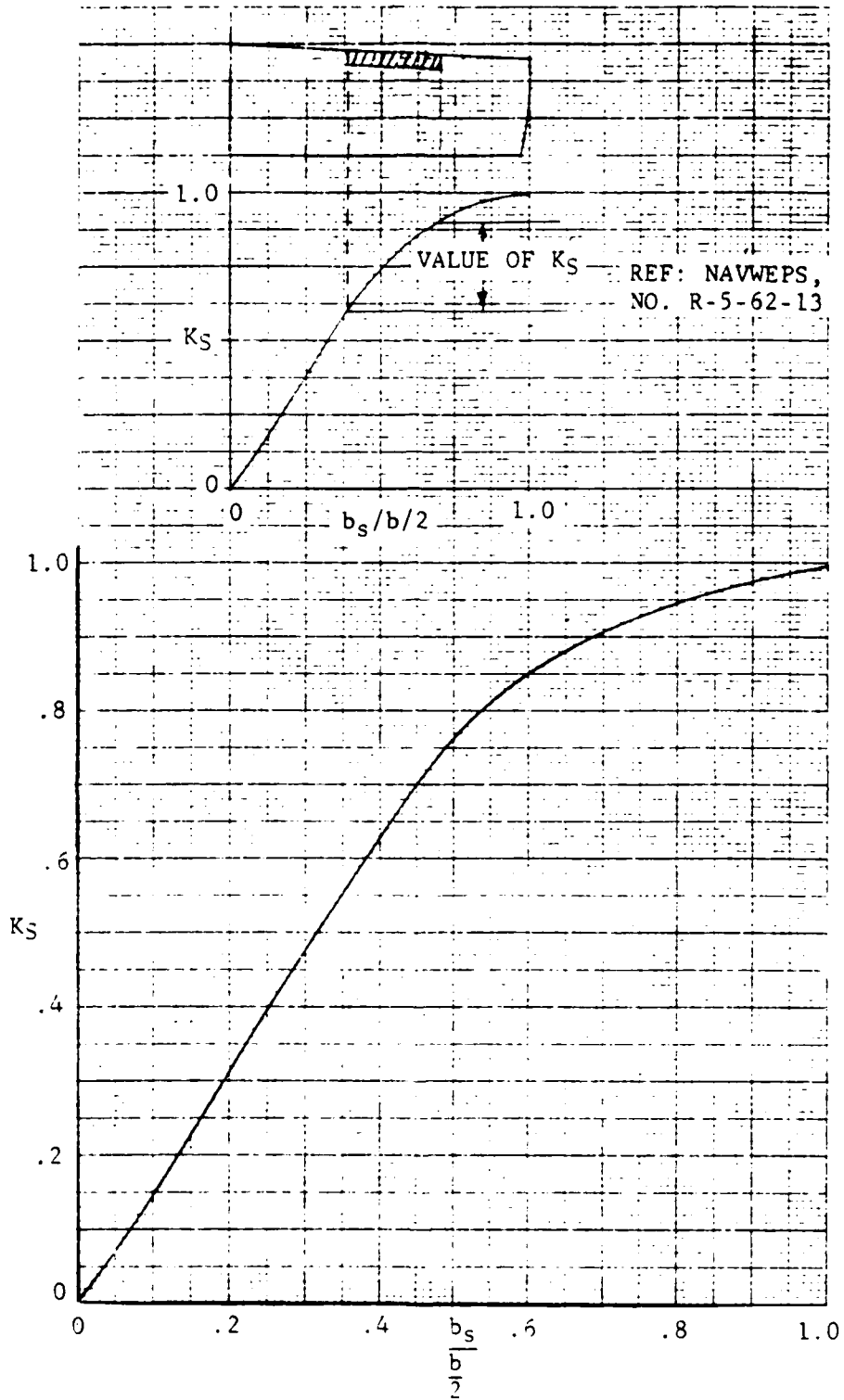


Figure 2.13.0 Slat Span Lift Factor

EFFECTS OF FLAP SPAN ON DRAG

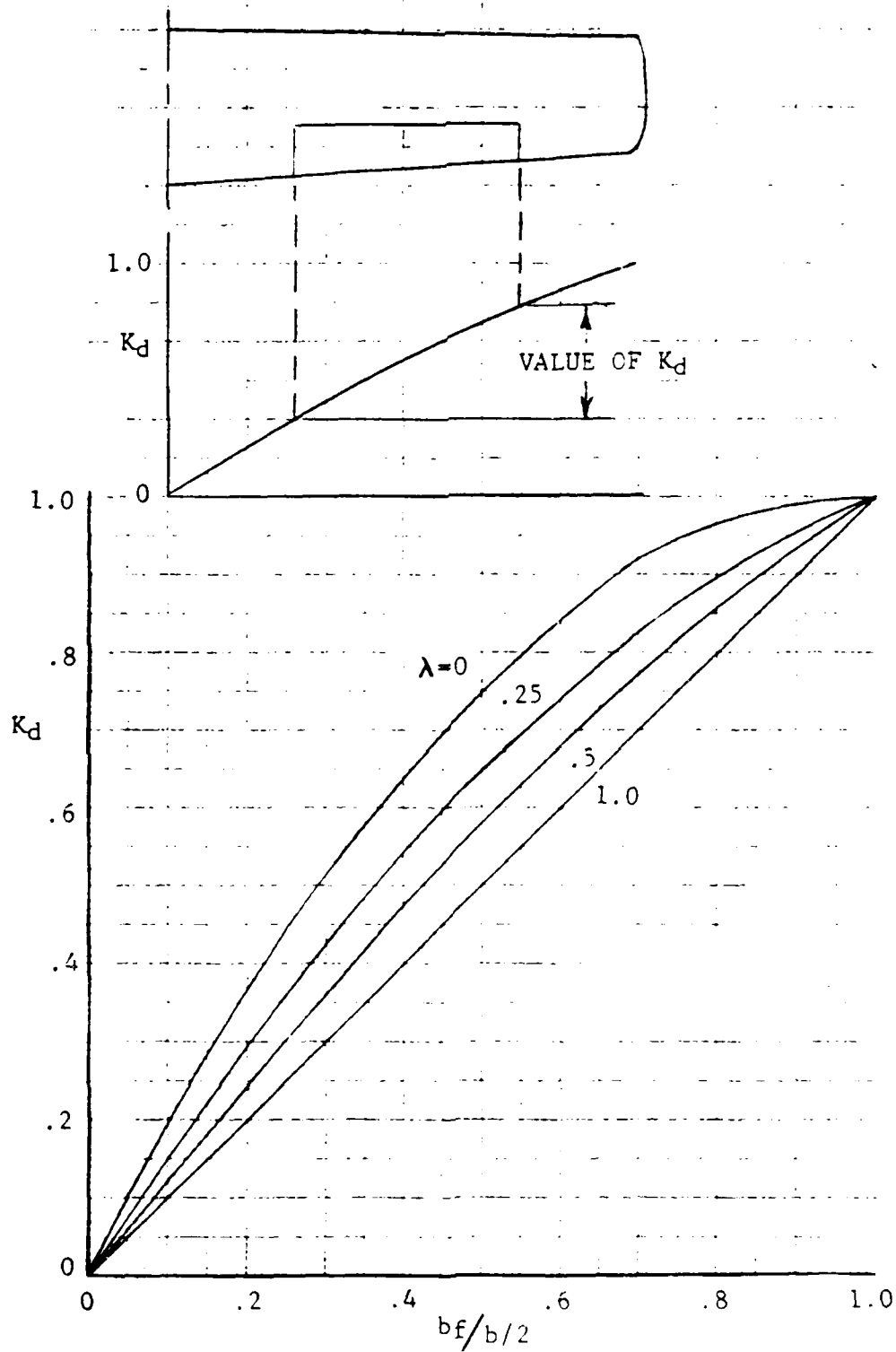


Figure 2.13.21 Flap Span Drag Factor

where

Ka is taken from the plot in figure 2.13.22

Kf is taken from the plot in figure 2.13.22

Ka and Kf are factors which account for the nonelectrical span loading of partial-span flaps.

The deflection of a flap increases the camber of the airfoil. In reference 33, thin-airfoil camber theory is used to relate the displacement of a polar with flaps to the lift increment of the flap at zero angle of attack by the equation.

$$DCL = DCL_{CLEAN} + DCLF$$

where

$$DCLF = \frac{(1 - 1/(\pi * ARW * AK)) * DCLOF}{(.5 - CF)} / (1 + 1.16 * CLOC1 * \dots) \quad (2.13.22)$$

and

AK is the drag due to lift

CF is the flap to wing chord ratio

DCLOF is the increment in CLO caused by a flap deflection from Section 2.13.2

2.13.4 Moment of High-Lift Devices

The pitching moment increment caused by a flap on a swept wing is represented by

$$DCMAF = DCMFS * CPF^2 * Km + .5 * ARW * \tan(SWEEPC2) * DCIF * Ksw \quad (2.13.23)$$

where

DCMFS is the sectional change in moment at zero alpha due to flap deflection

DC1F is the sectional change in lift at zero alpha due to flap deflection

CPF is the flap to wing chord ratio

ARW is the aspect ratio of the wing

SWEEPC2 is the half chord sweep of the wing

Km is taken from the plot in figure 2.13.23

Ksw is taken from the plot in figure 2.13.24

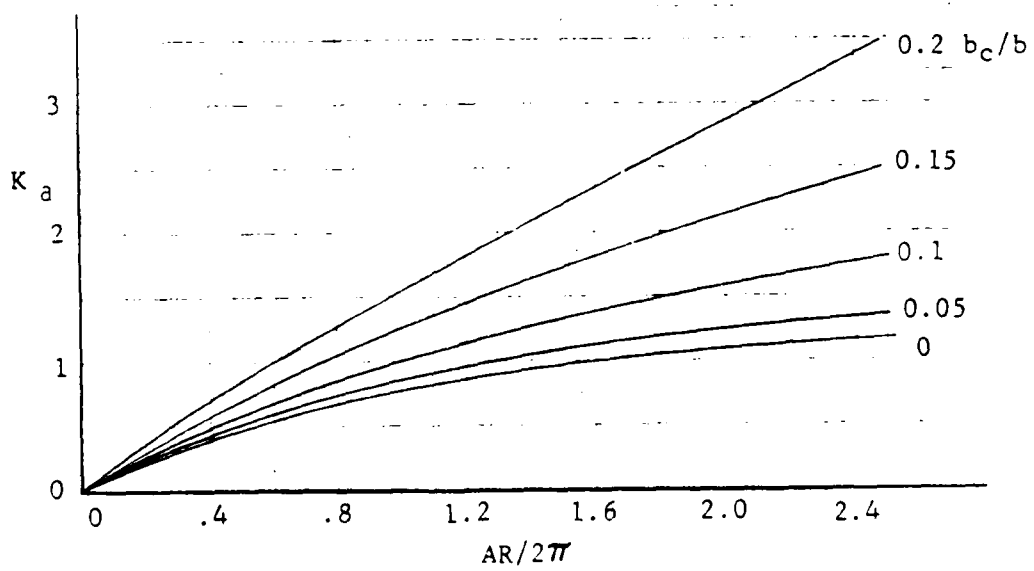
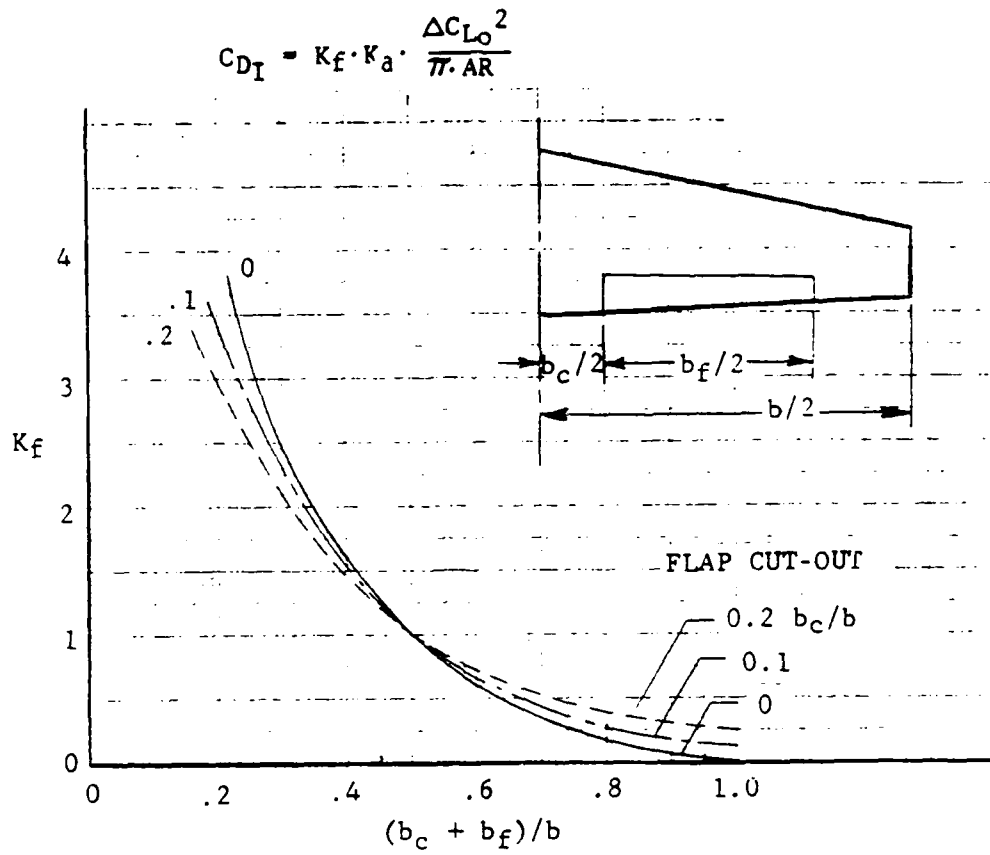


Figure 2.13.22 Flap-Induced Drag Factors

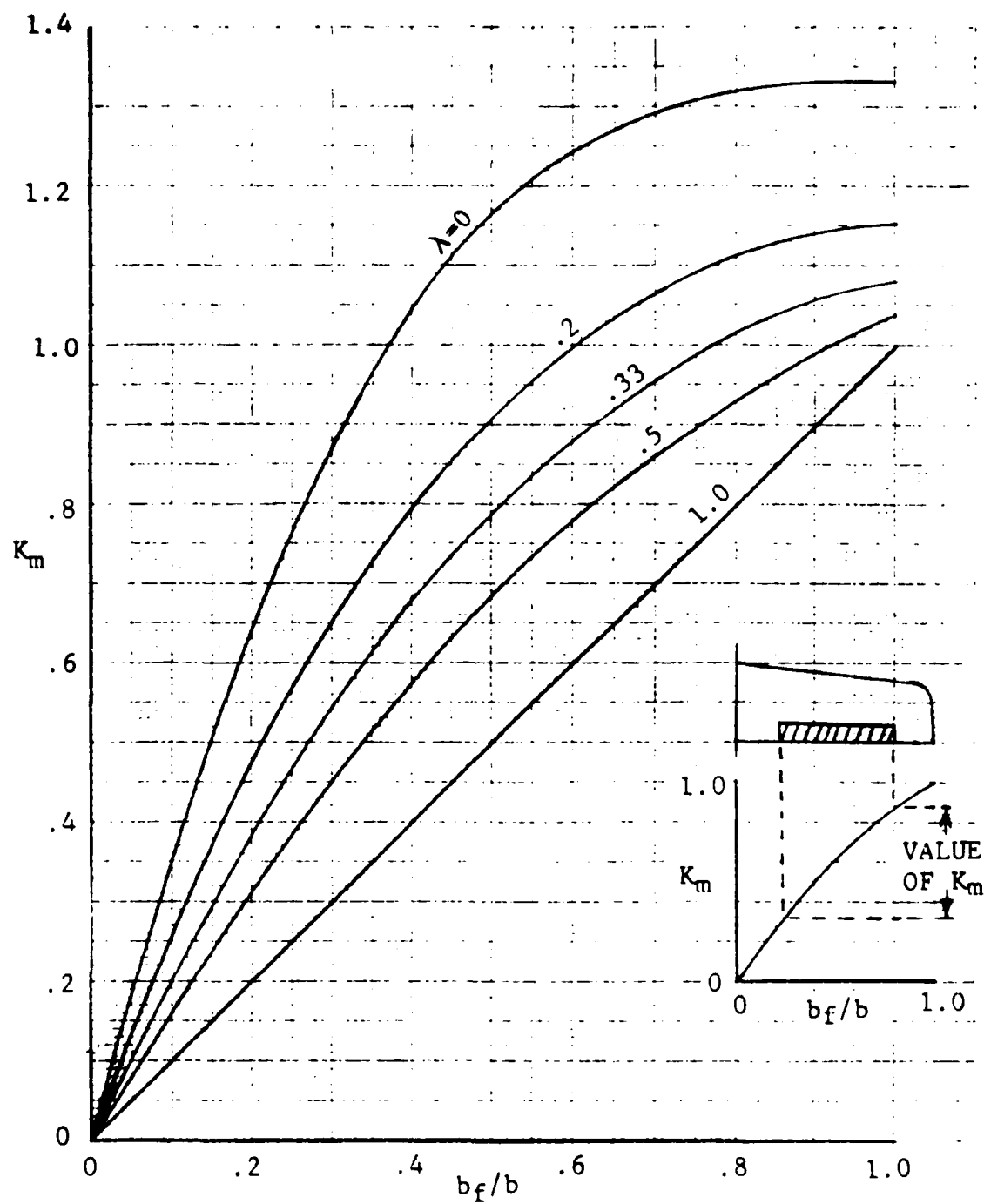


Figure 2.13.23 Span Effect on Moments

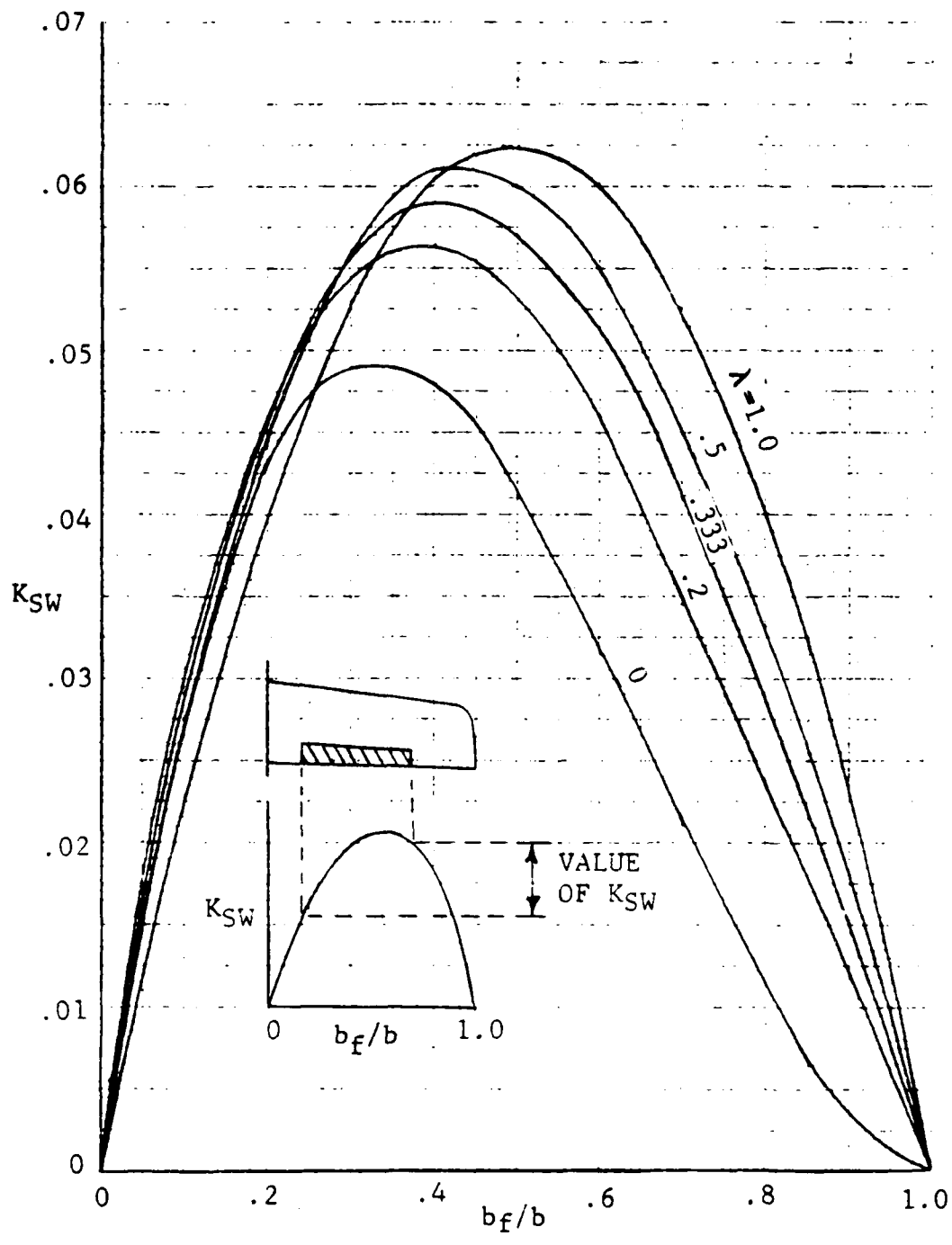


Figure 2.13.24 Span Effect on Moments of Sweptback Wings

3.0 STABILITY COEFFICIENTS METHODS

The methods described below are used to compute the lateral stability derivatives of an aircraft. The methods include some taken from DATCOM (8), and some that have been developed for use in SACP. The derivatives that are to be computed are; the variation of rolling moment coefficient with roll rate (CLP), the variation of rolling moment coefficient with aileron angle (CLDA), the variation of rolling moment coefficient with sideslip angle (CLB), the variation of yawing moment coefficient with sideslip angle (CNB), the variation of yawing moment coefficient with rudder angle (CNRD), and the variation of yawing moment coefficient with yaw rate (CNR).

3.1 CLP

The variation of rolling moment coefficient with roll rate (CLP) can be computed as the simple sum of; CLP for the Body with wing interference (CLPWB), CLP for the horizontal tail (CLPHT), CLP for the canard (CLPC) and CLP for the vertical tail (CLPVT). The equation for CLP is then just

$$CLP = CLPWB + CLPW + CLPHT + CLPC + CLPVT \quad (3.1.1)$$

where computation of each of the components is described below.

3.1.1 CLP For Lifting Surfaces

The method for computing the wing rolling derivative, CLPW, is given in the DATCOM. This method can be extended to other lifting surfaces by referencing the results to the appropriate reference area. This section presents the DATCOM methods for estimating the CLPS at subsonic and supersonic speeds for all lifting surfaces.

The DATCOM method for computation of CLPS at subsonic speeds accounts for the variations in wing lift curve slope, drag due to lift, and profile drag, as well as the effect of dihedral. The values of CLPS at a given lift coefficient at subsonic speeds, based on the product of the surface area and the square of the surface span, $SA * SPAN^2$, is given by

$$CLPS = (RDPZL * (K/BETA) * (CLALP/CLALPO) * DIHP) + DCLPD \quad (3.1.2)$$

where

RDPZL is the damping parameter at zero lift obtained from figure 3.1.1 as a function of SWPBETA and BA/K

SWPBETA is the compressible sweep parameter given by

$$SWPBETA = \text{ARCTAN}(\text{TAN}(C_4\text{SWEEP})/BETA)$$

SUBSONIC SPEEDS

(a) $\lambda = 0$

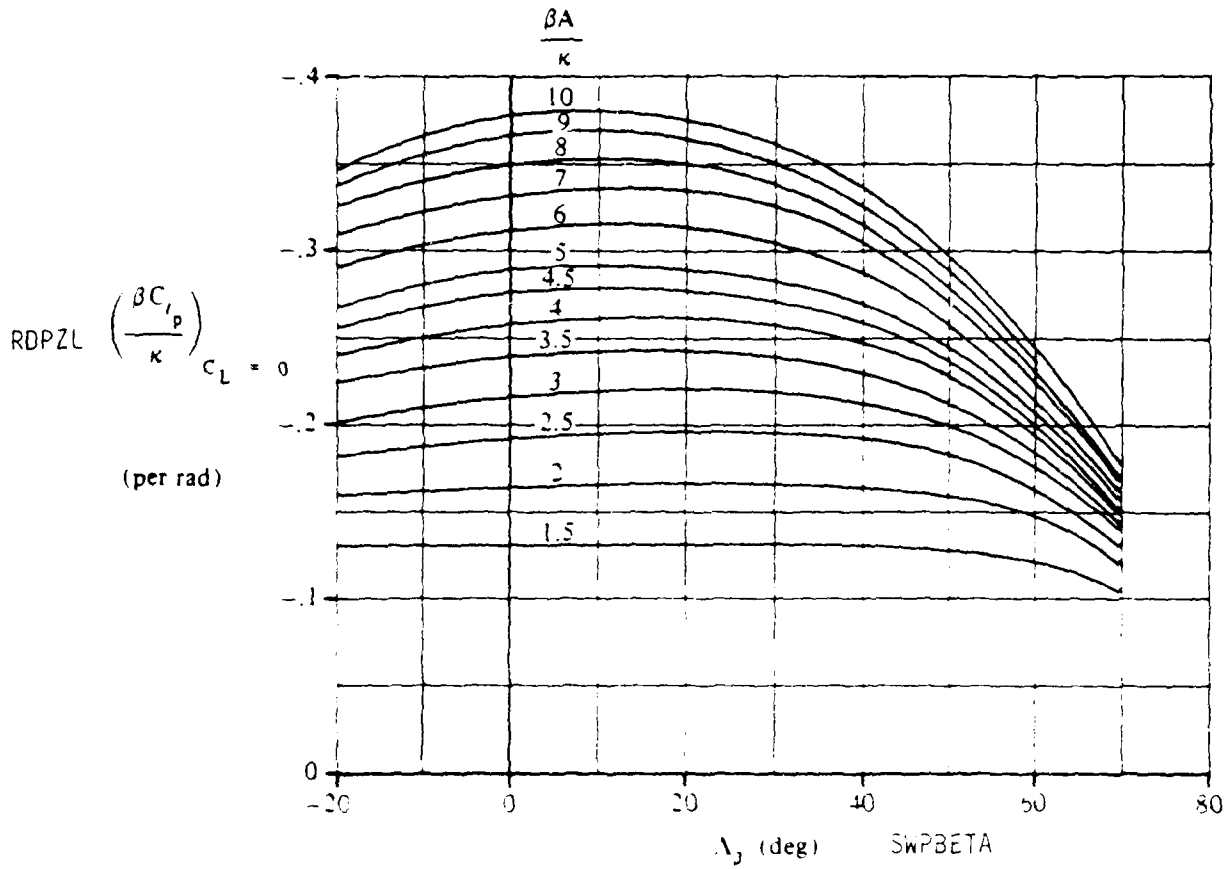


Figure 3.1.1 ROLL-DAMPING PARAMETER AT ZERO LIFT

SUBSONIC SPEEDS

(b) $\lambda = 0.25$

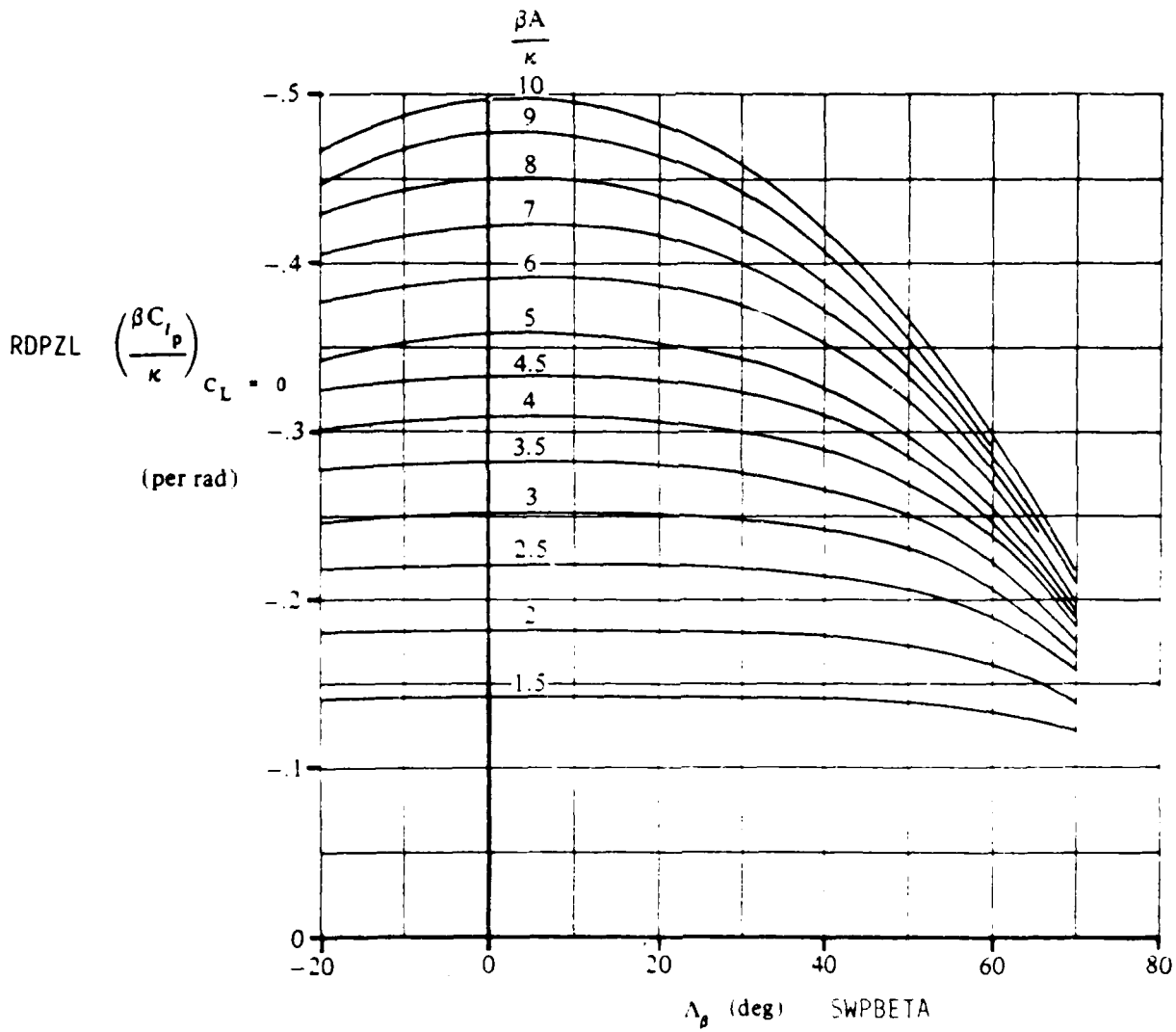


Figure 3.1.1 (CONTD)

SUBSONIC SPEEDS

(c) $\lambda = 0.50$

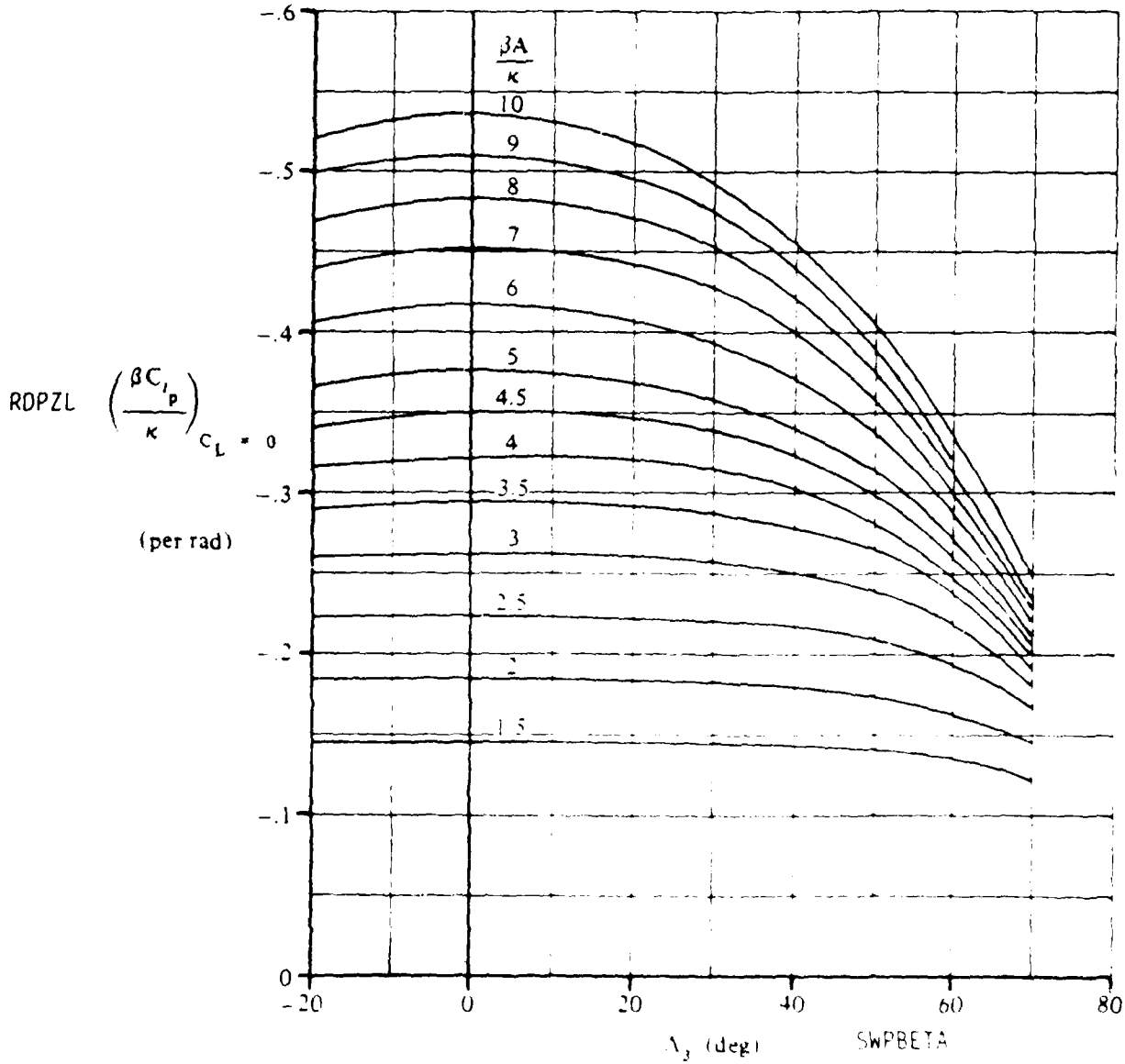


Figure 3.1.1 (CONTD)

SUBSONIC SPEEDS

(d) $\lambda = 1.0$

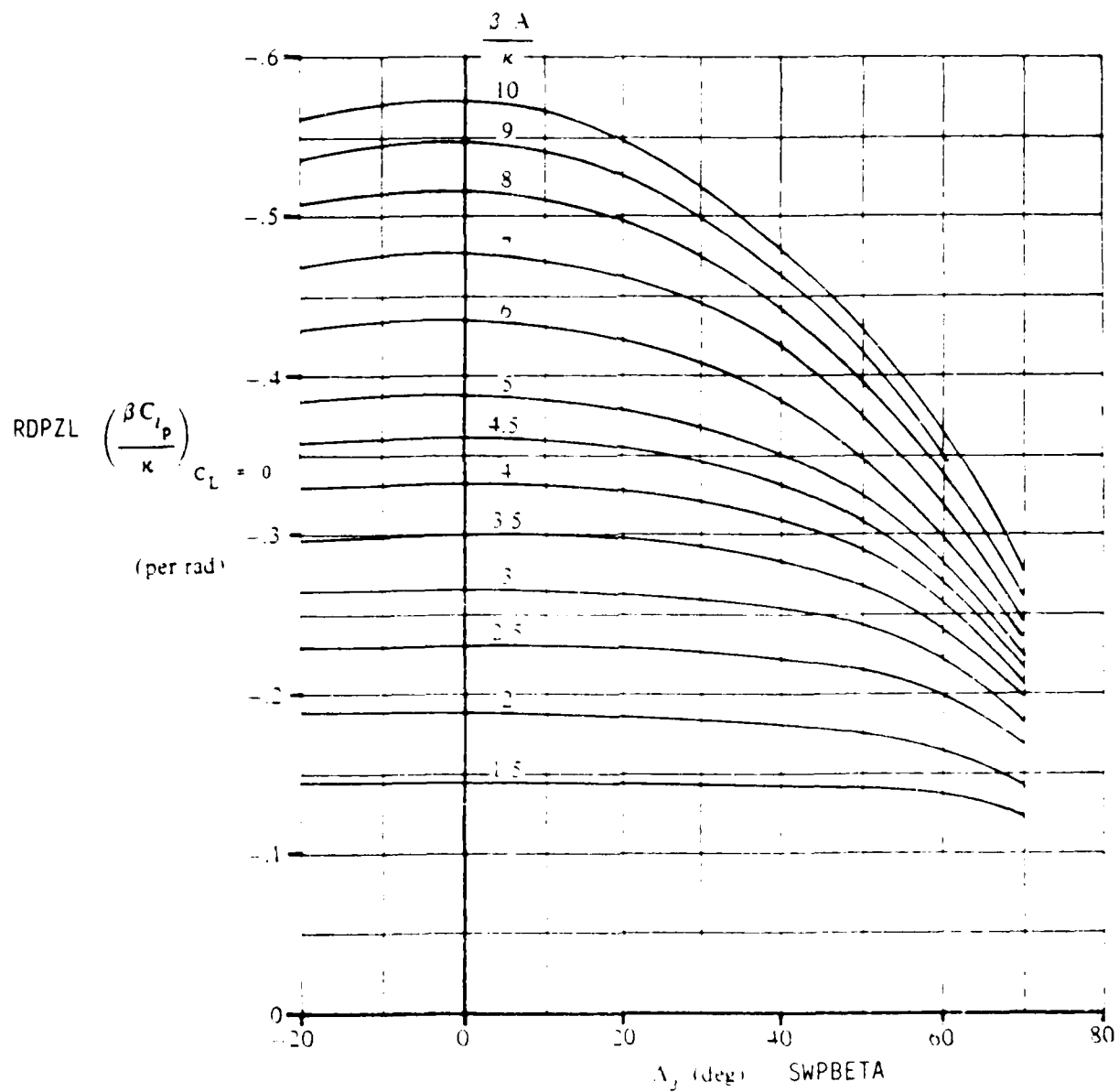


Figure 3.1.1 (CONTD)

$$BETA = \text{SQRT}(1.0 - \text{MACH}^2)$$

$$BAK = BETA * \text{ARS}/K$$

ARS is the aspect ratio of the surface

The parameter K is the ratio of the two-dimensional lift curve slope at the appropriate Mach number to $2.0 * \text{PI}/BETA$. i.e.,

$$K = \text{CLALP}/(2.0 * \text{PI}/BETA) \quad (3.1.3)$$

CLALP is the surface lift curve slope at any lift coefficient below stall

CLALPO is the surface lift curve slope at zero lift

DIHP is the dihedral-effect parameter given by

$$\text{DIHP} = 1.0 - 2.0 * (\text{ZCG}/(\text{SPAN}/2.0)) * \text{SIN}(\text{DIHSR}) + ((\text{ZCG}/(\text{SPAN}/2.0))^2 * ((\text{SIN}(\text{DIHSR})^2))) \quad (3.1.4)$$

DIHSR is the geometric dihedral angle, positive for surface tip above surface root.

ZCG is the vertical distance between the aircraft center of gravity and the surface root chord, positive for c.g. above the root chord

DCLPD is the increment in the roll damping derivative due to drag. It is given by

$$\text{DCLPD} = \text{DDL RDP} * \text{CL}^2 - 1/8 * \text{CDO} \quad (3.1.5)$$

where

DDL RDP is the drag due to lift roll damping parameter obtained from figure 3.1.2 as a function of ARS and C4SWEEP

CL is the surface lift coefficient

and

CDO is the total zero lift drag coefficient

For wings of low aspect ratio and/or high sweep the accuracy of the method rapidly deteriorates with increasing CL, even when experimental values of lift and drag are used. The error results from the fact that the high values obtained from figure 3.1.2 for these configurations are not realized in practice. Therefore, as CL increases the calculated values of the roll damping derivative become progressively smaller than those given by experiment.

At supersonic speeds, design charts based on theoretical calculations are presented for estimating CLP of surfaces. In this case CLP is given by

$$\text{CLP} = \text{CLPATF} * \text{ARS} * \text{CLPCLT} \quad (3.1.6)$$

SUBSONIC SPEEDS

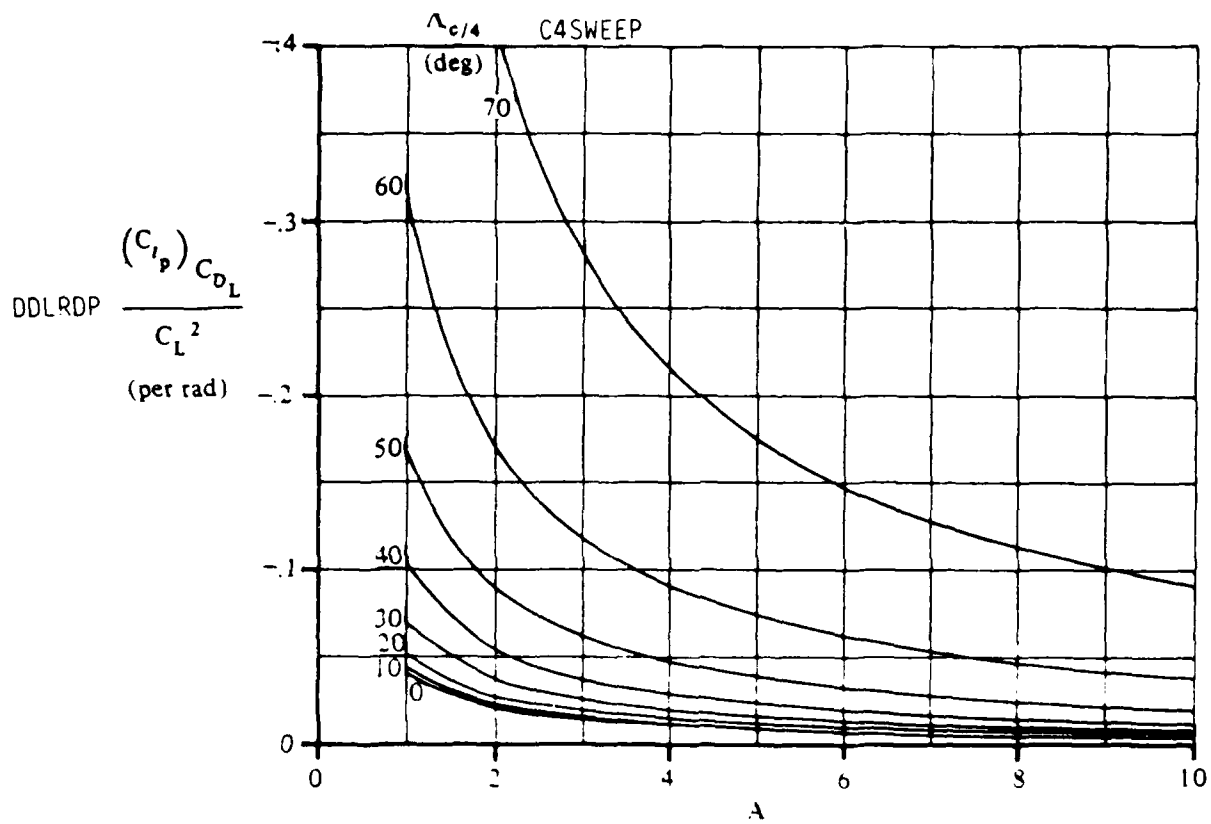


Figure 3.1.2 DRAG-DUE-TO-LIFT ROLL-DAMPING PARAMETER

where

CLPAT is the theoretical roll-damping parameter obtained from figure 3.1.3a through 3.1.3e

and

CLPCLPT is the empirical thickness correction factor obtained from figure 3.1.4

The sonic trailing edge boundaries on figure 3.1.3a through 3.1.3e represent an upper limit for the true theoretical values of the derivatives. Values below the sonic trailing-edge boundary are for wings with subsonic trailing edges and are in violation of one of the basic assumptions of the theory. For configurations with subsonic trailing edges the design charts will over-estimate the roll damping derivative.

It should be noted that the "kinks" in the curves of figure 3.1.3a through 3.1.3e correspond to the conditions of sonic leading edges. Experimental evidence shows that these kinks do not occur in practice.

3.1.2 CLP For the Vertical Tail

The contribution of CLP due to vertical tails is, according to Roskam (23),

$$CLPVT = -2.0 * CLALPVO * (ZV/SPAN)^2 * NV * SV/SW * VNO \quad (3.1.7)$$

where

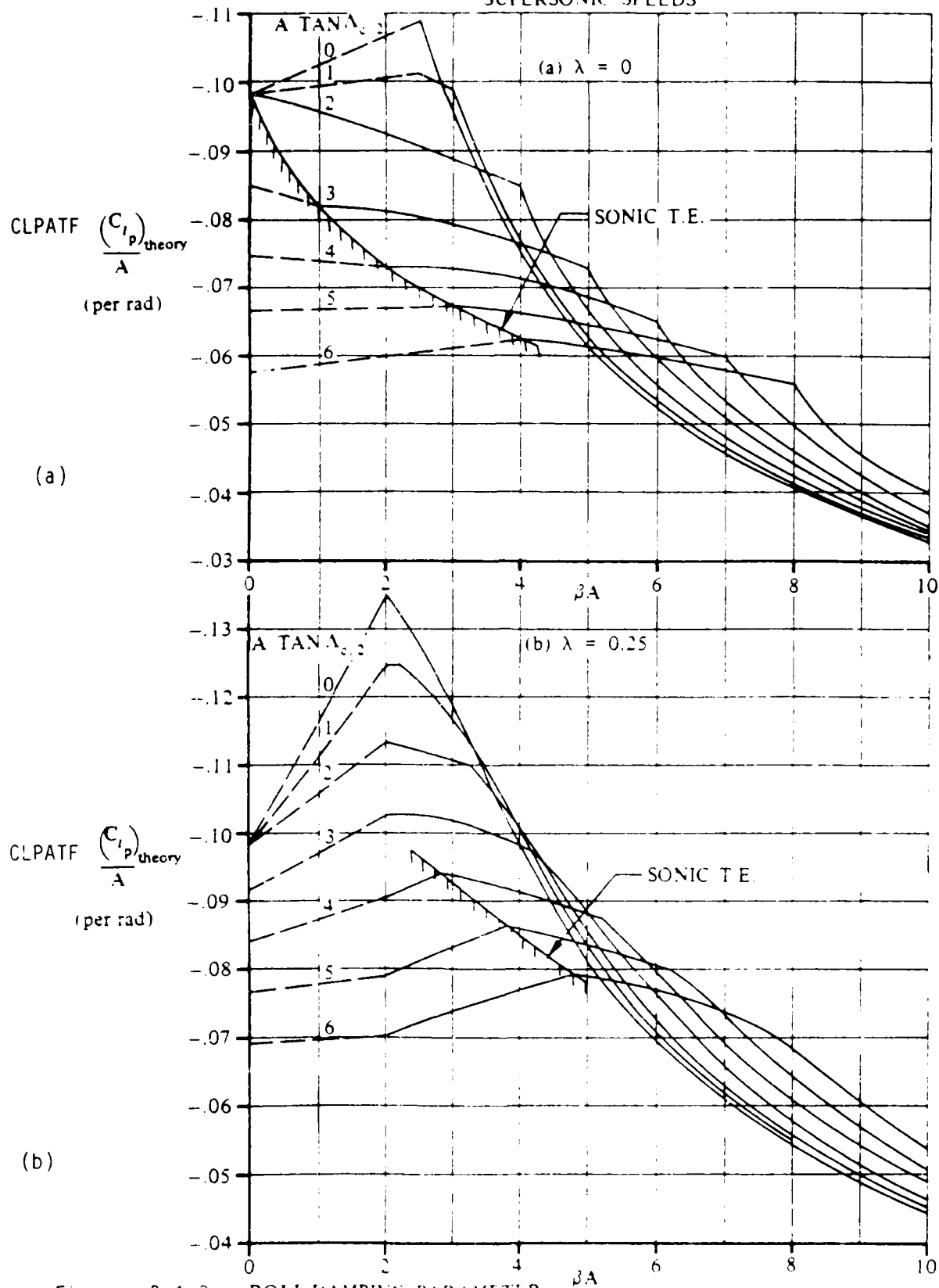
CLALPVO is the vertical tail lift curve slope
ZV is the vertical location of the mean aerodynamic chord of the vertical tail
NV is the vertical tail sidewash factor
SV is the area of the vertical tail
SW is the area of the wing
SPAN is the vertical tail span
VNO is the number of vertical tails

3.1.3 CLP for Wing-Body Interaction

This section presents methods for estimating the wing-body contribution to the rolling derivative CLP at subsonic and supersonic speeds. This derivative is the change in rolling-moment coefficient with change in the wing tip helix angle and is referred to as the roll damping derivative.

For subsonic speeds there is no body contribution to CLPWB so the value is simply

SUPERSONIC SPEEDS



SUPERSONIC SPEEDS

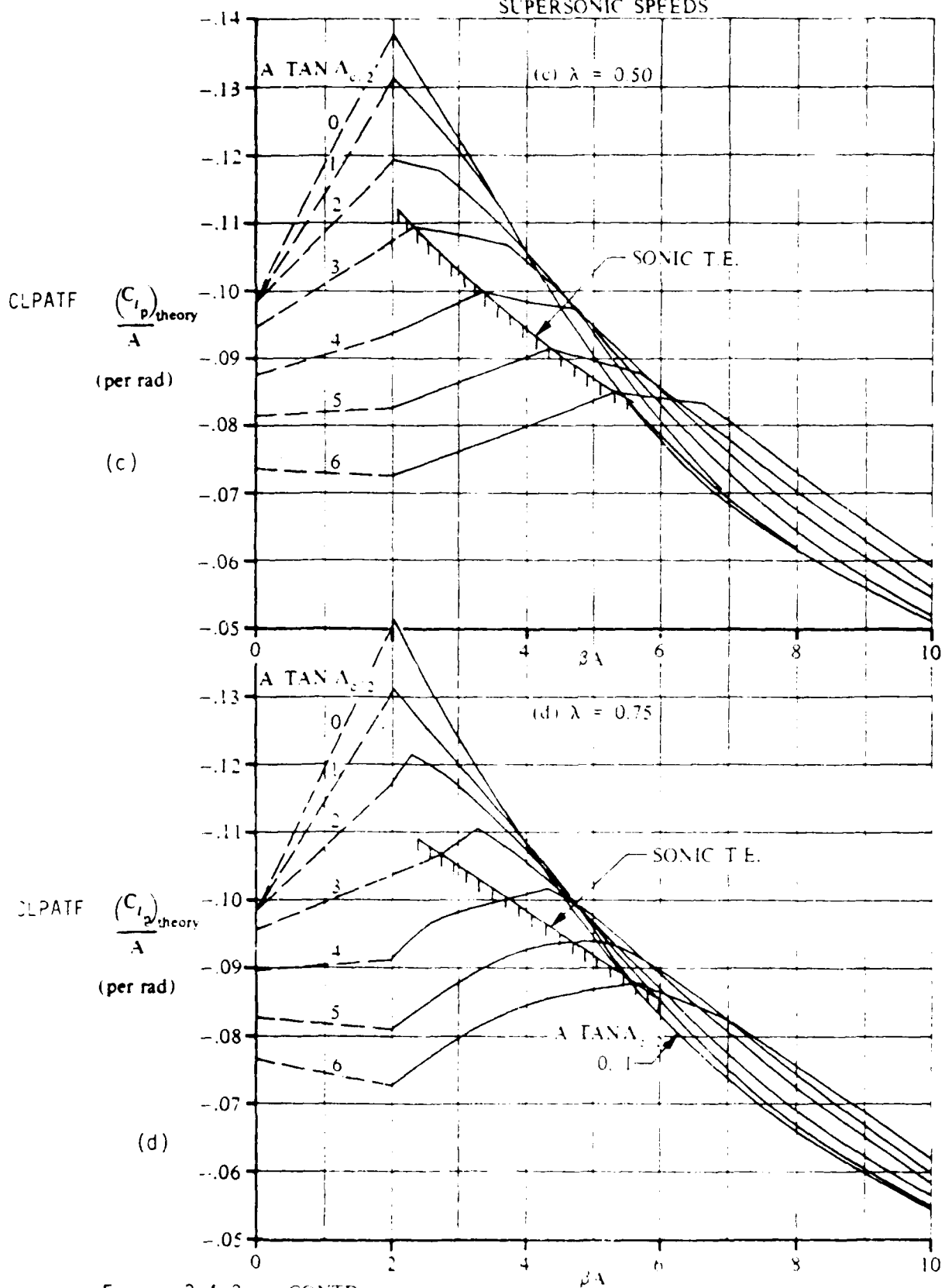


Figure 3.1.3 (CONTD)

SUPERSONIC SPEEDS

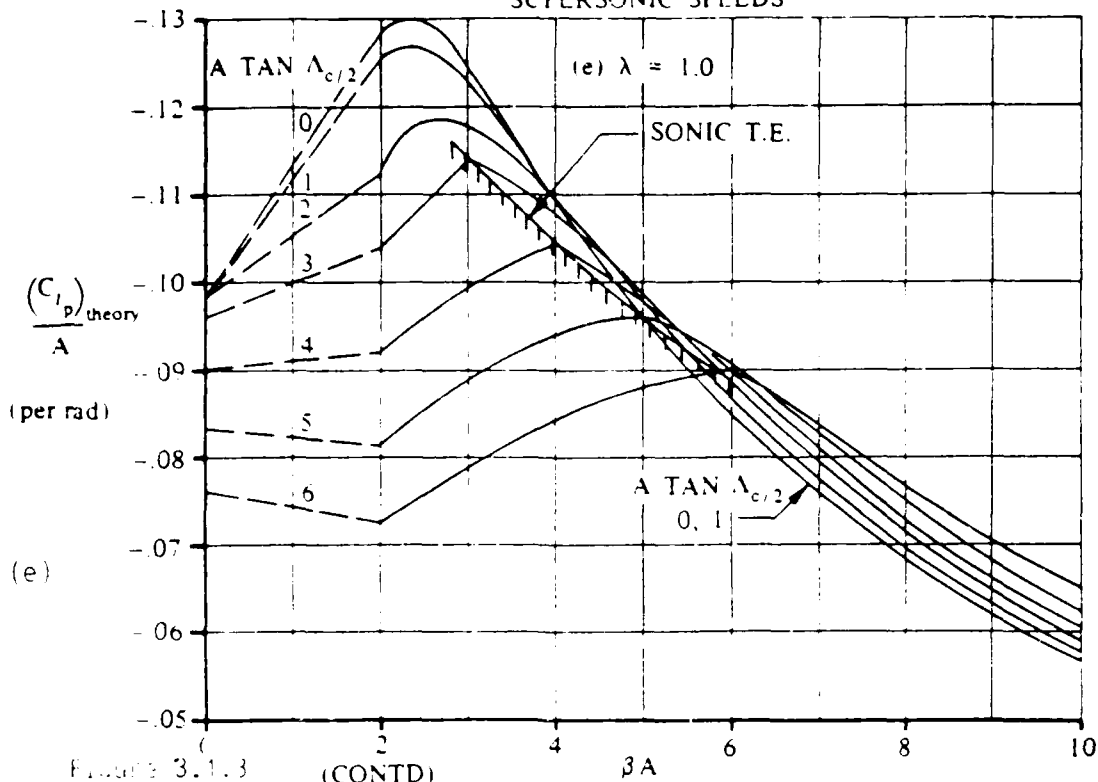


Figure 3.1.3 (CONTD)

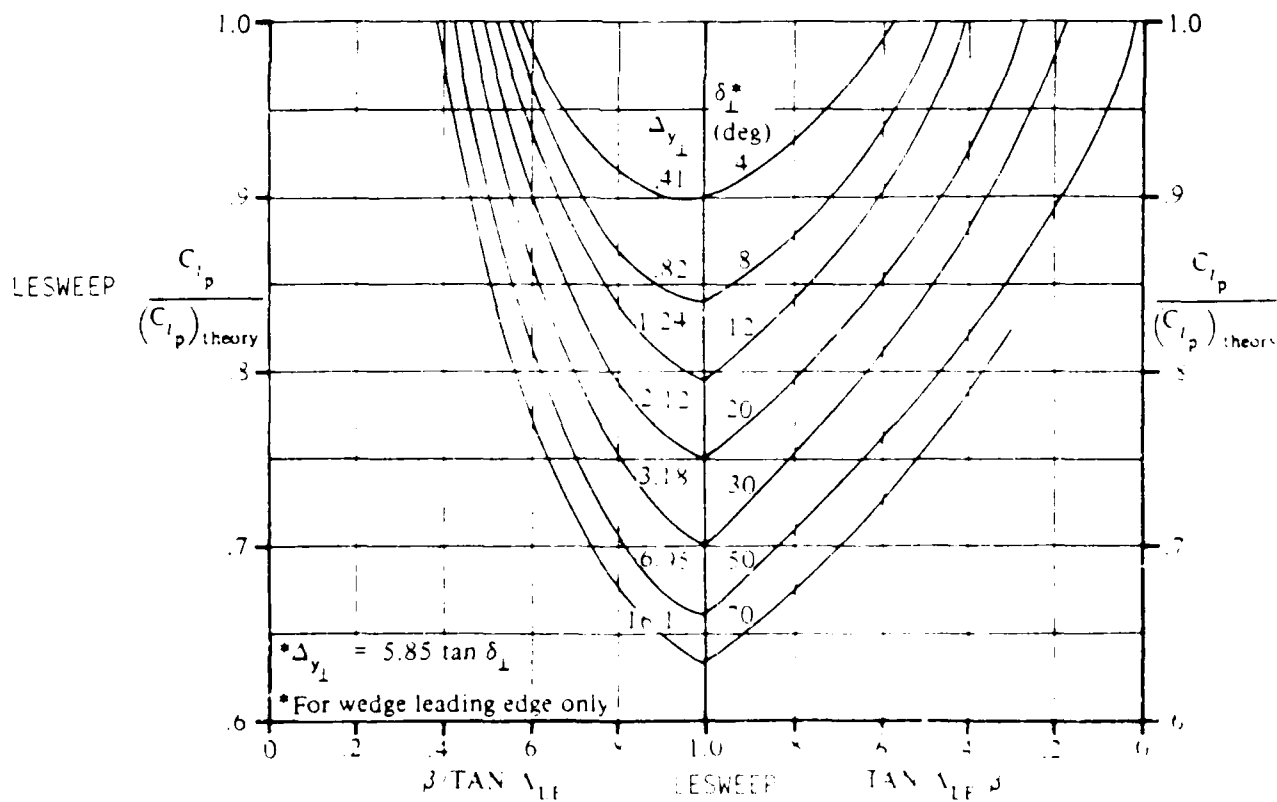


Figure 3.1.4 DAMPING-IN ROLL CORRECTION FACTOR FOR SONIC-LEADING-EDGE REGION

$$CLPWB = CLPW$$

where

CLPW is the same as calculated in section 3.1.1

The CLPWB for supersonic conditions is given in the DATCOM as

$$CLPWB = CLPW * SW/SREF * BCF \quad (3.1.8)$$

where

BCF is the semi-empirical body-correction factor obtained from figure 3.1.5 as a function of the ratio of maximum body diameter to wing span and the Mach number normal to the leading edge.

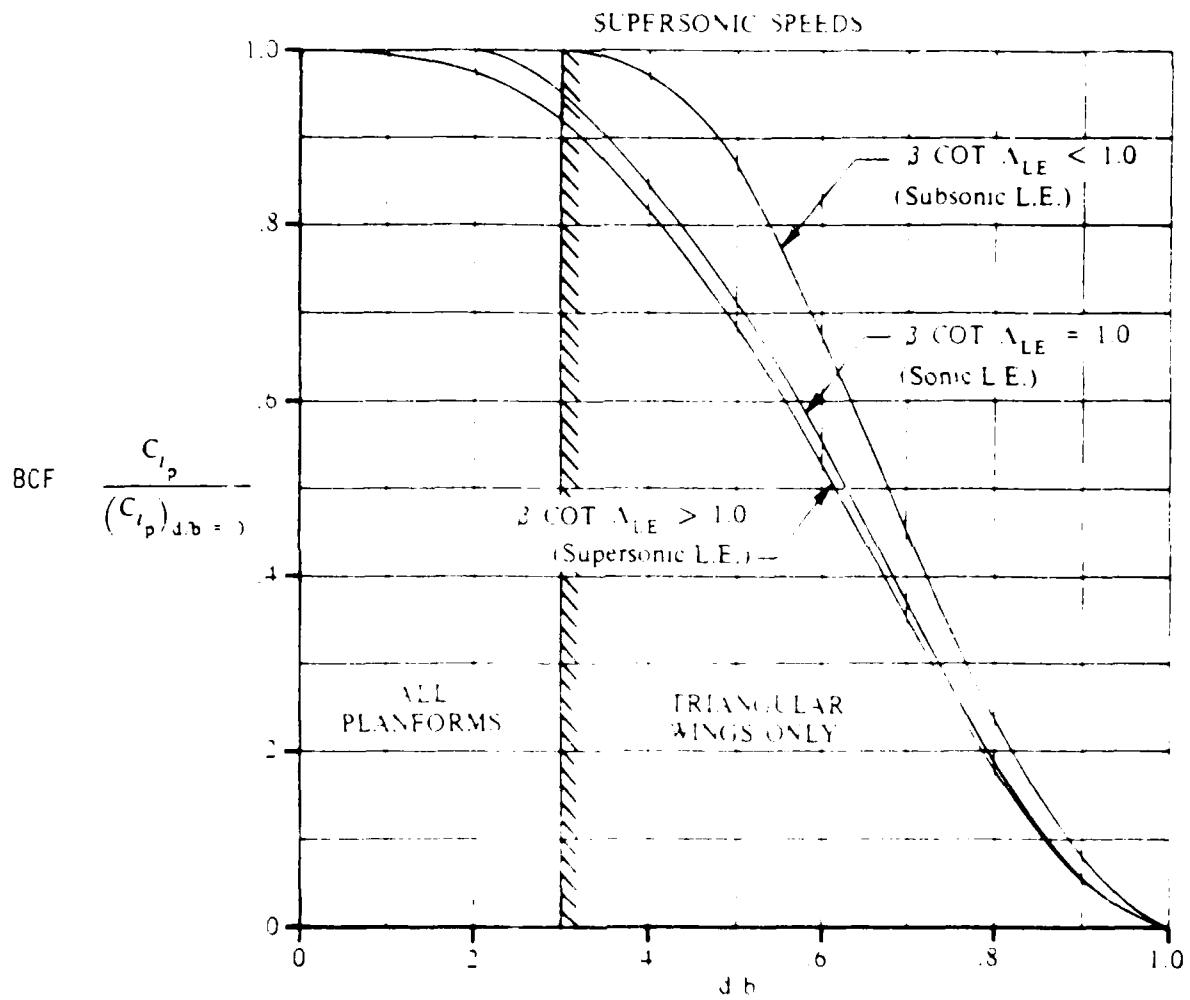


Figure 3.1.5 EFFECT OF THE FUSELAGE ON ROLL DAMPING

3.2 CLDA

The variation of rolling moment coefficient with aileron deflection, CLDA, can be computed by a procedure in Roskam (23) as follows.

STEP 1

Obtain the rolling-moment effectiveness parameter BCLPDK of two full-chord controls ($C_f/C = 1.0$) anti-symmetrically deflected, as a function of BA/K and SWPBETA from Figure 3.2.1.

The parameter K is the ratio of the two-dimensional lift-curve slope at the appropriate Mach number (CLALP) to $2 * \pi / \text{BETA}$, i.e. $\text{CLALP}_M / (2 * \pi / \text{BETA})$. For wings with airfoil sections varying in a reasonably linear manner at the Mach of the flapped portion of the wing is adequate. The parameter SWPBETA is the compressible sweep parameter, given as:

$$\text{SWPBETA} = \text{ATAN}(\text{TAN}(\text{C4SWEEP})/\text{BETA}) \quad (3.2.1)$$

Figure 3.2.1 gives directly the effectiveness parameter for control spans measured from the plane of symmetry outboard. For partial span controls having the inboard edge of the control at spanwise station N(i) and the outboard edge at N(o) the effectiveness parameter is obtained as illustrated in Figure 3.2.2.

STEP 2

Determine the rolling effectiveness of two-full-chord controls anti-symmetrically deflected by:

$$\text{CPLD} = \text{K}/\text{BETA} * (\text{BCLPDK}) \quad (3.2.2)$$

STEP 3

Determine the rolling effectiveness of the partial-chord controls ($C_f/C = \text{constant}$) anti-symmetrically deflected by:

$$\text{CLD} = \text{ABAD} * \text{CPLD} \quad (3.2.3)$$

where

ABAD is the absolute value of the section lift effectiveness, AD. AD is obtained from equation 3.2.4 for the particular control under consideration. For anti-symmetric control deflections, the value of AD is based on the deflection of the surface

$$\text{ABAD} = \text{CLD}/\text{CLALPH} \quad (3.2.4)$$

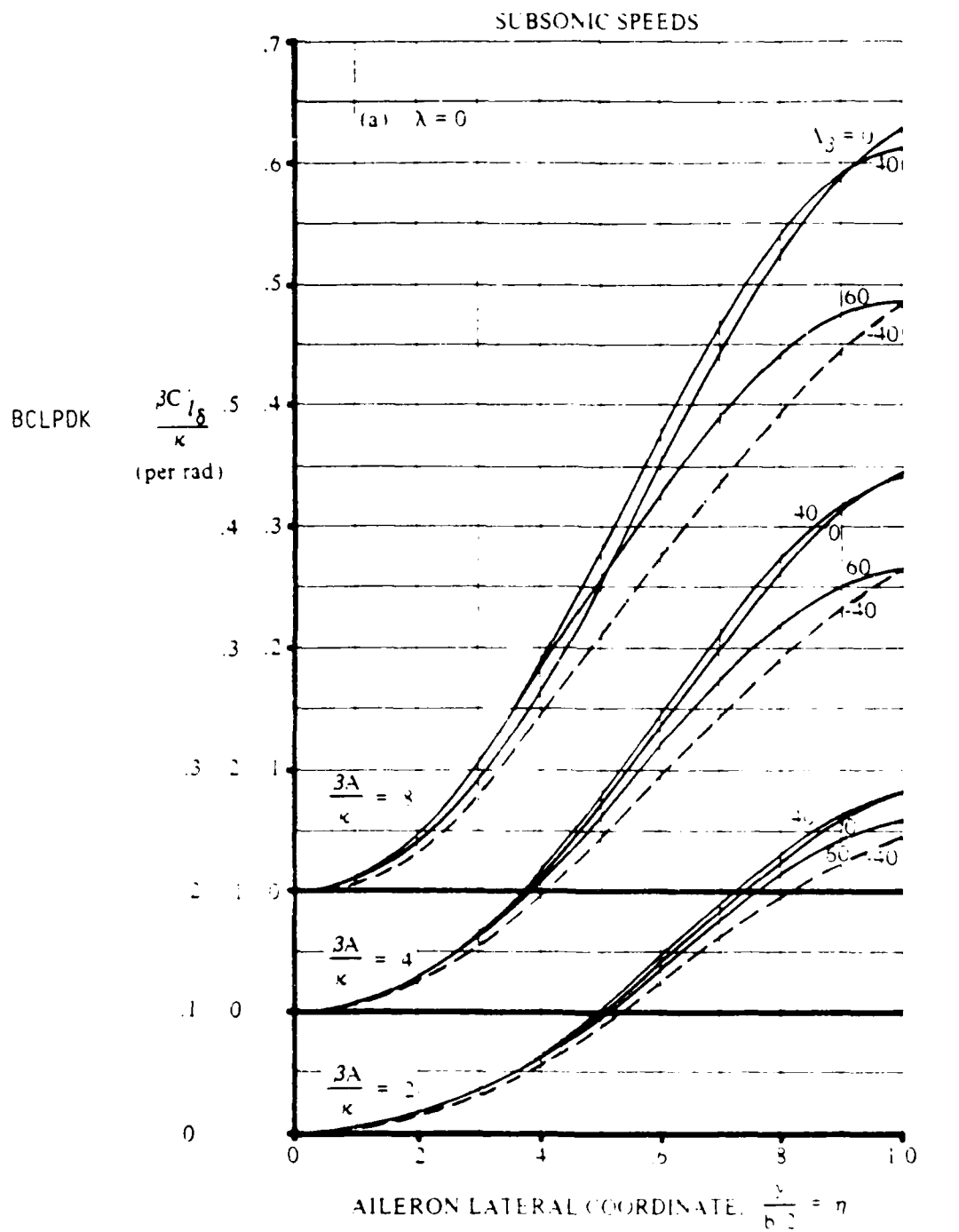


Figure 3.2.1

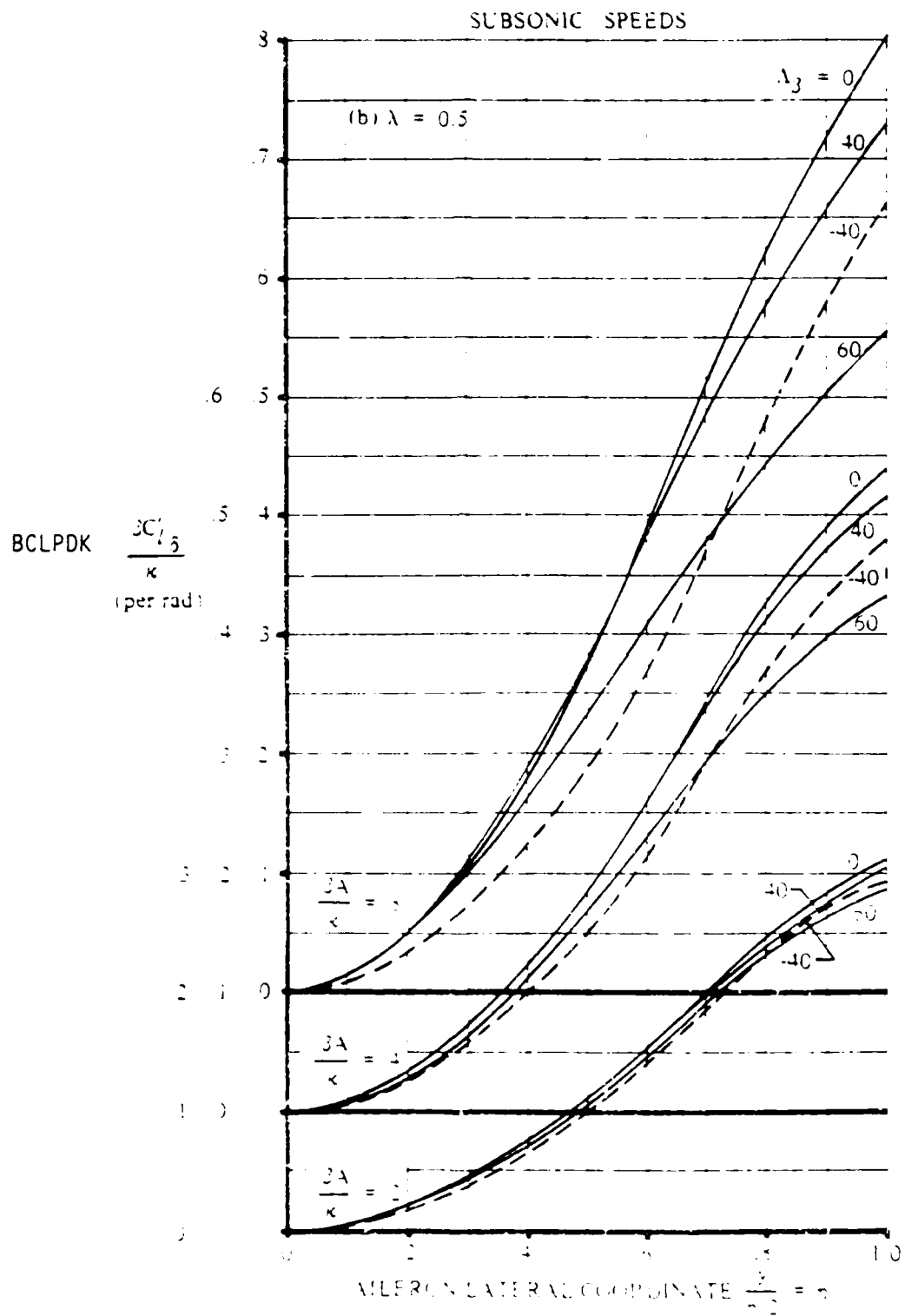


Figure 3.2.1 (CONTD)

SUBSONIC SPEEDS

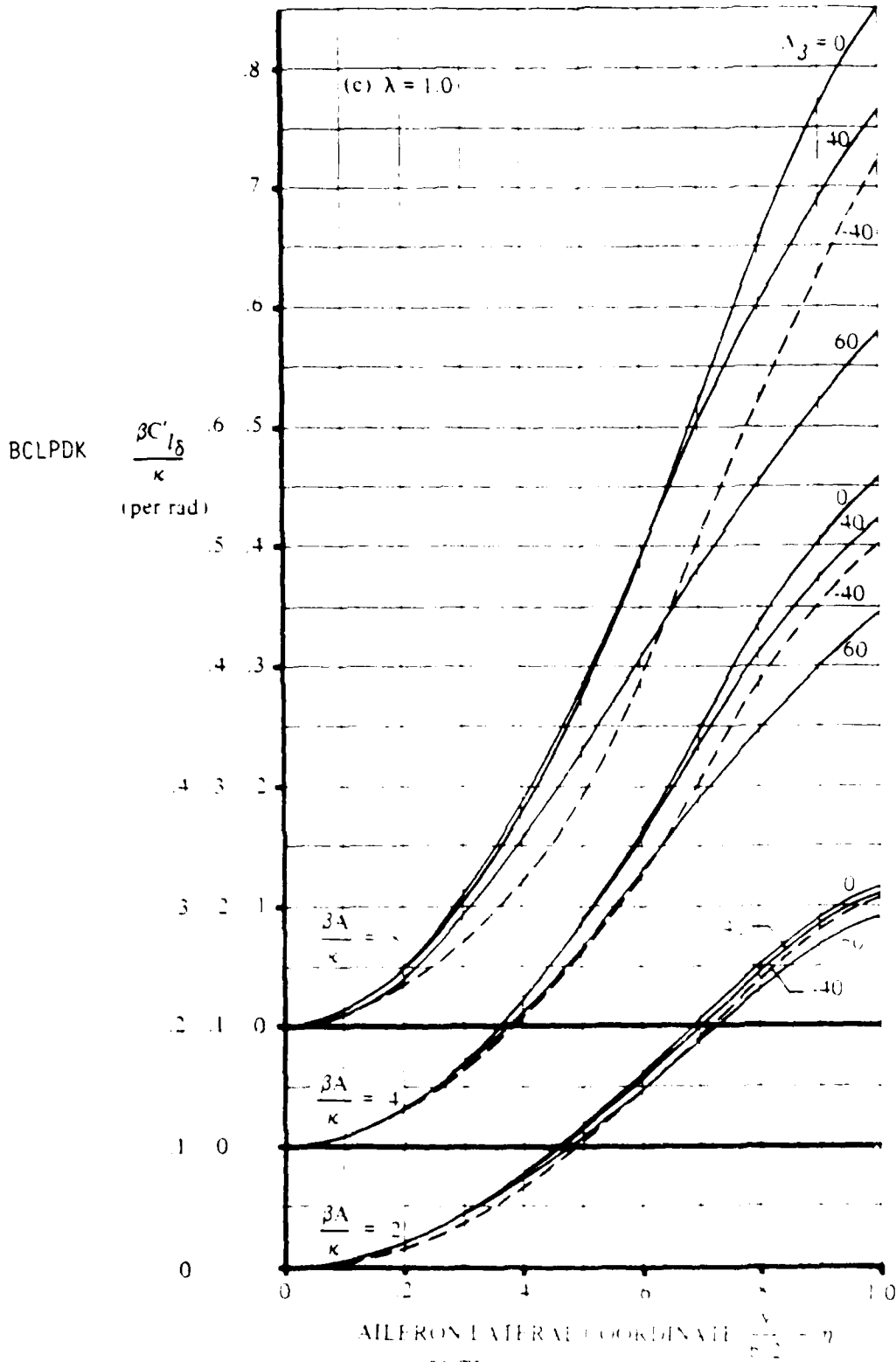


Figure 3.2.1 (CONTD)

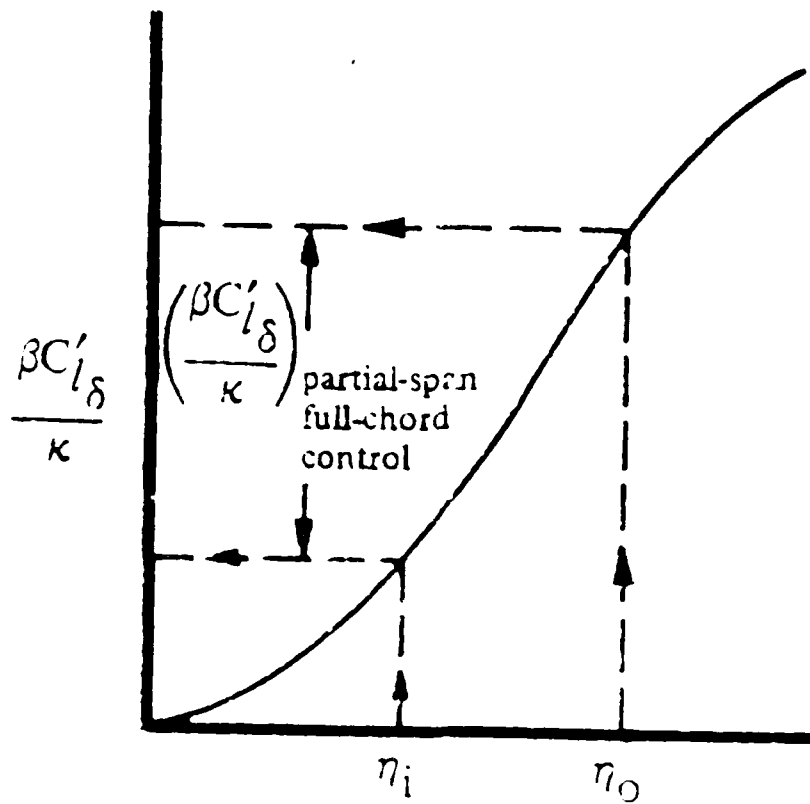


Figure 3.2.2 Instructions for Using Figure 3.2.1

where

$$CLD = CLDCLDT * CLDT \quad (3.2.5)$$

found in figures 3.2.4 and 3.2.3 respectively and where

CLALPH is the average section lift curve slope over the aileron span of the wing

STEP 4

The effect of a differential control deflection is taken into account by considering CLD of each control as one-half the anti-symmetrical value (equation 3.2.3) where ABAD is considered separately for each control and based on its respective deflection.

Then the total rolling-moment coefficient for differential-control deflection is obtained by:

$$CL = (CLD(L)/2.0 * AIL(L) - CLD(R)/2.0 * AIL(R)) \quad (3.2.6)$$

where it should be kept in mind that a positive control deflection is trailing edge down, and AIL(L) and AIL(R) are the left and right aileron deflections. "The" aileron deflection is defined as

$$DA = 1/2(AIL(L) - AIL(R)) \quad (3.2.7)$$

it follows that

$$CLDA = CLD(L) + CLD(R) \quad (3.2.8)$$

PLAIN TRAILING-EDGE FLAPS

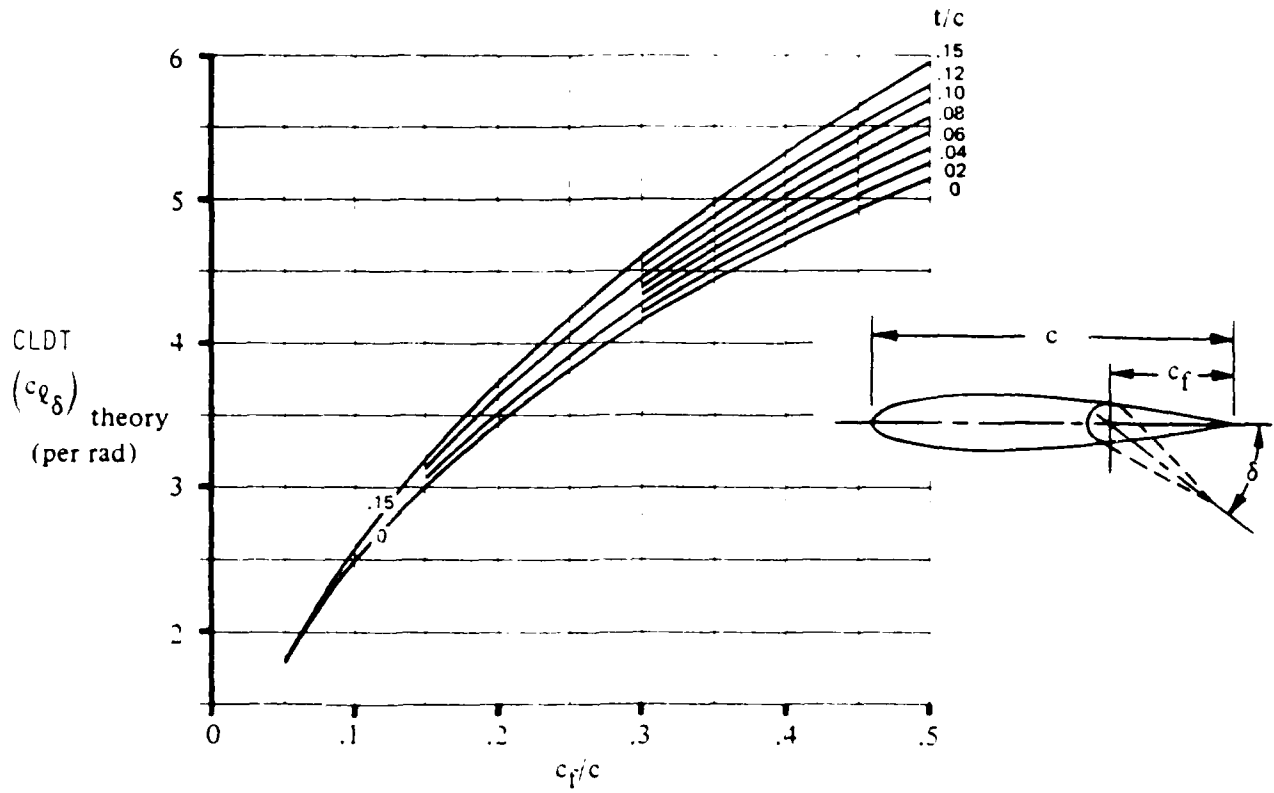


FIGURE 3.2.3 THEORETICAL LIFT EFFECTIVENESS OF PLAIN TRAILING-EDGE FLAPS

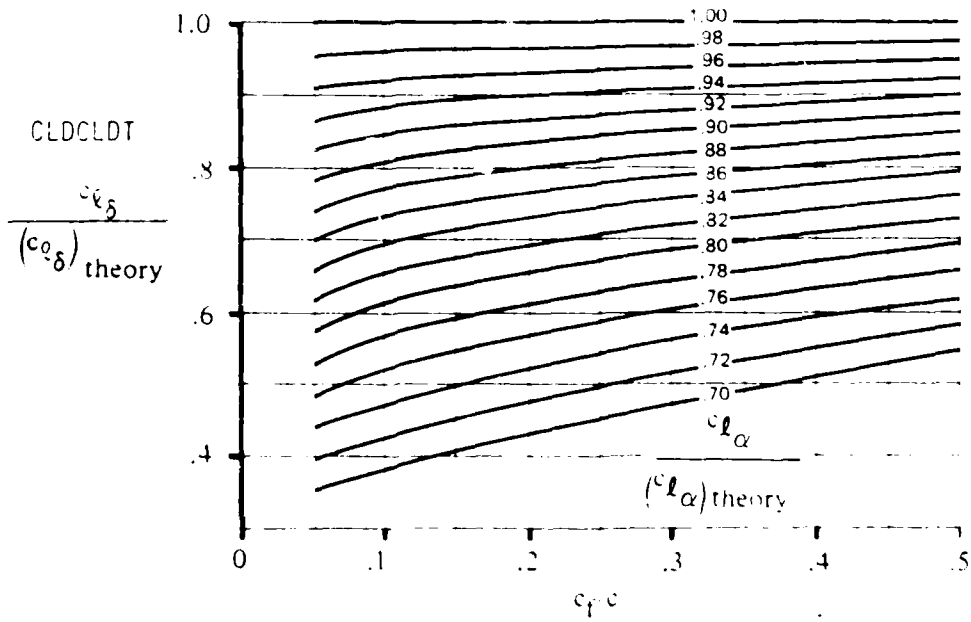


FIGURE 3.2.4 EMPIRICAL CORRECTION FOR LIFT EFFECTIVENESS OF PLAIN TRAILING-EDGE FLAPS

3.3 CLB

The variation of rolling moment coefficient with sideslip angle, CLB, is shown in Roskam (23) to be expressed as the sum of the component CLB's as:

$$CLB = CLBWB + CLBC + CLBH + CLBV \quad (3.3.1)$$

where

CLBWB is the CLB for wing-body interaction
CLBC can be treated as the canard-body interaction CLB
CLBH can be treated as the horizontal tail-body interaction CLB
CLBV is the vertical tail CLB

CLB for all of the lifting surfaces can be computed by the same method, while CLB_V must be treated separately.

3.3.1 CLB For Vertical Tails

According to Roskam (23) CLB for the vertical tail can be expressed as

$$CLBV = -CLALPV * SWFV * (SV/SW) * BV * VNO \quad (3.3.2)$$

where

$$BV = (ZV * \cos(\alpha) - LV * \cos(\alpha)) / \text{SPANW}$$

ZV is the vertical location of the vertical tail mean aerodynamic chord
LV is the axial location of the vertical tail mean aerodynamic chord
CLALPV is the vertical tail zero alpha lift curve slope
SWFV is the sidewash factor of the vertical tail
SV is the area of the vertical tail
SW is the area of the wing

and

VNO the number of vertical tails

3.3.2 CLB For Lifting Surfaces

The subsonic rolling moment due to sideslip, based on the product of the surface span and area, for straight-tapered surface-body combinations at low angles of attack is given by the DATCOM as;

$$CLB = ((CLSB * S1) + (DIHSD * S2) + DELTCLB + S3) * 57.3 \quad (3.3.3)$$

with

S1 = CLBCLC2 * KMS * FLEF + ARCF
S2 = SDEF * KMD + CLBDIH
S3 = TWISTS * TAN(C4SWEEP) * DELCLBH

where

CLSB is the lift coefficient of the body and surface
CLBCLC2 is the surface sweep contribution obtained from figure 3.3.1
KMS is the compressibility correction to the sweep contribution obtained from figure 3.3.2
FLEF is the empirical fuselage-length-effect correction factor obtained from figure 3.3.3
ARCF is the aspect ratio contribution obtained from figure 3.3.4
DIHSD is the geometric dihedral angle in degrees, positive for the surface tip above the plane of the root chord
SDEF is the surface dihedral effect for uniform geometric dihedral obtained from figure 3.3.5
KMD is the compressibility correction factor to the dihedral effect obtained from figure 3.3.6
CLBDIH is the body-induced effect on wing height due to uniform geometric dihedral given by

$$CLBDIH = -.0005 * \text{SQRT}(ARS) * (DIAEQ/SPANS)^2$$

ARS is the aspect ratio of the surface
DIAEQ is the average body diameter at the surface for non-body of revolution configuration, the average equivalent diameter at the surface root should be used

$$DIAEQ = \text{SQRT}(\text{average cross sectional area}/.07854)$$

SPANS is the span of the surface
DELTCALB is the increment in CLB due to the body-induced effect on wing height for configurations with surfaces located above or below the midfuselage height. The increment given by

$$DELTCALB = (1.2 * (\text{SQRT}(ARS)/57.3) * ZCG/SPANS) * 2 * DIAEQ/SPANS$$

where

ZCG is the vertical distance from the center of gravity to the quarter chord point of the surface
TWISTS is the surface twist between the root and tip sections in degrees (see Figure 3.3.7)
C4SWEEP is the sweep angle of the quarter chord point of the surface

SUBSONIC SPEEDS

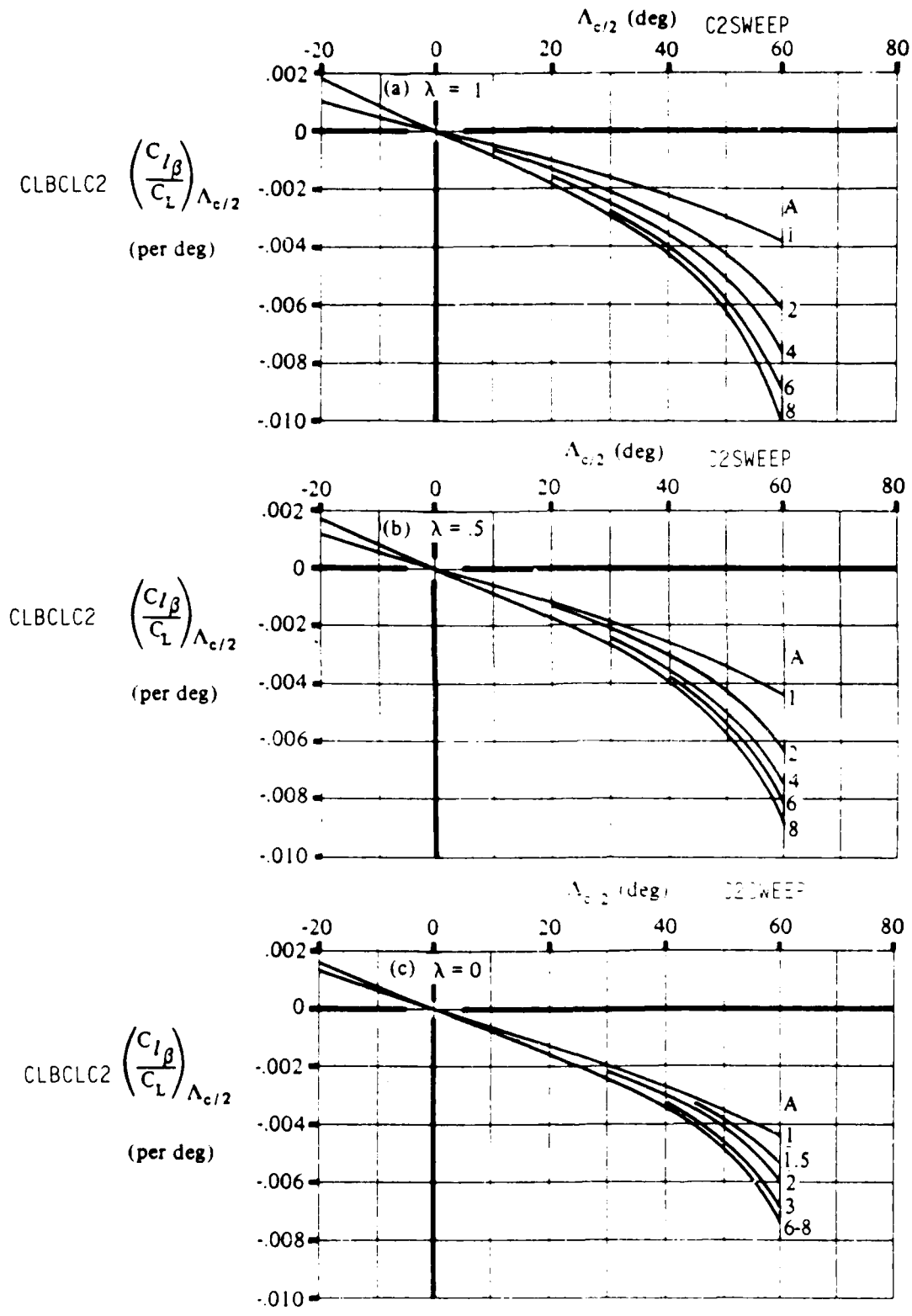


Figure 3.3.1 WING SWEEP CONTRIBUTION TO $C_{l\beta}$

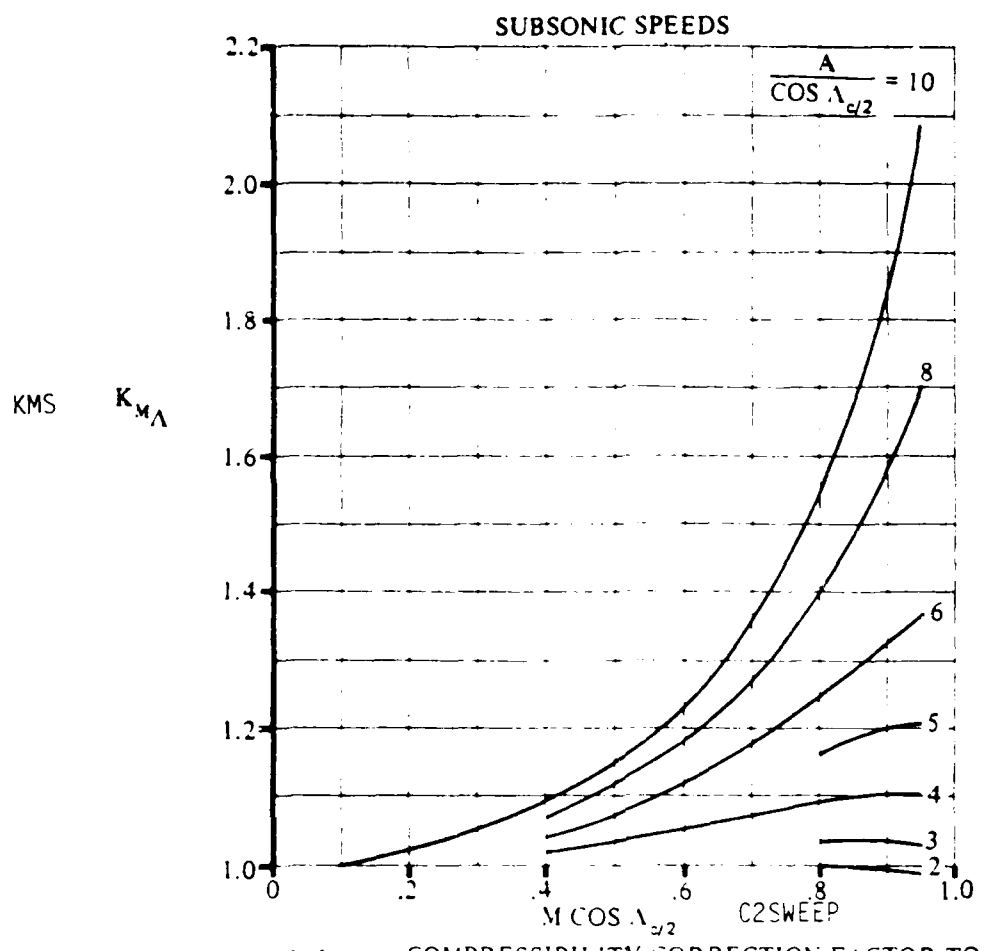


Figure 3.3.2 COMPRESSIBILITY CORRECTION FACTOR TO SWEEP CONTRIBUTION TO WING C_{l3}

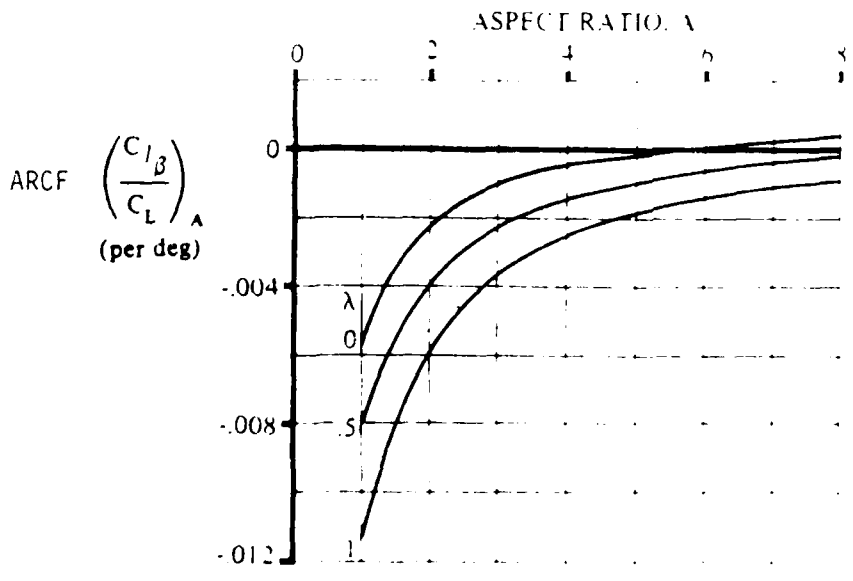


Figure 3.3.4 ASPECT RATIO CONTRIBUTION TO WING C_{l3}

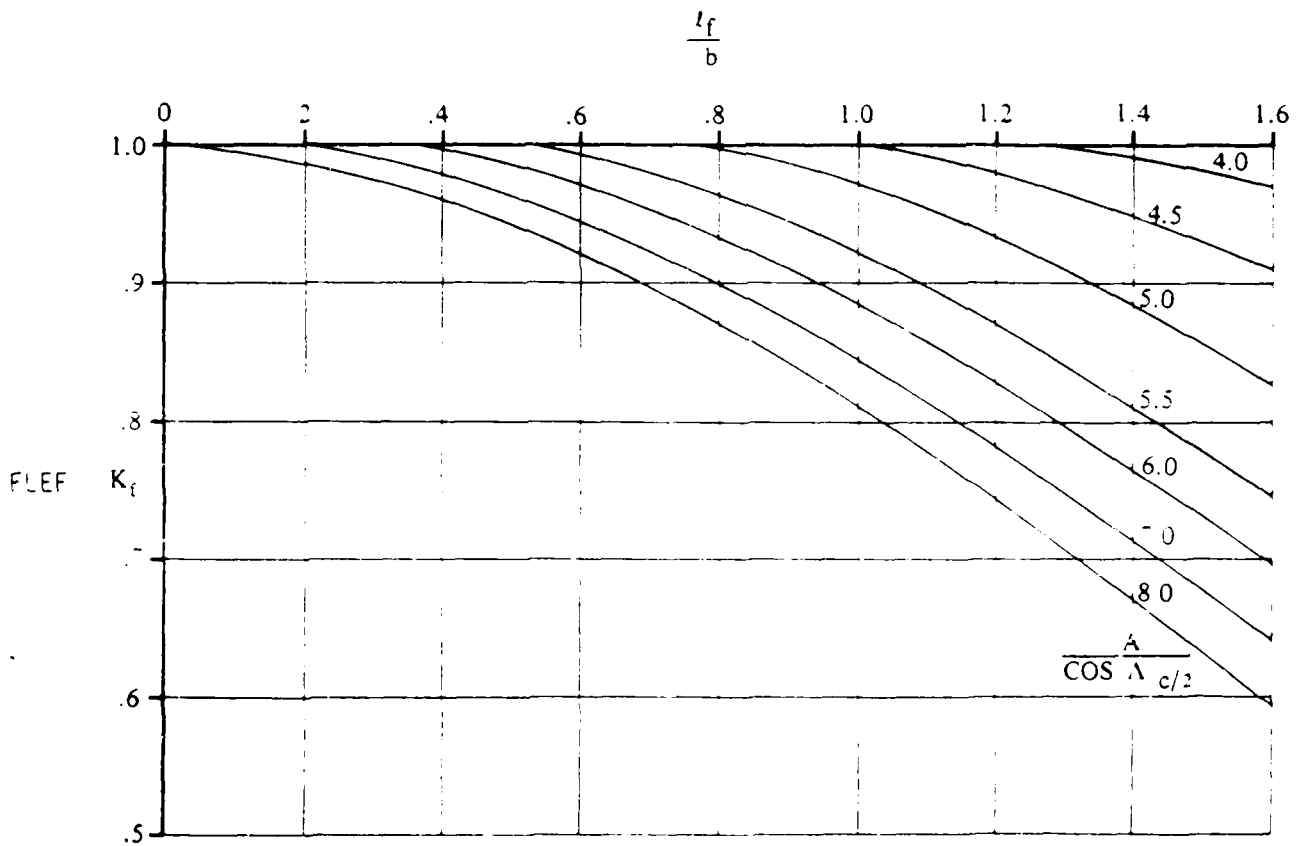
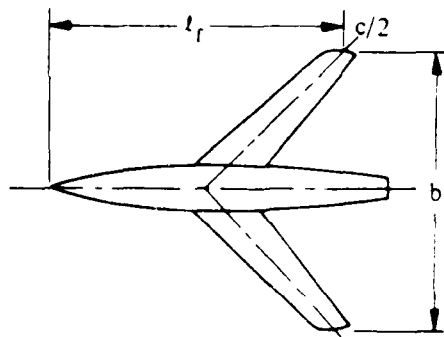


Figure 3.3.3 FUSELAGE CORRECTION FACTOR

SUBSONIC SPEEDS

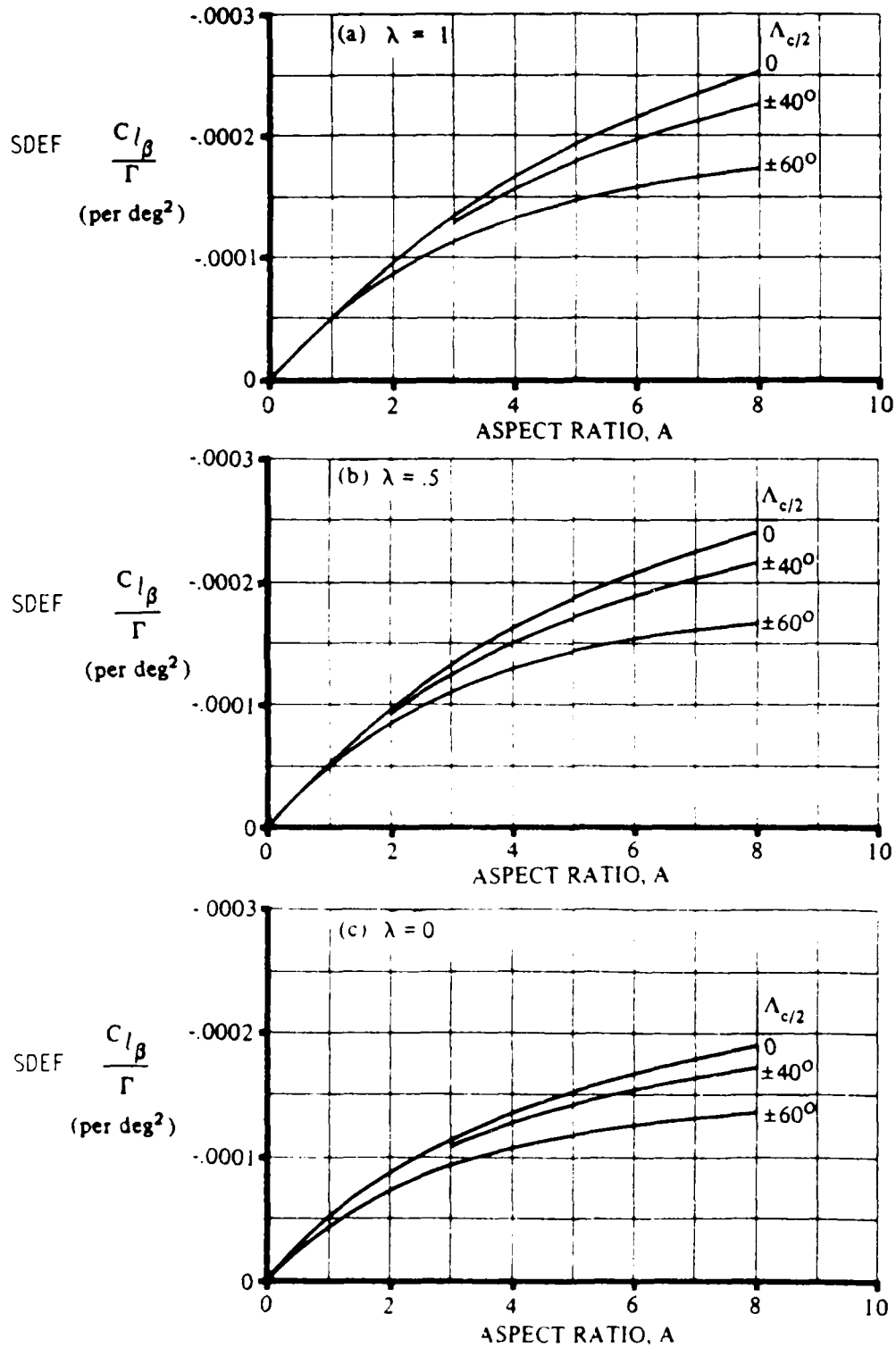


Figure 3.3.5 EFFECT OF UNIFORM GEOMETRIC DIHEDRAL ON WING $C_{l\beta}$

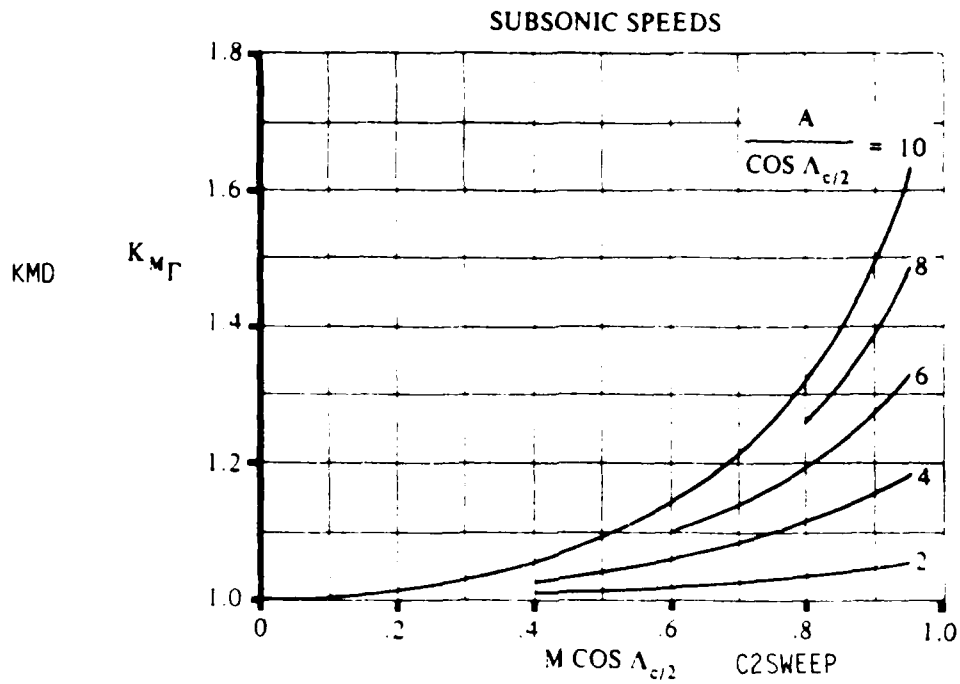


Figure 3.3.6 COMPRESSIBILITY CORRECTION TO DIHEDRAL EFFECT ON WING $C_{l\beta}$

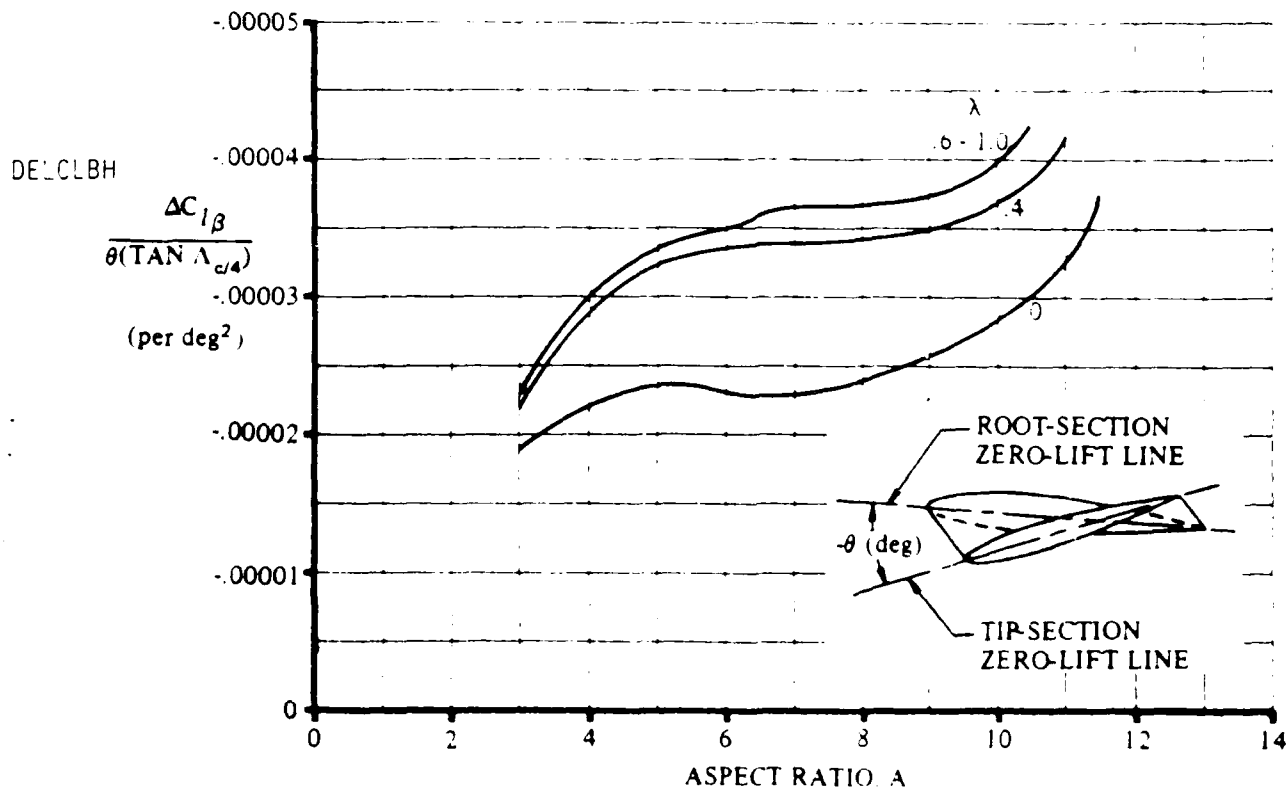


Figure 3.3.7 EFFECT OF WING TWIST ON WING $C_{l\beta}$

DELCLBH is the wing twist correction factor obtained from figure 3.3.7

The supersonic rolling moment due to sideslip for surface-body configurations with straight-tapered surfaces at low angles of attack is approximated in the DATCOM by

$$CLB = -.061 * CN * CLALPS * T1 * T2 * (T3 + T4) + T5 + DELTCLB \quad (3.3.4)$$

with

$$\begin{aligned} CN &= CLSB / \cos(\text{ALPHA}) \\ T1 &= 1.0 + (\text{TRS} * (1.0 + \text{LESWEEP})) \\ T2 &= (1.0 + (\text{LESWEEP}/2)) * \tan(\text{LESWEEP}) / \text{BETA} \\ T3 &= \text{MACH}^2 * (\cos(\text{LESWEEP}))^2 / \text{ARS} \\ T4 &= (\tan(\text{LESWEEP})/4)^{1.33} \\ T5 &= \text{DIHSD} * (\text{SDEFS} + \text{CLBDIH}) \end{aligned}$$

where

TRS is the taper ratio of the surface
LESWEEP is the leading edge sweep angle of the surface
CLALPS is the zero alpha lift curve slope of the surface
SDEFS is the surface dihedral effect given by
CLPS is the CLP for the surface from Section 3.1.1

and

$$\text{SDEFS} = 2/57.3^2 * (1.0 + (2.0 * \text{TRS})) / (1.0 + (3.0 * \text{TRS})) * \text{CLPS}$$

The value of CLB must now be adjusted for each surface by

$$\text{CLBS} = \text{CLB} * \text{NS} * \text{SS}/\text{SREF} * \text{SPANS}/\text{SPANW} \quad (3.3.5)$$

where

NS is the dynamic pressure ratio of the surface
SS is the reference area of the surface
SREF is the reference area of the aircraft
SPANS is the span of the surface

and

SPANW is the span of the wing

3.4 CNB

The variation of yawing moment coefficient with sideslip angle, CNB, can be obtained from the sum of the component CNB's by the equation

$$\text{CNB} = \text{CNBB} + \text{CNBN} + \text{CNBW} + \text{CNBC} + \text{CNBH} + \text{CNBV} + \text{CNBF} + \text{CNBHV} \quad (3.4.1)$$

where

CNBB is the CNB of the body
CNBN is the CNB of the nacelles
CNBW is the CNB of the wings
CNBC is the CNB of the canards
CNBH is the CNB of the horizontal tails
CNBV is the CNB of the vertical tails
CNBF is the CNB of the fins
CNBHV is the CNB of the horizontal tail (vertical component)

The derivatives for each of these components is described below.

3.4.1 CNB for Bodies and Nacelles

The total body or nacelle sideslip derivative CNB is given in the DATCOM as

$$\text{CNB} = -57.3 * \text{KN} * \text{KRL} * \text{BSA}/\text{SREF} * \text{LB}/\text{SPANW} \quad (3.4.2)$$

where

KN is the empirical factor related to the sideslip derivative for body plus wing interference obtained from figure 3.4.1 as a function of geometry
KRL is the empirical Reynolds-number factor obtained from figure 3.4.2
BSA is the side area of the body or nacelle
SREF is the reference area
LB is the length of the body or nacelle
SPANW is the span of the wing

For multiple nacelles, this result is summed over all of the nacelles.

3.4.2 CNB for Lifting Surfaces

The yawing moment of surface in sideslip is primarily caused by the asymmetrical induced-drag distribution associated with the asymmetrical lift distribution. The surface contribution to the derivative CNB is important only at large incidence.

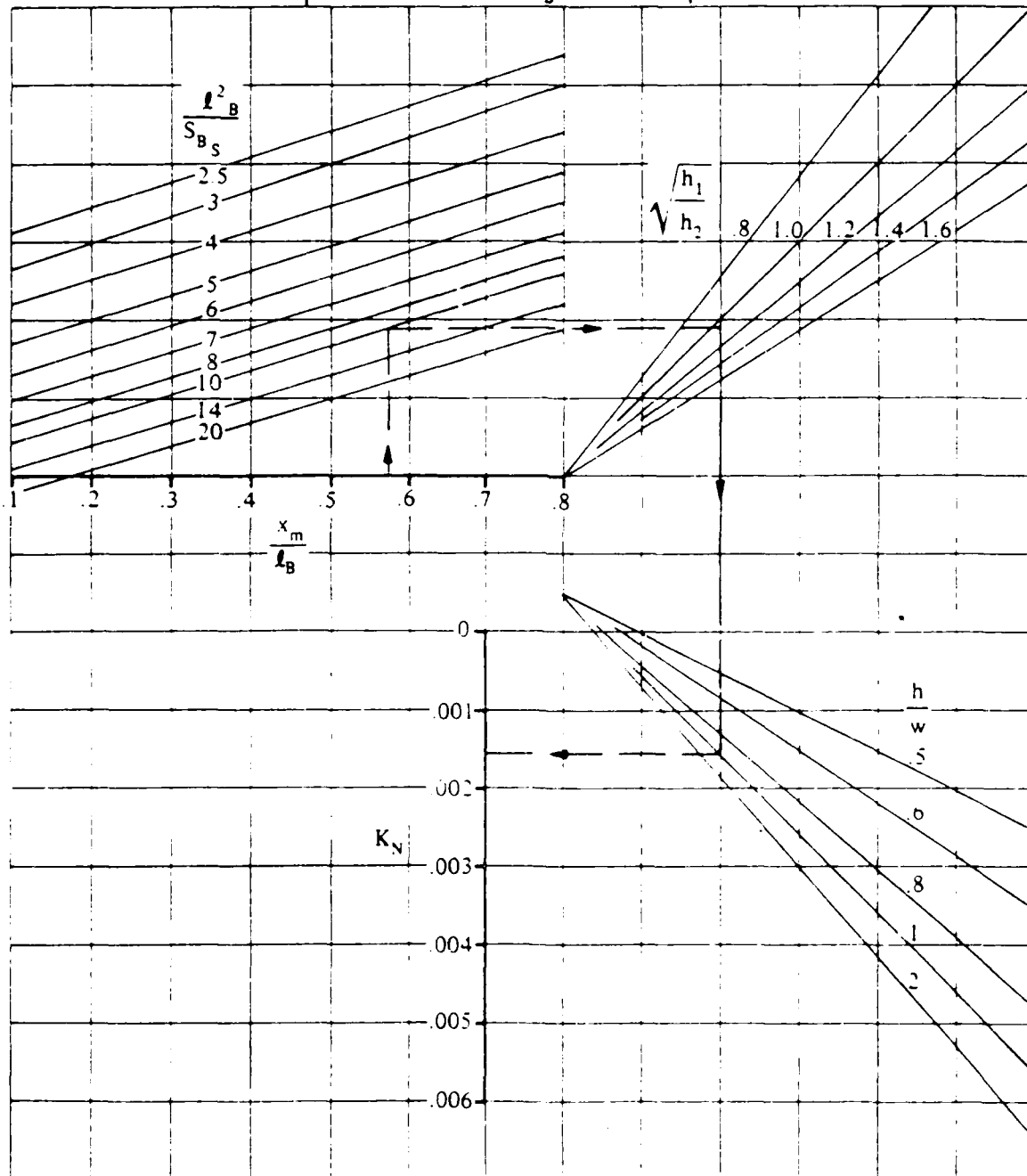
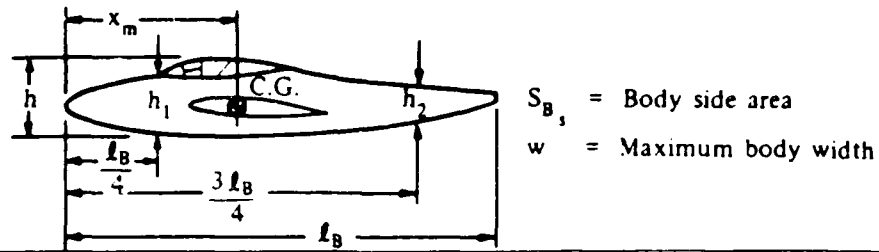


Figure 3.4.1 EMPIRICAL FACTOR K_N RELATED TO SIDESLIP DERIVATIVE $C_{n\beta}$ FOR BODY + WING-BODY INTERFERENCE

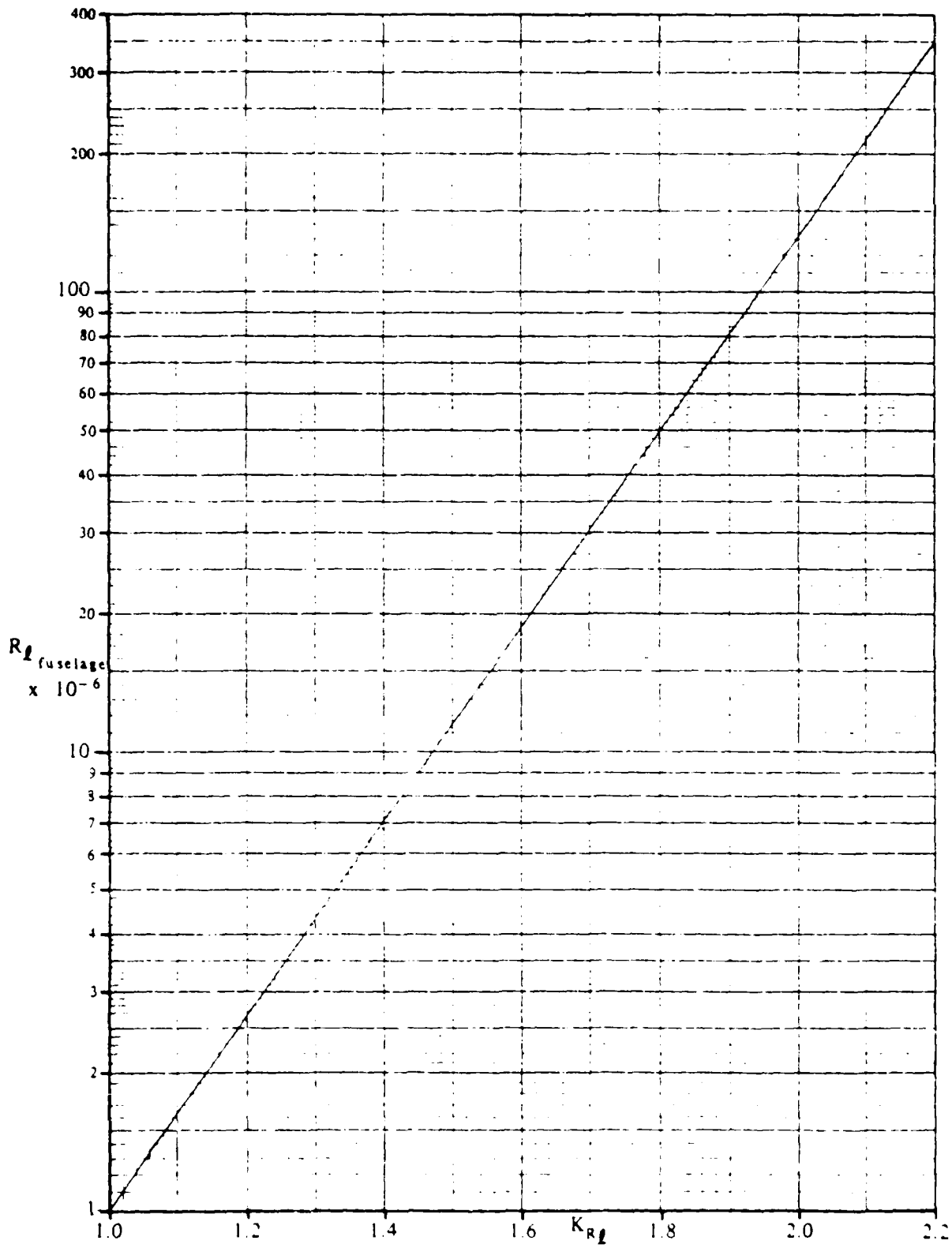


Figure 3.4.2 EFFECT OF FUSELAGE REYNOLDS NUMBER ON WING-BODY C_{n3}

The DATCOM method presented herein uses distinct equations for computation of low subsonic, high subsonic, and supersonic speeds.

The yawing moment derivatives at low speeds is given by

$$CNBLS = CL^2 * (Q1 - TAN(C4SWEEP)/Q2) * Q3 \quad (3.4.3)$$

with

$$\begin{aligned} Q1 &= 1.0 / (4.0 * PI * ARS) \\ Q2 &= PI * ARS * (ARS + 4.0 * COS(C4SWEEP)) \\ Q3 &= COS(C4SWEEP) - ARS / 2.0 - Q4 + Q5 \\ Q4 &= ARS^2 / (8.0 * COS(C4SWEEP)) \\ Q5 &= 6.0 * XB * SIN(C4SWEEP) / ARS \end{aligned}$$

where

CL is the lift coefficient of the surface
 C4SWEEP is the quarter chord sweep of the surface
 ARS is the aspect ratio of the surface
 XB is the axial distance from the surface aerodynamic center to the aircraft center of gravity

For subcritical speeds, the low-speed derivative can be modified by the Prandtl-Glauert rule to yield approximate corrections for the first order three-dimensional effects of compressibility. The resulting expression is

$$CNB = CNBLS * (Q6/Q7) * (Q8/Q9) \quad (3.4.4)$$

with

$$\begin{aligned} Q6 &= ARS + (4.0 * COS(C4SWEEP)) \\ Q7 &= (ARS * B) + (4.0 * COS(C4SWEEP)) \\ Q8 &= ARS^2 * B^2 + (4.0 * ARS * B * COS(C4SWEEP)) \\ &\quad - (8.0 * COS(C4SWEEP))^2 \\ Q9 &= ARS^2 + (4.0 * ARS * COS(C4SWEEP)) - (8.0 * COS(C4SWEEP))^2 \end{aligned}$$

where

$$B = SQRT(1.0 - MACH^2 * (COS(C4SWEEP))^2)$$

The DATCOM Methods for calculation of CNB at supersonic speeds is divided into methods for rectangular planforms, and fully tapered sweptback planforms with swept forward or sweptback trailing edges. The results are mainly functions of planform geometry and Mach number. The general trend of the variation of CNB with Mach number and aspect ratio is a reduction in the magnitude of the derivative with an increase in these parameters.

Rectangular Planforms $ARS * BETA \geq 1.0$

The wing yawing moment due to sideslip for rectangular planforms referred to an arbitrary moment center is given as

$$CNB = ALPHA^2 * Q10 * (Q11 + Q12 - PI * (Q13 + Q14)) \quad (3.4.5)$$

with

$$\begin{aligned} Q10 &= 1.0 / (PI * ARS^2 * BETA^2) \\ Q11 &= (4.0 * MACH^2) / 3.0 \\ Q12 &= 8.0 * MACH^2 * XOC1 \\ Q13 &= (ARS * (1.0 - BETA^2)) / BETA \\ Q14 &= (3.0 + BETA^2) / (3.0 * BETA^2) \end{aligned}$$

where

$$BETA = SQRT(MACH^2 - 1.0)$$

XOC1 is the distance of the origin of moments from the mean aerodynamic chord

Equation 3.4.5 is valid for Mach number and aspect ratio greater than that for which the Mach line from the leading edge of the tip section intersects the trailing edge of the opposite tip section ($ARS * BETA \geq 1.0$)

Sweptback Planform

The wing yawing moment due to sideslip for fully tapered sweptback planforms is:

$$CNB = ALPHA^2 * PI / 3 * (EBECT * F9N + (ARS^2 / 16 * F11N + XOC2) * MACH^2 * QBECT) \quad (3.4.6)$$

where

EBECT is obtained from figure 3.4.3
F9N is obtained from figure 3.4.4
F11N is obtained from figure 3.4.5
QBECT is obtained from figure 3.4.6

and

XOC2 is the distance of the origin of moments from the 2/3 chord point of the basic triangular wing, measured along the longitudinal axis.

SUPERSONIC SPEEDS

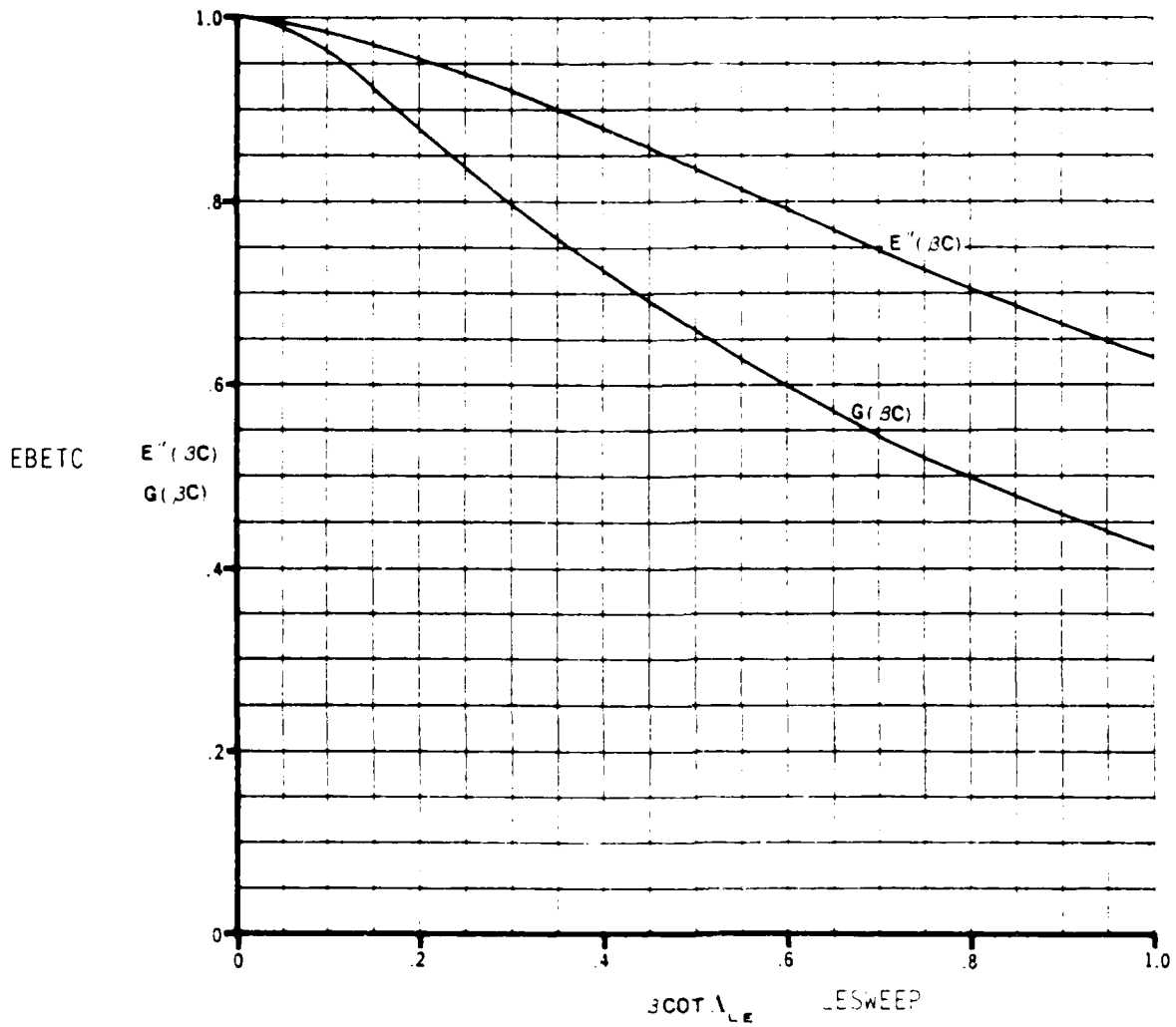


Figure 3.4.3 ELLIPTIC INTEGRAL FACTORS OF THE STABILITY DERIVATIVE

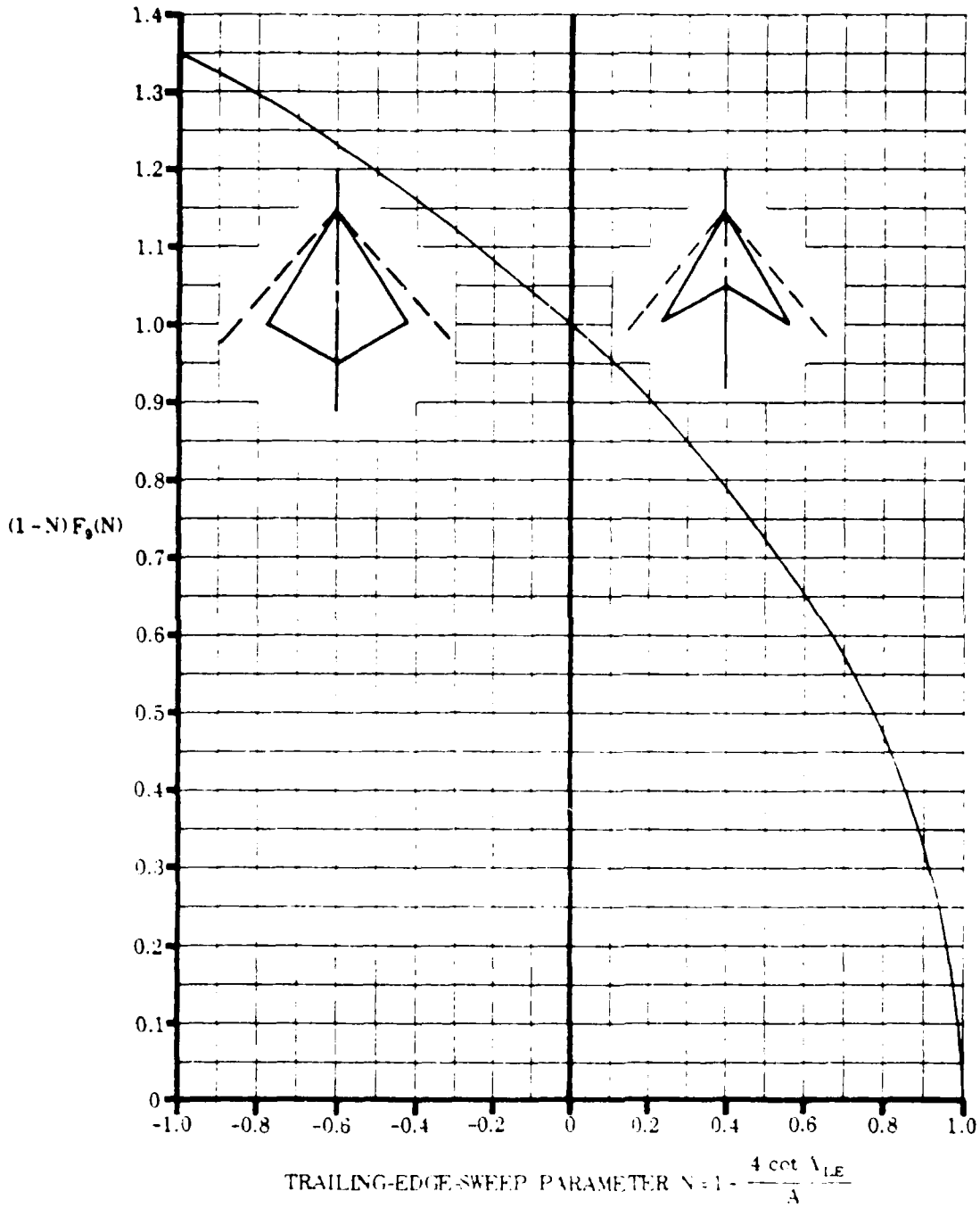


Figure 3.4.4 $F_9(N)$ FACTOR OF THE STABILITY DERIVATIVE

SUPERSONIC SPEEDS

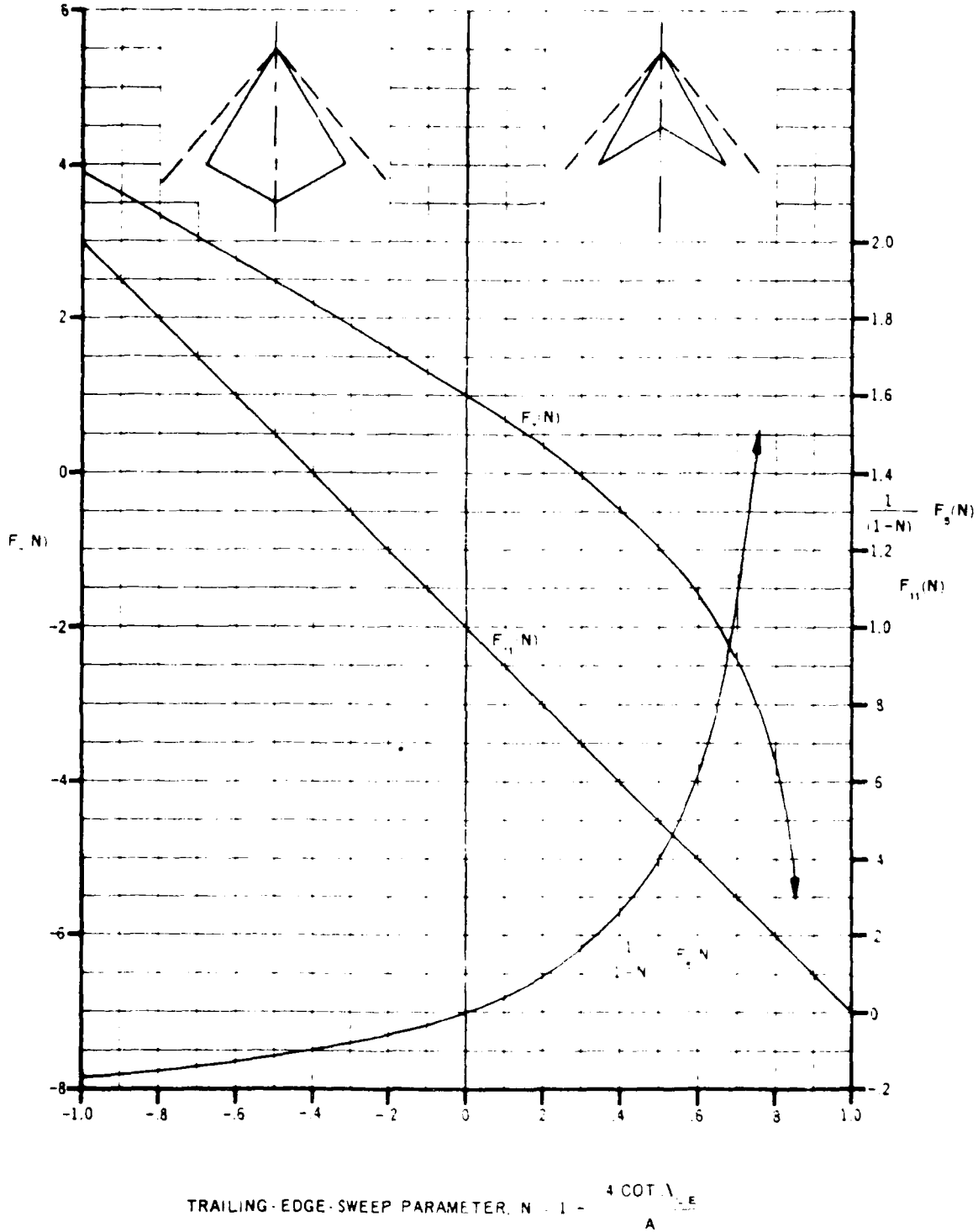


Figure 3.4.5 F(N) FACTORS OF THE STABILITY DERIVATIVE

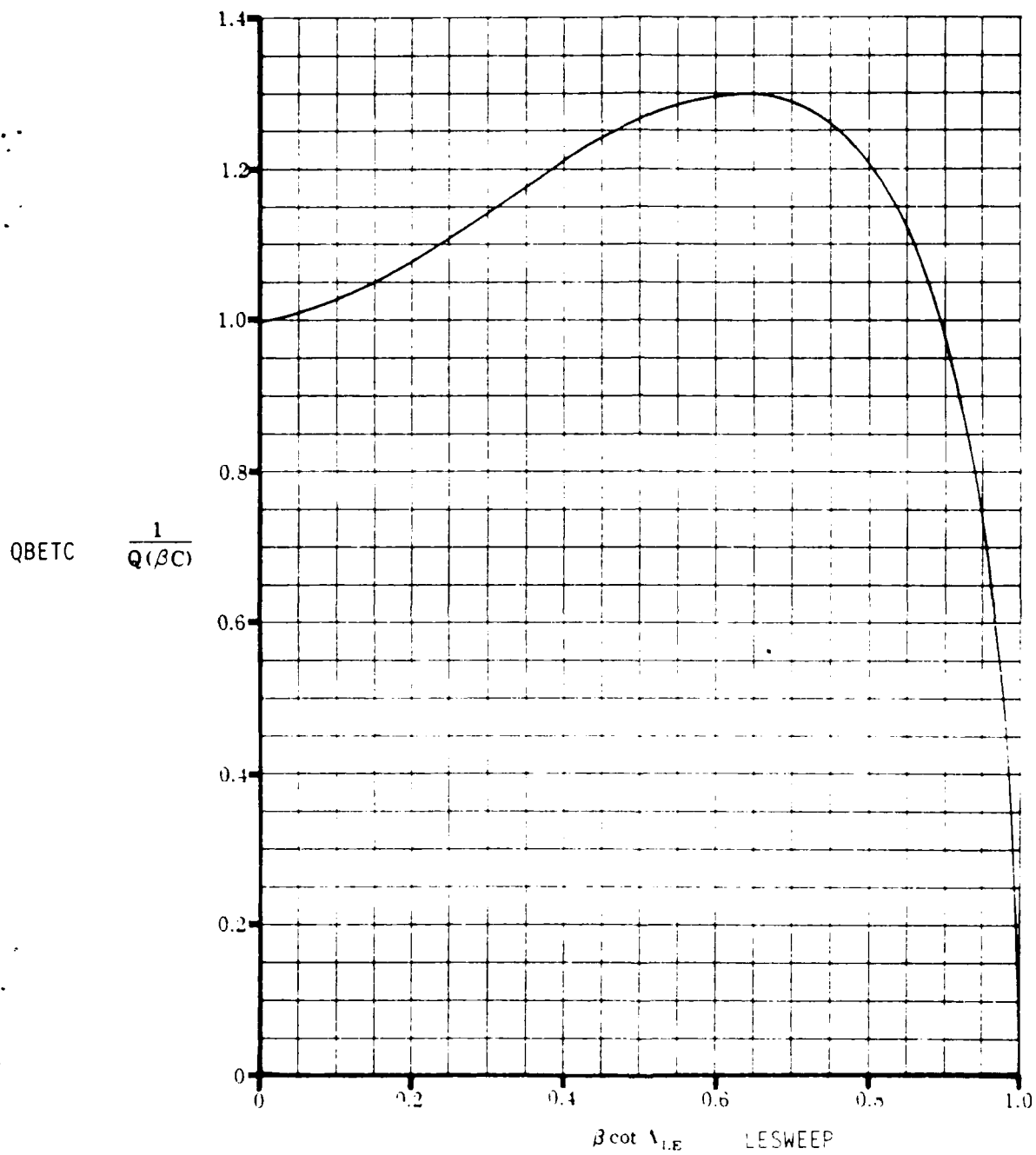


Figure 3.4.6 ELLIPTIC INTEGRAL FACTOR OF THE STABILITY DERIVATIVE

3.4.3 CNB for Vertical Tails

The variation of yawing moment coefficient with sideslip angle due to the vertical tail can be represented as

$$\text{CNBV} = \text{CLALPVO} * \text{SWFV} * \text{SV/SREF} * \text{BV} * \text{VNO} \quad (3.4.7)$$

where

CLALPVO is the zero alpha lift curve slope of the vertical tail
SWFV is the side-wash factor of the vertical tail
SV is the area of the vertical tail
SREF is the reference area
VNO is the number of vertical tails

$$\text{BV} = (\text{LV} * \text{COS}(\text{ALPHA}) + \text{ZV} * \text{SIN}(\text{ALPHA}))/\text{SPANW} \quad (3.4.8)$$

LV is the axial location of the vertical tail aerodynamic center
SPANW is the span of the wing

and

ZV is the vertical location of the mean aerodynamic chord of the vertical tail

3.4.4 CNB for Fins

The variation of yawing moment coefficient with sideslip angle due to fins is represented as

$$\text{CNBF} = \text{CLALPFO} * \text{SF/SREF} * \text{BF/SPANW} * \text{FNO} \quad (3.4.9)$$

where

CLALPFO is the zero alpha lift curve slope of the fin
SF is the area of the fin
SREF is the reference area
SPANW is the span of the wing
FNO is the number of fins

$$\text{BF} = \text{LF} * \text{COS}(\text{ALPHA}) + \text{ZF} * \text{SIN}(\text{ALPHA}) \quad (3.4.10)$$

where

LF is the X location of the fin aerodynamic center
ZF is the Z location of the fin mean aerodynamic chord

3.4.5 CNB for the Vertical Component of the Horizontal Tail

If the Horizontal tails have a slight dihedral angle then they will have a CNB component due to the vertical portion of the tail. This component is defined as

$$CN_{BH} = C_{L\alpha} * A_{EXH} / S_{REF} * \sin(\delta_{HH}) * N_H * B_H \quad (3.4.11)$$

where

$C_{L\alpha}$ is the horizontal tail lift coefficient due to α
 A_{EXH} is the exposed area of the horizontal tail
 S_{REF} is the reference area
 δ_{HH} is the dihedral angle of the horizontal tail
 N_H is the dynamic pressure ratio at the horizontal tail

$$B_H = ((L_H * \cos(\alpha) + (Z_H * \sin(\alpha))) / \text{SPANW}) \quad (3.4.12)$$

SPANW is the span of the wing
 L_H is the X location of the aerodynamic center of the horizontal tail
 Z_H is the Z location of the mean aerodynamic chord of the horizontal tail

3.5 CNDELTR

The variation of yawing moment coefficient with rudder angle CNDELTR can be computed by

$$\text{CNDELTR} = -\text{CLALPVO} * \text{SWFV} * \text{ALFDR} * \text{SV/SREF} * \text{BV} \quad (3.5.1)$$

where

ALFDR is the rudder effectiveness factor, obtained from figure 3.5.1

$$\text{ALFDR} = .2923253 + .4191569 * \text{CFC} + .4816274 * \text{CFC}^2$$

ALFDR = 1.0 for an all moveable tail

ALFDR = 0.0 for a fixed tail with no rudder

$$\text{CFC} = \text{RUDC/MACV}$$

RUDC is the average rudder chord

MACV is the mean aerodynamic chord of the vertical tail

CLALPVO is the zero alpha lift curve slope of the vertical tail

SWFV is the sidewash factor of the vertical tail

SV is the area of the vertical tail

SREF is the reference area

$$\text{BV} = (\text{LV} * \text{COS}(\text{ALPHA}) + \text{ZV} * \text{SIN}(\text{ALPHA}))/\text{SPANW} \quad (3.5.2)$$

LV the X location of the vertical tail aerodynamic center

SPANW the span of the wing

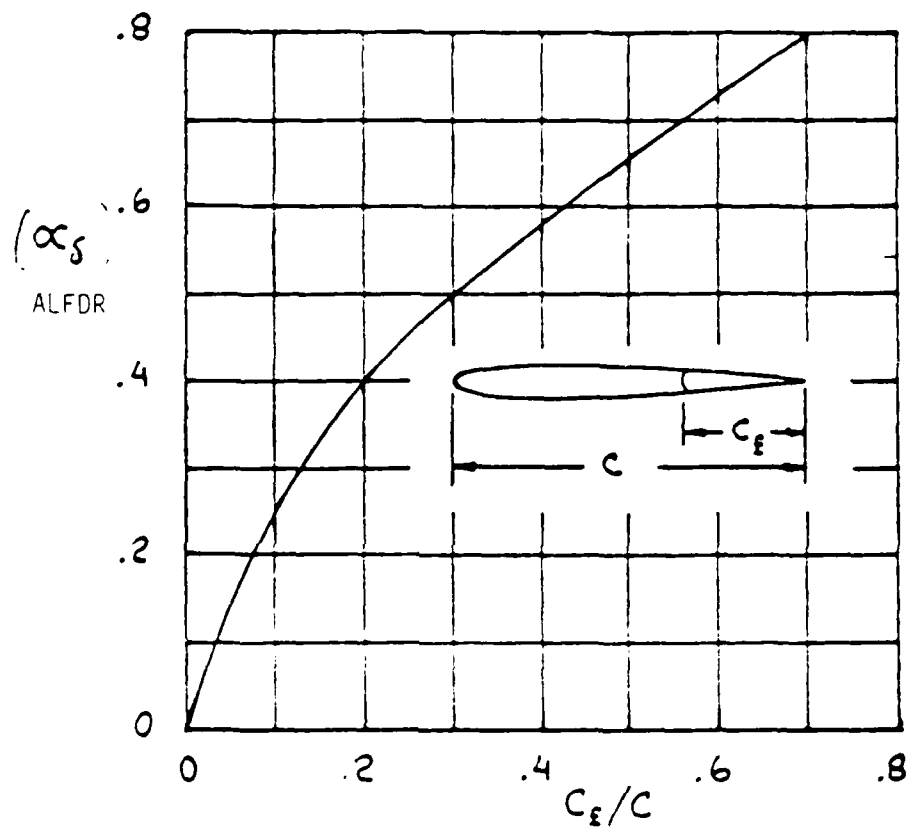


Figure 3.5.1

Angle-of-Attack Effectiveness of Trailing Edge Control Surfaces

3.6 CNR

The variation of yawing moment coefficient with yaw rate CNR is simply the sum of CNR for the vertical tail (CNRV) and CNR for the wing body combination (CNRWB). This is represented as

$$\text{CNR} = \text{CNRWB} + \text{CNRV} \quad (3.6.1)$$

where the components are computed below.

3.6.1 CNRWB

The variation of yawing moment coefficient with yaw rate due to the wing body-combination, CNRWB, cannot be predicted from a generalized method. However, the DATCOM considers the fuselage effects on this derivative as negligible and calculates the CNR for wing alone to represent CNRWB. In the DATCOM CNRWB is given as

$$\text{CNRWB} = \text{RCNRCL2} * \text{CLW}^2 + \text{RCNRCDO} * \text{CDOW} \quad (3.6.2)$$

where

CLW is the wing lift coefficient
RCNRCL2 is the low speed drag-due-to-lift yaw damping parameter obtained from figure 3.6.1 as a function of wing aspect ratio (ARW), taper ratio (TRW), sweepback (C4SWEEP), and mean aerodynamic chord (MACW).
RCNRCDO is the low-speed profile drag yaw-damping parameter obtained from figure 3.6.2 as a function of ARW, C4SWEEP, and MACW
CDOW is the wing profile drag coefficient evaluated at the appropriate Mach number

3.6.2 CNRV

The variation of yawing moment coefficient with yaw rate due to the vertical tail is represented as

$$\text{CNRV} = -\text{CLALPVO} * \text{BV} * \text{SWFV} * \text{SV/SREF} * \text{VNO} \quad (3.6.3)$$

where

CLALPVO is the zero alpha lift curve slope of the vertical tail
SWFV is the sidewash factor of the vertical tail
SV is the area of the vertical tail
SREF is the reference area
VNO is the number of vertical tails

$$\text{BV} = 2.0 * (\text{LV} * \text{COS}(\text{ALPHA}))^2 / \text{SPANW}^2 \quad (3.6.4)$$

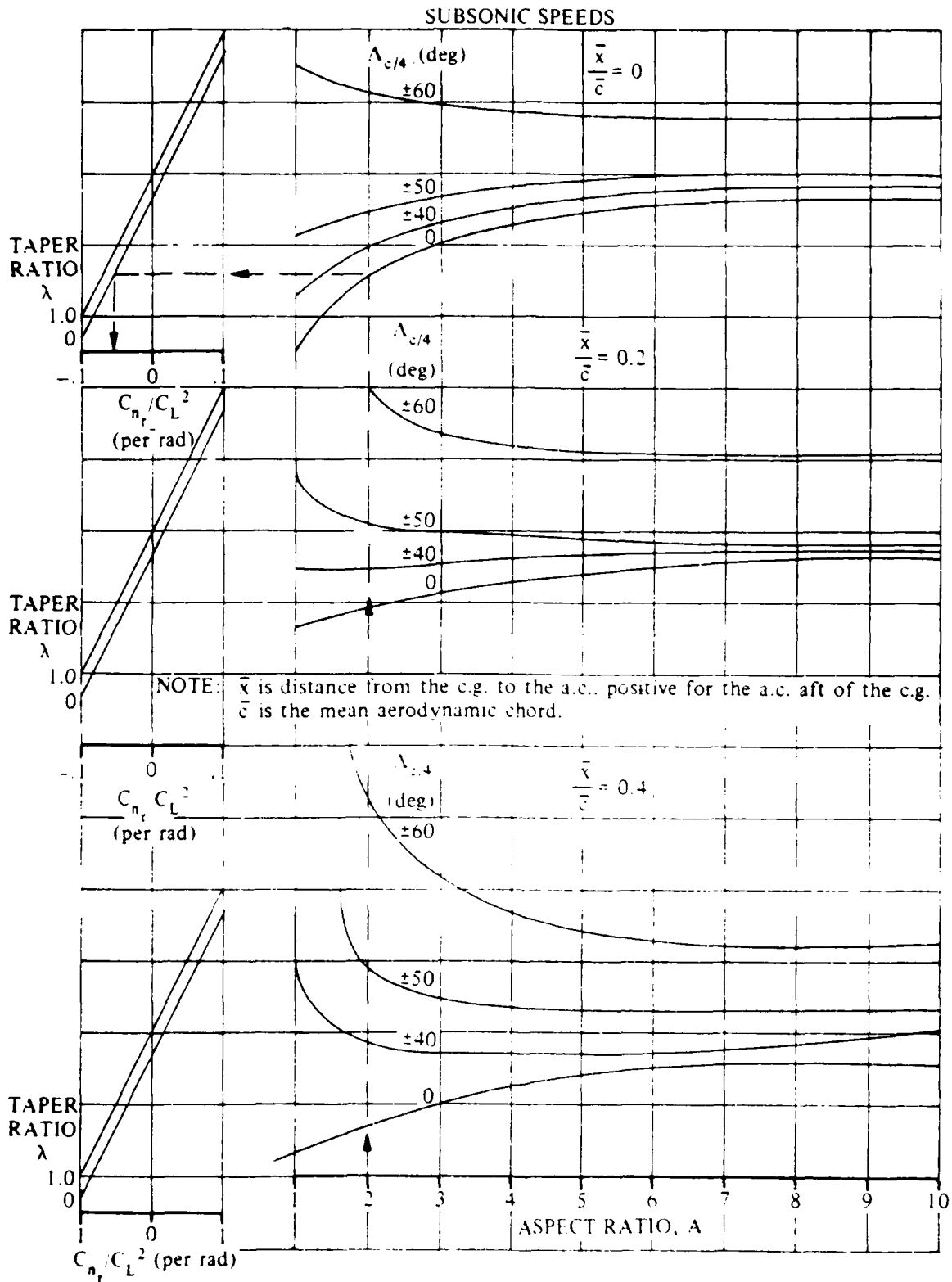
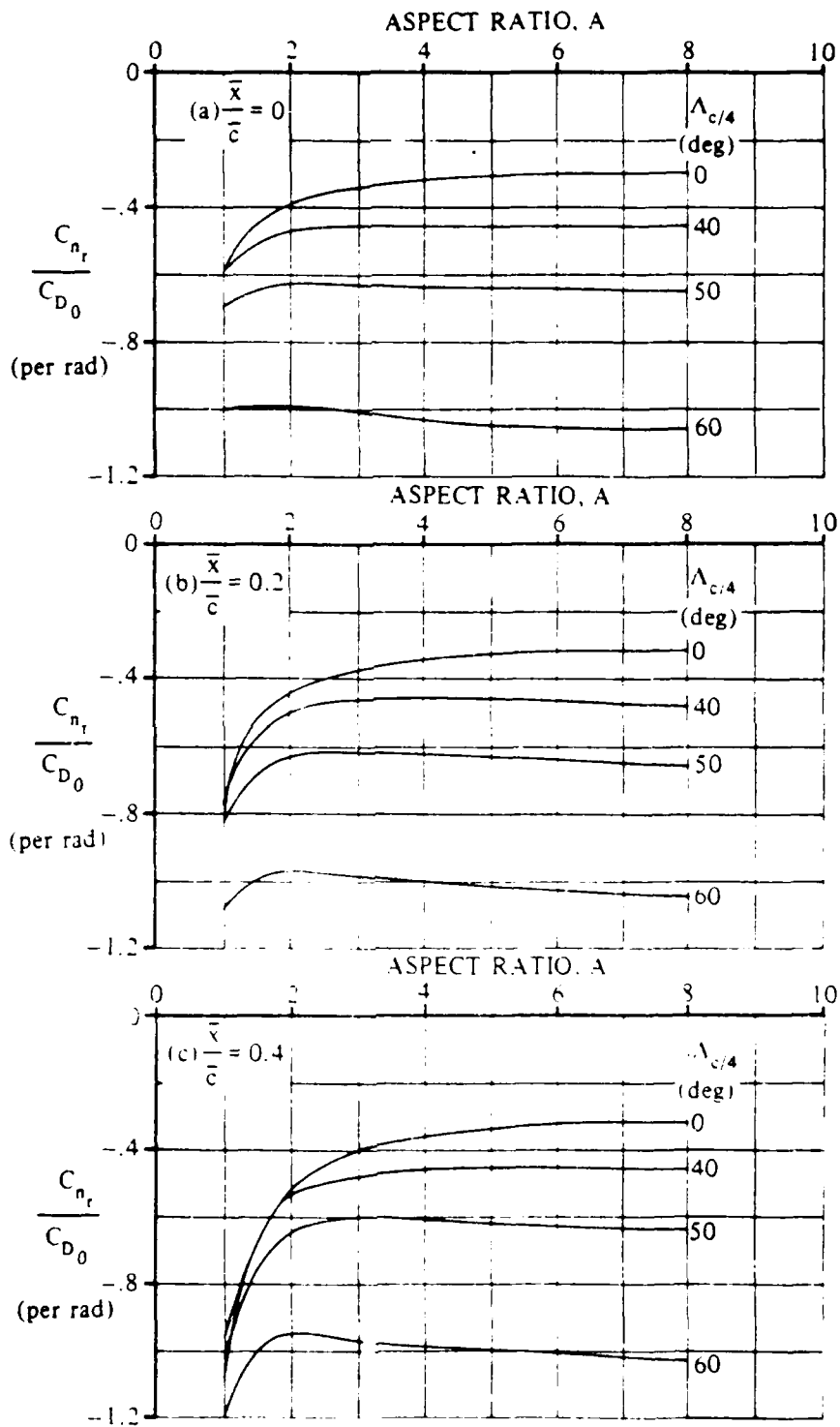


Figure 3.6.1 LOW-SPEED DRAG-DUE-TO-LIFT YAW-DAMPING PARAMETER

SUBSONIC SPEEDS



NOTE: \bar{x} is the distance from the c.g. to the a.c., positive for the a.c. aft of the c.g.
 \bar{c} is the wing mean aerodynamic chord.

Figure 3.6.2 LOW-SPEED PROFILE-DRAG YAW-DAMPING PARAMETER

LV is the axial location of the vertical tail aerodynamic center
ZV is the Z location of the vertical tail mean aerodynamic chord
SPANW is the span of the wing

4.0 DYNAMIC ANALYSIS ROUTINES

The methods described below represent the analysis of dynamic flying qualities of the aircraft of interest. These methods show how to compute the approximate characteristics for Short Period Mode, Phugoid Mode, Dutch-Roll Mode, and Rolling Mode. The dynamic analysis methods presented here are intended to give the user an approximate, rigid body, non-augmented dynamic analysis.

4.1 SHORT PERIOD MODE EQUATION

The short period oscillation of aircraft motion can be characterized by the equation:

$$S^2 + 2.0 * ZETA * OMEGAN * S + OMEGAN^2 = 0 \quad (4.1.1)$$

where

OMEGAN is the undamped natural frequency of oscillation
ZETA is the damping ratio
TS is the period of oscillation
T12S is the time to half amplitude

These characteristics are defined by

$$OMEGAN = \text{SQRT}((MQ * LALP/VEL) - MALP) \quad (4.1.2)$$

$$ZETA = ((LALP/VEL) - MQ - MALPD)/(2.0 * OMEGAN) \quad (4.1.3)$$

$$TS = (2.0 * PI)/(OMEGAN * \text{SQRT}(1.0 - ZETA^2)) \quad (4.1.4)$$

$$T12S = .6931472/(ZETA * OMEGAN) \quad (4.1.5)$$

where

$$LALP = (G * CLALP)/CLO$$

$$MALP = (G * CMALP)/(MACW * CLO * (KYS/MACW)^2)$$

$$MALPD = (G * CMALPD)/(2.0 * VEL * CLO * (KYS/MACW)^2)$$

$$MQ = (G * CMQ)/(2.0 * VEL * CLO * (KYS/MACW)^2)$$

and

G is the force of gravity (ft/sec²)
VEL is the aircraft velocity
CMALD is the variation of pitching moment coefficient with ALPHA
CMALPD is the variation of pitching moment coefficient with the rate of change of ALPHA

CLO is the zero ALPHA lift coefficient
CMQ is the variation of pitching moment coefficient with the pitch rate
MACW is the mean aerodynamic chord of the wing
KYS is the aircraft radius of gyration about the Y axis

4.2 PHUGOID MODE EQUATION

The Phugoid mode equation characterizes a lower frequency aircraft oscillation. The equation in this case is the same as 4.1.1;

$$S^2 + 2.0 * ZETA * OMEGAN * S + OMEGAN^2 = 0 \quad (4.2.1)$$

Where the characteristics of the equation are now represented by

$$OMEGAN = \text{SQRT}(2.0) * G/\text{VEL} \quad (4.2.2)$$

$$ZETA = \text{SQRT}(2.0)/2.0 * \text{CDO}/\text{CLO} \quad (4.2.3)$$

$$\text{TS} = (2.0 * \text{PI})/(\text{OMEGAN} * \text{SQRT}(1.0 - \text{ZETA}^2)) \quad (4.2.4)$$

$$\text{T12S} = .6931472/(\text{ZETA} * \text{OMEGAN}) \quad (4.2.5)$$

and

G is the force of gravity (ft/sec²)
VEL is the aircraft velocity (ft/sec)
CDO is the zero ALPHA drag coefficient
CLO is the zero ALPHA lift coefficient

4.3 DUTCH-ROLL MODE EQUATION

The Dutch-Roll mode equation is primary means of analyzing aircraft lateral stability. The characteristic equation is once again given as;

$$s^2 + 2.0 * ZETA * OMEGAN * s + OMEGAN^2 = 0 \quad (4.3.1)$$

with parameters defined as

$$OMEGAN = \text{SQRT}((G * CNB)/(\text{SPANW} * CLO * (KZS/\text{SPANW})^2)) \quad (4.3.2)$$

$$ZETA = ((G * CNR)/((2.0 * VEL * CLO * (KZS/\text{SPANW})^2)))/ (2.0 * OMEGAN) \quad (4.3.3)$$

$$TS = (2.0 * PI)/(OMEGAN * \text{SQRT}(1.0 - ZETA^2))$$

$$T12S = .6931472/(ZETA * OMEGAN)$$

and

G is the force of gravity (ft/sec²)
VEL is the aircraft velocity (ft/sec)
SPANW is the span of the wing
KZS is the aircraft radius of gyration about the Z axis
CNB is the variation of yawing moment coefficient with sideslip angle
CLO is the aircraft zero ALPHA lift coefficient
CNR is the variation of yawing moment coefficient with the yaw rate

4.4 ROLLING MODE EQUATION

The last dynamic analysis equation characterizes aircraft roll. This equation, known as the Rolling mode is given by

$$P(t) - LP * BANK(t) = LDELA * DELTAA$$

where

P(t) is the roll rate at time (t)
BANK(t) is the roll angle at time (t)
LP is the roll damping parameter
LDELA is the aileron power generating roll
DELTAA is the aileron input

The parameters LP and LDELA are given by

$$LP = (G * CLP)/(2.0 * VEL * CLO * (KXS/SPANW)^2)$$

$$LDELA = (G * CLDA)/(SPANW * CLO * (KXS/SPANW)^2)$$

where

G is the force of gravity (ft/sec²)
VEL is the aircraft velocity (ft/sec)
KXS is the aircraft radius of gyration about the X axis
SPANW is the span of the wing
CLO is the zero ALPHA lift curve slope of the aircraft
CLP is the variation of rolling moment coefficient with roll rate
CLDA is the variation of rolling moment coefficient with aileron angle

From the above results, the roll angle and roll rate at a certain time (t) after a unit step input is

$$BANK(t) = (-LDELA * DELTAA)/LP * (t + (1/LP) * (1.0 - e^{LP*t}))$$

$$P(t) = (-LDELA * DELTAA)/LP * (1.0 + e^{LP*t})$$

Simultaneously solving these equations for (t) with a given BANK(t) and P(t) = 0 gives the time required to achieve the BANK(t) angle. This solution can only be obtained by use of an iterative method.

5.0 STATIC ANALYSIS METHODS

The methods described below allow for the analysis of aircraft configurations under static conditions. The characteristics to be examined are engine out conditions, takeoff rotation, and crosswind landing. The objective of the methods is to determine how the aircraft reacts in these situations.

5.1 ENGINE OUT CONDITIONS

The objective of this method is to determine how the aircraft performance degrades when one or more of the engines are out. The affected systems are the required rudder deflection, the required aileron deflection, and the minimum control velocity.

First the moment forces for the remaining engines (TXM, TXD) must be determined. These are the sum of the moments of each individual engine. For each engine the moments are defined as

$$XM = THRUST * YTAP \quad (5.1.1)$$

$$XD = 1.17 * DQ * EIN * YTAP \quad (5.1.2)$$

where

THRUST is the thrust of the engine
YTAP is the Y location of the thrust application point
DQ is the atmospheric dynamic pressure
EIN is the engine inlet area

The Rudder deflection required (DELRR) can now be defined as

$$DELRR = ((TXM + TXD)/(DQ * SW * SPANW))/CNDELRT \quad (5.1.3)$$

where

SW is the area of the wing
SPANW is the span of the wing
CNDELRT is the variation of yawing moment coefficient with rudder angle (the sum of individual coefficients if two tails are present)

The Aileron deflection required DELAR is;

$$DELAR = (CLBE * (TXM + TXD))/(DQ * SW * SPANW * CNB * CLDA) \quad (5.1.4)$$

where

CLBE is the variation of rolling moment coefficient with sideslip angle

CNB is the variation of yawing moment coefficient with sideslip angle
CLDA is the variation of rolling moment coefficient with aileron angle

The minimum velocity for control of the aircraft can be found from

$$VMIN = \text{SQRT}(QMC / (.5 * DEN)) \quad (5.1.5)$$

where

$$QMC = \text{ABS}(-TXM - TXD) / (TN) \quad (5.1.6)$$

DEN is the atmospheric density

$$TN = CLALPVO * ALFDR * LMACVE * DEF * SV \quad (5.1.7)$$

ALFDR is the rudder effectiveness factor obtained from figure 5.1.1

ALFDR = 0 for non-moveable vertical tail
ALFDR = 1 for an all moveable vertical tail

$$ALFDR = .2923253 + .4191569 * CFC + .4816274 * CFC^2 \quad (5.1.8)$$

for a vertical tail rudder

CFC is the rudder chord to vertical tail chord ratio
CLALPVO is the vertical tail zero ALPHA lift curve slope
LMACVE is the mean aerodynamic chord of the exposed vertical tail
DEF is the tail or rudder deflection
SV is the area of the vertical tail

If multiple vertical tails are present then TN is summed for each tail.

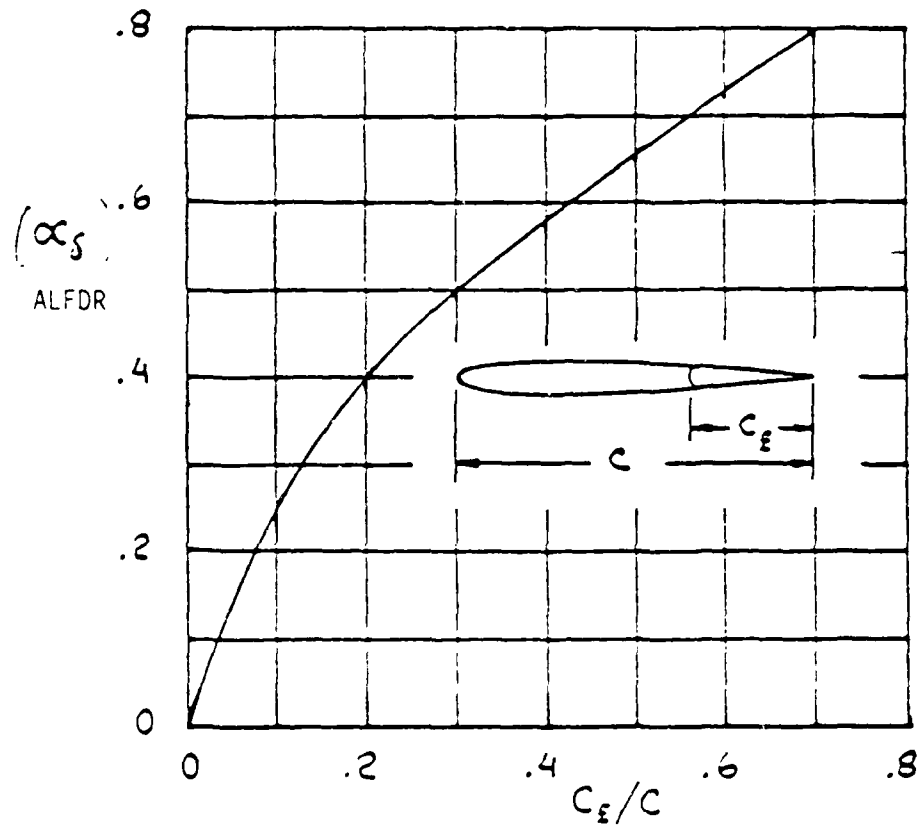


Figure 5.5.1

Angle-of-Attack Effectiveness of Trailing Edge Control Surfaces

5.2 TAKEOFF ROTATION

The methods described here compute the speed at which takeoff rotation occurs given the control surface deflections, and the takeoff power setting. The first step is the computation of the moments acting on the aircraft. These moments are

$$\text{Due to aircraft pitching moment} \\ \text{XMAPM} = \text{CM} * \text{QTOR} * \text{SREF} * \text{MACW} \quad (5.2.1)$$

where

CM is the total aircraft pitching moment coefficient
SREF is the reference area
MACW is the mean aerodynamic chord of the wing

and

$$\text{QTOR} = .5 * \text{DEN} * \text{TOVEL}^2 \quad (5.2.2)$$

where

DEN is the atmospheric density
TOVEL is the estimated takeoff velocity

Due to engines

$$\begin{aligned} \text{XMEZ} &= -\text{T} * \text{COS}(\text{XI}) * (-\text{ZTAP} - \text{ZGLCG}) \\ \text{XMEX} &= \text{T} * \text{SIN}(\text{XI}) * (\text{XTAP} * \text{MACW}) \\ \text{XME} &= \text{XMEX} + \text{XMEZ} \end{aligned} \quad (5.2.3)$$

where

T is the net thrust of the engine
XI is the thrust incidence angle
ZTAP is the thrust application point in the Z direction
XTAP is the thrust application point in the X direction
ZGLCG is the vertical distance between the ground line and the aircraft center line

These calculations are repeated for Body, Nacelle type 1, Nacelle type 2, and lift engines.

Due to Aircraft Weight

$$\text{XMAW} = -\text{WEIGHT} * (\text{XCG} - \text{XMG}) * \text{MACW} \quad (5.2.4)$$

where

XCG is the X location of the aircraft center of gravity
XMG is the X location of the main landing gear

Due to wing-body lift

$$\begin{aligned} \text{LWB} &= (\text{CLOW} * \text{QTOR} * \text{SW}) + (\text{CLALPWB} * \text{IW} * \text{QTOR} * \text{SREF}) \\ \text{XMWBL} &= \text{LWB} * (\text{XACWB} - \text{XMG}) * \text{MACW} \end{aligned} \quad (5.2.5)$$

where

LWB is the lift due to the wing body
CLOW is the wing zero alpha lift curve slope
SW is the wing area
CLALPWB is lift curve slope for the wing and body at ALPHA
IW is the incidence of the wing
XACWB is the aerodynamic center of the wing body combination

Due to drag

$$\begin{aligned} \text{CDTAC} &= \text{CDO} + \text{CDMG} + \text{CDOTO} \\ \text{DRAG} &= \text{CDTAC} * \text{QTOR} * \text{SREF} \\ \text{XMAD} &= \text{DRAG} * (-\text{ZMACWE} - \text{ZGLCG}) \end{aligned} \quad (5.2.6)$$

where

CDO is the zero ALPHA drag coefficient
CDMG is the drag coefficient due to the main gear
CDOTO is the drag coefficient for out of ground effects and high lift takeoff configurations
ZMACWE is the mean aerodynamic chord of the exposed wing

Due to horizontal tail and elevator

$$\begin{aligned} \text{LHT} &= (\text{CLALPH} * (\text{THORR} * (1.0 - \text{DEWH}) - \text{EWGHT} + \text{IH} + \\ &\quad (\text{ADE} * \text{TELER})) * \text{QTOR} * \text{NH} * \text{ASEXH}) + (\text{CLOH} * \text{QTOR} * \text{ASEXH}) \\ \text{XMHT} &= \text{LHT} * (\text{XACH} - \text{XMG}) * \text{MACW} \end{aligned} \quad (5.2.7)$$

where

CLALPH is the lift coefficient due to ALPHA of the horizontal tail
THORR is the control deflection of the horizontal tail
DEWH is the downwash gradient from the wing to the horizontal tail
EWGHT is the downwash angle on the horizontal tail
IH is the incidence angle of the horizontal tail
ADE is the elevator effectiveness parameter obtained from figure 5.1.1 (ALFDR)

$$\begin{aligned} \text{ADE} &= 0 \quad \text{for non-moveable horizontal tail} \\ \text{ADE} &= 1 \quad \text{for an all moveable horizontal tail} \\ \text{ADE} &= .2923253 + .4191569 * \text{CFC} + .4816274 * \text{CFC}^2 \end{aligned} \quad (5.2.8)$$

for a horizontal tail elevator

TELER is the control deflection of the elevator
NH is the dynamic pressure ratio at the horizontal tail
ASEXH is the exposed area of the horizontal tail

CLOH is the zero ALPHA lift coefficient of the horizontal tail
 XACH is the X location of the horizontal tail aerodynamic center

Due to canard and canard flaps

$$\begin{aligned}
 LC &= (CLALPC * (TCANR * (1.0 - DEWC) + IC + (ADCF * TCTFR)) * \\
 &\quad QTOR * NC * ASEXC) + (CLOC * QTOR * ASEXC) \\
 XMC &= LC * (XACC - XMG) * MACW \qquad (5.2.9)
 \end{aligned}$$

where

CLALPC is the lift coefficient due to ALPHA of the canard
 TCANR is the control deflection of the canard
 DEWC is the upwash gradient from the wing to the canard
 IC is the incidence of the canard

ADCF is the canard flaps effectiveness factor obtained from figure 5.1.1(ALFDR)

$$\begin{aligned}
 ADCF &= 0 \quad \text{for non-moveable canard} \\
 ADCF &= 1 \quad \text{for an all moveable canard} \\
 ADCF &= .2923253 + .4191569 * CFC + .4816274 * CFC^2 \quad (5.2.10) \\
 &\quad \text{for a canard flap}
 \end{aligned}$$

TCTFR is the control deflection of the canard flap
 NC is the dynamic pressure ratio at the canard
 ASEXC is the exposed area of the canard
 CLOC is the zero ALPHA lift coefficient of the canard
 XACC is the X location of the canard aerodynamic center

Due to acceleration

$$\begin{aligned}
 R &= WEIGHT - LWB - LHT - LC \\
 UDOT &= (G * (TTOTAL - (XMEU * R) - DRAG))/WEIGHT \\
 XMA &= -(WEIGHT/G) * UDOT * ZGLCG \quad (5.2.11)
 \end{aligned}$$

where

TTOTAL is the total thrust of the aircraft
 XMEU is the ground friction coefficient

Due to High lift devices

$$\begin{aligned}
 LHL &= (CLTO - CL) * QTOR * SW \\
 XMHL &= -LHL * (XHL - (XMG * MACW)) \quad (5.2.12)
 \end{aligned}$$

where

CLTO is the lift coefficient for high lift take off configurations
 CL is the aircraft lift coefficient
 XHL is the X location of high lift devices

Now the aircraft total moment without tail(s) deflection is

$$\begin{aligned} \text{XMTOTAL} = & \text{XMAPM} + \text{XMBE} + \text{XMN1E} + \text{XMN2E} + \text{XMLEX} + \text{XMLEZ} + \text{XMAW} + \\ & \text{XMWBL} + \text{XMAD} + \text{XMA} + \text{XMHL} \end{aligned} \quad (5.2.13)$$

The above calculations are repeated for a range of velocities. Two velocity points are then located, the first being the highest velocity where the aircraft moment is greater than the total control moment, the second being the lowest velocity where the aircraft moment is less than the total control moment. From these two points the takeoff rotation is then estimated with

$$\begin{aligned} \text{XT}(1) &= \text{TOVEL}(1) \\ \text{XT}(2) &= \text{TOVEL}(2) \\ \text{YT1}(1) &= \text{XMTOTAL}(1) \\ \text{YT1}(2) &= \text{XMTOTAL}(2) \\ \text{YT2}(1) &= \text{XMHT}(1) + \text{XMC}(1) \\ \text{YT2}(2) &= \text{XMHT}(2) + \text{XMC}(2) \end{aligned}$$

the velocity of takeoff rotation (VTOR) can be computed by

$$\begin{aligned} \text{TM1} &= (\text{YT1}(1) - \text{YT1}(2)) / (\text{XT}(1) - \text{XT}(2)) \\ \text{TM2} &= (\text{YT2}(1) - \text{YT2}(2)) / (\text{XT}(1) - \text{XT}(2)) \\ \text{B1} &= \text{YT1}(1) - (\text{TM1} * \text{XT}(1)) \\ \text{B2} &= \text{YT2}(1) - (\text{TM2} * \text{XT}(1)) \end{aligned}$$

and

$$\text{TOR} = (\text{B2} - \text{B1}) / (\text{TM1} - \text{TM2}) \quad (5.2.14)$$

5.3 CROSS-WIND LANDING

The methods described here are used to calculate the rudder deflection required to hold a side-slip angle of 11.5 degrees at landing conditions. The side-slip angle is found from an assumed 90 degree cross-wind equal to .2 times the takeoff velocity (.2 * VTO). The required angle is found from

$$\text{TAN}(B) = (\text{VCROSS}/V) = (.2 * \text{VTO}/\text{VTO}) = .2 \quad (5.3.1)$$

and

$$B = \text{ARCTAN}(.2) = 11.5 \text{ DEGREES}$$

Now using the equation of Equilibrium

$$\text{CNB} * B = -\text{CNDELRT} * \text{DELRCWT} \quad (5.3.2)$$

then the required deflection can be found from

$$\text{DELRCWT} = (-\text{CNB} * 11.5)/\text{CNDELRT}$$

where

CNB is the variation of yawing moment coefficient with side-slip angle evaluated at VTO

CNDELRT is the variation of yawing moment coefficient with rudder deflection evaluated at VTO.

APPENDIX A SIGN CONVENTIONS

The sign convention used in SACP is not the standard aerodynamic convention. It was changed to make the conventions used mathematically correct. This change greatly simplified the computations made in the computer program.

The convention for moment arms is to define negative arms forward and above the aircraft with positive arms below and behind. Figure A.1 shows the arms in relation to the aircraft, Note that there are not arms depicted in the Y direction. The Y axis is considered to be positive in both directions so components on that axis are not defined here.

The convention for forces acting on the aircraft is that positive forces act above and behind the aircraft, with negative forces forward and down. Figure A.2 shows this relationship.

The moment conventions are reversed from standard, aerodynamic definitions, but in the current configuration they are mathematically correct. With this convention, looking at the aircraft from the left wing tip, all positive moments act in the counter clockwise direction and negative moments act in the clockwise direction. Figure A.3 details these actions in each quadrant of the axis.

Figure A.4 illustrates an example of how the surface moment arms are defined. The surface is mounted at incidence (α) with forces of lift(L) and drag (D) acting upon it. In this case the moment arms are defined to be

$$X = (XAC_s * \cos \alpha) + (ZAC_s * \sin \alpha)$$

$$Z = (XAC_s * \sin \alpha) - (ZAC_s * \cos \alpha)$$

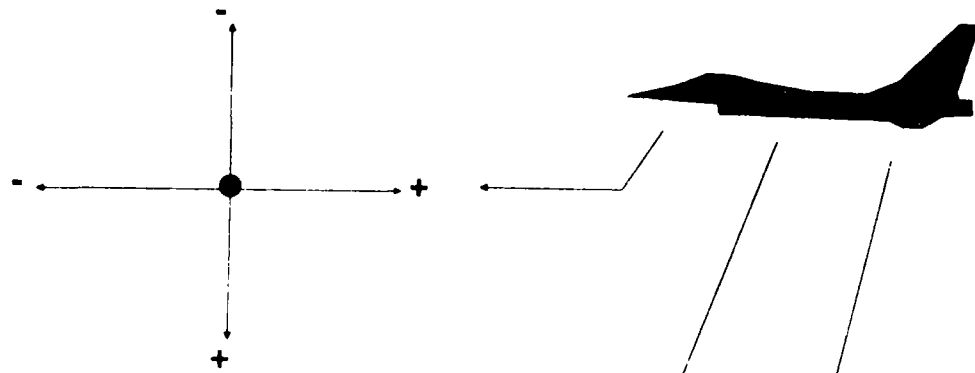


Figure A1 ARMS

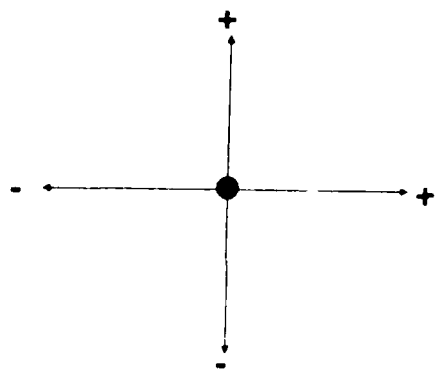


Figure A2 FORCES

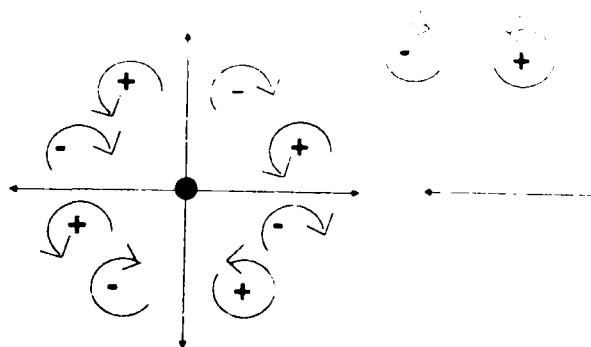


Figure A3 MOMENTS

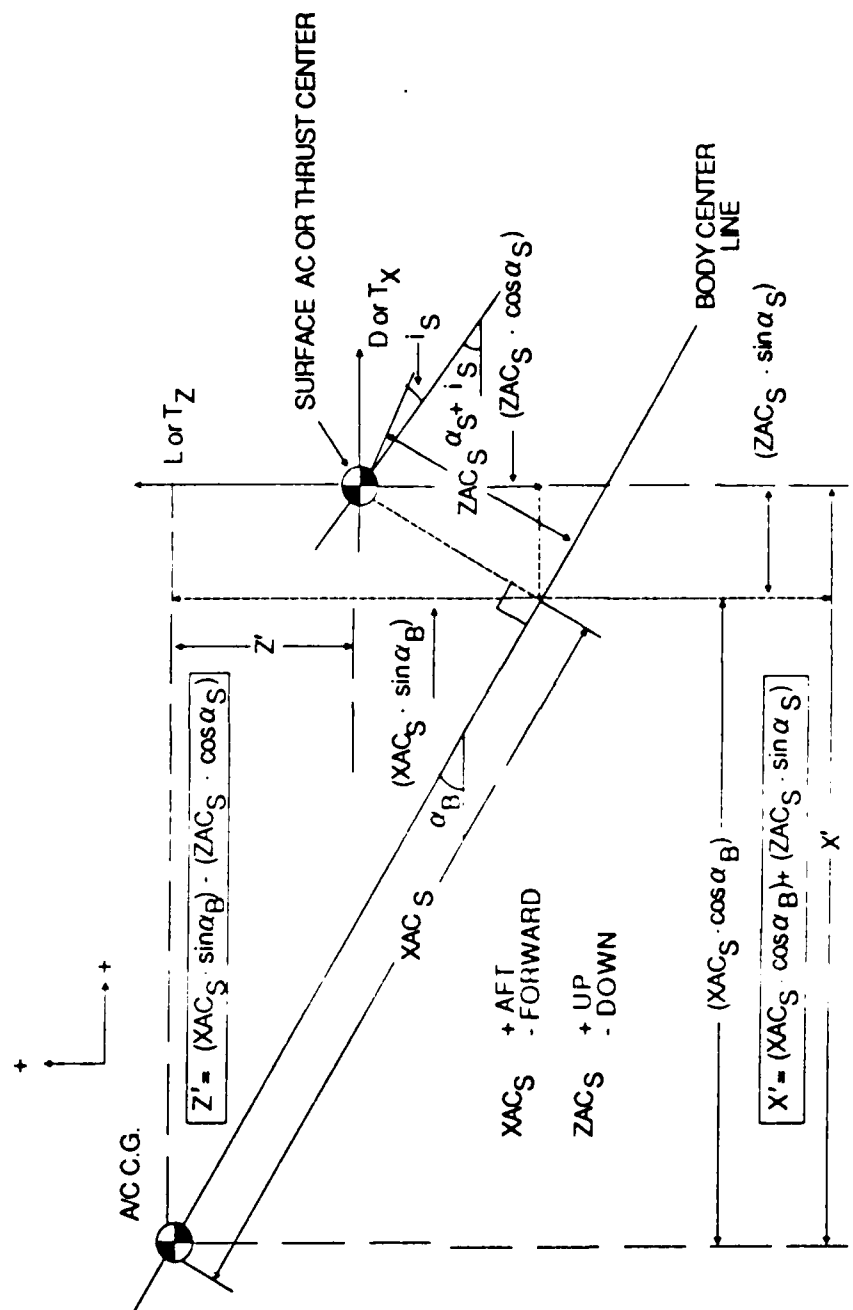


Figure A4. Surface Moment ARM Definition

APPENDIX B GEOMETRY

Though not an aerodynamic method, the proper calculation of geometry is essential to the accurate development of aerodynamic equations. The following section describes the input geometry for the wing, and the subsequent geometry calculations. The results obtained here can be extended directly to the other aircraft surfaces.

Figures 1 show the wing geometry inputs which are defined as follows:

NATW	the wing airfoil option flag
NPANSW	the number of wing panels (4 max)
CSAW	the average body cross-section area along the wing root chord (SQFT)
BDW	the body diameter along the wing root chord (ft)
XTCMW	the location of maximum t/c along the wing mean aerodynamic chord (% MAC)
IW	the wing incidence (DEG)
IFLEXW	the wing leading edge extension bluntness flag
SEXTW	the wing leading edge extension planform area (SQFT)
SLEXTW	the wing leading edge extension leading edge sweep (DEG)
XEXTW	the wing leading edge extension centroid x station (ft)
CREW	the wing exposed root chord length (ft)
TCREW	the wing T/C of exposed root chord leading edge (%)
XCREW	the wing x location of exposed root chord leading edge (ft)
YCREW	the wing y location of exposed root chord leading edge (ft)
ZCREW	the wing z location of exposed root chord leading edge (ft)
WSPLEP(NP)	the leading edge sweep of each panel of the wing (DEG)
WTOCP(NP)	the t/c at the tip chord of each panel of the wing (%)
WSPANP(NP)	the span of each panel of the wing (ft)
WTCP(NP)	the tip chord length of each panel of the wing (ft)
WOFFP(NP)	the leading edge offset length (- forward) of the wing (ft)
WCAMP(NP)	the design lift camber coefficient of each panel of the wing
WTWISTP(NP)	the twist of each panel (- for washout) of the wing
WDIHP(NP)	the dihedral angle of each panel (+ up) of the wing (DEG)

FIGURE WING PANEL INPUTS

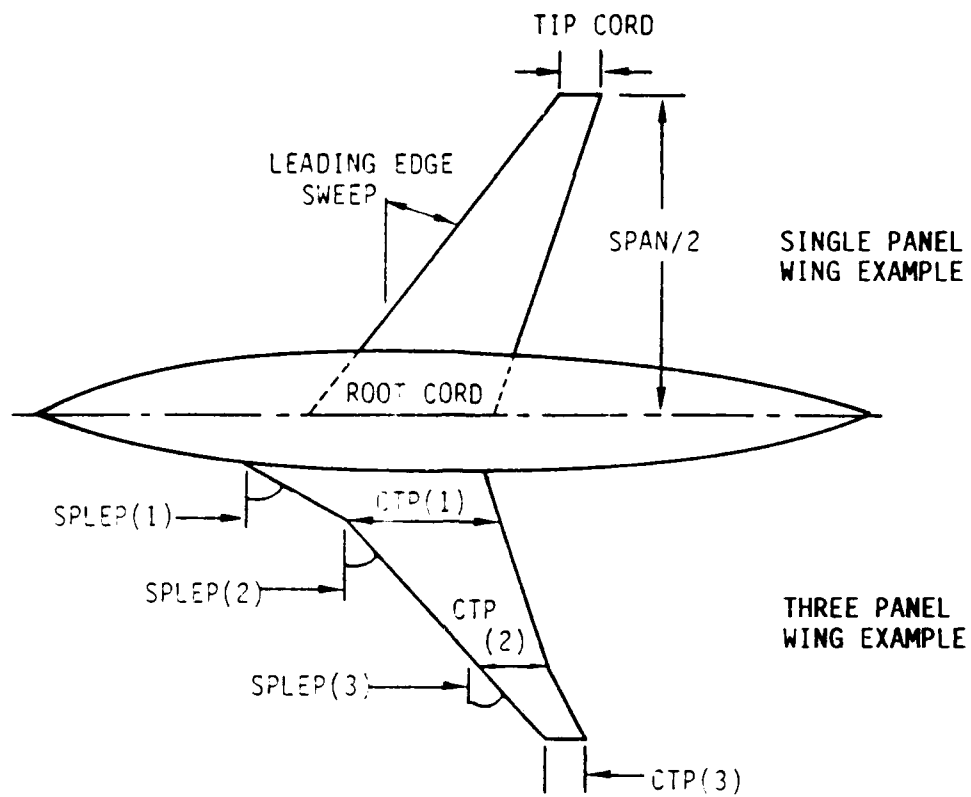


Figure B1 WING SURFACE GEOMETRY

With these inputs some additional properties can be computed by

SXXW(NP) the exposed area of each panel

$$SXXW(NP) = (WCTP(NP) + WCTP(N-1)) * WSPANP(NP)$$

$$WCTP(0) = CREW$$

ASEXW the exposed area of the wing

$$ASESW = SXXN(NP)$$

ARWPE(NP) the exposed aspect ratio of each panel

$$ARWPE(NP) = (2. * WSPANP(NP))^2 / SXXW(NP)$$

TRWPE(NP) the exposed aspect ratio of each panel

$$TRWPE(NP) = WCTP(NP) / WCTP(NP-1)$$

XCRW(NP) the exposed root chord of each panel

$$XCRW(NP) = XCRS(NP-1) + TAN(WSPLEP(NP-1)) * WSPANP(NP-1) + SOFFP(NP)$$

$$XCRW(1) = XCREW$$

SPANWE the exposed wing span

$$SPANWE = WSPANP(NP) * 2.$$

SPANW the wing span

$$SPANW = SPANWE + YCREW * 2.$$

WSPC4P(NP) the quarter chord sweep of each panel

$$WSPC4P(NP) = ATAN((((WSPANP(NP) * 2. * (TAN(WSPLEP(NP)))) + (.5 * WCTP(NP)) - (.5 * WCTP(NP-1)))/(WSPANP * 2.))$$

WSPC2P(NP) the half chord sweep of each panel

$$WSPC2P(NP) = ATAN((((WSPANP(NP) * 2. * (TAN(WSPLEP(NP)))) + (WCTP(NP)) - (WCTP(NP-1)))/(WSPANP * 2.))$$

WSPTEP(NP) the trailing edge sweep of each panel

$$WSPTEP(NP) = ATAN((((WSPANP(NP) * 2. * (TAN(WSPLEP(N2)))) + (2. * WCTP(NP)) - (2. * WCTP(NP-1)))/(WSPANP * 2.))$$

WSPMTP(NP) the maximum thickness sweep of each panel

$$WSPMTP(NP) = ATAN((((WSPANP(NP) * 2. * (TAN(WSPLEP(N2)))) + (XTCMW * 2. * WCTP(NP)) - (XTCMW * 2 * WCTP(NP-1)))/(WSPANP * 2))$$

$$SUM1 = TAN(WSPLEP(NP)) * SXXW(NP)$$

$$SUM2 = TAN(WSPC4P(NP)) * SXXW(NP)$$

$$SUM3 = TAN(WSPC2P(NP)) * SXXW(NP)$$

$$SUM4 = TAN(WSPTEP(NP)) * SXXW(NP)$$

$$SUM5 = TAN(WSPMTP(NP)) * SXXW(NP)$$

SPLEWR the total wing leading edge sweep

$$SPLEWR = ATAN(SUM1/ASEXW)$$

SPC4WR the total wing quarter chord sweep
SPCRWR = $ATAN(SUM2/ASEXW)$

SPC2WR the total wing half chord sweep
SPC2WR = $ATAN(SUM3/ASEXW)$

SPTEWR the total wing trailing edge sweep
SPTEWR = $ATAN(SUM4/ASEX)$

SPMTWR the total wing maximum thickness sweep
SPMTWR = $ATAN(SUM5/ASEX)$

WMACP(NP) the mean aerodynamic chord of each panel
 $WMACP(NP) = \frac{2}{3} * (WCTP(NP - 1) - WOFFP(NP)) * (1. + TRWPE(NP) + TRWPE(NP)^2) / (1. + TRWPE(NP))$

AWET(NP) the wetted area of each panel
 $AWET(NP) = SXXW(NP) * (2 + .1843 * WTOCP(NP) + 1.5268 * STOCP(NP)^2 - .8395 * STOCP(NP)^3)$

ARW the aspect ratio of the wing
 $ARW = SPANW^2/SW$

ARWE the exposed aspect ratio of the wing
 $ARWE = SPANWE^2/ASEXW$

XCR23W the X location of the 2/3 chord point
 $XCR23W = XCREW + (2/3 * CREW)$

ZCGCRW the Z distance between the center of gravity and the root chord of the wing
 $ZCGCRW = ZCREW - ((.25 * CREW) * SIN(IW))$

REFERENCES

1. Schemensky, R. T., Development of an Empirically Based Computer Program to Predict the Aerodynamic Characteristics of Aircraft, Volume 1, Empirical Methods. General Dynamics Corporation, November 1973, AFFDL-TR-73-144.
2. Schemensky, R. T., Development of an Empirically Based Computer Program to Predict the Aerodynamic Characteristics of Aircraft, Volume 2, Program User Guide. General Dynamics Corporation, November 1973, AFFDL-TR-73-144.
3. A Method of Estimating Drag-Rise Mach Number for Two-Dimensional Aerofoil Sections, Royal Aerodynamic Society Transonic Data Memorandum 6407, July 1964.
4. Sinnott, C. S., "Theoretical Prediction of the Transonic Characteristics of Airfoils", Journal of Aerospace Sciences, Volume 29, No. 3 (March 1962).
5. Method for Predicting the Pressure Distribution on Swept Wings with Subsonic Attached Flow, Royal Aerodynamic Society Transonic Data Memorandum 6312, December 1963.
6. Miller, B.D., Notes on Wing Design Methods for Supercritical Airfoils, General Dynamics Convair Aerospace Division Report ARM-061, October 1971.
7. Drag-Rise Mach Number of Aerofoils Having a Specified Form of Upper-Surface Pressure Distribution: Charts and Comments on Design, Royal Aerodynamic Society Transonic Data Memorandum 67009, January 1967.
8. USAF Stability and Control DATCOM, Air Force Flight Dynamics Laboratory, October 1960 (Revised August 1968).
9. Henderson, W. P., Studies of Various Factors Affecting Drag Due to Lift at Subsonic Speeds, NASA TN D-3584, October 1966.
10. Lowry, J. G., and Polhamus, E. C., A Method for Predicting Lift Increments Due to Flap Deflection at Low Angles of Attack in Incompressible Flow, NACA TN 3911, 1957.
11. Polhamus, E. C., Summary of Results Obtained by Transonic-Bump Method on Effects of Planform and Thickness on Lift and Drag Characteristics of Wings at Transonic Speeds, NACA RM L51H30, 30 November 1951.
12. Nelson, W. H., and McDevitt, J. B., The Transonic Characteristics of 17 Rectangular, Symmetrical Wing Models of Varying Aspect Ratio and Thickness, NACA RM A51A12, 10 May 1951.

13. Tinling, B. E. and Kolk, W. R., The Effects of Mach Number and Reynolds Number on the Aerodynamic Characteristics of Several 12-Percent-Thick Wings Having 35 Degrees of Sweepback and Various Amounts of Camber, NACA RM A50K27, 23 February 1951.
14. Dolan, C. J., and Weil, J., Characteristics of Swept Wings at High Speeds, NACA RM L52A15, January 1952.
15. Gilman, B. G., and Burdges, K. P., "Rapid Estimation of Wing Aerodynamic Characteristics for Minimum Induced Drag", Journal of Aircraft, Volume 4, No. 6 (November - December 1967).
16. White, F. M., and Christoph, G. H., A Simple New Analysis of Compressible Turbulent Two-Dimensional Skin Friction Under Arbitrary Conditions, AFFDL-TR-70-133, February 1971.
17. Aerospace Handbook, Second Edition, (C. W. Smith, ed.), General Dynamics Convair Aerospace Division Report FZA-381-II, October 1972.
18. Linnell, R. D., Similarity Rule Estimation Methods III, Flow Around Cones and Parabolic Noses, General Dynamics Convair Aerospace Division Report MR-A-1059, 10 August 1955.
19. Hoerner, S. F., Fluid-Dynamic Drag (Published by the author, Midland Park, New Jersey, 1965).
20. Axelson, J. A., AEROX - Computer Program for Transonic Aircraft Aerodynamics to High Angles of Attack, Volume I: Aerodynamic Methods and Program Users' Guide Ames Research Center, Moffitt Field, California Report number TM X-73;208, February 1977.
21. Axelson, J.A. and A.D. Levin, Extension of the AEROX Aerodynamics Computer Program to Include Canard Aircraft. Ames Research Center, May 1980.
22. Behrhohm, Hermann, Basic Low-Speed Aerodynamics of Short-Coupled Canard Configurations of Small Aspect Ratio. SAAB TN 60, July 1965.
23. Roskam, Jan, Methods for Estimating Stability and Control Derivatives of Conventional Subsonic Airplanes. Copywrite 1971.
24. Flax, Alexander H.: Comment on "Simplification of the Wing-Body Problem", AIAA Journal of Aircraft, Volume II, No. 10, October 1973, pp640.
25. Flax, Alexander H.: Comment on "Correlation of Wing-Body, Combination Lift Data", AIAA Journal of Aircraft, Volume 11, No.5,, May 1974, pp 303-304.
26. Axelson, John A., Estimation of Transonic Aircraft Aerodynamics to High Angles of Attack, AIAA Paper No.. 75-996, August 1975.

27. Laitone, E. V., "Limiting Velocity of Momentum Relations for Hydrofoils Near the Surface and Airfoils in Near Sonic Flow", Proceedings of the Second U.S. National Congress of Applied Mechanics, June 14 - 18, 1954, pp 751-753.
28. Laitone, E. V., "Local Supersonic Region on a Body Moving at Subsonic Speeds", Symposium Transonicum, Aachen, Germany, September 3-7, 1962, Edited by Klaus Oswatitsch.
29. Ames Research Staff, Equations, Tables and Chart for Compressible Flow, NACA TR 1135, 1953.
30. Cleary, J. W. and Axelson, J. A., Theoretical Aerodynamic Characteristics of Sharp and Circularly Blunt-Wedge Airfoils at Hypersonic Speeds, NASA TR R-202, July 1964.
31. Mager, J. P., A Limit Pressure and an Estimation of Limit Forces on Airfoils at Supersonic Speeds, NACA RM L8F23, 1948.
32. Jorgenson, L. H., Prediction of Static Aerodynamic Characteristics for Space Shuttle-like and Other Bodies at Angles of Attack from 0° to 180°, NASA TN D-6996, 1973.
33. Shemensky, R. T., High-Lift Prediction Techniques, General Dynamics' Fort Worth Division Report AIM-170, 12 February 1969.
34. Hebert, J., et al., Effects of High-lift Devices on V/STOL Aircraft Performance, USAAVLABS Technical Report 70-33A, October 1970.
35. Hebert, J., et al., STOL Tactical Aircraft Investigation, Volume II - Design Compendium, AFFDL-TR-73-21, 13 January 1973.
36. Roskam, J.A., Airplane FLight Dynamics and Automatic Flight Controls. Roskam Aviation and Engineering Corporation 1979.

END

DATE

FILMED

5-88

DTIC